

STRUCTURAL STUDIES OF THE  
MINERAL SULFOSALTS

by

NOBUKAZU NIIZEKI

Rigakushi, Tokyo University  
(1952)

SUBMITTED IN PARTIAL FULFILLMENT OF THE  
REQUIREMENTS FOR THE DEGREE OF  
DOCTOR OF PHILOSOPHY

at the

MASSACHUSETTS INSTITUTE OF TECHNOLOGY  
(1957)

Signature of Author. . . . .  
Department of Geology and Geophysics, March 5, 1957

Certified by. . . . .

Accepted by. . . . .  
Chairman, Departmental Committee on Graduate Students



Room 14-0551  
77 Massachusetts Avenue  
Cambridge, MA 02139  
Ph: 617.253.5668 Fax: 617.253.1690  
Email: docs@mit.edu  
<http://libraries.mit.edu/docs>

## **DISCLAIMER OF QUALITY**

Due to the condition of the original material, there are unavoidable flaws in this reproduction. We have made every effort possible to provide you with the best copy available. If you are dissatisfied with this product and find it unusable, please contact Document Services as soon as possible.

Thank you.

### **Pages are missing from the original document.**

Missing pages 230-234 and page 250.  
Two pages numbered 253.

## ABSTRACT

## STRUCTURAL STUDIES OF THE MINERAL SULFOSALTS

by

Nobukazu Niizeki

Submitted to the Department of Geology and Geophysics on March 6, 1957, in partial fulfillment of the requirements for the degree of Doctor of Philosophy.

The crystal structure of livingstonite has been determined. A new chemical analysis of the mineral gives the formula  $\text{HgSb}_4\text{S}_8$  instead of the previously assigned  $\text{HgSb}_4\text{S}_7$ . The space group is  $A2/a$ , and the unit cell dimensions are:  $a = 30.25\text{\AA}$ ,  $b = 4.00\text{\AA}$ ,  $c = 21.48\text{\AA}$ , and  $\beta = 104^\circ 12'$ . This unit cell contains  $8\text{HgSb}_4\text{S}_8$ . Intensities were measured by the single-crystal Geiger-counter method with  $\text{CuK}\alpha$  and  $\text{MoK}\alpha$  radiations. The structure was analyzed by direct interpretations of the Patterson map  $P(xz)$ , and the three-dimensional Patterson sections,  $P(x, n/60, z)$ . The refinement of the structure was performed by the successive Fourier and difference-Fourier trials, and finally by the three-dimensional least-squares method. The structure obtained confirms the new chemical formula.

In the structure an  $S_2$  group is found with S-S distance of  $2.07\text{\AA}$ . The existence of this  $S_2$  group was suggested from the new chemical formula. In the structure, there are two kinds of layers, both running parallel to  $((001))$ . In one kind of layer, two  $\text{Sb}_2\text{S}_4$  double chains are joined together by an S-S bond to form an  $S_2$  group between them. In the other, two  $\text{Sb}_2\text{S}_4$  double chains are cemented together by Hg atoms. Each Sb atom has three closest neighboring S atoms and four additional ones at greater distances. The coordination of Hg atom is a distorted octahedral of six S atoms, of which two are strongly bonded ones arranged in a linear way as found in cinnabar, HgS. The perfect cleavage  $((001))$  can be explained as the breaking of the weaker bonds between the two kinds of layers.

The crystal structure of jamesonite has been determined. The space group of the mineral is  $P2_1/a$ , and its unit cell dimensions are:  $a = 15.08\text{\AA}$ ,  $b = 18.98\text{\AA}$ ,  $c = 4.03\text{\AA}$ , and  $\beta = 91^\circ 48'$ . This unit cell contains  $2\text{FePb}_4\text{Sb}_6\text{S}_{14}$ . The intensities were measured by the single-crystal Geiger-counter method with  $\text{CuK}\alpha$  radiation. The projected structure along  $c$  axis was solved by the minimum function method. The  $z$  parameters of the atoms were determined by the implication method. The structure was refined by the successive Fourier and difference-Fourier trials, and finally by the three-dimensional least-squares method.

In the structure three  $\text{SbS}_3$  groups are arranged parallel to  $[120]$ , and can be described as forming  $\text{Sb}_3\text{S}_7$  groups. Two  $\text{Sb}_3\text{S}_7$  groups are loosely bonded together into a larger  $\text{Sb}_6\text{S}_{14}$  group. Fe and two kinds of Pb atoms are

...yren (Geol) Sept. 9, 1957

located in the interstices provided by the S atoms of the  $Sb_6S_{14}$  groups, and play the role of cementing these  $Sb-S$  groups. Fe has a distorted octahedral coordination of six S atoms. The Pb atoms have either 7 or 8 atoms of sulfur as closest neighbors. The strongly bonded chains or layers running parallel to the acicular axis of the mineral are not well defined in jamesonite. The cleavage of the mineral has been accounted for in terms of the observed interatomic distances.

The crystal structures of the sulfosalts minerals have been systematically studied. The arrangements of the S atoms around the central metal and submetal atoms were examined. The first and the second coordination polyhedra of each central atom were described. As the structural basis of the crystal chemistry of sulfosalts, the stacking of these polyhedra was considered. The chemical parameter  $f$  defined as  $(Cu+Ag+Pb+As+Sb+Bi)/S$  was introduced, and the relations between this value and the mode of stacking of the polyhedra were developed.

The sulfosalts can be classified into three main groups. They are: (1) acicular sulfosalts, (2) sulfosalts with structures closely related to the simple sulfides (PbS type or ZnS type), and (3) sulfosalts with the value of  $f$  greater than 1.0.

The acicular sulfosalts are characterized by a shortest unit cell dimension of  $4\text{\AA}$ . The values of  $f$  are generally less than 1.0, and are equal to 1.0 only when the formula contain Cu. The coordination polyhedra are stacked in such a way that the  $4\text{\AA}$  dimensions of polyhedra are oriented parallel to each other. In the most structures of this group, the first coordinations of the submetal atoms, the  $SbS_3$  pyramids, are well defined and are built into the larger groups sharing the S atoms with adjacent pyramids.

When the dimension of  $4\text{\AA}$  is not found as the true unit cell dimension, but as an asymmetric or a sub-multiple dimension of the structures, these structures are considered as related closely to the acicular group.

In the structures closely related to the simple sulfides, the value of  $f$  is equal to 1.0 or very close to it. The structures of the acicular sulfosalts were considered as the deviated ones from the simple structures, and the existence of the fragmental layers of the simpler type in the structure was pointed out.

As one possible type of the structure with the value of  $f$  greater than 1.0, the structures with independent  $SbS_3$  groups were considered. The physical properties of the minerals of this group are found as more covalent than metallic, and the relation between this nature and the type of coordination in the structure was discussed.

"Thesis Supervisor: Martin J. Buerger

Title: Professor of Mineralogy and Crystallography

## TABLE OF CONTENTS

	PAGE
Title and Certificate of Approval	
Abstract	i
List of illustrations	viii
Table index	xii
Introduction	1

## PART I

The crystal structure of livingstonite,  $\text{HgSb}_4\text{S}_8$ 

Introduction	4
Preliminary structure investigation	4
Chemical composition of livingstonite	8
Unit cell dimensions and space group	13
Relations between unit cell data	15
Three-dimensional intensity determination	16
Refinement of the projected structure	19
Determination of y coordinates	20
Introduction	20
Three-dimensional Patterson sections	20
Interpretation of three-dimensional Patterson peaks	26
Refinement of y coordinates	34
Three-dimensional refinement	34
Discussion of the structure	41

## PART II

The crystal structure of jamesonite,  $\text{FePb}_4\text{Sb}_6\text{S}_{14}$

	PAGE
Introduction	61
Unit cell and space group	62
Intensity determination	62
General outline of the structure determination	64
Interpretation of Patterson peaks	67
Solutions by the image-seeking method	72
False structure	75
Correct structure	79
Determination of z coordinates of atoms	82
Three-dimensional refinement	90
Discussion of the structure	90

### PART III

#### Crystal chemistry of the sulfosalt minerals

Introduction	110
1. Geometrical basis of crystal chemistry of sulfosalts	116
Coordination polyhedra	116
First coordination polyhedra	116
Second coordination polyhedra	118
Geometry of polyhedra	119
Interatomic distances in second coordination	121
Sulfosalt structures as the open stacking of second coordination polyhedra	122
Classification of sulfosalt minerals	132
Chemical parameter, f	142
2 Polygonal network of the projected structure of the minerals in group A and A'	146

	PAGE
Introduction	146
Nature of polygonal network	155
Solution of polygonal network	157
Polygonal network and chemical formula	157
Theorems of network theory	158
Ambiguities in the solutions of polygonal network	159
Systematic solution of the polygonal network	162
Examples of systematic treatment	164
Summary of polygonal network theory	172
3. The Sb(As,Bi)-S chains and layers	174
Introduction	174
Electronic configurations of Sb and S atoms, and structures of the elements Sb and S	174
Independent $SbS_3$ pyramid	177
Finite groups of Sb and S atoms	179
$SbS_2$ chain	179
$Sb_2S_4$ double chain	183
$Sb_2S_3$ band	183
$Sb_2S_3$ sheet	184
$Sb_4S_8$ group	185
Structure of stibnite	185
Chains and double chains of metal-sulfur	188
Polyhedral interstices provided by two or more chains	191
Relation between the first and second coordination polyhedra of Sb(As,Bi) atom	194
Cleavage of acicular sulfosalts	196
Sub-multiple unit cell dimension of 4A in sulfosalt structures	197

	PAGE
4. Relation between sulfosalts structures and simple sulfide structures	201
Sulfosalts of group B	201
Relation between atomic ratio in the formula and C.N. ratio in the structure	203
Relation between C.N. and chemical parameter $f = 1.0$	204
Relation between C.N. and deviation of $f$ -value from 1.0	205
Fragments of simple coordinations in sulfosalts structures	205
Minerals of group C.	208
5. Minerals with $f$ -value greater than 1.0	216
Minerals containing Ag	216
Minerals containing Cu	219
Minerals containing Cu and Ag	220
Minerals in group E	220
6. Summary	222

#### PART IV

Appendix I. Historical introduction to the crystal-structure analysis of sulfosalts	227
Appendix II. A note on absorption correction	230
Appendix III. A note on Wilson's statistical method	233
Appendix IV. Proof of Theorem 1	235
Appendix V. Proof of Theorem 2	239
Appendix VI. Proof of Theorem 3	242
Appendix VII. Proof of Theorem 4	244
Appendix VIII. Proof of Theorem 5	247
Appendix IX. Proof of solution of jamesonite network	248



	PAGE
Appendix X. Valences in submetals As, Sb, and Bi	250
Bibliography	251
Acknowledgment	257
Biographical note	258

## LIST OF ILLUSTRATIONS

	PAGE
PART I	
Fig. 1. Patterson diagram $P(xz)$	6
Fig. 2. Statistical test of centrosymmetry	7
Fig. 3. The first electron-density map $\rho(xz)$	9
Fig. 4. Representations of space group $A2/a$	18
Fig. 5. Determination of scale factor and temperature coefficient by Wilson's method	21
Fig. 6. Final electron-density map $\rho(xz)$	22
Fig. 7. Representations of space group $A2/m$	24
Fig. 8. Projection of Sb atoms in the unit cell	25
Fig. 9. Vector set of Sb atoms	27
Fig. 10. Three-dimensional Patterson sections	
a. Section at $y = 0/60$	29
b. Section at $y = 2/60$	29
c. Section at $y = 4/60$	30
d. Section at $y = 6/60$	30
e. Section at $y = 8/60$	31
f. Section at $y = 10/60$	31
g. Section at $y = 12/60$	32
h. Section at $y = 14/60$	32
Fig. 11. Final electron-density map $\rho(xy)$	35
Fig. 12. Determination of non-uniform scaling factor for each level	40
Fig. 13. Schematic representation of the structure	48
Fig. 14. Schematic representation of the structure (whole unit cell)	49

## PART II

Fig. 15	Determination of scale factor and temperature coefficient by Wilson's method	63
Fig. 16	Patterson diagram, $P(xy)$	65
Fig. 17	Geometrical relation between a rotation peak and its reflection satellites	66
Fig. 18	Solution of rotation peaks from satellite-like peaks	68
Fig. 19	$I_{M_4}$ map.	69
Fig. 20	$II_{M_4}$ map	70
Fig. 21	$III_{M_4}$ map	71
Fig. 22	$I+a_{M_8}$ map	73
Fig. 23	Comparison of two $M_8$ maps	74
Fig. 24	$\rho(xy)$ of false structure	76
Fig. 25	Structural scheme of correct structure	77
Fig. 26	$\rho(xy)$ of correct structure	78
Fig. 27	$I+a_{M_8}$ map and $b+c_{M_8}$ map	80
Fig. 28	Final electron-density map $\rho(xy)$	81
Fig. 29	Harker section $P(x\frac{1}{2}z)$	83
Fig. 30	Relations between crystal space, Patterson space, and implication space	84
Fig. 31	Implication map $I(x\frac{1}{2}z)$	85
Fig. 32	Final electron-density map $\rho(xz)$	88
Fig. 33	Schematic representation of the structure	89

## PART III

Fig. 34	Geometry of tetrahedron	123
Fig. 35	Geometry of octahedron	124
Fig. 36	Geometry of complex polyhedra	125
Fig. 37	Schematic representation of the structure of stibnite	127

	PAGE
Fig. 38 Schematic drawing of the structure of galena	128
Fig. 39 Schematic drawing of a double layer of 7-vertex-8-hedra	128
Fig. 40 Structural scheme of aikinite	143
Fig. 41 Structural scheme of bournonite	143
Fig. 42 Polygonal network of chalcostibite	147
Fig. 43 Polygonal network of aikinite	148
Fig. 44 Polygonal network of bournonite	149
Fig. 45 Polygonal network of berthierite	150
Fig. 46 Polygonal network of galenobismutite	151
Fig. 47 Polygonal network of jamesonite	152
Fig. 48 Polygonal network of livingstonite	153
Fig. 49 Alternative representation of polygonal network of chalcostibite	161
Fig. 50 Idealized network of chalcostibite	168
Fig. 51 Second type of arrangement of 3-gons and 5-gons	169
Fig. 52 Schematic representation of Sb-S groups (1)	178
Fig. 53 Structural scheme of berthierite	180
Fig. 54 Schematic representation of Sb-S groups (2)	181
Fig. 55 Structural scheme of chalcostibite	182
Fig. 56 Structural scheme of orpiment	186
Fig. 57 Structural scheme of stibnite	187
Fig. 58 Structural scheme of galenobismutite	190
Fig. 59 Schematic representations of the polyhedral interstices	192

	PAGE
Fig. 60 Relations between the first and second coordinations of Sb atom	195
Fig. 61 Fragmental groups of atoms in sulfosalts	207
Fig. 62 Structure of tennantite	209
Fig. 63 Structure of enargite and its relation to structures of wurtzite and chalcostibite	213
Fig. 64 Structure of chalcostibite in terms of octahedral and tetrahedral coordinations	214
Fig. 65 Structure of proustite	218

## TABLE INDEX

	PAGE
PART I	
Table 1	Coordinates of atoms in projection on (010) 10
Table 2	Analysis of livingstonite 12
Table 3	Interpretation of chemical data 14
Table 4	Comparison of cell data 17
Table 5a	Sb-Sb peaks used for the determination of $y_{Sb}$ 's. 36
Table 5b	Determination of $y_{Sb}$ 's 36
Table 6	Atomic coordinates from several processes 37
Table 7a	Analysis of three-dimensional refinement cycles by the least-squares method of IBM 42
Table 7b	Level-by-level comparison of R-values 43
Table 8	Final atomic coordinates 44
Table 9	Interatomic distances 47
Table 10	Observed and computed structure factors 50
PART II	
Table 11	Atomic coordinates determined by several methods 86
Table 12	Final atomic coordinates 94a
Table 13	Interatomic distances 95
Table 14	Observed and calculated structure factors 96
PART III	
Table 15	Sulfosalts structures determined 115
Table 16	Dimensions in tetrahedron and octahedron 126

	PAGE
Table 17 The first and second coordination polyhedra characteristics of central atoms	129
Table 18 Chemical classifications of sulfosalts	
a. Sulfosalt minerals containing Cu	134
b.     "           "           "           Ag	135
c.     "           "           "           Pb	136
d.     "           "           "           Cu, Ag	138
e.     "           "           "           Cu, Pb	138
f.     "           "           "           Ag, Pb	139
g.     "           "           "           Cu, Ag, Pb	140
Table 19 Classifications of sulfosalts based on the possible stacking type of the second coordination polyhedra	145
a. Group A	167
b. Group A'	199
c. Group B	202
d. Group C	208
e. Group D	217
f. Group E	221
Table 20 Coordination polygons	154
Table 21 Nature of polygonal networks of the projection of structures of acicular sulfosalts	156
Table 22 Metal-S distances in sulfosalts	193

## INTRODUCTION

The work described in this thesis is composed of three related papers and one supplementary section.

The crystal chemistry of the sulfosalt minerals is one of the important subjects of mineralogy and crystallography yet to be investigated. There are two factors which have prevented a systematic treatment of the problem. One is the lack of the structural knowledge itself of the minerals. The other is the lack of understanding of the basic principles relating the chemical formula and structure types.

In recent years, however, the structural knowledge has been significantly increased. Several investigators have determined the crystal structures of the minerals berthierite ( $\text{FeSb}_2\text{S}_4$ ), galenobismutite ( $\text{PbBi}_2\text{S}_4$ ), aikinite ( $\text{CuPbBiS}_3$ ), and seligmannite ( $\text{CuPbAsS}_3$ ). The first two parts of the thesis are a contribution along the same line. In Part I, the structure determination of the mineral livingstonite,  $\text{HgSb}_4\text{S}_8$ , is presented. In Part II, the structure determination of the mineral jamesonite,  $\text{FePb}_4\text{Sb}_6\text{S}_{14}$ , is described.

Except seligmannite, all the minerals mentioned above are the members of the group of acicular sulfosalts. These minerals have unit cells with one shortest dimension of  $4\text{\AA}$  length, and exhibit the acicular crystal habits. The structures of the sulfosalts in general must



be further investigated. Nevertheless, the structural features found among the previously determined crystal structures reveal certain structural principles of sulfosalt minerals.

In the crystal chemistry of the ionic crystals, the structures can be described by means of the packing of the spheres of anions and cations. When there is a strongly bonded structural unit, as in the silicate minerals, the structures can be described in terms of the structural motifs built from this unit. In the sulfide minerals the directional properties of the chemical bonds between the metallic and sulfur atoms play an important role. These different aspects are directly related to the nature of the chemical bonds holding the different types of the crystals together.

In sulfosalt minerals, however, the nature of the chemical bonds is an intricate one. The physical properties of the minerals indicate a partial metallic character of the chemical bonds in the sulfosalt crystals. Presumably related to this kind of nature, the characteristic covalency in many sulfide minerals is modified in the sulfosalts. Beside the directional bonds characteristics of each metallic or submetallic atom, in sulfosalt crystals, these atoms tend to have larger coordination numbers for sulfur atoms. This fact applies especially to the atom Pb, and to the V-b elements As, Sb, and Bi.

It has been found that, in many of the sulfosalt structures, the spatial arrangements of sulfur atoms are determined by the kind of central metallic atom. These sulfur atoms can be considered as located at the vertices of a polyhedron characteristics of the central atom. The crystal structure can be regarded as the stacking of these coordination polyhedra, each polyhedron sharing its vertices, edges, or faces with neighboring ones.

In Part III of the thesis, the above-mentioned viewpoint will be taken as the structural base of the crystal chemistry of sulfosalt minerals. The relations between the possible types of polyhedral stacking and the unique shortest dimensions of unit cells are discussed. The chemical parameter,  $f = (Ag + Cu + Pb + As + Sb + Bi)/S$  is introduced, and the relation between this value and the structural types is developed. Finally a classification based on these principles is tentatively presented.

In Part IV, a supplementary section, matters related to the problem treated in the main text are discussed. They are: (1) a historical introduction to the crystal structure analysis of the sulfosalt minerals, (2) a note on the process of structure determination when the effect of x-ray absorption by crystals is not negligible, and (3) the proofs of the geometrical theorems used in the Part III.

## PART I

The crystal structure of livingstonite,  $\text{HgSb}_4\text{S}_8$

## Introduction

There have been two crystallographic investigations of the mineral livingstonite. Richmond<sup>1</sup> described it as monoclinic, and Gorman's presentation<sup>2</sup> was triclinic. Buerger and Niizeki<sup>3</sup> carried out a preliminary structure determination of the mineral assuming Gorman's triclinic cell was correct. They succeeded in obtaining the structure projected along the shortest axis ( $4\text{\AA}$ ). Our result suggested doubt concerning the number of sulfur atoms in the chemical formula.

Livingstonite crystallizes in an elongated needle form with one perfect prismatic cleavage. The mineral belongs to the group of acicular sulfosalts. Structure determinations for several minerals of this group have recently been published<sup>4,5,6,7,8</sup>. Livingstonite is the only known sulfosalt mineral containing mercury.

## Preliminary structure investigation

For the preliminary phase of the structure investigation we are greatly indebted to Dr. Gorman of the University of Toronto, Canada. We were kindly offered not only a massive aggregate of the cleavage flakes of livingstonite from Guerrero, Mexico, but also his original single crystal used for the above-mentioned description of his triclinic

unit cell.

The first intensity data were collected from the equator Weissenberg photograph taken with  $\text{CuK}\alpha$  radiation. The intensities were measured by the M.I.T. modification of the Dawton method<sup>9</sup>. The intensities were then corrected for Lorentz and polarization factors, but no allowance was made for absorption. The resulting  $F^2(h0l)$ 's were used to prepare the Patterson map,  $P(xz)$ , Fig. 1.

Since Gorman's unit cell contained  $\text{HgSb}_4\text{S}_7$ , there is only one Hg atom in the cell. Its position is fixed at the center of symmetry if the space group is  $\bar{P}1$ . A statistical check of the centrosymmetry<sup>10</sup> was applied to the observed intensity data, and the resulting curve is shown in Fig. 2. Although the chemical composition of the mineral is not ideal for the statistical treatment, the result was considered as indicating a center of symmetry in the projection.

Once the position of the mercury atom was fixed, the interpretation of the Patterson map, Fig. 1, was straightforward. The two heavy peaks, indicated by crosses in Fig. 1, must be due to Hg-Sb interactions. Since Hg is at the origin, these peaks could be assumed as the atomic sites for the two Sb atoms in the asymmetric unit. The first Fourier map of the projection, Fig. 3, was computed using signs determined by heavy atoms only, provided the contribution to the amplitude by them exceeded one third of the observed values. From this map information concer-

Fig. 1 Patterson diagram  $\underline{P}(\underline{xz})$ . The dotted contours represent depressions. The details of the heavy peak at the origin are omitted.

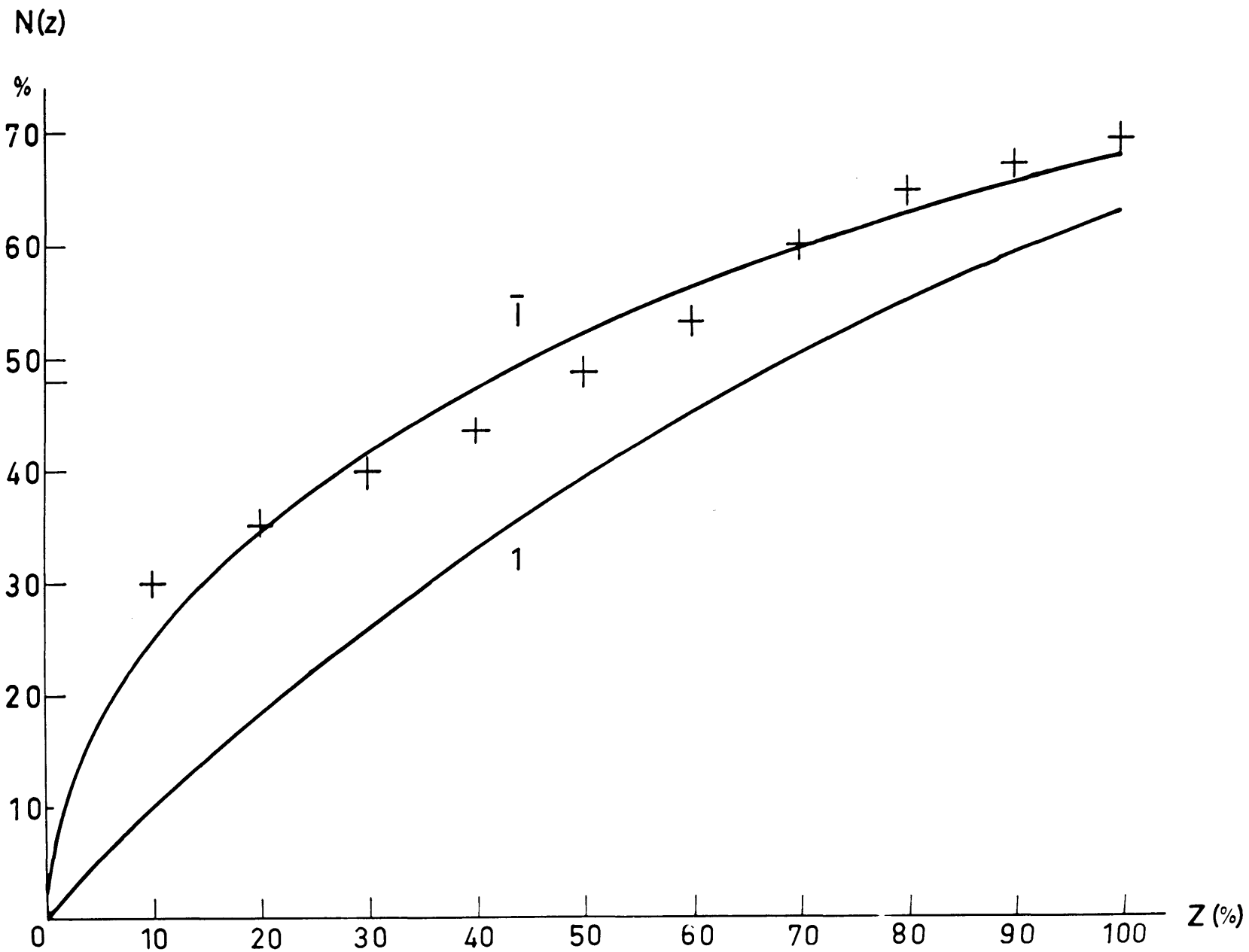
$$c' = \frac{c}{2}$$



0

$$a' = \frac{a}{4}$$

Fig. 2 Statistical test of the centrosymmetry.  
The theoretical curve for the centrosymmetric crystal is designated by  $\bar{1}$ , and for the non-centrosymmetric crystal by 1. The crosses represent the result with  $\underline{F}^2(\underline{h0l})$ 's of livingstonite.





ning the locations of the S atoms could be obtained. The structure was refined by four successive Fourier trials. With an assumed chemical formula of  $\text{HgSb}_4\text{S}_7$ , one of the S atoms must be placed on one set of centers of symmetry. From these Fourier trials, however, the following facts became evident. First, there are two peaks surrounding the center of symmetry at  $(\frac{1}{2}0\frac{1}{2})$  with peak heights as high as the other three kinds of S atoms. Second, there is no indication of an atom on the center of symmetry, and the sign changes caused by placing one S atom on this inversion center did not bring back the assumed atom onto the center in the resulting Fourier map. The atomic coordinates of the fourth trial are tabulated in Column I of Table 1.

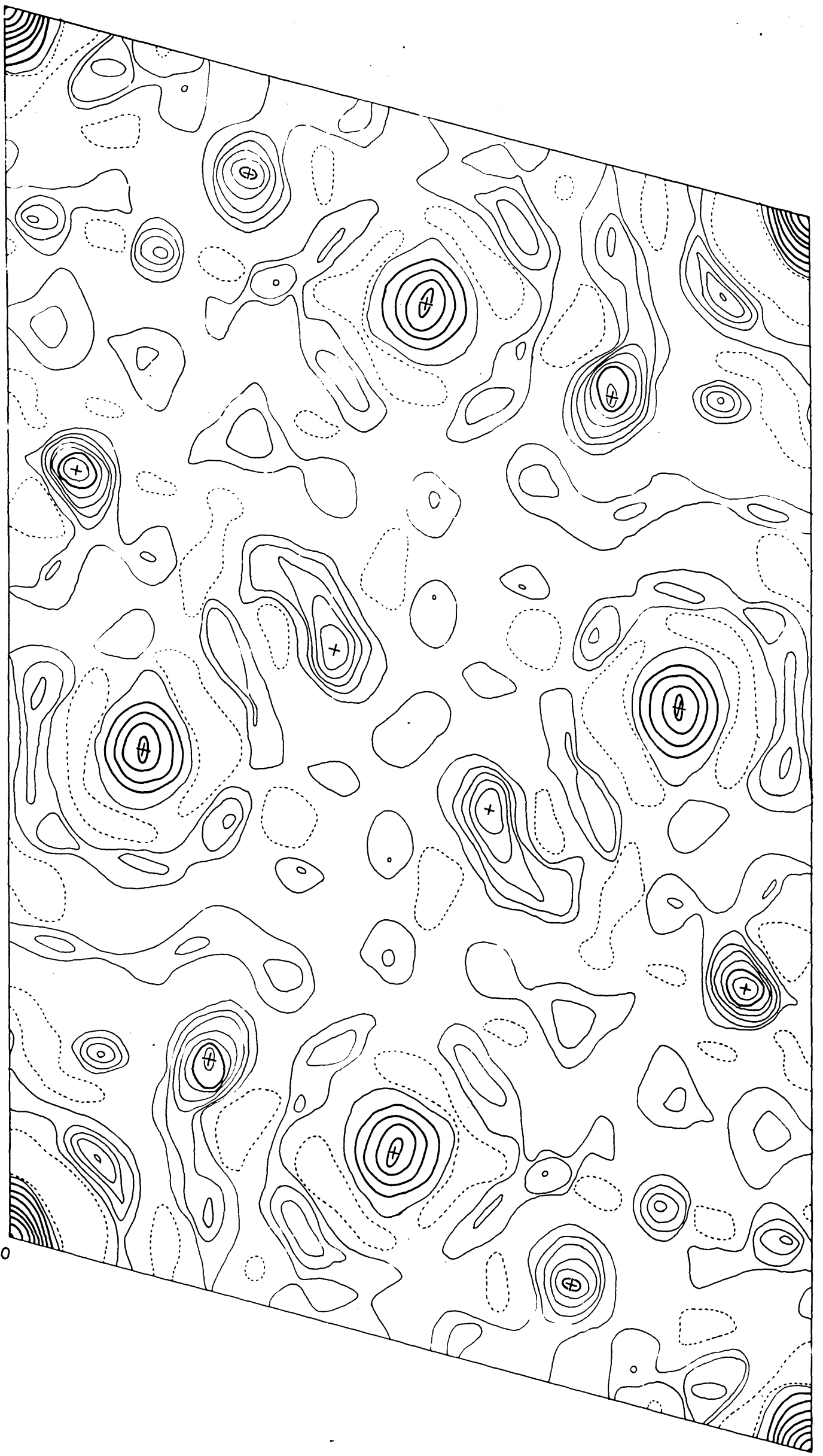
If the peak at  $\underline{x} = .598$ ,  $\underline{z} = .444$  did actually represent the fourth S atom in the asymmetric unit, the chemical formula of livingstonite should be  $\text{HgSb}_4\text{S}_8$  instead of  $\text{HgSb}_4\text{S}_7$ .

#### Chemical composition of livingstonite

In the face of this anomaly of composition, it was keenly felt that new data for the chemical composition of the mineral, as well as the more exact x-ray diffraction data, were essential to solve the problem. A specimen from Huitzco, Mexico, was kindly offered for this purpose by Dr. Foshag of the National Museum, Washington, D.C. This specimen (U.S. National Museum No. 105163) was a

Fig. 3 The first electron-density map  $\rho(\underline{xz})$ .  
The broken lines represent depressions. One interval  
between heavy contours corresponds to five intervals  
of light contours. The details between successive heavy  
contours are omitted. The crosses indicate the atomic  
sites listed in Column I of Table 1.

2/6



0

5/10

Table 1. Coordinates of atoms referred to projected cell with  $a' = \frac{a}{4}$ , and  $c' = \frac{c}{2}$ .

Atom		I	II
		Dawton data	Geiger-counter data
Hg	$x'$	.000	.000
	$z'$	.000	.000
Sb <sub>I</sub>	$x'$	.479	.482
	$z'$	.150	.153
Sb <sub>II</sub>	$x'$	.170	.170
	$z'$	.429	.423
S <sub>I</sub>	$x'$	.243	.237
	$z'$	.160	.185
S <sub>II</sub>	$x'$	.915	.910
	$z'$	.364	.363
S <sub>III</sub>	$x'$	.693	.685
	$z'$	.085	.081
S <sub>IV</sub>	$x'$	.598	.597
	$z'$	.444	.443

beautiful crystal of selenite with numerous inclusions of fine needles of livingstonite.

First the selenite crystal was carefully cleaved to separate the livingstonite needles. After repeated washings in a warm dilute solution of hydrochloric acid, the remaining grains of selenite were separated by the heavy liquid method. Finally the sample was placed under the binocular for the manual separation of the mineral. The material collected was then chemically and spectrographically analyzed. The result of this analysis is tabulated in Table 2.

The interpretation of the chemical data was carried out under the following two assumptions. First, Si and Al detected by the spectrograph were due to minor impurities of some kind of unidentified silicate minerals which escaped separation. Later it was observed that some livingstonite needles were aggregated around impurity grains as cores. Second, As substitutes for Sb, and Pb and Fe could occupy Hg sites.

The weight percentages of Si and Al were subtracted from the total amount. The amount subtracted was half of the value of the maximum estimated by the spectrographical method. The values determined in this way, 1.1% for Si, and 0.6% for Al, summed to 1.7%, which was very close to the deficiency of the total weight percentage of the major elements from 100%. The elements Hg, Pb, and Fe were grouped

Table 2. Analysis of livingstonite

Element	Weight percent	
Hg	19.49%	
Sb	50.46	
S	27.61	
As	0.29	
Fe	0.22	
Pb	0.24	
Si	0.1 - 1.0%	estimated
Al	0.1 - 1.0	"
Ca	500 - 3000 ppm	"
Cu	200 - 1000	"
Mg	100 - 500	"
Bi	100 - 500	"
Mn	50 - 300	"
Ag	5 - 25	"
Na	5 - 25	"
Tl	2 - 10	"

together in one group, and Sb and As into another group, as shown in Column II of Table 3. All the other minor elements were neglected. Then these three values for (Hg,Pb,Fe), (Sb,As) and S were converted into the values listed in Table 3 to make up the total to 100%.

In Column III and IV of Table 3, the ideal weight percentages of the composition  $\text{HgSb}_4\text{S}_7$  and  $\text{HgSb}_4\text{S}_8$  are tabulated. Comparison of the result in the Column II with these two kinds of ideal composition indicated definitely the composition of  $\text{HgSb}_4\text{S}_8$  as that of livingstonite. The value of density, 5.00, measured by Frondel<sup>11</sup> was found to agree well with 5.06, the calculated density of  $\text{HgSb}_4\text{S}_8$ .

#### Unit cell dimensions and space group

Several good single crystals were selected for the x-ray investigation from the livingstonite needles used for the chemical analysis. Weissenberg, precession, and de Jong photographs were taken for the equator and up to the 4th layer, with the crystal set so that the needle axis was parallel to the goniometer axis. The crystals used for the preliminary stage were re-examined by the same methods, and were identified as the same material as the needles.

The crystal was monoclinic, and the unit cell dimensions obtained were as follows:

Table 3. Interpretation of chemical data

Element	I Original Analysis	II Normalized to 100%	III HgSb <sub>4</sub> S <sub>7</sub>	IV HgSb <sub>4</sub> S <sub>8</sub>
Hg	19.49 %			
Pb	0.24	19.95 %	20.29 %	21.99 %
Fe	0.22			
Sb	50.46			
As	0.29	50.75	51.63	53.40
S	27.61		28.08	24.61
Total	98.31		100.00	100.00
Density measured	5.00 (Fronde <sup>11</sup> )			
Density computed			4.88	5.06



$$a = 30.25\text{\AA}$$

$$b = 4.00\text{\AA} \quad \beta = 104^\circ 12'$$

$$c = 21.48\text{\AA}$$

This unit cell contains  $8\text{HgSb}_4\text{S}_8$ .

The following systematic absences were observed for the recorded spectra:

$$\underline{hkl} \text{ with } \underline{k} + \underline{l} = \text{even only,}$$

$$\underline{h0l} \text{ with } \underline{l} = \text{even, and } \underline{h} = 4n \text{ (} n = 0, 1, 2, 3, \dots \text{) only,}$$

$$0\underline{k}0 \text{ with } \underline{k} = \text{even only.}$$

From these rules the space group is  $\underline{A2/a}$  if it is centrosymmetric, and  $\underline{Aa}$  if non-centrosymmetric. The observed systematic absences for the type reflections  $\underline{h0l}$  are rather unusual. For the two possible space groups the required systematic absences for this type reflections are  $\underline{h} = \text{odd}$ , and  $\underline{l} = \text{odd}$ . Therefore, the extra systematic absences with  $\underline{h} = 4n + 2$ , and  $\underline{l} = \text{odd}$  are to be interretated as due to the structural arrangement. Satisfactory twinning rules to explain the above-mentioned facts could not be obtained. The centrosymmetrical space group  $\underline{A2/a}$  was assumed for the starting point.

#### Relations between unit cell data

Because of the extinction already described, a submultiple cell with  $\underline{a}' = \underline{a}/4$ , and  $\underline{c}' = \underline{c}/2$  could be taken for the projection on (010). These dimensions are as follows:

$$a' = 7.56\text{\AA}$$

$$b' = 10.74\text{\AA} \quad \beta = 104^\circ 12'$$

These values were identical with those obtained at the stage of checking Gorman's result from the equator Weissenberg photograph. There must be some relations between the present unit cell and the ones previously described by Richmond and Gorman. The relations between these unit cells are tabulated in Table 4.

Our cell and Richmond's are almost identical except that the former's  $\underline{a}$  unit is double the  $\underline{a}$  unit of the latter. Gorman's triclinic cell can be explained as the triclinic setting of our  $\underline{A}$ -centered monoclinic cell if taken with the sub-multiple units,  $\underline{a}' = \underline{a}/4$ , and  $\underline{c}' = \underline{c}/2$ . The three shortest vectors of this setting of our cell are represented by vectors  $\underline{A}$ ,  $\underline{B}$ , and  $\underline{C}$  in Table 4. The vectorial expression of these three new axes is also found in Table 4. The good agreement between this cell and Gorman's cell supports the relation discussed above.

Space group  $\underline{A}2/\underline{a}$  is illustrated in Fig. 4 by two projections along  $\underline{b}$  and  $\underline{c}$  axes. The sub-multiple unit cell in the projection on (010) is indicated by a heavy outline in the drawing. The statistical test with  $\underline{F}^2(\underline{h}0\underline{l})$ 's, which was considered to indicate the existence of the center of symmetry in the projection, must now be interpreted as the proof of the pseudo center of symmetry at  $(\frac{1}{8}, 0, \frac{1}{4})$ , which is indicated by a cross in Fig. 4.

#### Three-dimensional intensity determination

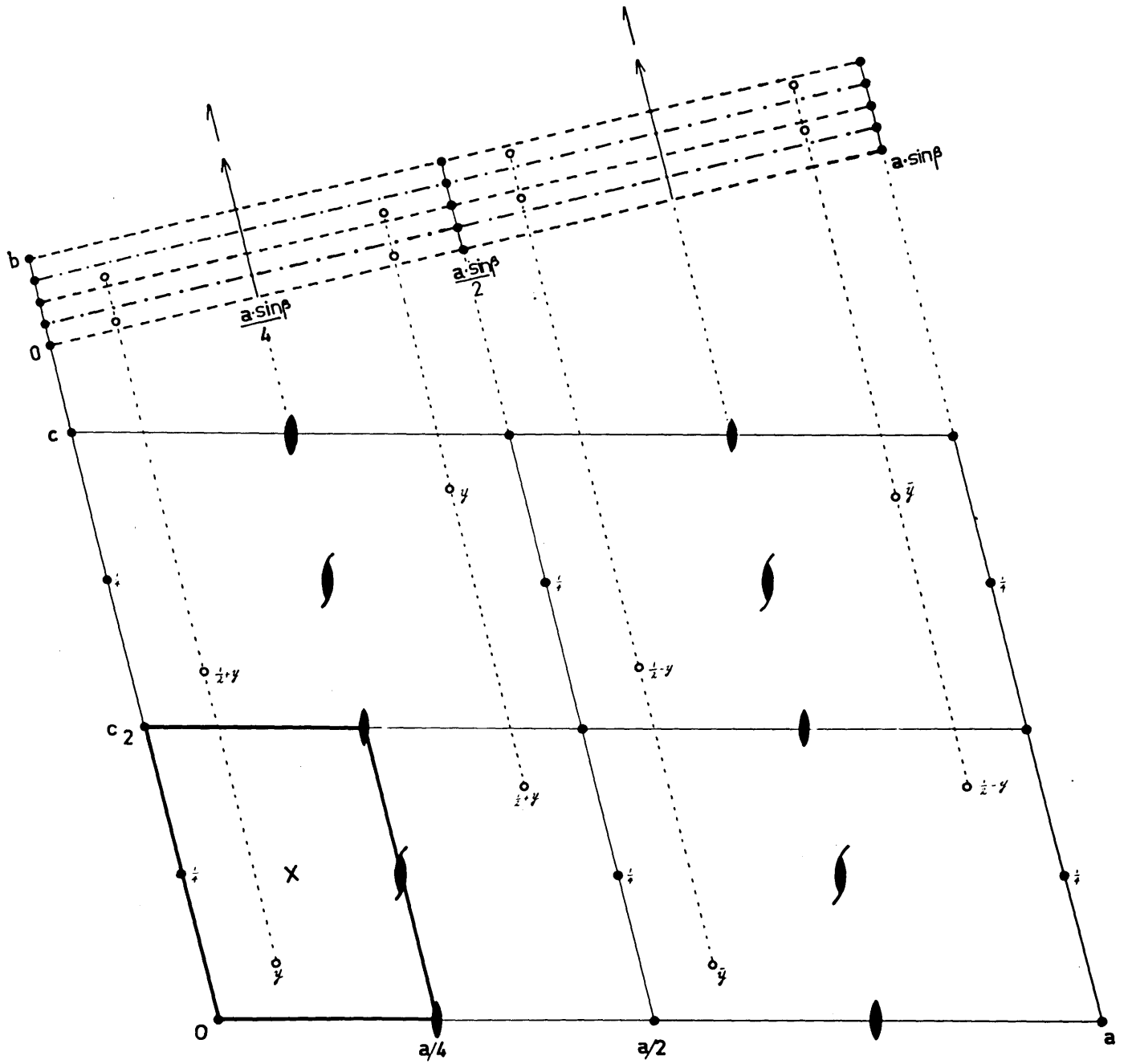
Three-dimensional intensities were collected by the

Table 4. Comparison of cell data for livingstonite

Richmond	Gorman (original <u>KX</u> units converted to Å units)	Niizeki and Buerger	Niizeki and Buerger's cell referred to $A = \frac{1}{4}a - \frac{1}{2}b$ $B = \frac{1}{2}b - \frac{1}{2}c$ $C = b$
15.14 Å		30.25 Å	
$a = 7.57 \times 2$	$= 7.67 \text{ Å}$	$= 7.64 \times 4$	$7.62 \text{ Å}$
b 3.98	4.00	4.00	4.00
21.60		21.49	
$c = 10.80 \times 2$	10.84	$= 10.75 \times 2$	10.93
$\alpha$ _____	99°12'	_____	100°31'
$\beta$ 104°00'	102°01'	104°12'	104°49'
$\gamma$ _____	73°48'	_____	73°46'
cell contents			
4 HgSb <sub>4</sub> S <sub>7</sub>	HgSb <sub>4</sub> S <sub>7</sub>	8 HgSb <sub>4</sub> S <sub>8</sub>	HgSb <sub>4</sub> S <sub>8</sub>

Fig. 4 Representations of space group  $\underline{A2/a}$ . The lower drawing shows the symmetry elements and the general equipoints  $8(\underline{f})$  in the projection on  $(010)$ . The heavy outline in this drawing indicates the sub-multiple unit cell of the projection. A cross inside this unit shows the location of the pseudo center of symmetry.

The upper drawing represents the projection on the plane normal to  $\underline{c}$  axis.



single-crystal Geiger-counter-goniometer method developed in the Crystallographic Laboratory of M.I.T. The  $h0l$  intensities were first measured with  $MoK\alpha$  radiation. But the large size of the true unit-cell dimensions made the successive reciprocal lattice-points in the upper levels too close to be resolved by this radiation. Thus  $CuK\alpha$  radiation was necessary to collect the  $hkl$  intensities, although this longer wavelength resulted in an increase in the linear absorption coefficient of the crystal. These intensities were corrected for Lorentz and polarization factors, but no allowance was made for absorption factor until the last stage of analysis.

#### Refinement of the projected structure

With the new set of  $F^2(h0l)$ 's collected with  $MoK$  radiation, the refinement of the electron density map was carried out. The statistical treatment by Wilson's<sup>12</sup> method applied to the  $F^2$  values, shown in Fig. 5, determined the scaling factor and temperature coefficient. With the final atomic coordinates determined in the preliminary stage, and these new  $F^2$  values, the refinement of the projection was done by the successive Fourier and difference-Fourier trials. The final atomic coordinates are tabulated in Column II of Table 1. The temperature coefficient determined from Fig. 5 was  $B = 1.32$ . The reliability factor with the final atomic coordinates was computed as  $R = .133$ . The final electron-density map  $\rho(xz)$

is presented in Fig. 6. In this map it is clearly shown that the structure determination confirms the new chemical composition of livingstonite,  $\text{HgSb}_4\text{S}_8$ .

#### Determination of $y$ coordinates

Introduction. The comparison between the projection of the structure, Fig. 6, and the structures of other acicular sulfosalts previously analyzed permitted understanding the general scheme of the structure without difficulty. All the atoms were found to be located very close to the  $a$  glide-planes at  $y = 0$ , or  $\frac{1}{2}$ . The deviations of the  $y$  coordinates from these values were considered too small to be detected by crystal-chemical considerations. Also the other two available projections along the longer axes were expected to give results with considerable overlappings of atoms. More exact  $y$  coordinates of the heavy atoms were determined from the direct interpretation of the three-dimensional Patterson sections.

Three-dimensional Patterson sections. The three-dimensional Patterson sections were prepared with  $F^2(hkl)$ 's collected with  $\text{CuK}$  radiation. The Fourier summations of the type

$$P(\underline{x}, \frac{n}{60}, \underline{z}) = \sum_h \sum_k \sum_l |F(hkl)|^2 \cos 2\pi (hx + k \frac{n}{60} + lz)$$

were computed for the values of  $n = 0, 2, 4, \dots$  and up to 14. The resulting maps representing eight sections are shown in Fig. 10

The space group of the crystal is  $A2/a$ . The space

Fig. 5 Determination of scale factor and temperature coefficient of livingstonite by Wilson's statistical method. The observed  $F^2(h0l)$ 's collected with MoK radiation were used to obtain the result.



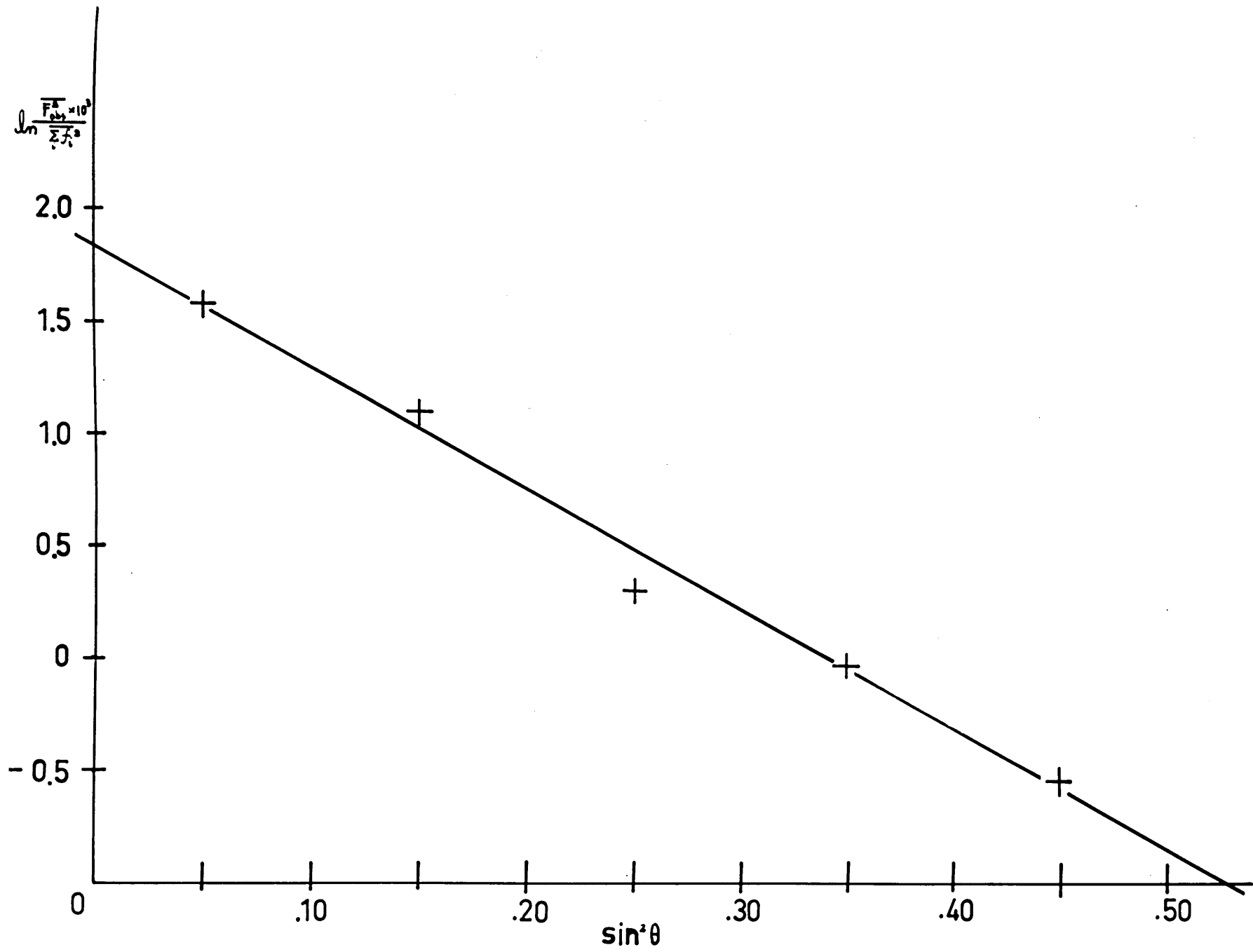
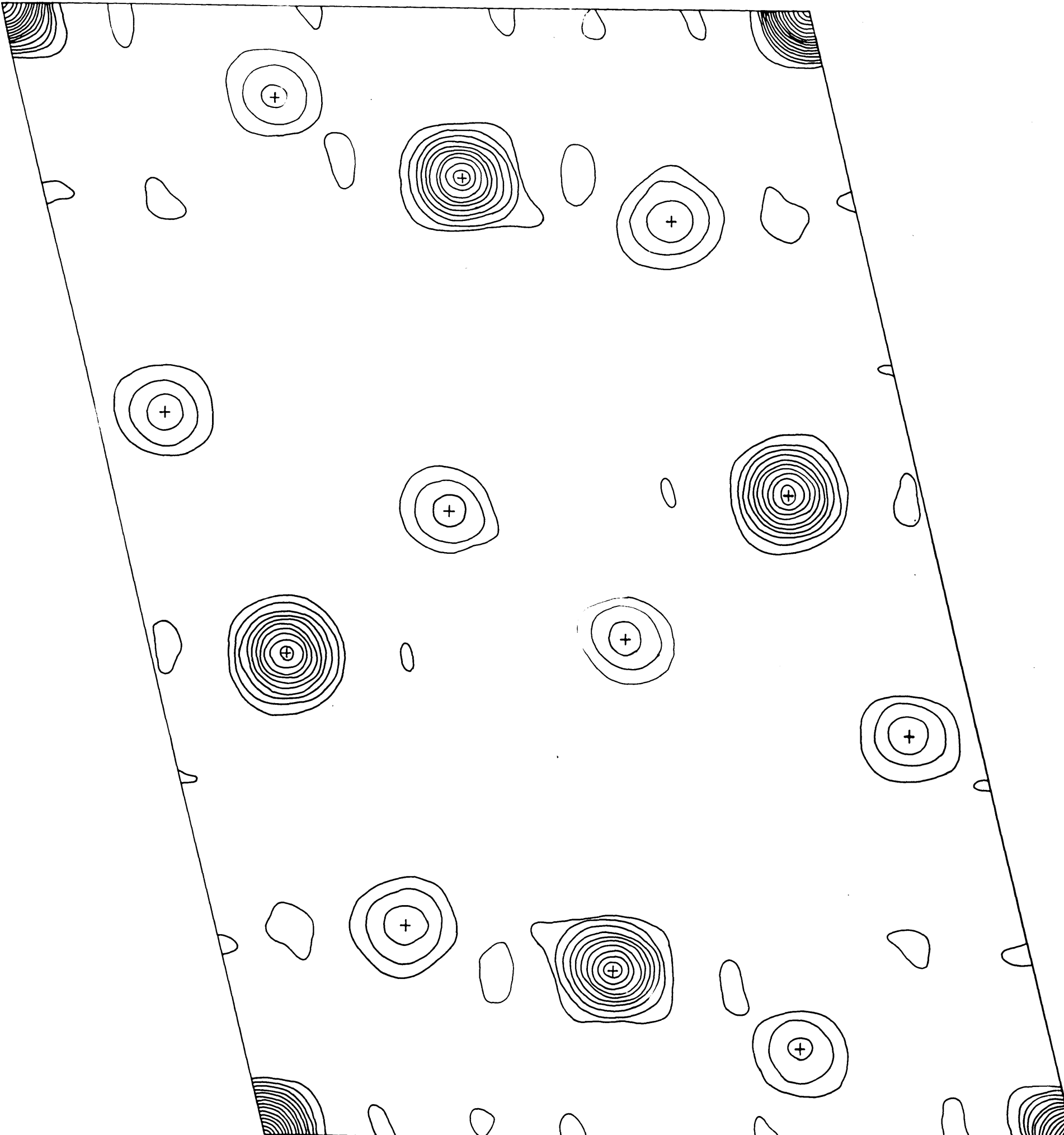


Fig. 6 Final electron-density map of the projection on (010). This  $\rho(\underline{xz})$  map represents the crystal structure in the sub-multiple unit cell outlined by heavy lines in Fig. 4. Negative contours are omitted.



of Patterson space corresponding to  $\underline{A2/a}$  is  $\underline{A2/m}$ . This space group  $\underline{A2/m}$  is illustrated in Fig. 7. Because of the  $\underline{A}$  centering, the section at  $y = \frac{1}{2}$  is identical with that at  $y = 0$  combined with the shift of origin by  $\underline{c}/2$ . The following relation exists among the various sections:

Section  $(30 + n)/60 =$  section  $n/60$  plus shift of origin by  $\underline{c}/2$ .

Also there are two mirror planes at  $y = 0$ , and  $\frac{1}{2}$ . Because of these mirror operations there are two further relations among sections:

Section  $n/60 =$  section  $(-n)/60$ , and

Section  $(30 + n)/60 =$  section  $(30 - n)/60$

The above considerations show that the sections between  $0/60$  and  $15/60$  are enough to represent the whole Patterson space. The other sections are related to these as indicated in the following table.

Section					
16/60	=	14/60	plus a shift of origin	by $\underline{c}/2$	
17/60	=	13/60	"	"	"
.					
29/60	=	1/60	"	"	"
30/60	=	0/60	"	"	"
31/60	=	1/60	"	"	"
.					
44/60	=	14/60	"	"	"
45/60	=	15/60	without shift		

Fig. 7 Two projections of space group  $A2/m$ . The lower drawing shows the symmetry elements and the general equipoints  $8(\underline{j})$  in the projection on (010). The upper drawing shows the projection on the plane normal to  $\underline{c}$  axis.

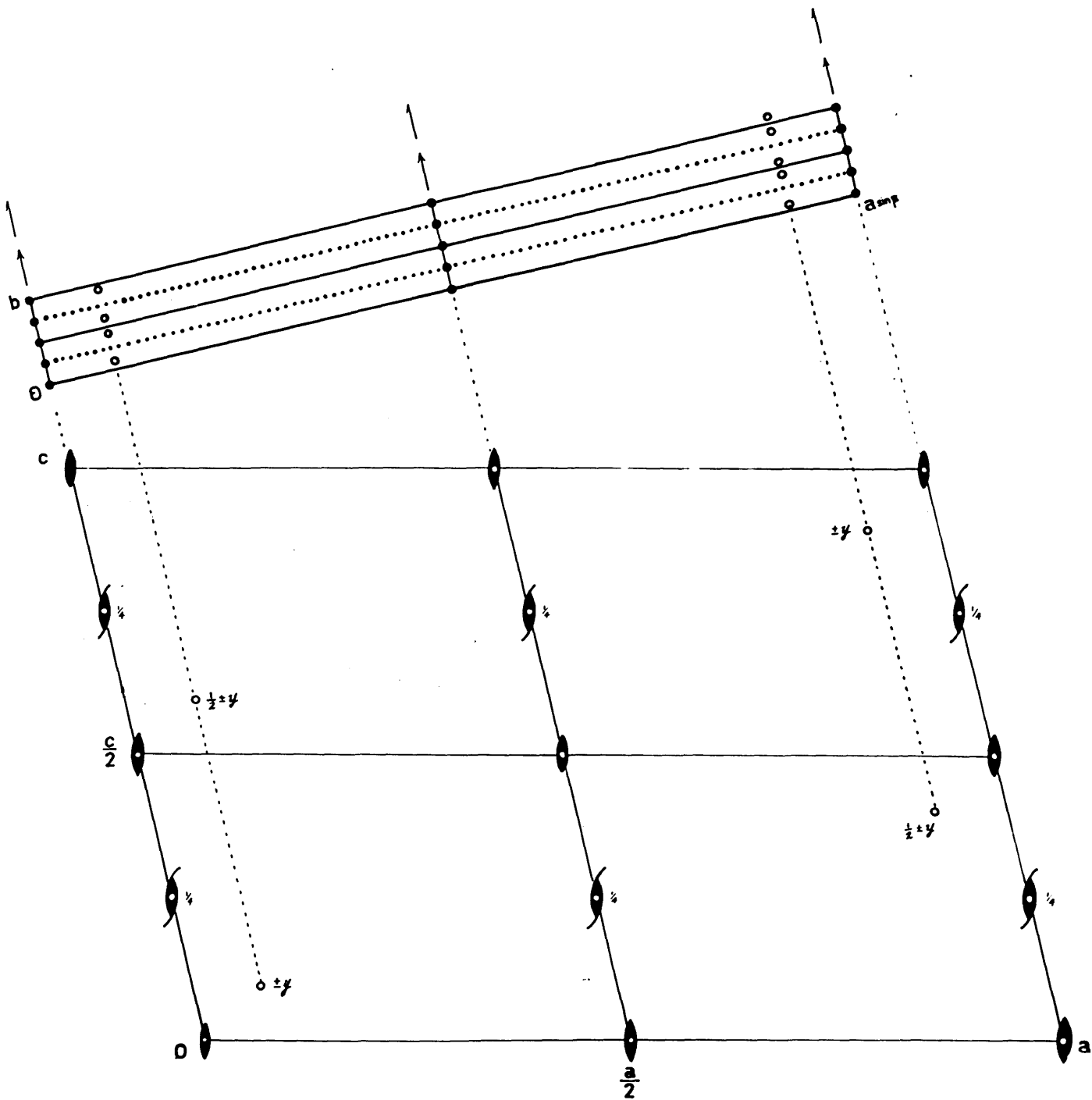
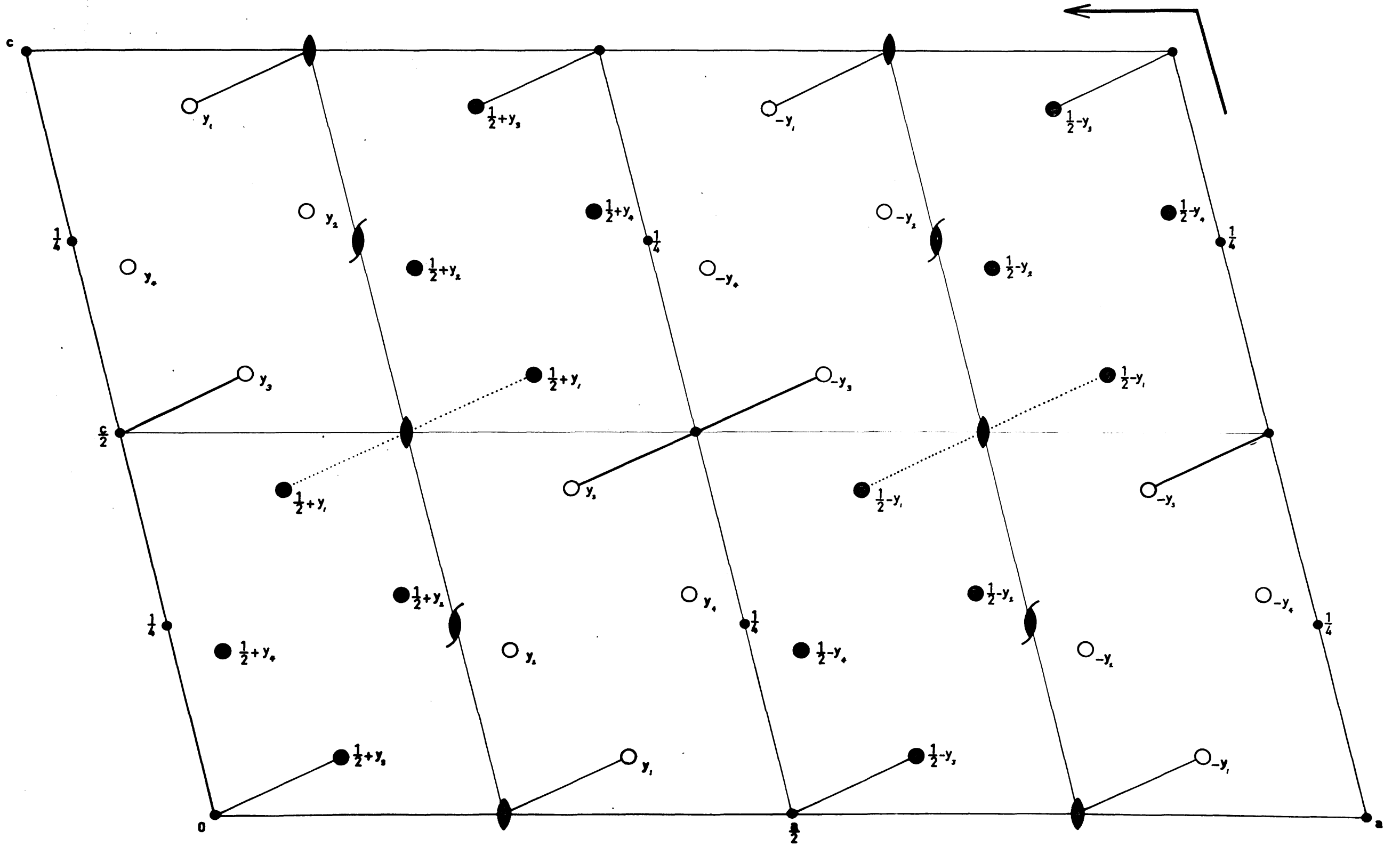


Fig. 8 Projection of the Sb atoms in the whole unit cell on (010). The open circles indicate  $y$  coordinates close to zero, and the shaded circles indicate  $y$  coordinates close to  $1/2$ .





Section			
46/60	=	14/60	without shift
47/60	=	13/60	" "
:			
:			
59/60	=	1/60	" "

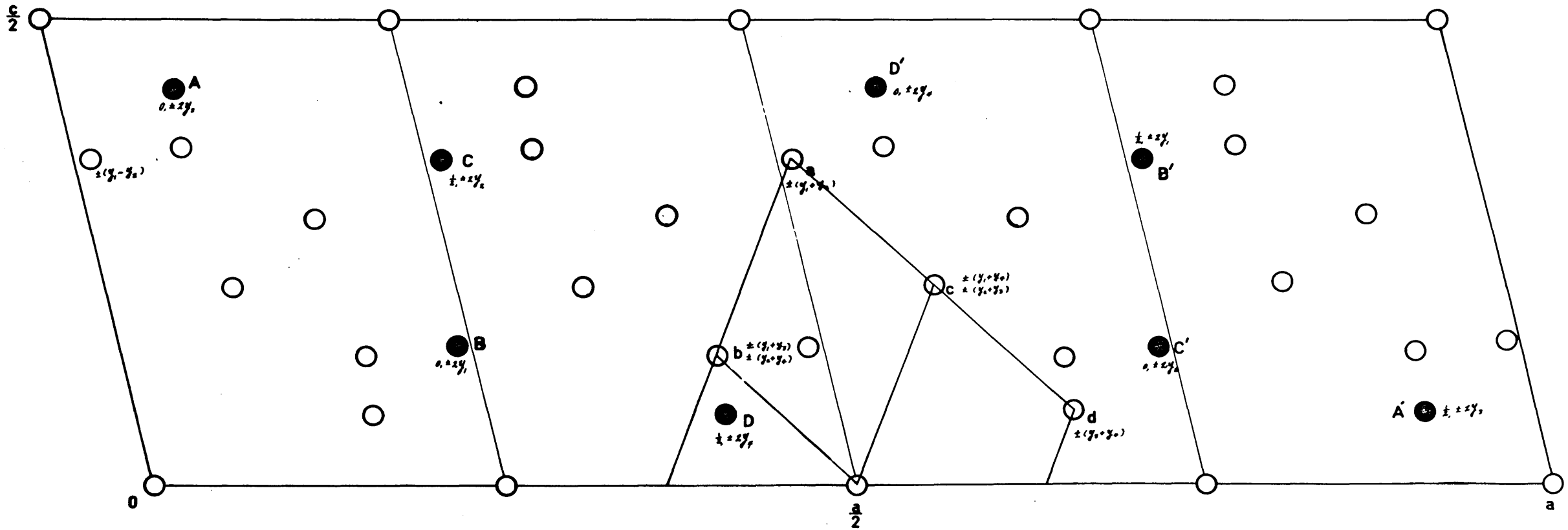
Interpretation of the three-dimensional Patterson peaks.

The unit cell contains  $8\text{HgSb}_4\text{S}_8$ . Equipoint considerations fix the locations of two kinds of Hg.  $\text{Hg}_I$  is placed at the center of symmetry  $4(\underline{b})$ .  $\text{Hg}_{II}$  is on the two fold axis  $4(\underline{e})$ . All the rest of the atoms occupy the general position  $8(\underline{f})$ . The  $\text{Hg}_I - \text{Hg}_{II}$  Patterson peaks were easily identified, and it was found that between  $y_{\text{Hg}_I}$  and  $y_{\text{Hg}_{II}}$  there was a difference of  $b/2$ . There are four different kinds of Sb atoms in the unit cell.

Two kinds of approach to determine the  $y$  coordinates of these Sb atoms were tried:

Interpretation of Hg-Sb peaks. The Hg -Sb peaks could easily be identified in the Patterson sections. Since one kind of Hg is located on a center of symmetry, the  $y$  coordinates of Sb atoms can be determined if the Hg -Sb peaks are clearly defined in the sections. Unfortunately the deviations of the  $y$  coordinates from zero or  $\frac{1}{2}$  are small, so that the maximum contour of the  $\text{Hg}_I - \text{Sb}$  peak should be located very close to section 0/60. As mentioned above there is a mirror operation at level 0/60. Thus the peak very close to section 0/60 overlaps its mirror equivalent. As the result, all the  $\text{Hg}_I - \text{Sb}$  peaks give

Fig. 9 The vector set constructed from the point set of Sb atoms, Fig. 8. The positions of Patterson peaks are indicated by circles. Shaded circles designated by letters A, B, C, and D indicate the inversion peaks. The open circles with letters a, b, c, and d are the peaks used for the determination of y coordinates of the Sb atoms. These peaks are connected by straight lines so that the identification of them in the Patterson sections (Fig. 10) becomes easy. Computed y coordinates of these peaks are also found in the diagram.



elongated peak-volume with their maximum contours in the section 0/60. Thus the more exact determination of  $y_{Sb}$ 's from this approach was impractical.

Interpretation of Sb - Sb peaks. In Fig. 8, the projected locations of Sb atoms are illustrated. Approximate  $y$  coordinates determined as 0 and  $\frac{1}{2}$  are indicated respectively by open and shaded circles. From this projection of the heavy atoms the vector set of Sb atoms can be constructed, and the result is shown in Fig. 9. There are two kinds of Sb-Sb peaks. One corresponds to the interatomic vector between an Sb and its symmetrical equivalents. They are, for example,  $Sb_I-Sb_I$  inversion peaks, rotation peaks generated by a 2-fold rotation axis or a 2-fold screw axis, and glide-related peaks. The rotation peaks were not useful in determining the  $y$  coordinates; that is, the coordinates along the rotation axis. Since the glide peaks have special values for  $x$  and  $z$ , considerable overlapping results and the decomposition of the glide peak into each component was impossible. Although the consideration of the inversion peaks is most appropriate in the usual case, the situation with livingstonite makes the interpretation of the inversion peak difficult. The reason is as follows: Because of the sub-multiple unit cell observed in the projection on (010), the inversion peak of an atom and the rotation peak of an atom, related to the former atom by the pseudo center

Fig. 10a Three-dimensional Patterson section  
at  $y = 0/60$ .

The heavy contours represent the fifth intervals of light contours. The details of some of the heavy peaks are omitted. All the negative contours are not shown. The maximum contours of peaks a, b, c, and d of Fig. 9 will be evident if the illustrated 4-gons are traced in the following sections.

Fig. 10b Three-dimensional Patterson section  
at  $y = 2/60$ .

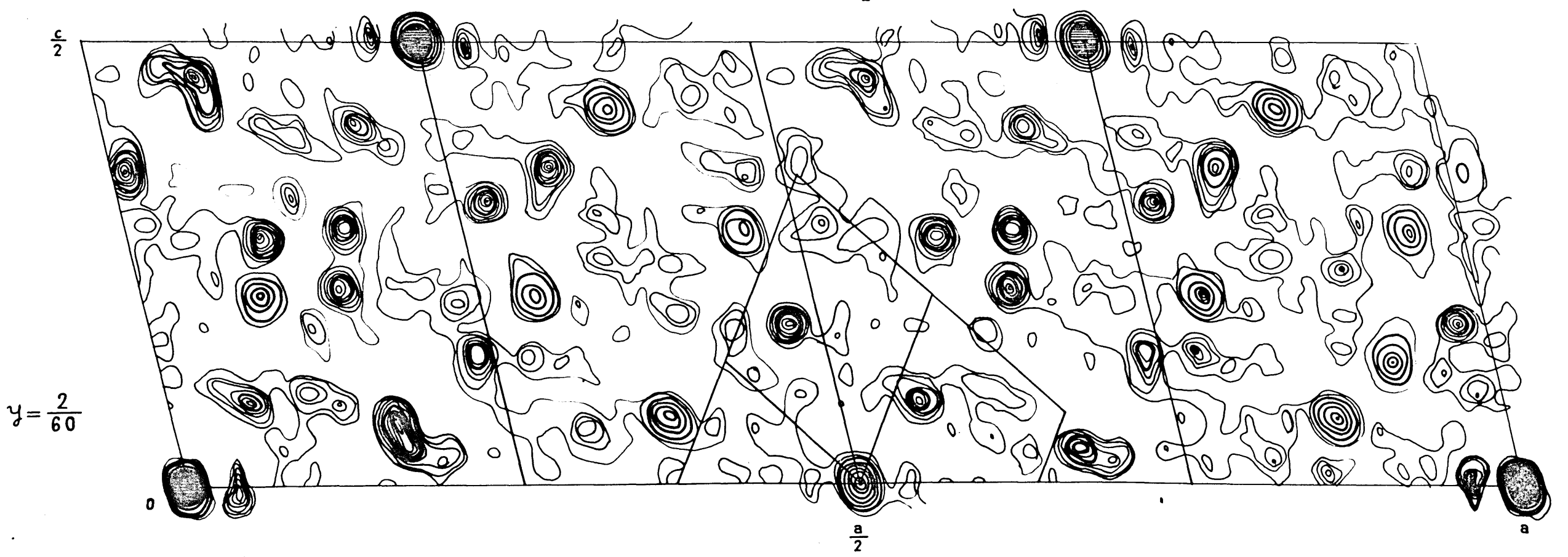
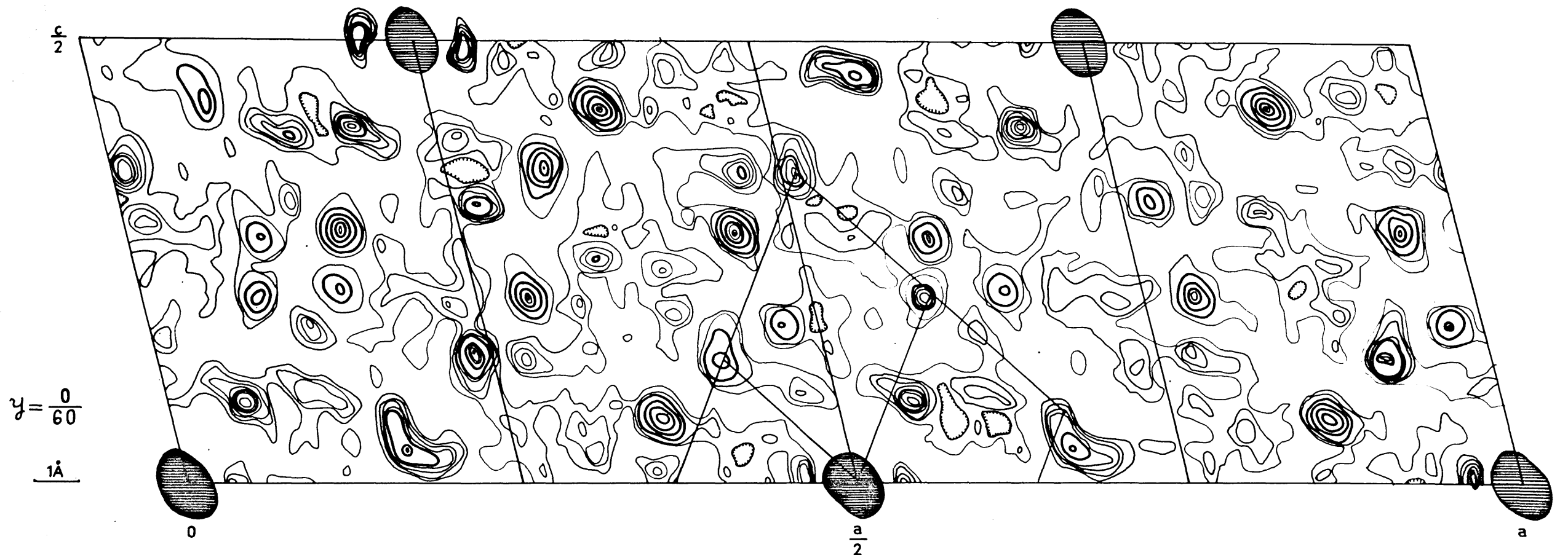


Fig. 10c Three-dimensional Patterson section  
at  $y = 4/60$ .

Fig. 10d Three-dimensional Patterson section  
at  $y = 6/60$ .

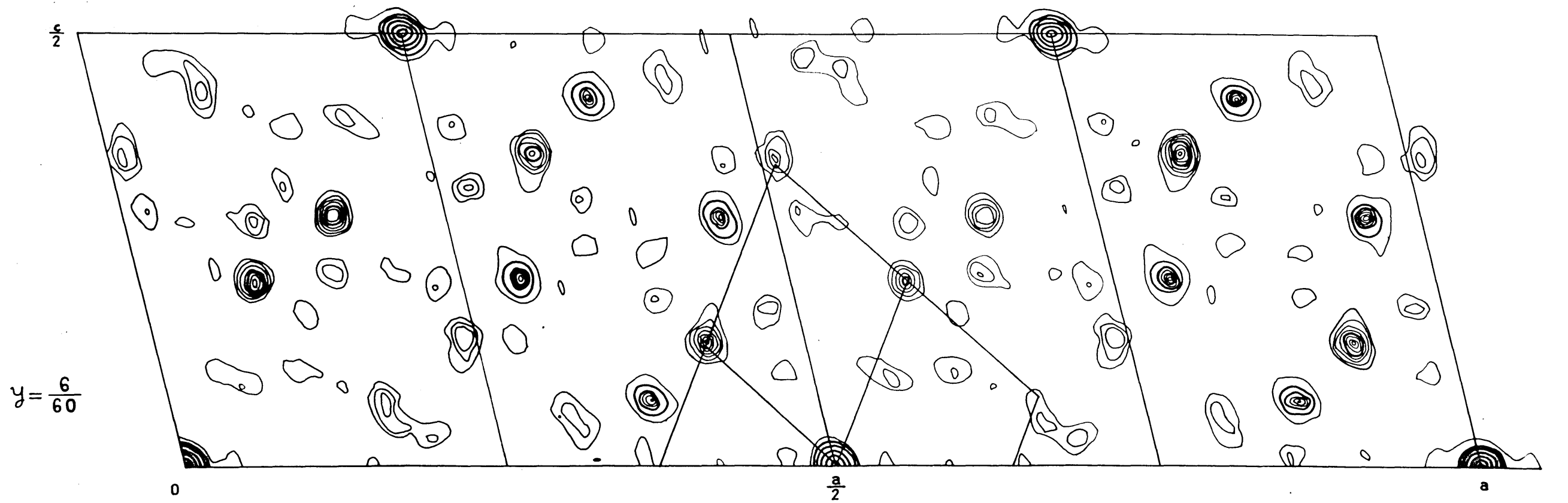
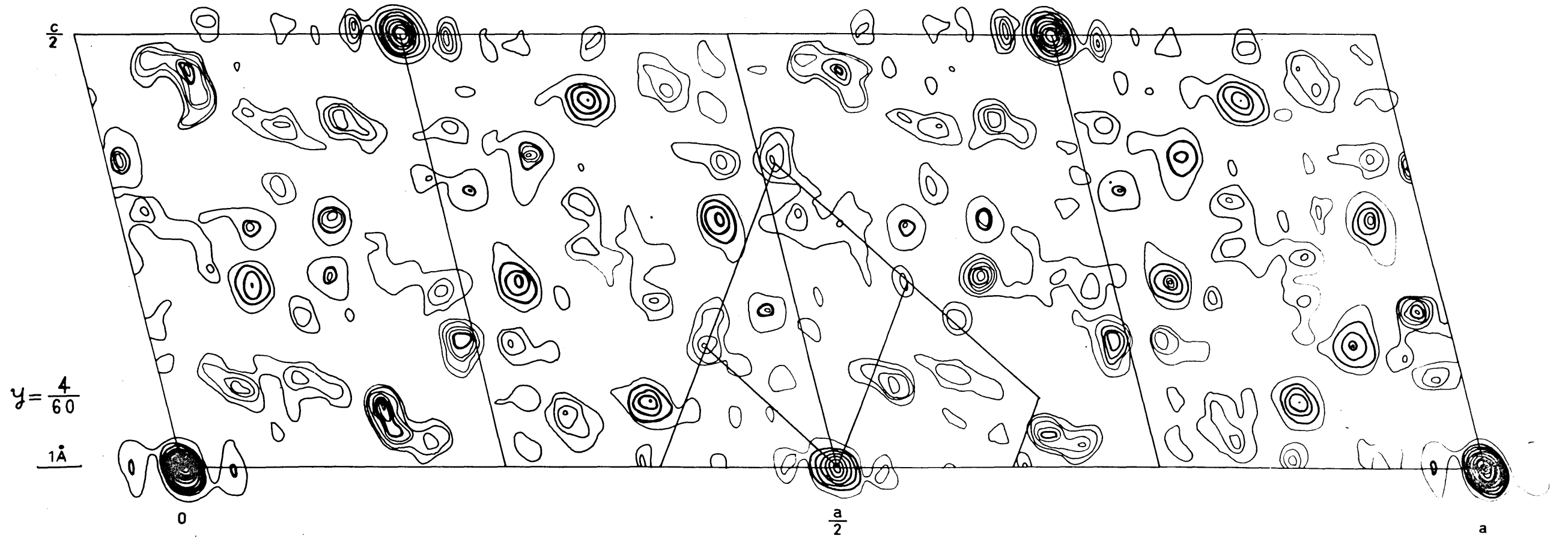




Fig. 10d Three-dimensional Patterson section  
at  $y = 8/60$ .

Fig. 10f Three-dimensional Patterson section  
at  $y = 10/60$ .

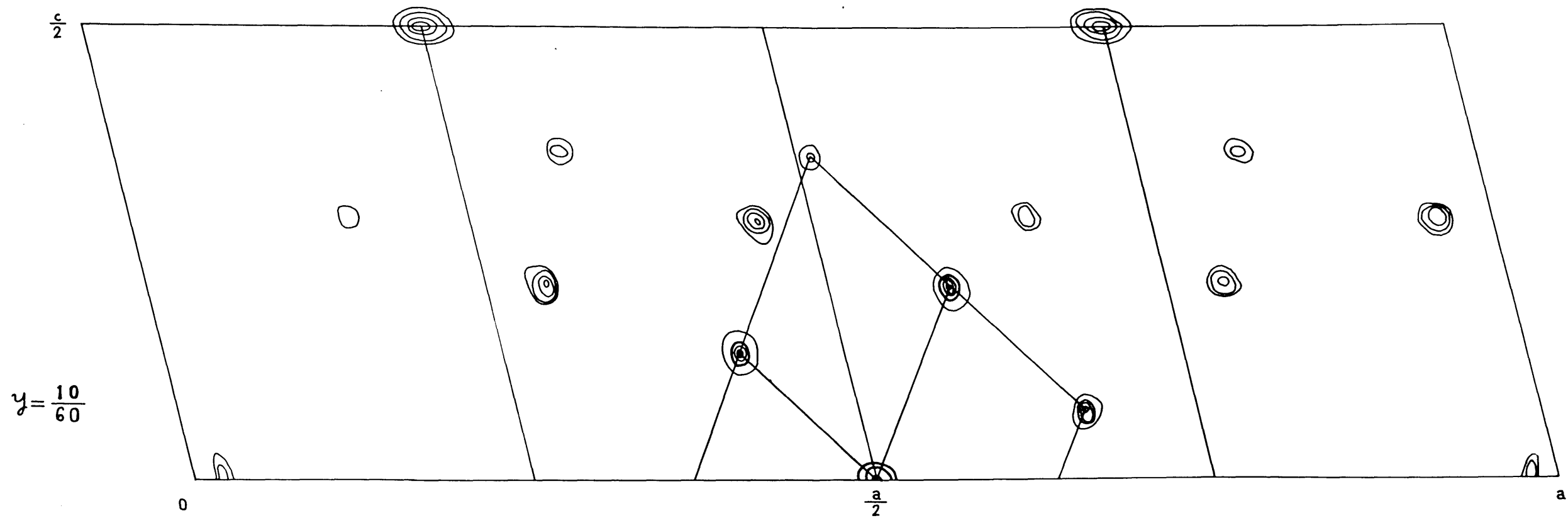
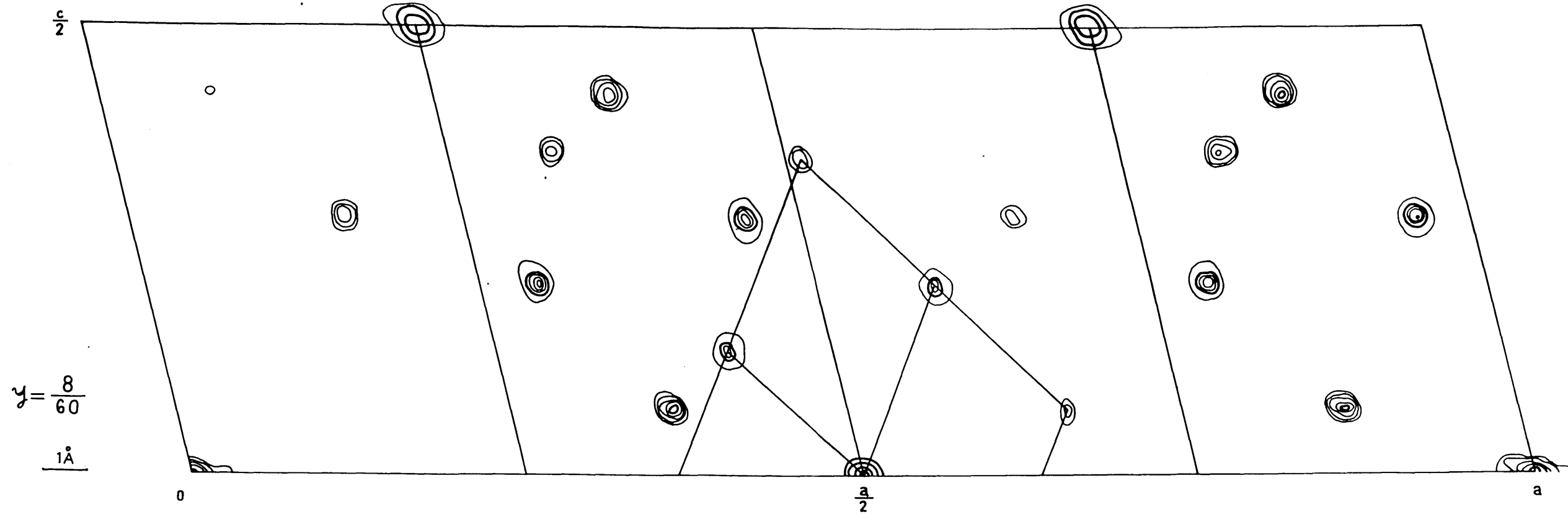
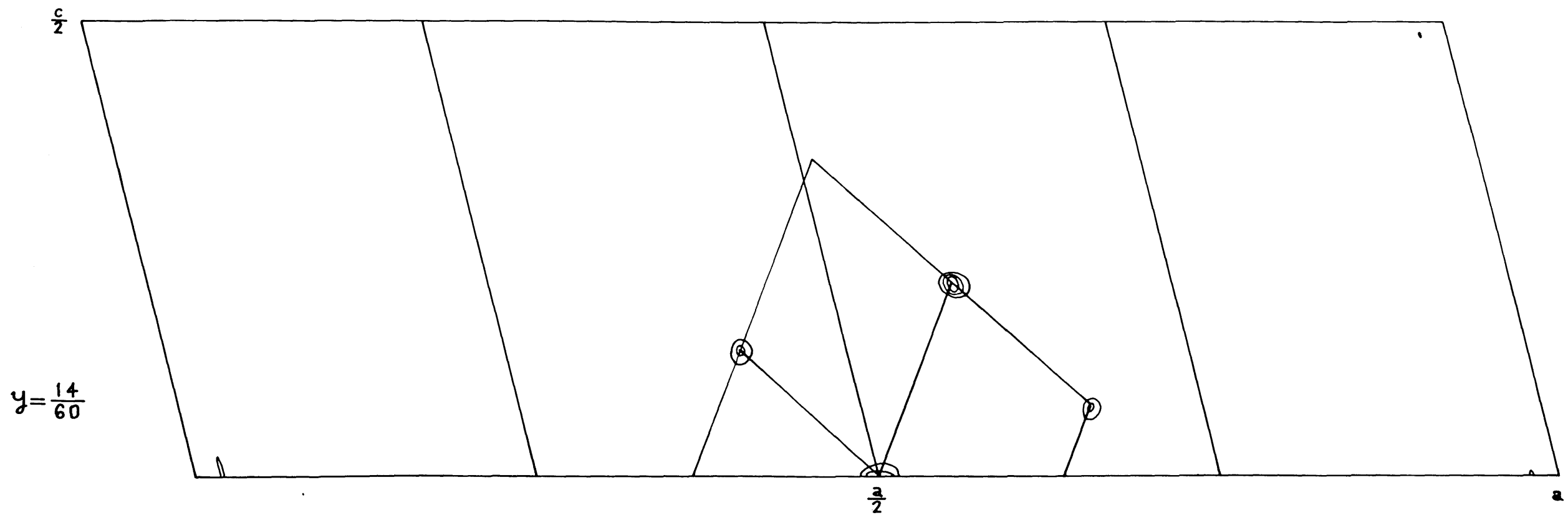
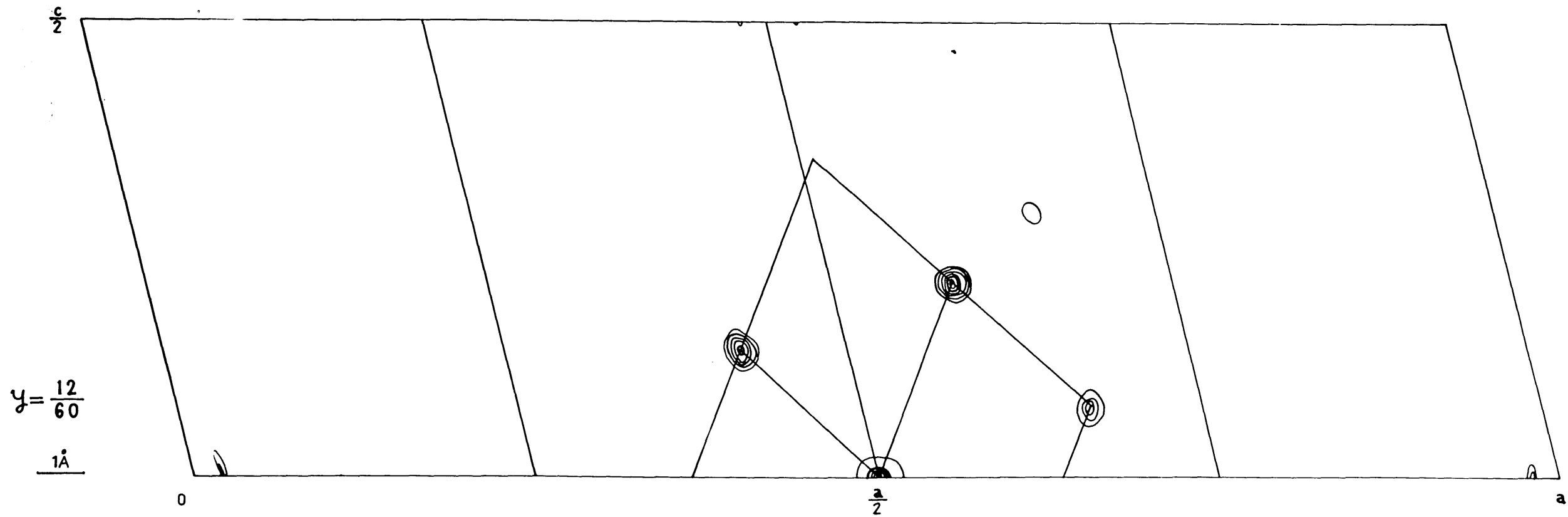


Fig. 10g Three-dimensional Patterson section  
at  $y = 12/60$ .

Fig. 10h Three-dimensional Patterson section  
at  $y = 14/60$ .



of symmetry, have identical  $x$  and  $z$  coordinates. For example, in Fig. 8, the  $Sb_{III}-Sb_{III}$  inversion vector is drawn with a heavy line, and the  $Sb_I-Sb_I$  rotation vector with a dotted line. These two vectors give their peak at the same location indicated by the letter B in Fig. 9. The  $y$  coordinates of the peaks are  $2y_3$  and zero. It also can be seen that the  $Sb_I-Sb_I$  inversion vector, and the  $Sb_{III}-Sb_{III}$  rotation vector indicated by light lines in Fig. 8, also give their peaks at the same location in the projection, with  $y$  coordinates of  $2y_1$  and zero. Thus if the  $y$  coordinates do not deviate much from zero, the overlapping with the rotation peak at section 0/60 obscures the definite maximum contours representing  $2y_1$  and  $2y_3$ .

The second kind of Sb-Sb peak represents the interatomic vectors between different kinds of Sb atoms, such as  $Sb_I-Sb_{II}$ 's. The examination of the three-dimensional Patterson space showed that there were four peaks with definite maximum contours at levels other than zero. The comparison with the vector set map, Fig. 9, indicated these peaks as all of the second kind. In Fig. 9 these peaks are designated by letters a, b, c, and d. The computed  $y$  coordinates of these peaks are given beside the circles indicating the locations of the peaks. The observed  $y$  coordinates of the maximum contour of these peaks are tabulated in Table 5. It is noticed that the

$y$  coordinates of these peaks have a sum form, such as  $Y_1 + Y_2$ . The approximate  $y$  coordinates were obtained by analysing these values. They are tabulated in Table. 5b.

#### Refinement of $y$ coordinates

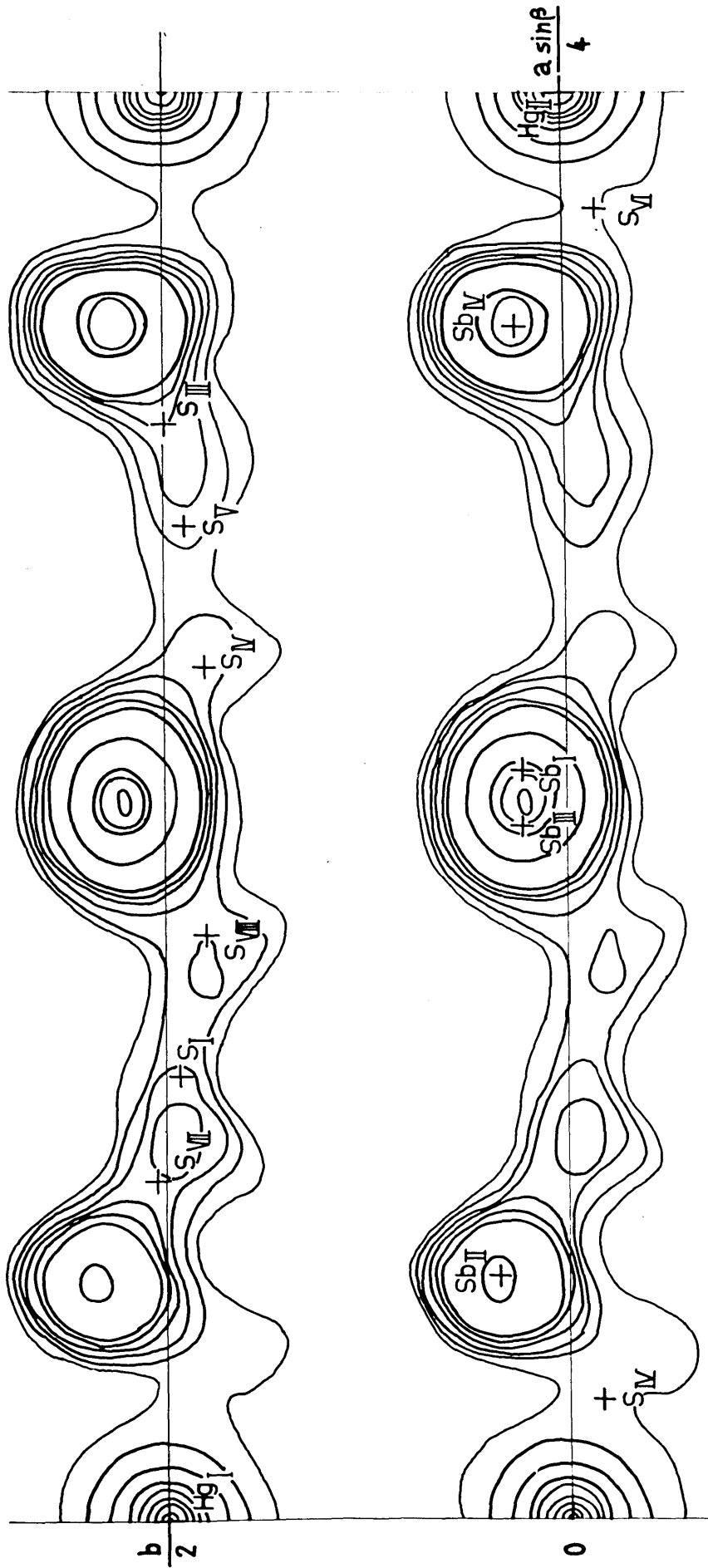
With the approximate  $y$  coordinates of the heavy atoms determined by the above method, the structure factors  $F(hk0)$  could be computed. The resulting electron density map  $\rho(\underline{xy})$  represents the projection of the structure along  $\underline{c}$  axis. The refinement of  $y$  coordinates was carried out by successive Fourier trials with this projection. Final atomic coordinates determined in this way are tabulated in Column I of Table 6. Those of the heavy atoms are listed in Table 5b. The final electron-density map  $\rho(\underline{xy})$  is shown in Fig. 11. The reliability factor for this projection was computed as  $\underline{R} = .24$ .

#### Three-dimensional refinement

The three-dimensional refinement of the structure was performed by the least-squares method developed by Sayre at the International Business Machine Corp., New York. The initial atomic coordinates were these values given in Column I of Table 6. The number of structure factors used in this refinement process was 1950  $F(\underline{hkl})$ 's.

The reliability factor started as  $\underline{R} = .39$  and after three cycles of refinement went down to  $\underline{R} = .31$ , obviously

Fig. 11 Final electron-density map  $\rho(\underline{xy})$ .  
The asymmetric unit of projection of (001) is illustrated.  
Negative contours are omitted.



$1 \text{ \AA}$



Table 5a. Sb-Sb peaks used for the determination of  $y_{Sb}$ 's.

Peaks	Computed $y$ 's	Observed $y$ 's of the maximum contours in Patterson section
a	$y_1 + y_2$	5/60
b	$y_1 + y_3$	10/60
	$y_2 + y_4$	
c	$y_1 + y_4$	10/60
	$y_2 + y_3$	
d	$y_3 + y_4$	11/60

Table 5b. Determination of  $y_{Sb}$ 's from the three-dimensional Patterson sections, and  $\rho(xy)$  map.

Atom	$y$		
	I From Patterson sections	II From $(xy)$	III From least-squares refinement
Sb <sub>I</sub>	3.5/60 = .058	.056	.063
Sb <sub>II</sub>	4.5/60 = .075	.087	.095
Sb <sub>III</sub>	3.5/60 = .058	.056	.064
Sb <sub>IV</sub>	4.5/60 = .075	.063	.078

Table 6. Atomic coordinates from several processes.

Atom		I From Fourier maps	II From first least- squares refinement	III From second least-squares refinement
Hg <sub>I</sub>	x =	.000	.000	.000
	y =	.500	.500	.500
	z =	.000	.000	.000
Hg <sub>II</sub>	x =	.250	.250	.250
	y =	.000	.004	.001
	z =	.000	.000	.000
Sb <sub>I</sub>	x =	.120	.120	.120
	y =	.056	.062	.063
	z =	.075	.075	.075
Sb <sub>II</sub>	x =	.042	.042	.042
	y =	.087	.094	.095
	z =	.213	.214	.214
Sb <sub>III</sub>	x =	.130	.130	.131
	y =	.056	.062	.064
	z =	.426	.425	.425
Sb <sub>IV</sub>	x =	.208	.208	.208
	y =	.063	.073	.078
	z =	.287	.287	.287
S <sub>I</sub>	x =	.059	.062	.062
	y =	.495	.503	.493
	z =	.093	.092	.092
S <sub>II</sub>	x =	.229	.228	.229
	y =	.962	.026	.028
	z =	.183	.181	.180
S <sub>III</sub>	x =	.173	.172	.172
	y =	.475	.510	.506
	z =	.040	.039	.039
S <sub>IV</sub>	x =	.149	.148	.149
	y =	.450	.523	.521
	z =	.223	.221	.222
S <sub>V</sub>	x =	.191	.189	.189
	y =	.488	.502	.494
	z =	.407	.408	.407
S <sub>VI</sub>	x =	.021	.022	.022
	y =	.962	.020	.021
	z =	.317	.318	.318
S <sub>VII</sub>	x =	.077	.078	.078
	y =	.488	.509	.507
	z =	.460	.461	.460
S <sub>VIII</sub>	x =	.101	.102	.102
	y =	.450	.483	.483
	z =	.277	.278	.277

a value too high for an acceptable structure. The atomic coordinates determined by these processes are given in Column II of Table 6.

After numerous trials, which only proved that different structure models could not improve the  $\underline{R}$  factor, the result of this refinement process was closely examined. An analysis is given in Table 7a and 7b. In Table 7a, the variations of  $\underline{R}$ ,  $\underline{K}$ , and averaged  $\underline{B}$  values after each cycle are tabulated. In Table 7b, the reliability factor computed for each level is given first. These  $\underline{R}$ -values are computed with a uniform scaling factor  $\underline{K}$  after the second cycle, i.e., with  $\underline{K} = 50.7$ . In the second column of Table 7b are given the optimum values of scaling factor  $\underline{K}$ . These  $\underline{K}$  values were determined by the formula,  $\underline{K} = \frac{\sum F_c}{\sum F_o}$ . For example, the optimum  $\underline{K}$  value of the second level is computed by the formula,  $\underline{K} = \frac{\sum F_c(h21)}{\sum F_o(h21)}$ . In the third column, the  $\underline{R}$  values computed with thus determined  $\underline{K}_{\text{optimum}}$  values are tabulated. The values of  $\underline{R}$  given in this column are acceptable considering the highly absorbing nature of the material. As a result of this analysis it was suspected that the use of a uniform scaling factor caused a large  $\underline{R}$ -value even if the structure was close to the final solution.

The best way to proceed was to correct the individual intensities for absorption factor. In the present case, however, as the second best procedure, the use of a scaling

factor which differed with different levels, was applied. That this procedure is equivalent to the partial correction of the absorption factor is shown in Appendix II.

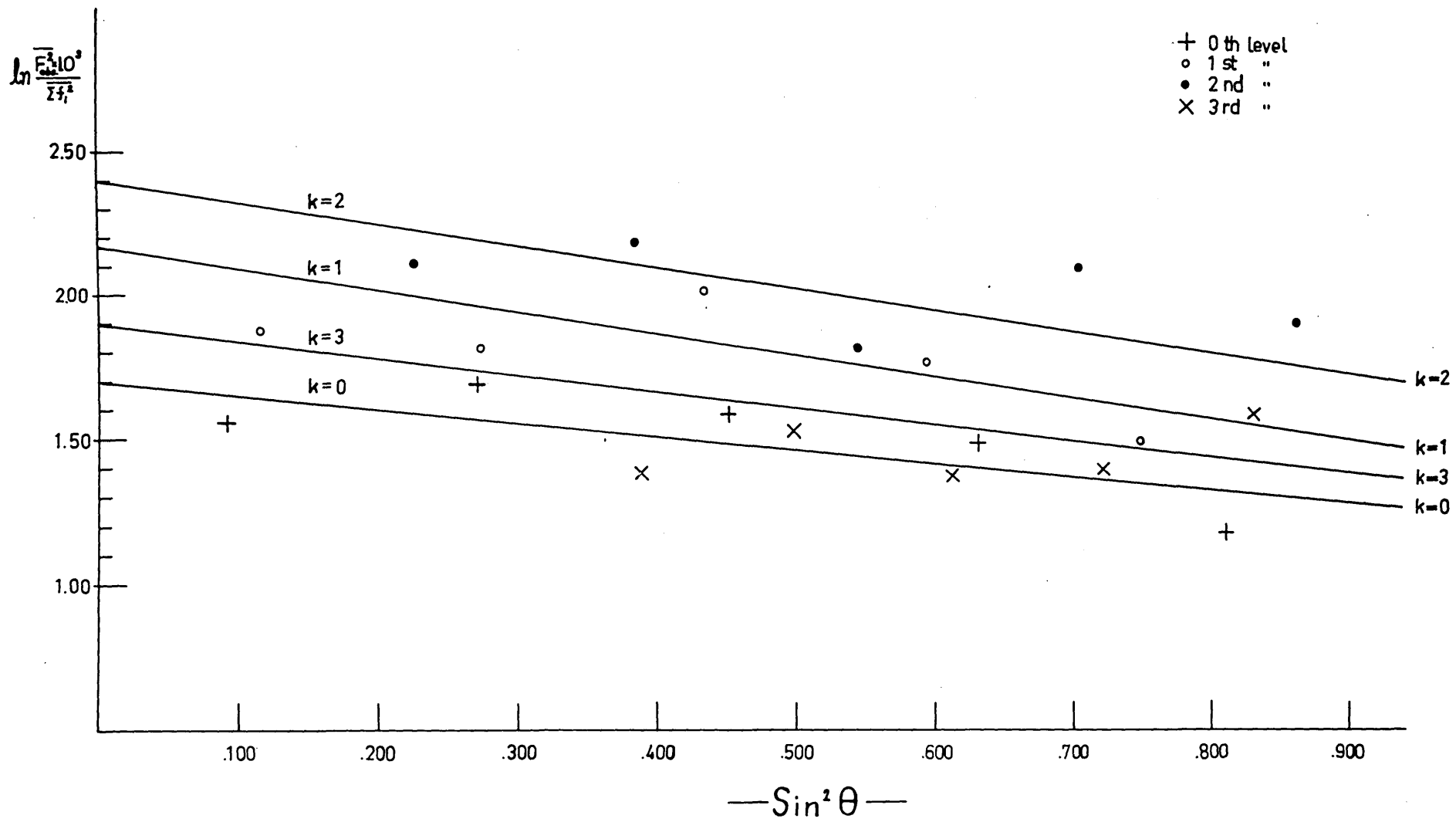
These non-uniform scaling factors were determined in the following way: The observed  $F^2(hkl)$ 's with different  $k$  values were grouped together. For the  $F^2$ 's in each group, the scaling factor was determined by Wilson's<sup>12</sup> statistical method. The result of the treatment is represented in Fig. 12. The individual values of the scaling factor for each level are tabulated in the fourth column of Table 7b.

Since a uniform scaling factor was necessary for the IBM procedure of refinement, the  $K$  value thus determined with  $F^2(h0l)$ 's was used as such.  $F$  values observed for the first, second, and third levels were corrected by multiplying by the factors given in the last column of Table 7b. These factors are ratios between the  $K$  value of each level to the  $K$  value of the equator.

With the  $F_0$  values thus corrected, three further cycles of refinement were carried out. The final  $R$  value was computed as .19. This treatment of structure factors represents the correction of the differences between the averaged effect of absorption for different levels. The correction within each level was not considered. The final  $R$  value was considered as reasonably low. The final atomic coordinates are tabulated in Table 8, and also, for

Fig. 12 Determination of non-uniform scaling factor for each level. Wilson's statistical method was applied to  $\underline{F}^2(\underline{h01})$ 's,  $\underline{F}^2(\underline{h11})$ 's,  $\underline{F}^2(\underline{h21})$ 's, and  $\underline{F}^2(\underline{h31})$ 's treated separately.

The result obtained for each level is expressed by different symbols as indicated in the drawing.



a comparison with previously obtained values, in Column III of Table 6.

The comparison between the observed and computed structure factors is listed in Table 10.

#### Discussion of the structure

The interatomic distances between the neighboring atoms are tabulated in Table 9. These distances are also shown in the diagrammatic representation of the structure, Fig. 13. In Fig. 14, the structural scheme is illustrated for the whole unit cell.

The structure of livingstonite can be described as a double layered structure. Both kinds of layers run parallel to (001). All the Sb atoms have as closest neighbors three S atoms at distances of  $2.5\text{\AA}$ – $2.6\text{\AA}$ . This  $\text{SbS}_3$  unit, together with its equivalent related by translation  $\underline{b}$ , is built into a chain of composition  $\text{SbS}_2$ . There are three groups of two  $\text{SbS}_2$  chains in the structure. In one group these two  $\text{SbS}_2$  chains are related by a center of symmetry. In another, by a two-fold screw axis, and in the third, by no symmetry element. In all of the three cases two  $\text{SbS}_2$  chains are combined into an  $\text{Sb}_2\text{S}_4$  double chain. This  $\text{Sb}_2\text{S}_4$  double chain was also described in the crystal structure of bertierite<sup>4</sup>,  $\text{FeSb}_2\text{S}_4$ .

In one kind of layer, neighboring double chains of composition  $\text{Sb}_2\text{S}_4$  are built into a layer through a mutual

Table 7a. Analysis of three-dimensional refinement cycles by the least-squares method of IBM.

	Value			
	Initial	First cycle	Second cycle	Third cycle
<u>K</u>	61.0	52.9	50.7	49.7
<u>B</u>	1.32	0.90	0.89	0.97
<u>R</u>		.39	.33	.315



Table 7b. Level by level comparison of R-value after second cycle.

Level	R-value after second cycle	$\underline{K}_{\text{optimum}}$	R-value with $\underline{K}_{\text{optimum}}$	$\underline{K}$ -determined from Fig. 12	Correction factor
k = 0	.354	63.6	.172	58.1	1.00
k = 1	.233	44.7	.222	42.8	0.74
k = 2	.281	38.6	.197	39.9	0.69
k = 3	.227	51.8	.193	51.2	0.88
k = 4	.664	82.1	.489	--	--

Table 8. Final atomic coordinates.

Atom	x	y	z	B
Hg <sub>I</sub>	.000	.500	.000	1.58
Hg <sub>II</sub>	.250	.001	.000	1.58
Sb <sub>I</sub>	.120	.063	.075	1.09
Sb <sub>II</sub>	.042	.095	.214	1.14
Sb <sub>III</sub>	.131	.064	.425	0.94
Sb <sub>IV</sub>	.208	.078	.287	0.21
S <sub>I</sub>	.062	.493	.092	1.06
S <sub>II</sub>	.229	.028	.180	0.50
S <sub>III</sub>	.172	.506	.039	1.21
S <sub>IV</sub>	.149	.521	.222	0.47
S <sub>V</sub>	.189	.494	.407	0.96
S <sub>VI</sub>	.022	.021	.318	0.76
S <sub>VII</sub>	.078	.507	.460	0.89
S <sub>VIII</sub>	.102	.483	.277	0.69

Note. Temperature coefficient of each atom listed under B has been determined during the refinement processes by least-squares method.

$S_2$  group. The S-S distance in this  $S_2$  group is found to be  $2.07\text{\AA}$ . An  $S_2$  group in the structure of a sulfosalt mineral has not been reported before, but three examples are known in the sulfide structures, i.e. in pyrite,  $FeS_2$ , in marcasite,  $FeS_2$ , and in covellite,  $CuS$ . The S-S distance in livingstonite is in good agreement with those values found in sulfides. The  $S_2$  group is located in the structure so that the middle point of the group is at  $(\frac{1}{8}0\frac{1}{4})$  i.e., at a pseudo center of symmetry. These sulfur atoms are the ones which require the new chemical formula of the mineral. The chemical formula of this layer can be expressed as  $(Sb_4S_6)S_2$ .

In another type of layer, two  $Sb_2S_4$  double chains are cemented together by Hg atoms. Both  $Hg_I$  and  $Hg_{II}$  atoms have as nearest neighbors two S atoms at  $2.3\text{\AA} - 2.4\text{\AA}$ . If S atoms at larger distance are counted, there are four more S atoms at distances of about  $3.4\text{\AA}$ . Counting these additional atoms, both Hg atoms have six sulfur atoms in a distorted octahedral coordination. In sulfide structures two types of Hg-S coordination are known. In metacinnabar,  $HgS$ , the coordination is a regular tetrahedral one, and the Hg-S distances are  $2.53\text{\AA}$ . In cinnabar<sup>13</sup>, the more stable form of  $HgS$ , the Hg atom is located at the center of a distorted octahedral arrangement of six S atoms with the following Hg-S distances:

2.36Å(2), 3.10Å(2), and 3.30Å(2). The two strong linear bonds of about 2.35Å length, characteristics of Hg, are present in livingstonite. In cinnabar, these strong Hg-S bonds are found to share S atoms with neighboring Hg-S bonds to form a spiral chain, while in livingstonite these bonds are orientated parallel to (010), sharing S atoms with Sb atoms. This type of layer has the chemical formula  $\text{HgSb}_2\text{S}_4$ . Thus the structural formula of livingstonite can be expressed as  $(\text{HgSb}_2\text{S}_4)_2(\text{Sb}_4\text{S}_6)\text{S}_2$ .

The interatomic distances between the atoms in the different kinds of layers are not less than 3.3Å. These weak bonds can explain the existence of a perfect cleavage parallel to (001).

Table 9. Interatomic distances in livingstonite.

	S <sub>I</sub>	S <sub>II</sub>	S <sub>III</sub>	S <sub>IV</sub>	S <sub>V</sub>	S <sub>VI</sub>	S <sub>VII</sub>	S <sub>VIII</sub>
Hg <sub>I</sub>	2.37Å(2)						3.34Å(2) 3.38 (2)	
Hg <sub>II</sub>			3.34Å(2) 3.37 (2)		2.33Å(2)			
Sb <sub>I</sub>	2.54 2.95		2.70 2.94	3.57Å <sup>o</sup> 3.75			2.49	
Sb <sub>II</sub>	3.25 3.62					2.44Å <sup>o</sup> 2.47 3.11		2.52Å <sup>o</sup> 3.15
Sb <sub>III</sub>			2.47		2.55 2.96		2.62 2.95	3.51 3.86
Sb <sub>IV</sub>		2.54Å <sup>o</sup> 2.59 2.88		2.66 2.98	3.24 3.63			
S <sub>II</sub>			3.64 3.74					
S <sub>IV</sub>								2.07
S <sub>VI</sub>							3.66 3.72	

Fig. 13 Schematic representation of the structure. The structure is represented in the asymmetric unit of the projection of (010). The open circles represent the atoms with  $y$  coordinates close to zero. The shaded circles represent the atoms with  $y$  coordinates close to  $1/2$ . The chemical bonds between the neighboring atoms are shown by straight lines. The broken lines are used to indicate the weaker bonds between Hg and S. The dotted lines are used to indicate the weaker Sb-S bonds between the different kinds of layers. The figures accompanying these bonds are interatomic distances in Å units.

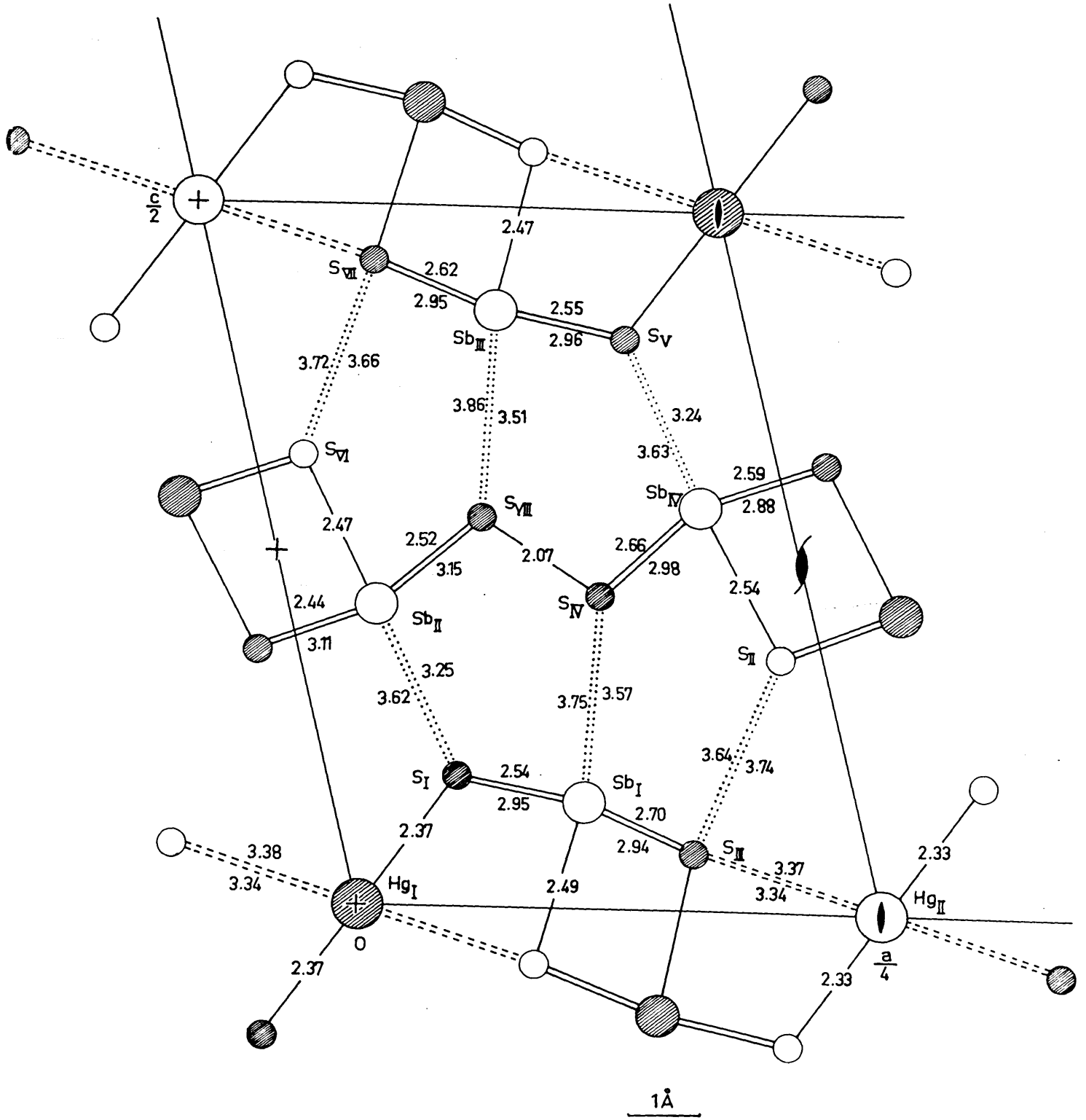


Fig. 14 Schematic representation of the structure projected on (010). The projection of the whole unit cell is shown. The perfect cleavage parallel to (001) can be understood as the breaking of the weaker bonds represented by dotted lines.



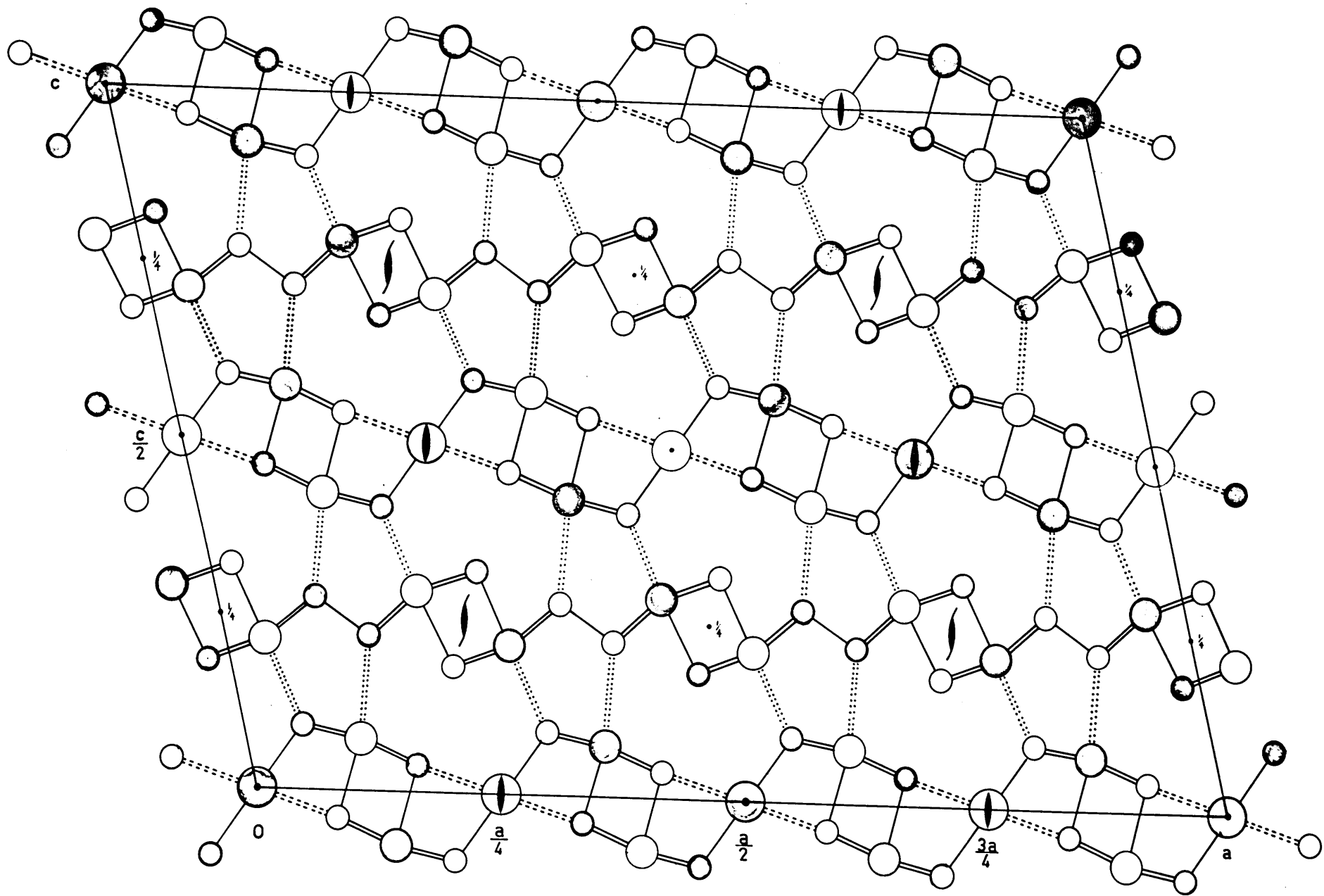


Table 10  
Observed and Calculated Structure Factors

hkl	F <sub>obs</sub>	F <sub>calc</sub>	hkl	F <sub>obs</sub>	F <sub>calc</sub>	hkl	F <sub>obs</sub>	F <sub>calc</sub>
400	161	+ 144	20,04	125	- 92	40,10	690	+ 562
800	486	+ 683	24,04	800	+ 697	80,10	621	- 548
12,00	505	- 538	28,04	942	+ 690	12,0,10	114	+ 71
16,00	587	+ 589	32,04	671	+ 439	16,0,10	224	+ 206
20,00	255	+ 175	006	445	- 335	20,0,10	968	+ 935
24,00	877	+ 734	406	1103	+1034	24,0,10	121	+ 62
28,00	356	+ 233	806	533	- 458	28,0,10	346	+ 244
32,00	205	+ 139	12,06	1006	+ 1027	32,0,10	52	- 100
36,00	182	- 182	16,06	505	+ 489	00,12	412	+ 308
002	372	+ 306	20,06	761	+ 703	40,12	74	+ 73
402	489	- 541	24,06	112	+ 32	80,12	1174	+1188
802	597	+ 812	28,06	52	- 134	12,0,12	465	+ 452
12,02	716	+ 902	32,06	119	- 113	16,0,12	722	+ 697
16,02	1384	+1650	008	551	- 388	20,0,12	126	- 178
20,02	377	- 355	408	1406	+1539	24,0,12	227	- 215
24,02	511	+ 433	808	596	+ 548	28,0,12	208	+ 151
28,02	348	- 306	12,08	755	+ 698	00,14	1193	+1125
32,02	651	+ 495	16,08	186	- 169	40,14	124	- 82
004	942	+ 923	20,08	588	+ 498	80,14	684	+ 542
404	935	+1016	24,08	179	- 188	12,0,14	439	- 392
804	635	+ 651	28,08	1006	+ 815	16,0,14	400	+ 290
12,04	68	- 53	32,08	142	+ 159	20,0,14	304	+ 248
16,04	90	- 65	00,10	1058	+ 945	24,0,14	935	+ 750

hkl	F <sub>obs</sub>	F <sub>calc</sub>	hkl	F <sub>obs</sub>	F <sub>calc</sub>	hkl	F <sub>obs</sub>	F <sub>calc</sub>
28,0,14	270	+ 176	40 $\bar{2}$	120	+ 157	40 $\bar{8}$	116	- 50
00,16	200	- 117	80 $\bar{2}$	887	+1059	80 $\bar{8}$	445	- 410
40,16	206	- 183	12,0 $\bar{2}$	589	+ 726	12,0 $\bar{8}$	922	+1193
80,16	780	+ 675	16,0 $\bar{2}$	563	+ 578	16,0 $\bar{8}$	519	+ 537
12,0,16	163	- 164	20,0 $\bar{2}$	110	- 66	20,0 $\bar{8}$	864	+ 886
16,0,16	608	+ 613	24,0 $\bar{2}$	205	+ 106	24,0 $\bar{8}$	336	+ 306
20,0,16	164	+ 222	28,0 $\bar{2}$	508	+ 376	28,0 $\bar{8}$	182	- 100
24,0,16	307	+ 213	32,0 $\bar{2}$	506	+ 372	32,0 $\bar{8}$	344	+ 213
00,18	319	+ 297	36,0 $\bar{2}$	826	+ 789	36,0 $\bar{8}$	250	+ 131
40,18	851	+ 791	40 $\bar{4}$	584	+ 482	40, $\bar{10}$	780	+ 868
80,18	589	+ 541	80 $\bar{4}$	241	- 253	80, $\bar{10}$	903	+1088
12,0,18	192	+ 148	12,0 $\bar{4}$	664	+ 860	12,0, $\bar{10}$	218	- 174
16,0,18	192	+ 148	16,0 $\bar{4}$	30	+ 26	16,0, $\bar{10}$	269	+ 322
20,0,18	365	+ 239	20,0 $\bar{4}$	1458	+1486	20,0, $\bar{10}$	0	+ 1
00,20	256	- 226	24,0 $\bar{4}$	507	+ 307	24,0, $\bar{10}$	709	+ 658
40,20	320	+ 225	28,0 $\bar{4}$	364	+ 252	28,0, $\bar{10}$	333	+ 282
80,20	490	- 473	32,0 $\bar{4}$	496	- 549	32,0, $\bar{10}$	671	+ 516
12,0,20	483	+ 445	36,0 $\bar{4}$	303	+ 255	36,0, $\bar{10}$	326	- 284
16,0,20	288	+ 226	40 $\bar{6}$	1187	+1580	40, $\bar{12}$	263	- 250
00,22	260	+ 210	80 $\bar{6}$	710	+ 854	80, $\bar{12}$	703	+ 777
40,22	551	+ 534	12,0 $\bar{6}$	834	+1052	12,0, $\bar{12}$	127	+ 182
80,22	272	+ 315	16,0 $\bar{6}$	703	- 786	16,0, $\bar{12}$	877	+1086
12,0,22	506	+ 506	20,0 $\bar{6}$	97	+ 134	20,0, $\bar{12}$	86	- 114
00,24	455	+ 498	24,0 $\bar{6}$	32	+ 32	24,0, $\bar{12}$	203	+ 208
40,24	0	+ 17	28,0 $\bar{6}$	1045	+ 836	28,0, $\bar{12}$	697	- 510
00,26	152	+ 152	32,0 $\bar{6}$	309	+ 177	32,0, $\bar{12}$	922	+ 810
40,26	0	+ 17	36,0 $\bar{6}$	800	+ 543	36,0, $\bar{12}$	451	+ 329

hkl	F <sub>obs</sub>	F <sub>calc</sub>	hkl	F <sub>obs</sub>	F <sub>calc</sub>	hkl	F <sub>obs</sub>	F <sub>calc</sub>
40, $\overline{14}$	108	+ 138	12,0, $\overline{20}$	506	+ 688	311	33	- 14
80, $\overline{14}$	614	+ 664	16,0, $\overline{20}$	127	- 126	411	23	+ 13
12,0, $\overline{14}$	611	- 696	20,0, $\overline{20}$	39	+ 50	511	189	- 201
16,0, $\overline{14}$	373	+ 516	24,0, $\overline{20}$	56	+ 11	611	884	-1222
20,0, $\overline{14}$	615	+ 703	28,0, $\overline{20}$	793	+ 703	711	181	+ 160
24,0, $\overline{14}$	787	+ 737	32,0, $\overline{20}$	204	+ 271	811	64	+ 25
28,0, $\overline{14}$	404	+ 303	40, $\overline{22}$	174	+ 145	911	126	- 79
32,0, $\overline{14}$	39	+ 37	80, $\overline{22}$	213	- 244	10,11	809	- 979
36,0, $\overline{14}$	113	- 116	12,0, $\overline{22}$	299	+ 496	11,11	202	+ 239
40, $\overline{16}$	543	+ 626	16,0, $\overline{22}$	299	+ 497	13,11	111	+ 177
80, $\overline{16}$	742	+ 885	20,0, $\overline{22}$	302	+ 335	14,11	292	- 329
12,0, $\overline{16}$	595	+ 683	24,0, $\overline{22}$	145	- 71	17,11	201	+ 169
16,0, $\overline{16}$	154	+ 194	28,0, $\overline{22}$	214	- 204	18,11	175	- 130
20,0, $\overline{16}$	112	- 34	40, $\overline{24}$	221	+ 378	19,11	173	- 143
24,0, $\overline{16}$	277	- 206	80, $\overline{24}$	230	+ 316	23,11	114	- 106
28,0, $\overline{16}$	321	+ 297	12,0, $\overline{24}$	298	- 379	25,11	63	- 55
32,0, $\overline{16}$	312	+ 230	16,0, $\overline{24}$	144	+ 219	26,11	172	- 136
40, $\overline{18}$	210	+ 233	20,0, $\overline{24}$	165	- 119	013	35	+ 18
80, $\overline{18}$	443	- 459	24,0, $\overline{24}$	630	+ 692	113	143	- 67
12,0, $\overline{18}$	255	+ 343	40, $\overline{26}$	177	- 217	213	942	- 902
16,0, $\overline{18}$	32	+ 27	80, $\overline{26}$	384	+ 514	313	279	+ 330
20,0, $\overline{18}$	768	+ 945	12,0, $\overline{26}$	290	+ 373	513	395	+ 405
24,0, $\overline{18}$	47	- 7	16,0, $\overline{26}$	290	+ 373	613	864	+ 780
28,0, $\overline{18}$	599	+ 550	20,0, $\overline{26}$	88	- 90	713	299	- 247
32,0, $\overline{18}$	370	- 298				813	35	- 29
40, $\overline{20}$	716	+ 955	111	259	- 303	10,13	622	- 685
80, $\overline{20}$	182	+ 172	211	595	- 816	11,13	77	- 71

hkl	F <sub>obs</sub>	F <sub>calc</sub>	hkl	F <sub>obs</sub>	F <sub>calc</sub>	hkl	F <sub>obs</sub>	F <sub>calc</sub>
13,13	46	+ 13	22,15	504	+ 423	319	395	- 298
14,13	57	+ 61	23,15	281	- 223	519	115	- 132
15,13	276	- 271	017	55	+ 30	619	590	- 488
17,13	208	- 250	117	184	- 104	719	76	- 84
18,13	916	- 907	217	1103	- 911	919	62	- 69
19,13	212	+ 155	317	239	+ 198	10,19	78	- 69
21,13	55	- 38	417	28	+ 21	11,19	76	- 90
22,13	780	- 624	517	90	+ 112	13,19	243	- 198
23,13	159	+ 100	617	572	- 480	14,19	993	- 954
25,13	45	+ 7	717	96	+ 107	15,19	233	+ 205
26,13	577	- 428	817	32	- 5	18,19	292	- 238
27,13	168	+ 125	917	158	+ 146	19,19	70	+ 60
015	65	- 27	10,17	481	- 490	11,11	89	- 80
115	65	- 127	11,17	61	- 35	21,11	729	- 604
215	332	- 284	12,17	36	- 28	51,11	291	- 185
315	64	- 62	13,17	161	+ 98	61,11	1071	- 939
515	49	- 54	14,17	286	+ 252	71,11	366	+ 318
615	572	- 519	15,17	212	- 202	91,11	215	+ 217
715	103	- 167	17,17	117	- 127	11,1,11	105	- 35
915	361	- 311	18,17	554	- 504	14,1,11	436	- 312
10,15	1374	- 1447	19,17	44	- 8	17,1,11	147	+ 164
11,15	326	+ 287	21,17	99	- 90	18,1,11	341	+ 346
13,15	119	+ 154	22,17	761	- 606	19,1,11	251	- 229
14,15	36	+ 22	23,17	45	+ 18	11,13	250	+ 193
18,15	381	- 323	019	113	- 34	31,13	122	- 44
19,15	83	+ 107	119	447	+ 336	51,13	112	+ 59
21,15	301	+ 242	219	710	+ 559	61,13	81	+ 68

hkl	F <sub>obs</sub>	F <sub>calc</sub>	hkl	F <sub>obs</sub>	F <sub>calc</sub>	hkl	F <sub>obs</sub>	F <sub>calc</sub>
71,13	170	- 117	10,1,17	386	- 272	23,11̄	244	+ 210
10,1,13	91	- 59	01,19	31	- 25	25,11̄	300	+ 233
11,1,13	150	- 161	21,19	287	- 179	26,11̄	697	+ 537
13,1,13	212	- 210	31,19	76	- 89	27,11̄	222	- 148
14,1,13	1129	-1056	61,19	303	- 262	113̄	88	- 58
15,1,13	161	+ 95	71,19	43	- 74	213̄	309	- 316
17,1,13	62	- 39	91,19	203	- 186	313̄	32	- 79
18,1,13	287	- 229	10,1,19	622	- 567	413̄	50	+ 14
19,1,13	74	+ 65	11,1,19	148	+ 144	513̄	228	- 233
11,15	202	- 189	111̄	299	+ 362	613̄	1677	-1826
21,15	651	- 515	211̄	95	- 146	713̄	275	+ 420
31,15	94	+ 17	311̄	108	- 125	813̄	34	+ 15
51,15	94	- 58	411̄	67	- 20	913̄	181	+ 305
61,15	361	- 292	511̄	76	+ 45	10,13̄	204	+ 301
71,15	97	+ 50	611̄	262	- 348	11,13̄	99	- 90
91,15	140	- 76	711̄	115	- 119	13,13̄	46	+ 44
10,1,15	761	- 656	911̄	128	+ 76	14,13̄	206	- 266
11,1,15	172	+ 156	10,11̄	407	+ 433	15,13̄	32	+ 22
13,1,15	125	+ 129	11,11̄	182	- 280	17,13̄	180	+ 146
14,1,15	65	- 5	13,11̄	289	- 322	18,13̄	119	- 113
01,17	62	+ 44	14,11̄	1064	-1058	19,13̄	270	- 271
11,17	139	- 75	15,11̄	188	+ 142	21,13̄	243	- 223
21,17	1084	- 963	17,11̄	35	+ 11	22,13̄	871	- 792
31,17	258	+ 221	18,11̄	486	- 398	23,13̄	67	+ 45
51,17	251	+ 223	19,11̄	65	+ 42	24,13̄	31	+ 28
61,17	244	+ 199	21,11̄	57	- 55	25,13̄	74	- 59
71,17	177	- 133	22,11̄	974	- 806	26,13̄	527	- 344

hkl	F <sub>obs</sub>	F <sub>calc</sub>	hkl	F <sub>obs</sub>	F <sub>calc</sub>	hkl	F <sub>obs</sub>	F <sub>calc</sub>
11 $\bar{5}$	320	+ 289	81 $\bar{7}$	46	- 14	21,1 $\bar{9}$	279	+ 238
21 $\bar{5}$	241	+ 181	91 $\bar{7}$	234	+ 252	22,1 $\bar{9}$	627	+ 537
31 $\bar{5}$	298	- 290	10,1 $\bar{7}$	191	- 252	23,1 $\bar{9}$	260	- 214
51 $\bar{5}$	110	- 175	11,1 $\bar{7}$	77	- 50	11,1 $\bar{1}$	99	- 54
61 $\bar{5}$	884	-1051	12,1 $\bar{7}$	37	- 24	21,1 $\bar{1}$	1264	-1299
71 $\bar{5}$	28	- 95	13,1 $\bar{7}$	175	+ 161	31,1 $\bar{1}$	219	+ 255
91 $\bar{5}$	82	- 128	14,1 $\bar{7}$	347	+ 397	51,1 $\bar{1}$	291	+ 309
10,1 $\bar{5}$	371	- 384	15,1 $\bar{7}$	245	- 299	61,1 $\bar{1}$	554	+ 564
13,1 $\bar{5}$	192	- 210	17,1 $\bar{7}$	144	- 198	71,1 $\bar{1}$	189	- 167
14,1 $\bar{5}$	993	-1126	18,1 $\bar{7}$	645	- 681	81,1 $\bar{1}$	38	- 32
15,1 $\bar{5}$	229	+ 234	19,1 $\bar{7}$	27	+ 15	91,1 $\bar{1}$	38	- 2
17,1 $\bar{5}$	35	+ 67	20,1 $\bar{7}$	23	+ 17	10,1,1 $\bar{1}$	262	- 341
18,1 $\bar{5}$	325	- 329	21,1 $\bar{7}$	81	- 81	11,1,1 $\bar{1}$	89	- 74
19,1 $\bar{5}$	84	+ 127	22,1 $\bar{7}$	213	- 212	14,1,1 $\bar{1}$	102	- 170
20,1 $\bar{5}$	19	+ 2	23,1 $\bar{7}$	52	- 16	15,1,1 $\bar{1}$	131	- 176
21,1 $\bar{5}$	177	+ 161	25,1 $\bar{7}$	264	- 138	17,1,1 $\bar{1}$	181	- 195
22,1 $\bar{5}$	50	- 72	26,1 $\bar{7}$	1090	- 974	18,1,1 $\bar{1}$	716	- 804
23,1 $\bar{5}$	60	- 20	11 $\bar{9}$	92	- 144	19,1,1 $\bar{1}$	148	+ 124
25,1 $\bar{5}$	158	+ 95	21 $\bar{9}$	658	- 675	11,1 $\bar{3}$	114	- 137
26,1 $\bar{5}$	106	+ 80	61 $\bar{9}$	90	- 120	21,1 $\bar{3}$	486	- 537
11 $\bar{7}$	179	- 134	71 $\bar{9}$	106	- 172	51,1 $\bar{3}$	142	- 154
21 $\bar{7}$	974	- 975	91 $\bar{9}$	300	- 321	61,1 $\bar{3}$	658	- 748
31 $\bar{7}$	254	+ 266	10,1 $\bar{9}$	1064	-1282	71,1 $\bar{3}$	147	+ 129
41 $\bar{7}$	38	+ 19	11,1 $\bar{9}$	273	+ 313	10,1,1,1 $\bar{3}$	206	- 243
51 $\bar{7}$	164	+ 223	13,1 $\bar{9}$	67	+ 138	11,1,1,1 $\bar{3}$	108	+ 117
61 $\bar{7}$	54	- 33	14,1 $\bar{9}$	541	- 636	13,1,1,1 $\bar{3}$	62	+ 110
71 $\bar{7}$	41	+ 59	18,1 $\bar{9}$	560	- 589	14,1,1,1 $\bar{3}$	269	- 345

hkl	F <sub>obs</sub>	F <sub>calc</sub>	hkl	F <sub>obs</sub>	F <sub>calc</sub>	hkl	F <sub>obs</sub>	F <sub>calc</sub>
17,1,13	170	+ 174	91,19	70	- 109	22,20	72	- 43
18,1,13	228	+ 177	10,1,19	363	- 543	23,20	384	+ 311
19,1,13	172	- 188	13,1,19	99	- 110	24,20	494	+ 384
11,15	200	+ 233	14,1,19	495	- 652	25,20	390	- 299
21,15	163	+ 112	15,1,19	88	+ 114	022	396	+ 395
31,15	154	- 135	11,21	60	- 103	122	92	+ 39
61,15	234	- 271	21,21	395	- 559	222	101	+ 60
71,15	70	- 65	31,21	106	+ 164	322	352	- 308
91,15	41	+ 32				422	74	- 43
10,1,15	123	- 164	020	1516	+1689	522	443	+ 530
11,1,15	130	- 195	120	366	- 628	622	43	+ 26
13,1,15	214	- 280	220	57	- 53	722	315	+ 435
14,1,15	773	- 994	320	119	- 269	822	415	+ 492
15,1,15	163	+ 165	420	83	+ 134	922	65	- 39
18,1,15	116	+ 165	820	364	+ 516	10,22	65	- 27
19,1,15	77	+ 57	920	179	- 299	11,22	110	+ 106
51,17	168	- 126	10,20	84	+ 49	12,22	494	+ 596
61,17	742	- 962	11,20	415	- 469	14,22	102	- 51
71,17	224	+ 261	12,20	106	- 137	15,22	379	+ 353
91,17	137	+ 198	13,20	443	+ 480	16,22	961	+1034
17,1,17	99	+ 98	14,20	102	+ 46	17,22	510	- 474
18,1,17	372	+ 383	15,20	121	+ 161	18,22	42	- 34
19,1,17	150	- 213	16,20	479	+ 464	19,22	335	- 334
11,19	126	+ 152	18,20	33	- 6	20,22	208	- 177
21,19	272	+ 332	19,20	34	+ 58	024	588	+ 543
31,19	63	- 99	20,20	179	+ 112	224	98	- 53
71,19	141	- 170	21,20	154	+ 147	324	351	+ 283



hkl	F <sub>obs</sub>	F <sub>calc</sub>	hkl	F <sub>obs</sub>	F <sub>calc</sub>	hkl	F <sub>obs</sub>	F <sub>calc</sub>
524	379	- 351	16,26	295	+ 273	12,12	132	+ 133
624	92	- 47	028	184	- 106	22,12	65	+ 29
724	66	- 116	128	502	+ 472	32,12	57	- 29
824	415	+ 419	328	522	+ 484	42,12	168	+ 165
924	208	- 234	428	961	+ 905	52,12	274	+ 262
11,24	256	- 294	528	390	- 274	62,12	34	- 19
12,24	123	+ 126	628	63	- 55	72,12	471	+ 417
13,24	130	+ 122	728	18	+ 1	82,12	813	+ 740
14,24	88	+ 50	828	358	+ 335	92,12	288	- 236
15,24	201	- 172	928	92	- 56	10,2,12	62	- 47
16,24	166	+ 125	10,28	50	- 45	11,2,12	57	+ 40
17,24	219	+ 191	11,28	177	+ 154	12,2,,2	280	+ 255
18,24	50	+ 41	12,28	439	+ 395	13,2,12	152	- 168
19,24	44	- 0	13,28	326	- 363	02,14	677	+ 609
026	121	- 49	02,10	631	+ 585	12,14	451	- 390
126	182	+ 87	12,10	363	- 307	22,14	74	- 44
226	75	+ 35	32,10	165	- 175	32,14	172	- 164
426	871	+ 884	42,10	620	+ 508	42,14	137	- 79
626	79	+ 59	52,10	92	- 83	82,14	526	+ 439
726	341	- 286	62,10	63	+ 47	92,14	183	- 185
826	121	- 63	72,10	424	- 337	10,2,14	42	+ 37
926	459	+ 470	82,10	255	- 203	02,16	44	+ 22
11,26	331	+ 357	92,10	324	+ 253	12,16	52	+ 48
12,26	677	+ 673	10,2,10	75	+ 49	32,16	72	+ 55
13,26	157	- 107	12,2,10	168	+ 135	42,16	241	- 206
14,26	33	- 33	13,2,10	169	+ 163	52,16	62	+ 36
15,26	135	+ 132	02,12	400	+ 350	72,16	295	+ 276

hkl	F <sub>obs</sub>	F <sub>calc</sub>	hkl	F <sub>obs</sub>	F <sub>calc</sub>	hkl	F <sub>obs</sub>	F <sub>calc</sub>
12 $\bar{2}$	201	+ 202	42 $\bar{4}$	404	+ 473	15,2 $\bar{6}$	490	- 513
22 $\bar{2}$	46	+ 31	52 $\bar{4}$	84	- 142	16,2 $\bar{6}$	370	- 330
32 $\bar{2}$	39	- 24	62 $\bar{4}$	64	+ 51	17,2 $\bar{6}$	362	+ 315
42 $\bar{2}$	144	+ 216	72 $\bar{4}$	319	- 431	18,2 $\bar{6}$	118	+ 54
52 $\bar{2}$	175	+ 331	82 $\bar{4}$	108	+ 146	12 $\bar{8}$	161	+ 110
62 $\bar{2}$	30	- 30	92 $\bar{4}$	284	+ 381	22 $\bar{8}$	77	+ 41
72 $\bar{2}$	310	+ 447	10,2 $\bar{4}$	77	+ 62	32 $\bar{8}$	141	- 111
82 $\bar{2}$	386	+ 531	11,2 $\bar{4}$	128	+ 194	42 $\bar{8}$	101	+ 121
92 $\bar{2}$	183	- 178	12,2 $\bar{4}$	588	+ 710	52 $\bar{8}$	121	+ 88
10,2 $\bar{2}$	83	- 55	13,2 $\bar{4}$	85	+ 85	62 $\bar{8}$	90	+ 57
11,2 $\bar{2}$	110	+ 83	17,2 $\bar{4}$	130	+ 162	72 $\bar{8}$	261	- 236
12,2 $\bar{2}$	339	+ 376	18,2 $\bar{4}$	52	- 34	82 $\bar{8}$	119	- 54
13,2 $\bar{2}$	263	- 266	19,2 $\bar{4}$	486	+ 393	92 $\bar{8}$	358	+ 451
14,2 $\bar{2}$	41	- 24	20,2 $\bar{4}$	993	+ 916	11,2 $\bar{8}$	257	+ 346
15,2 $\bar{2}$	71	- 106	21,2 $\bar{4}$	537	- 409	12,2 $\bar{8}$	658	+ 804
16,2 $\bar{2}$	455	+ 448	22,2 $\bar{4}$	79	- 59	13,2 $\bar{8}$	66	- 33
17,2 $\bar{2}$	150	- 140	12 $\bar{6}$	428	+ 457	14,2 $\bar{8}$	74	- 45
18,2 $\bar{2}$	32	+ 20	32 $\bar{6}$	533	+ 558	15,2 $\bar{8}$	171	+ 200
19,2 $\bar{2}$	275	- 236	42 $\bar{6}$	768	+ 839	16,2 $\bar{8}$	257	+ 256
20,2 $\bar{2}$	133	+ 112	52 $\bar{6}$	415	- 410	12, $\bar{10}$	85	- 31
21,2 $\bar{2}$	177	+ 132	62 $\bar{6}$	88	- 61	22, $\bar{10}$	97	- 49
22,2 $\bar{2}$	100	+ 64	82 $\bar{6}$	420	+ 542	32, $\bar{10}$	214	+ 205
23,2 $\bar{2}$	198	- 127	92 $\bar{6}$	84	- 58	42, $\bar{10}$	475	+ 461
24,2 $\bar{2}$	301	+ 239	10,2 $\bar{6}$	56	- 43	52, $\bar{10}$	283	- 267
25,2 $\bar{2}$	396	+ 257	11,2 $\bar{6}$	124	+ 90	62, $\bar{10}$	63	- 29
12 $\bar{4}$	262	- 251	12,2 $\bar{6}$	557	+ 649	72, $\bar{10}$	99	+ 33
32 $\bar{4}$	88	- 136	13,2 $\bar{6}$	354	- 426	82, $\bar{10}$	677	+ 753

hkl	F <sub>obs</sub>	F <sub>calc</sub>	hkl	F <sub>obs</sub>	F <sub>calc</sub>	hkl	F <sub>obs</sub>	F <sub>calc</sub>
92, $\bar{1}0$	280	- 322	12, 2, $\bar{1}4$	301	- 306	233	303	- 283
11, 2, $\bar{1}0$	287	- 341	13, 2, $\bar{1}4$	338	+ 390	333	400	+ 408
13, 2, $\bar{1}0$	151	+ 137	14, 2, $\bar{1}4$	86	+ 62	533	502	+ 543
14, 2, $\bar{1}0$	54	+ 49	15, 2, $\bar{1}4$	94	+ 153	733	353	- 409
16, 2, $\bar{1}0$	348	+ 404	16, 2, $\bar{1}4$	320	+ 432	833	126	- 67
17, 2, $\bar{1}0$	117	+ 112	12, $\bar{1}6$	146	+ 166	10, 33	510	- 585
22, $\bar{1}2$	70	+ 144	32, $\bar{1}6$	79	+ 113	135	178	- 139
32, $\bar{1}2$	308	- 276	42, $\bar{1}6$	404	+ 533	235	264	- 223
42, $\bar{1}2$	83	+ 90	72, $\bar{1}6$	201	+ 270	635	334	- 355
52, $\bar{1}2$	455	+ 464	82, $\bar{1}6$	462	+ 562	735	206	- 191
72, $\bar{1}2$	321	+ 359	92, $\bar{1}6$	150	- 144	835	84	+ 52
82, $\bar{1}2$	475	+ 467	10, 2, $\bar{1}6$	79	- 62	935	488	- 466
92, $\bar{1}2$	115	- 106	11, 2, $\bar{1}6$	107	+ 112	10, 35	506	- 442
10, 2, $\bar{1}2$	55	- 43	12, 2, $\bar{1}6$	331	+ 402	037	128	+ 68
14, 2, $\bar{1}2$	68	- 48	13, 2, $\bar{1}6$	219	- 286	137	204	- 180
15, 2, $\bar{1}2$	272	+ 273				237	362	- 286
16, 2, $\bar{1}2$	530	+ 631	131	279	- 361	337	293	+ 247
17, 2, $\bar{1}2$	360	- 393	231	239	- 289	437	61	+ 39
12, $\bar{1}4$	339	- 385	431	72	+ 46	537	135	+ 109
22, $\bar{1}4$	68	- 42	531	194	- 262	637	352	- 314
32, $\bar{1}4$	159	- 211	631	304	- 432	737	152	+ 108
42, $\bar{1}4$	95	+ 125	731	153	+ 240	837	55	- 34
72, $\bar{1}4$	34	- 66	831	80	+ 63	937	164	+ 177
82, $\bar{1}4$	502	+ 570	931	101	- 166	10, 37	595	- 569
92, $\bar{1}4$	119	- 138	10, 31	286	- 359	039	99	- 62
10, 2, $\bar{1}4$	59	+ 40	033	79	+ 49	139	600	+ 533
11, 2, $\bar{1}4$	289	- 314	133	130	- 165	239	125	- 135

hkl	F <sub>obs</sub>	F <sub>calc</sub>	hkl	F <sub>obs</sub>	F <sub>calc</sub>	hkl	F <sub>obs</sub>	F <sub>calc</sub>
339	537	- 454	435	101	- 60	33,11	346	+ 362
439	104	- 48	535	228	- 219	53,11	476	+ 455
539	219	- 171	635	584	- 668	73,11	266	- 284
639	380	- 324	735	58	- 65	83,11	114	- 61
739	91	- 84	935	74	- 123	10,3,11	313	- 379
13,11	100	- 95	10,35	160	- 177	13,13	172	- 160
23,11	328	- 284	137	168	- 227	23,13	224	- 239
43,11	97	+ 56	237	234	- 267	43,13	83	+ 51
53,11	335	- 331	337	376	+ 346	53,13	182	- 229
63,11	293	- 219	437	56	+ 38	63,13	195	- 199
73,11	526	+ 507	537	308	+ 290	73,13	172	+ 200
431	59	- 69	637	66	- 114	83,13	84	+ 59
631	283	- 435	737	90	+ 30			
731	71	- 134	837	35	- 35			
831	70	- 42	937	132	+ 189			
931	144	+ 190	10,37	302	- 375			
10,31	33	+ 330	139	223	- 185			
233	36	- 72	239	480	- 429			
333	85	- 129	439	36	- 4			
433	76	+ 67	539	37	- 39			
533	242	- 367	639	52	- 96			
633	422	- 614	739	239	- 235			
733	390	+ 565	839	119	+ 51			
933	310	+ 384	939	434	- 499			
135	398	+ 408	10,39	300	- 316			
235	324	- 389	13,11	147	- 162			
335	366	- 387	23,11	595	- 680			

## PART II

The crystal structure of jamesonite,  $\text{FePb}_4\text{Sb}_6\text{S}_{14}$

## Introduction

The crystallographic description of the mineral jamesonite,  $\text{FePb}_4\text{Sb}_6\text{S}_{14}$ , has been presented by Berry<sup>14</sup>. Jamesonite is a member of the group of acicular sulfosalts, concerning which there has been a considerable increase in structural knowledge in recent years<sup>4,5,6,8,15</sup>. As in the case of livingstonite<sup>15</sup>,  $\text{HgSb}_4\text{S}_8$ , the crystal system of jamesonite is monoclinic. The needle axis of jamesonite is parallel to  $\underline{c}$  axis, while in livingstonite it is parallel to unique 2-fold (or  $\underline{b}$ ) axis.

The cleavage of the members of the group of acicular sulfosalts are known to occur in two ways. In one type, cleavage parallel to the acicular axis, or prismatic cleavage only, is observed. All the sulfosalts crystals of the acicular group with previously determined structures are of this type. In these crystal structures there are layers or chains composed of submetal atoms and sulfur atoms running parallel to the needle axis of the mineral. The prismatic cleavage of the mineral has been explained as due to the breaking of the weaker chemical bonds between the layers or chains in the structure, and, as a result, parallel to the acicular axis. The second type of cleavage occurs perpendicularly to acicular axis.

This basal cleavage is observed with or without accompanying prismatic cleavage. Among the minerals with this type of cleavage are jamesonite, owyheeite,<sup>16</sup> and falkmannite<sup>17</sup>. Accordingly, a somewhat different structural scheme than found in the previously determined structures can be expected for jamesonite.

#### Unit cell and space group

The unit cell and space group of the mineral were determined from precession and de Jong photographs using crystals from Cornwall, England, kindly furnished for our investigation from the Harvard mineralogical collection by Professor Clifford Frondel. The results obtained for the unit cell dimensions are:

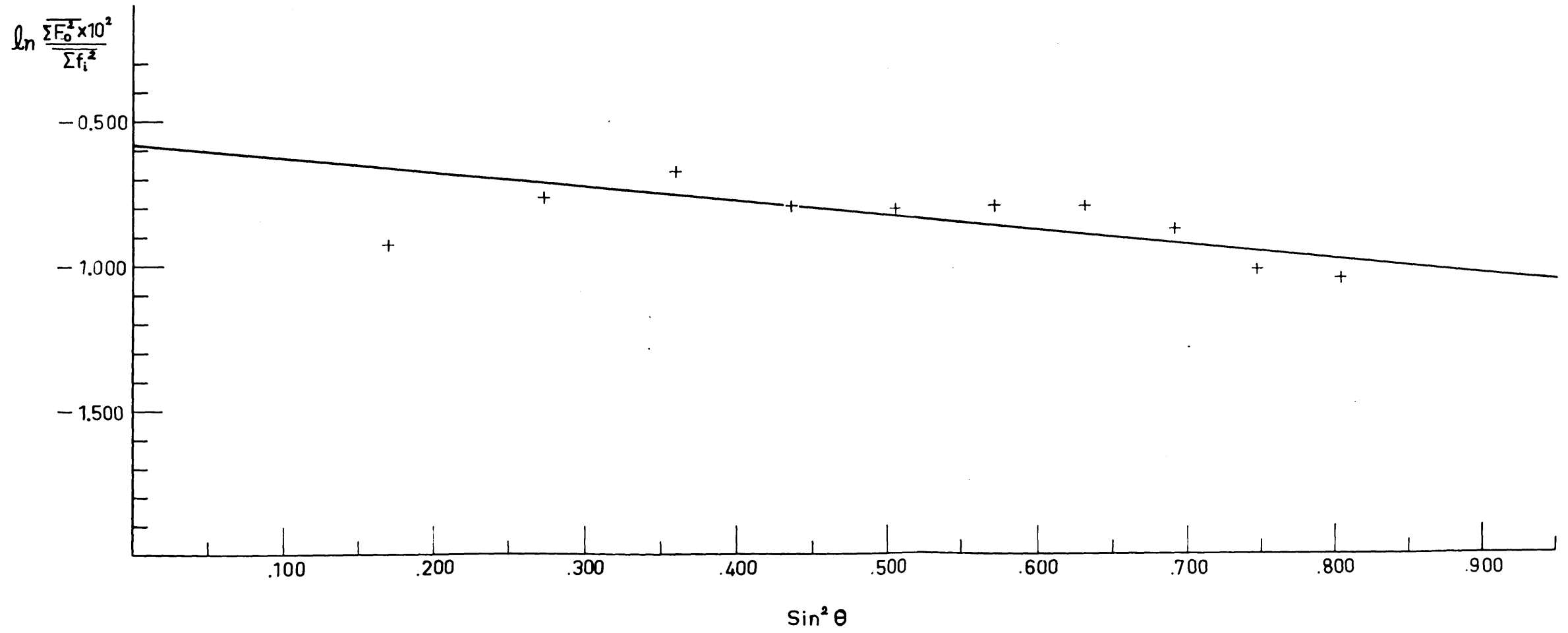
$$\begin{aligned} \underline{a} &= 15.57\text{\AA} \\ \underline{b} &= 18.98\text{\AA} & \beta &= 91^{\circ}48' \\ \underline{c} &= 4.03\text{\AA} \end{aligned}$$

These values are in good agreement with those of Berry. The space group  $\underline{P}2_1/\underline{a}$  assigned by Berry<sup>14</sup> was confirmed. The unit cell contains  $2\text{FePb}_4\text{Sb}_6\text{S}_{14}$ .

#### Intensity determination

A single crystal of needle form having dimensions 0.03mm x 0.04mm x 1.5mm was selected for the intensity determination. The three-dimensional intensities were measured by the single-crystal Geiger-counter-goniometer method developed in the Crystallographic Laboratory,

Fig. 15 Determination of scale factor and temperature coefficient by Wilson's statistical method applied to three-dimensional intensity data.





M.I.T., using  $\text{CuK}\alpha$  radiation. Intensities were then corrected for Lorentz and polarization factors, but no allowance was made for the absorption factor. The  $F^2(hkl)$  values were then placed on an absolute basis using Wilson's method<sup>12</sup> applied three-dimensionally, Fig. 15. The temperature coefficient obtained by this method was  $B = 0.59$ .

#### General outline of the structure determination

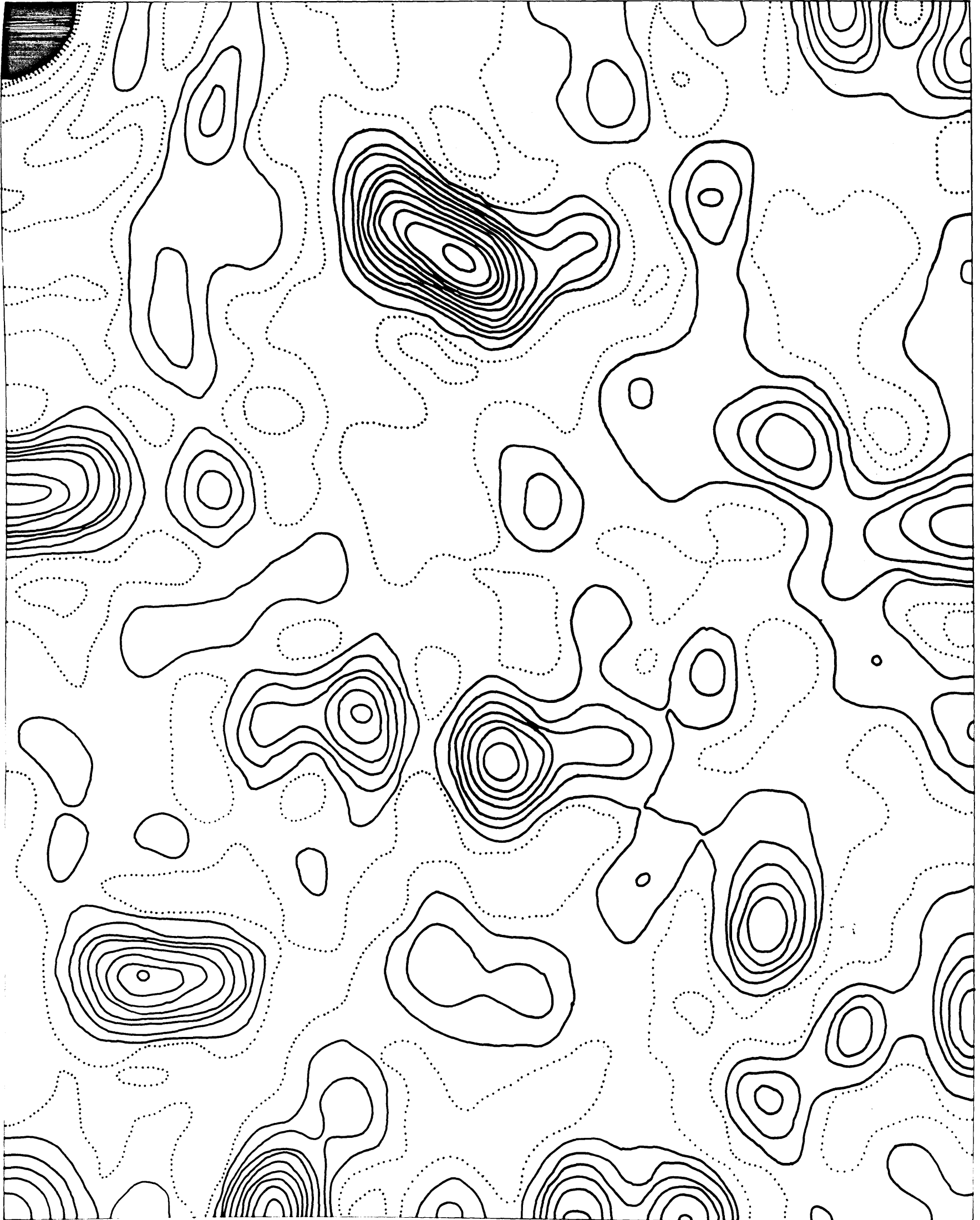
Space-group equipoint considerations fix the position of Fe atoms on one set of centers of symmetry. All the rest of the atoms presumably must occupy the general position  $4(e)$ . The existence of one short axis of length  $4\text{\AA}$  suggests the possibility of solving the crystal structure projected along this axis by means of minimum function method<sup>18</sup>.

As pointed out by Buerger and Hahn elsewhere<sup>4</sup>, errors in the solution by the minimum function method can arise if the Patterson peak chosen as the image point is not a single peak, but rather a coalescence of several peaks. During the present case of structure determination of jamesonite, a false structure was obtained from the image point incorrectly selected. This false structure appeared very similar to the expected structure, at least in numbers of heavy peaks representing Pb and Sb atoms. The falseness of the structure could not be detected until

Fig. 16 Patterson diagram  $P(\underline{xy})$ . The dotted contours represent depressions. The details of the heavy peaks at the origin are omitted.

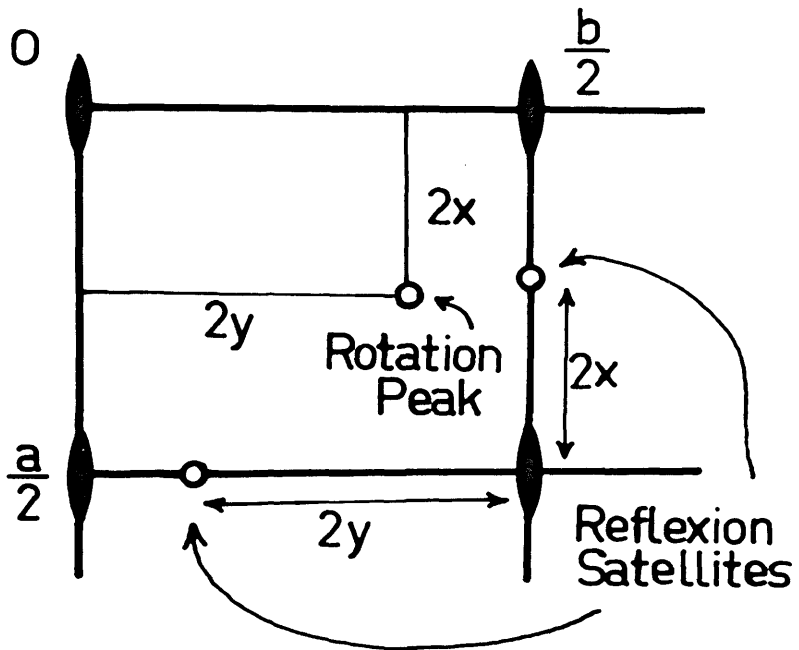
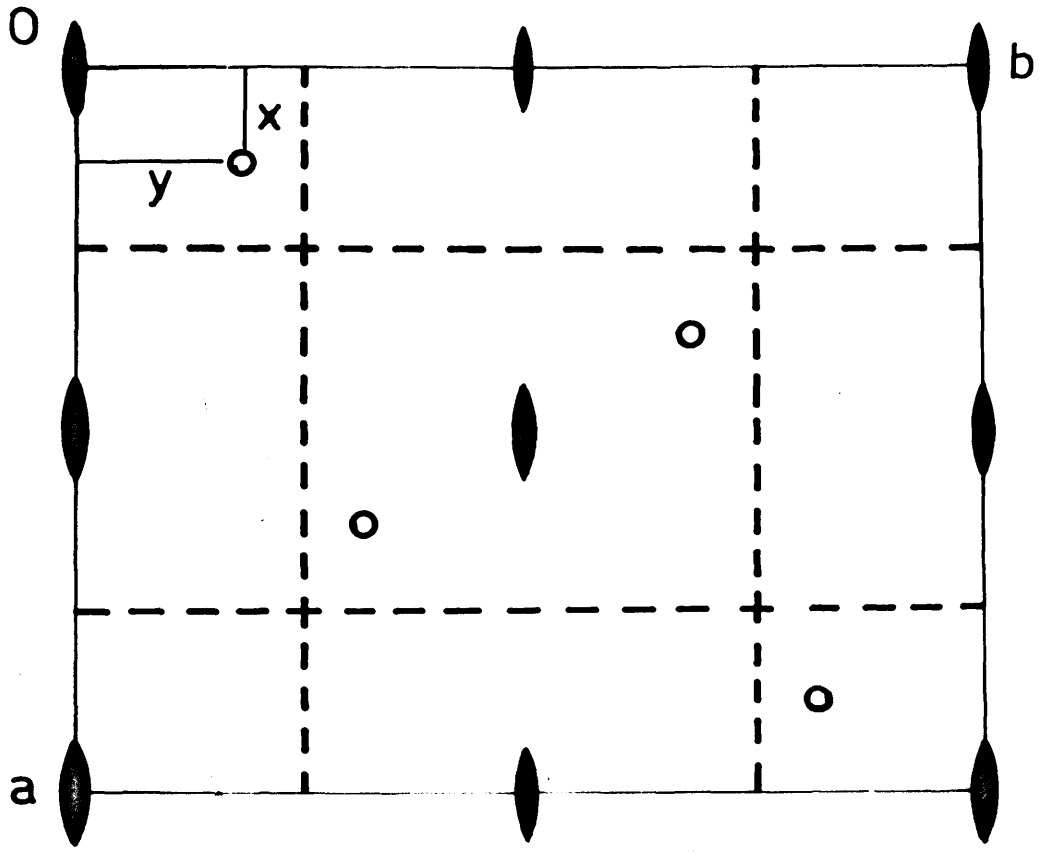
0

$\frac{a \cdot \sin^2 \theta}{2}$



b/2

Fig. 17 Geometrical relation between a rotation peak and its reflection satellites in Patterson diagrams having plane group symmetry  $\underline{p2mm}$ .



a final electron density map indicated certain abnormalities of the structure. Since this kind of confusion is apt to occur when the image-seeking method is applied to solve structures with large unit cells having many heavy atoms, such as of many sulfosalt minerals, the discussion of the procedure will be given in some detail below.

#### Interpretation of Patterson peaks

The Patterson map  $P(\underline{xy})$ , Fig. 16, was obtained from  $F^2(hk0)$ 's. The plane group of projection along  $c$  axis of space group  $P2_1/a$  is  $p2gg$ , and the corresponding Patterson plane group is  $p2mm$ . The relation between rotation peak and its reflection satellites in this plane group is illustrated in Fig. 17. Since there are 2 Pb atoms and 3 Sb atoms in the asymmetric unit, if no overlapping occurred, there must be 5 rotation peaks of single weight, and 10 reflection satellites of double weight in a quarter of Patterson space. Actually, as shown in Fig. 16, there are 6 peaks along the line  $\underline{x} = \frac{1}{2}$ , and 8 peaks along the line  $\underline{y} = \frac{1}{2}$ . These peaks have various heights, and the broadened shapes of some peaks at once suggest a considerable amount of overlapping at these locations. The excess number of peaks appearing along these lines is considered due to either the interatomic vectors with accidental  $\underline{x}$  or  $\underline{y}$  component

Fig. 18 Solution of rotation peaks from satellite-like peaks. Solution are obtained at the intersections of horizontal and vertical lines drawn according to the relation illustrated in Fig. 17. Satellite-like peaks are designated by letters a to l, and the corresponding lines are designated by letters A to L. Three probable rotation peaks obtained by this method are indicated by I, II, and III.

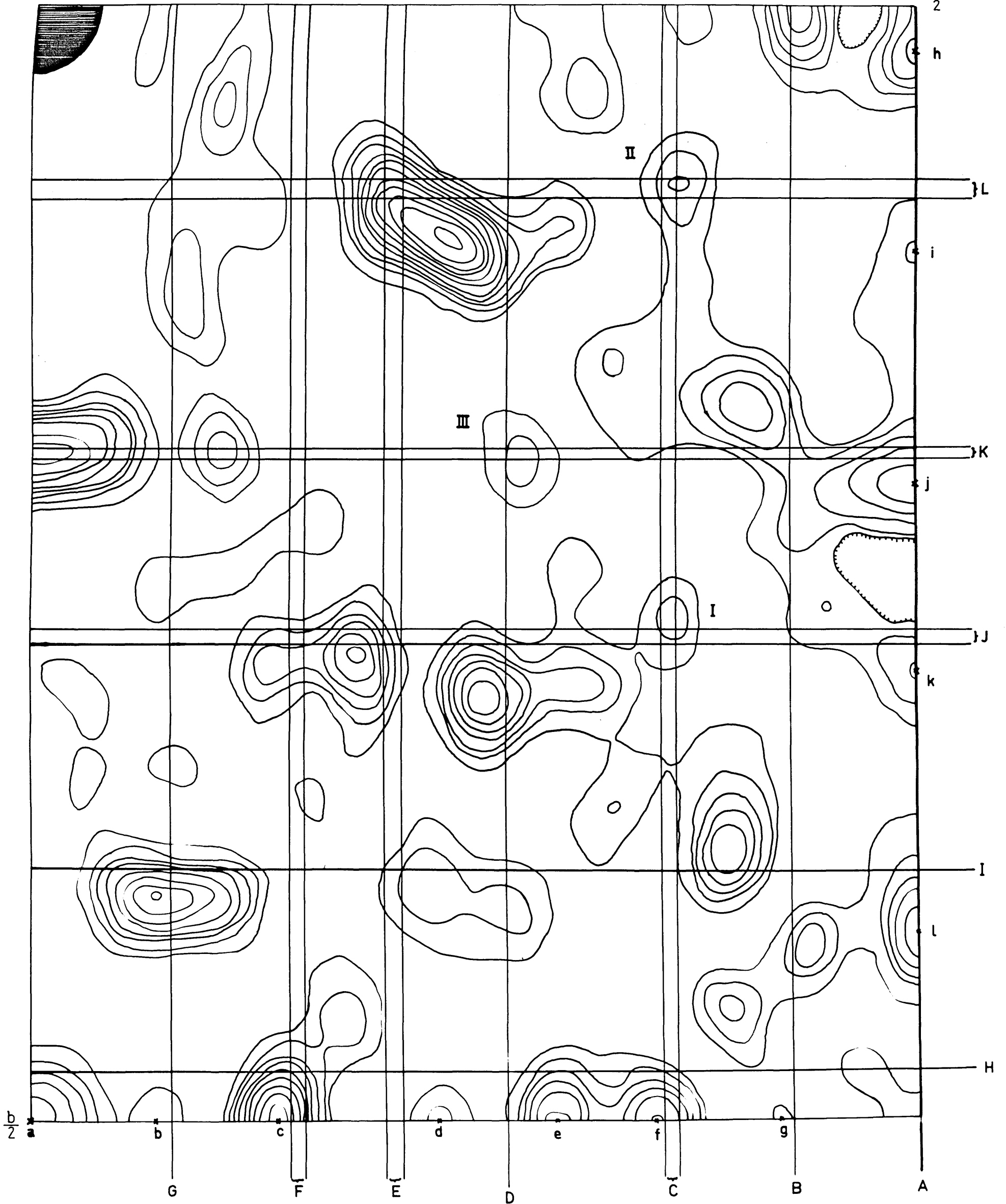
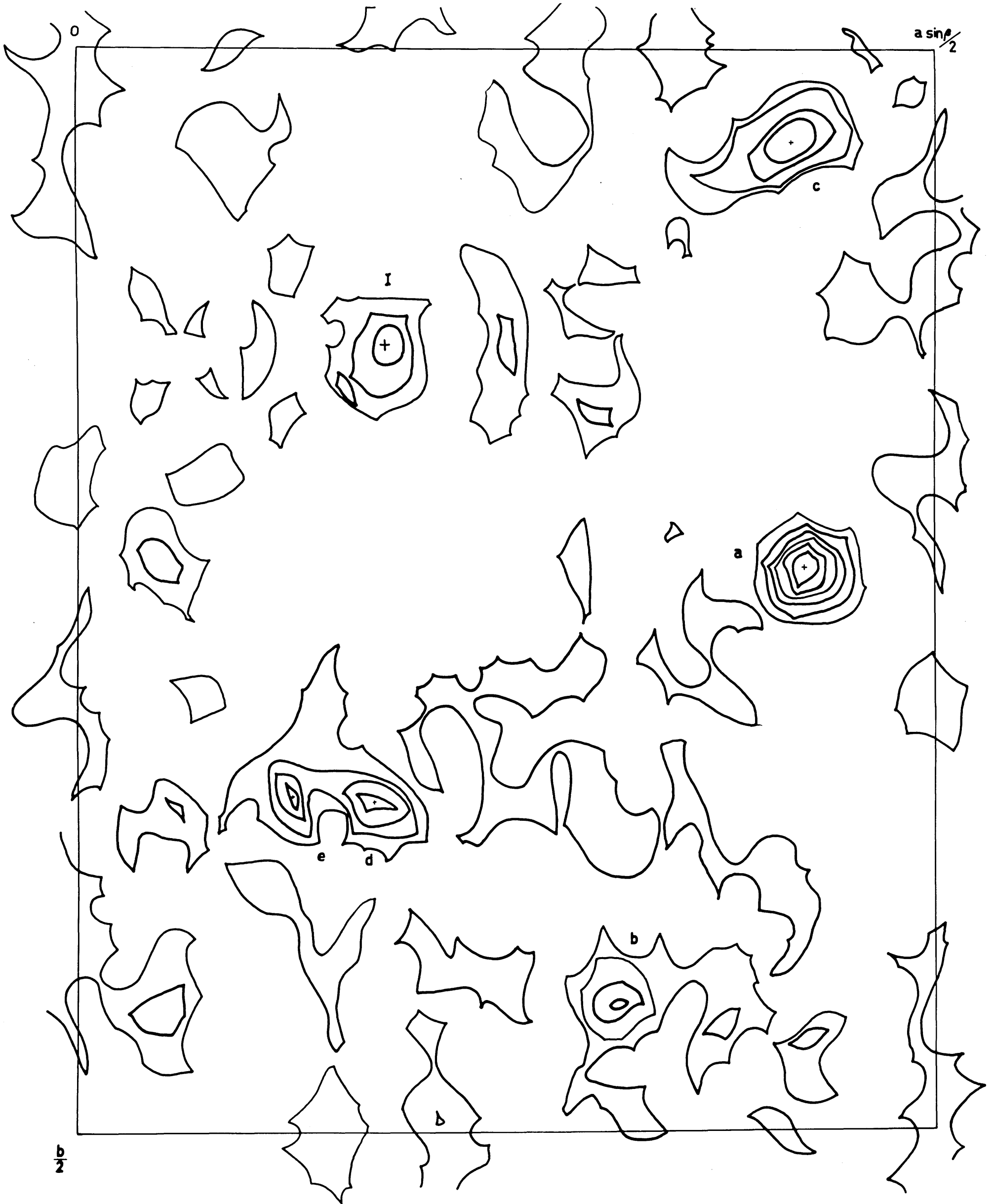




Fig. 19  $\underline{I}_{M_4}$  map.



$a \sin^2/2$

$b/2$

i

a

e

d

b

Fig. 20  $II_{\underline{M}_4}$  map.

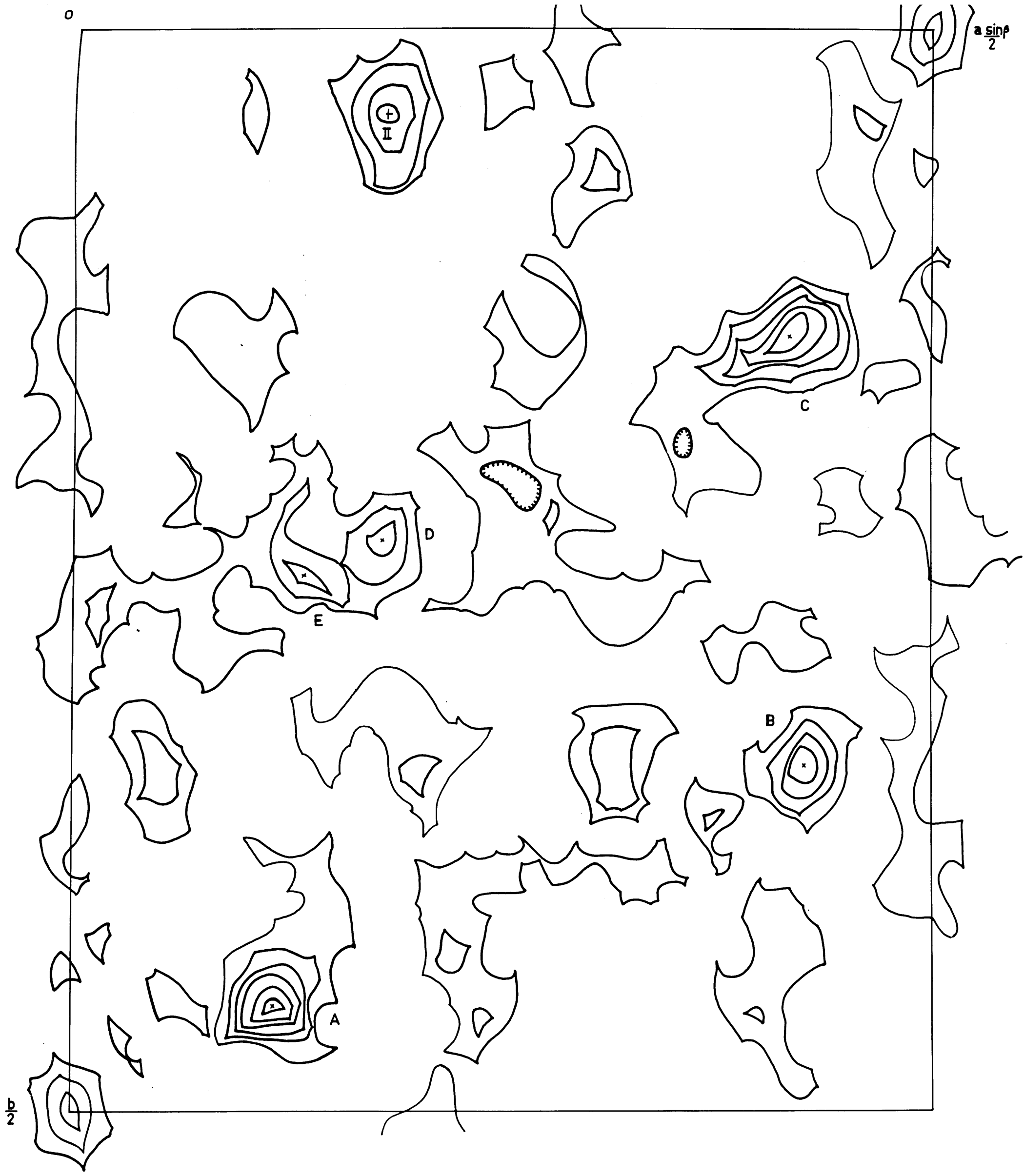
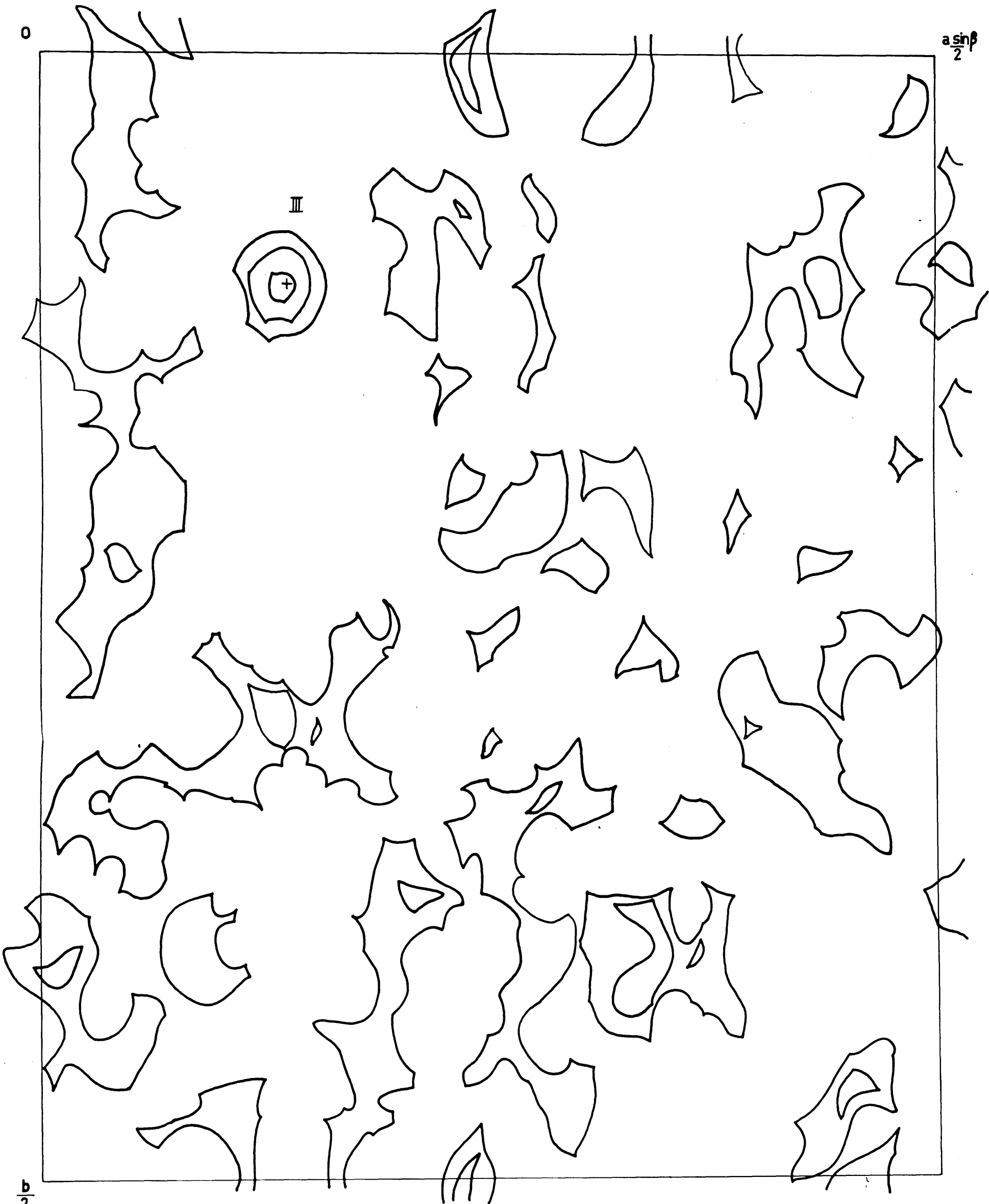


Fig. 21  $III_{\underline{M}_4}$  map.

$a \sin \beta$   
2

0



$\frac{b}{2}$

of  $\frac{1}{2}$ , or coalescence of reflection satellites of S atoms.

Since it was impossible to choose definite satellite peak among them, all the satellite-like peaks were used to find possible rotation peaks. Among 48 possible positions for rotation peaks, Fig. 18, only three of them are associated with peaks which can be assumed reasonably as single-weight rotation peaks. The peak height analysis was done assuming a probable zero contour, and it was found that all three of the peaks could be Pb-Pb rotation peaks. These peaks are numbered as peak I, II, and III in Fig. 18.

#### Solutions by the image-seeking method

Assuming each of these three peaks as an image point, three sets of  $\underline{M}_2$  functions in turn were obtained, and each of them was folded into an  $\underline{M}_4$  function using a glide operation. These three  $\underline{M}_4$  maps are shown in Figs. 19, 20, and 21. Among them the  $^{III}\underline{M}_4$  map (an  $\underline{M}_4$  map based upon the assumption that peak III is a Pb-Pb rotation peak) gave a result completely unrelated to the expected number of heavy atoms in the structure, Fig. 21, and was accordingly discarded. Since both the  $^I\underline{M}_4$  map and the  $^{II}\underline{M}_4$  map gave 6 heavy peaks, no choice between them was considered at this stage. Henceforth, the structures based on peak I and II will be identified as structures I and II respectively. To resolve an extra peak in each

Fig. 22  $I+a_{\underline{M}_8}$  map. Black dots indicate the final atomic sites for S atoms determined by Fourier method.

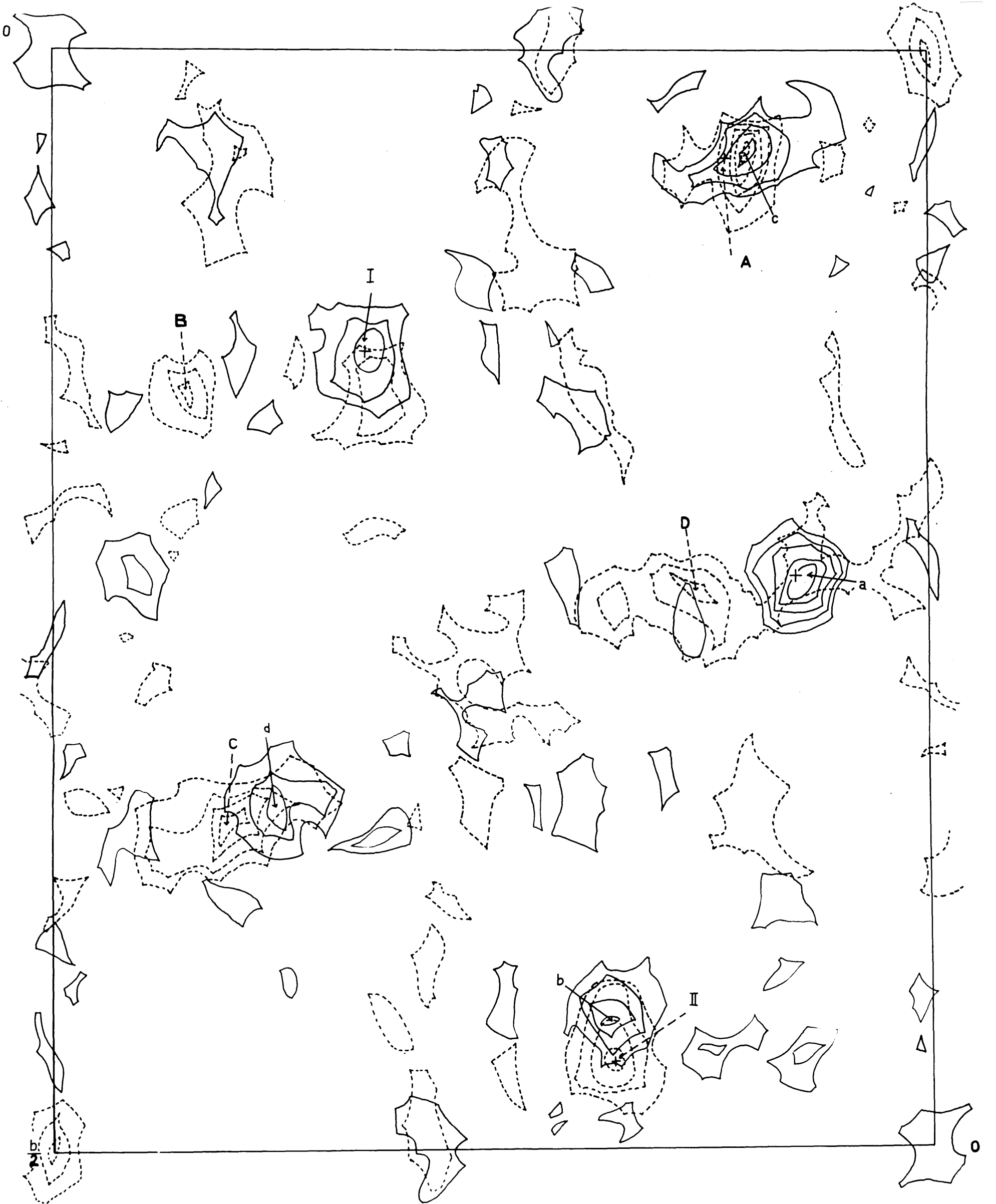


$a \sin^2 \frac{\rho}{2}$



$\frac{b}{2}$

Fig. 23 Comparison of two  $\underline{M}_8$  maps. The  $\text{I}+\text{a}_{\underline{M}_8}$  map is drawn in full lines, and the  $\text{II}+\text{A}_{\underline{M}_8}$  map in broken lines.



map, another  $\underline{M}_4$  map was tried for each structure. The peak with the heaviest contour in each  $\underline{M}_4$  map was assumed as the second probable site for the Pb atom. In structure I, Fig. 19, it is designated as peak  $\underline{a}$ , and in structure II, Fig. 20, as peak  $\underline{A}$ . The  $\underline{aM}_4$  map and the  $\underline{AM}_4$  map were then prepared. Under the assumption that the atoms at  $\underline{I}$  and  $\underline{a}$  in one structure, and  $\underline{II}$  and  $\underline{A}$  in the other, are all of the same atomic specie, i.e. Pb, the  $\underline{I+aM}_8$  and  $\underline{II+A M}_8$  maps can be obtained by superposing the proper  $\underline{M}_4$  maps. The  $\underline{I+aM}_8$  map, which was later found to represent the correct structure, is shown in Fig. 22. Also in Fig. 23, two  $\underline{M}_8$  maps were compared, one map  $\underline{I+aM}_8$  in full lines, and the other  $\underline{II+A M}_8$  in dotted lines. From this comparison, however, nothing indicates which is the correct one.

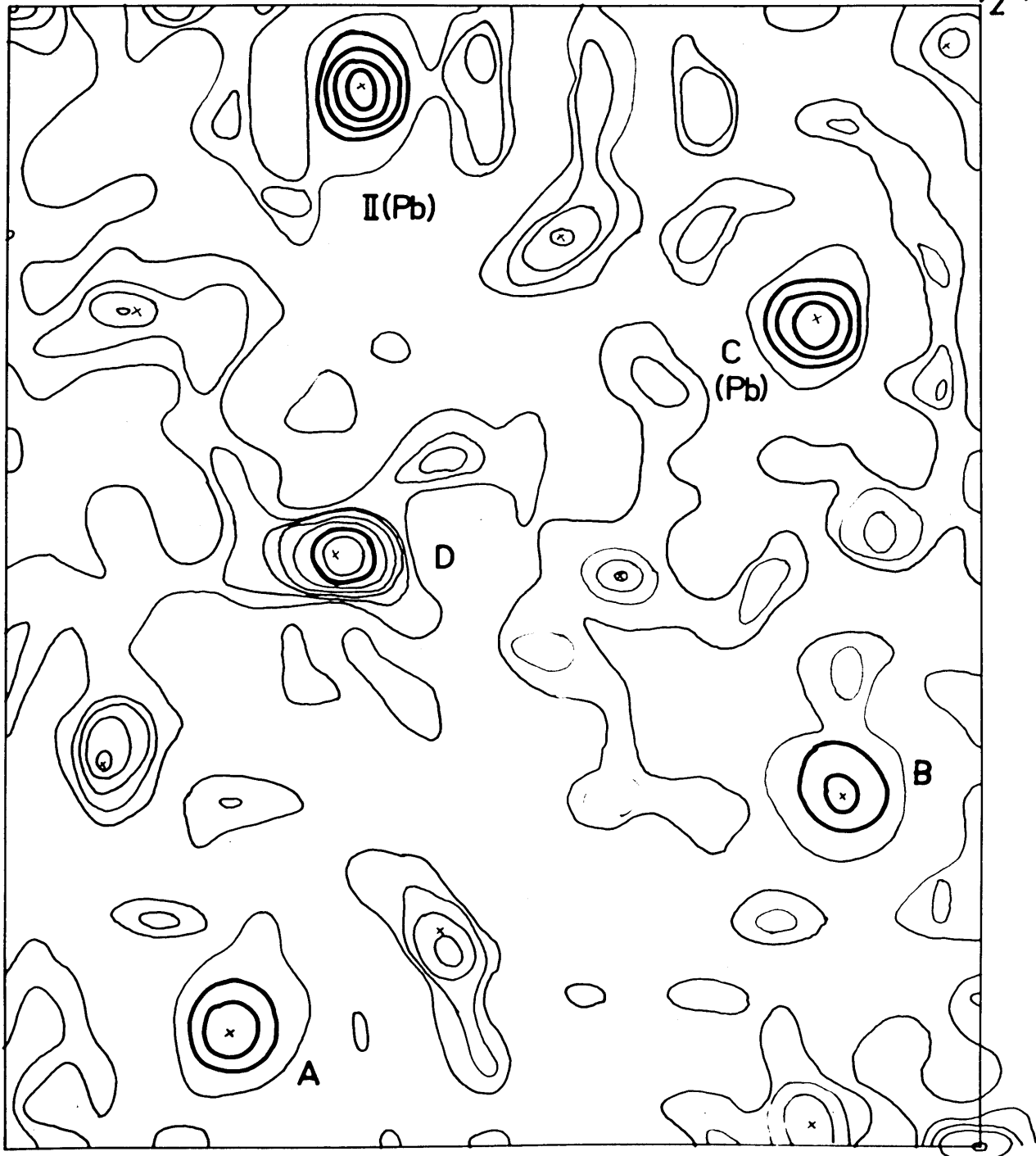
#### False structure

First the structure II was assumed to be correct, and since the identification of heavy peaks in the  $\underline{M}_8$  map with Pb and Sb was impossible, structure factors were computed using an average  $\underline{f}$ -curve,  $\frac{1}{2}(f_{\text{Pb}} + f_{\text{Sb}})$ . The electron-density map was prepared using signs determined in this way, and then refined by the usual procedures. The final electron-density map of structure II and its structural scheme, are shown respectively in Figs. 24 and 25. The examination of  $\rho(\underline{xy})$ , Fig. 24, in detail, however, reveals several peculiarities which are enough to

Fig. 24 Electron-density map  $\rho(\underline{xy})$  of false structure based on  $II+A_{\underline{M}_8}$  map.

0

$\frac{a}{2}$



$\frac{b}{2}$

Fig. 25 Structural scheme of false structure,  
Fig. 10.

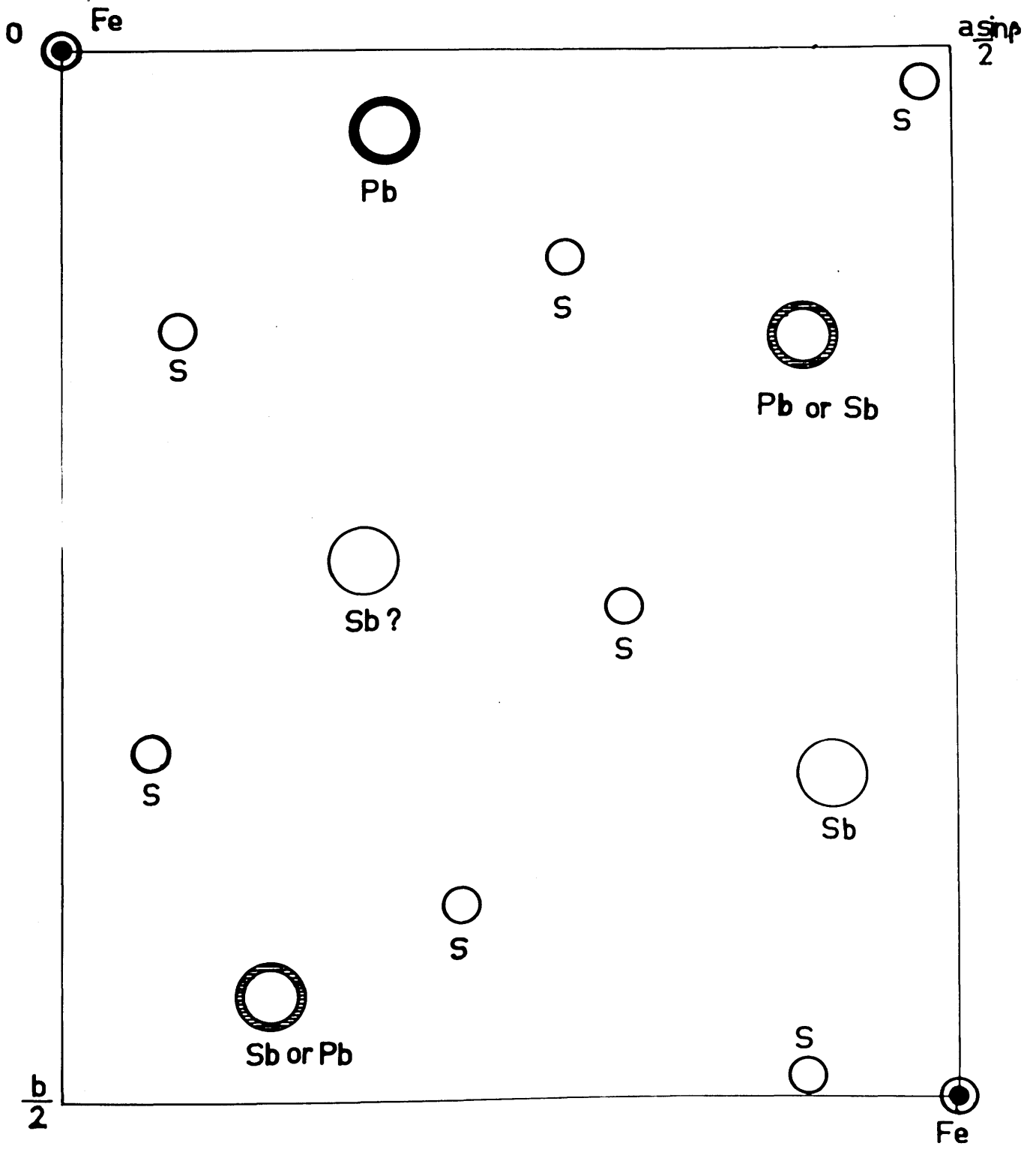
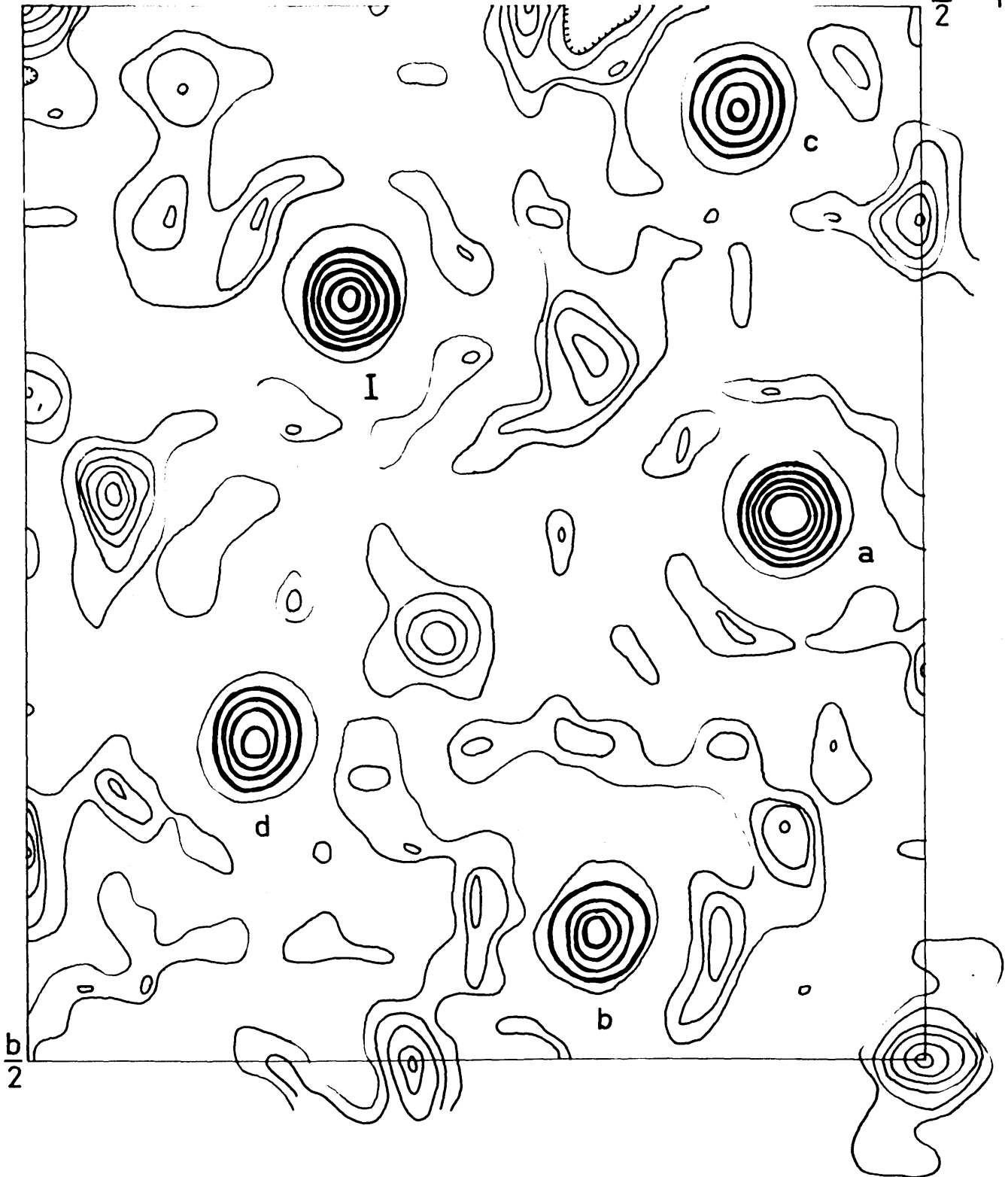




Fig. 26 Electron-density map  $\rho(\underline{xy})$  of correct structure based on  $I^{+a}_{\underline{M}_8}$  map.

0

$\frac{a \sin \beta}{2}$



raise a question as to the validity of this structure. First, the relative weights of the five heavy peaks do not correspond to the chemical formula of jamesonite in a clear-cut way. Above all, there is one peak, peak D in Fig. 24, much too low to be assigned to an Sb atom. Furthermore, the shape of this particular peak is not well defined. The above-mentioned aspects for the structure could not be improved by exchanging Pb with Sb in some of the atomic sites. Second, the peak shapes of the lighter atoms, especially of the Fe atom at the origin, are obscure. For these reasons structure II was considered incorrect. The significance of those features in the Fourier diagrams which suggest an incorrect structure was recently pointed out by Pinnock et al<sup>19</sup>.

#### Correct structure

The alternative structure I based on the  $I+a_{\underline{M}_8}$  map was then tried. Structure factors were computed as before with the averaged  $\underline{f}$ -curve. The electron-density map is shown in Fig. 26. In this map the shapes and the weight relations among the five heavy peaks are well defined. Peaks I and a are assigned to Pb atoms, and peaks b, c, and d to the three Sb atoms.

Because of the identity of peaks I and a, the superposition of the  $I_{\underline{M}_4}$  and  $a_{\underline{M}_4}$  maps was justified, and this  $I+a_{\underline{M}_8}$  map, Fig. 26, should contain enough information concerning the locations of S atoms. Although the

Fig. 27 Two  $\underline{M}_8$  maps superposed. The  $\overset{I+a}{\underline{M}_8}$  map is drawn in full lines, and the  $\overset{b+c}{\underline{M}_8}$  map is in dotted lines. Black dots indicate the final locations of S atoms determined by Fourier method.

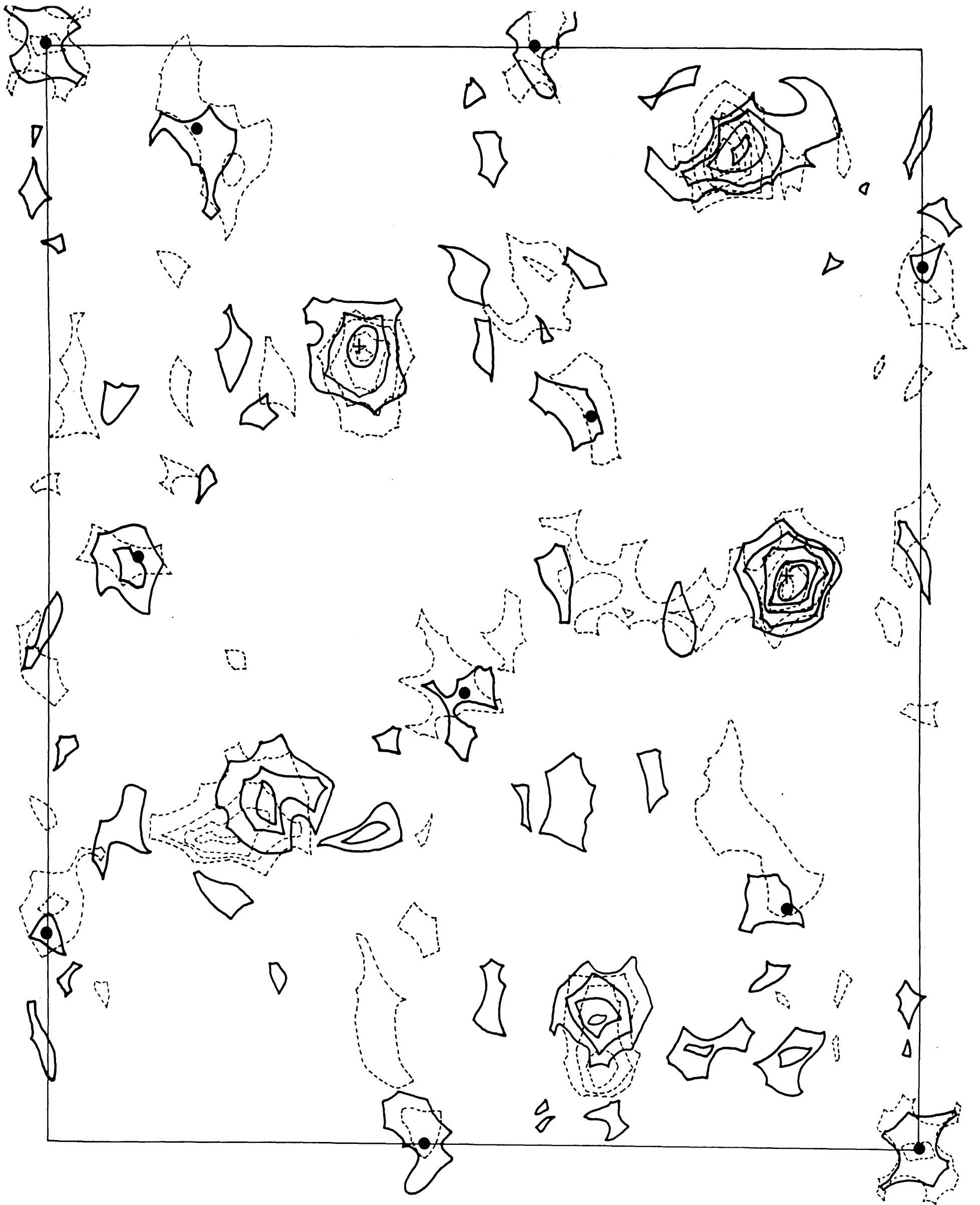
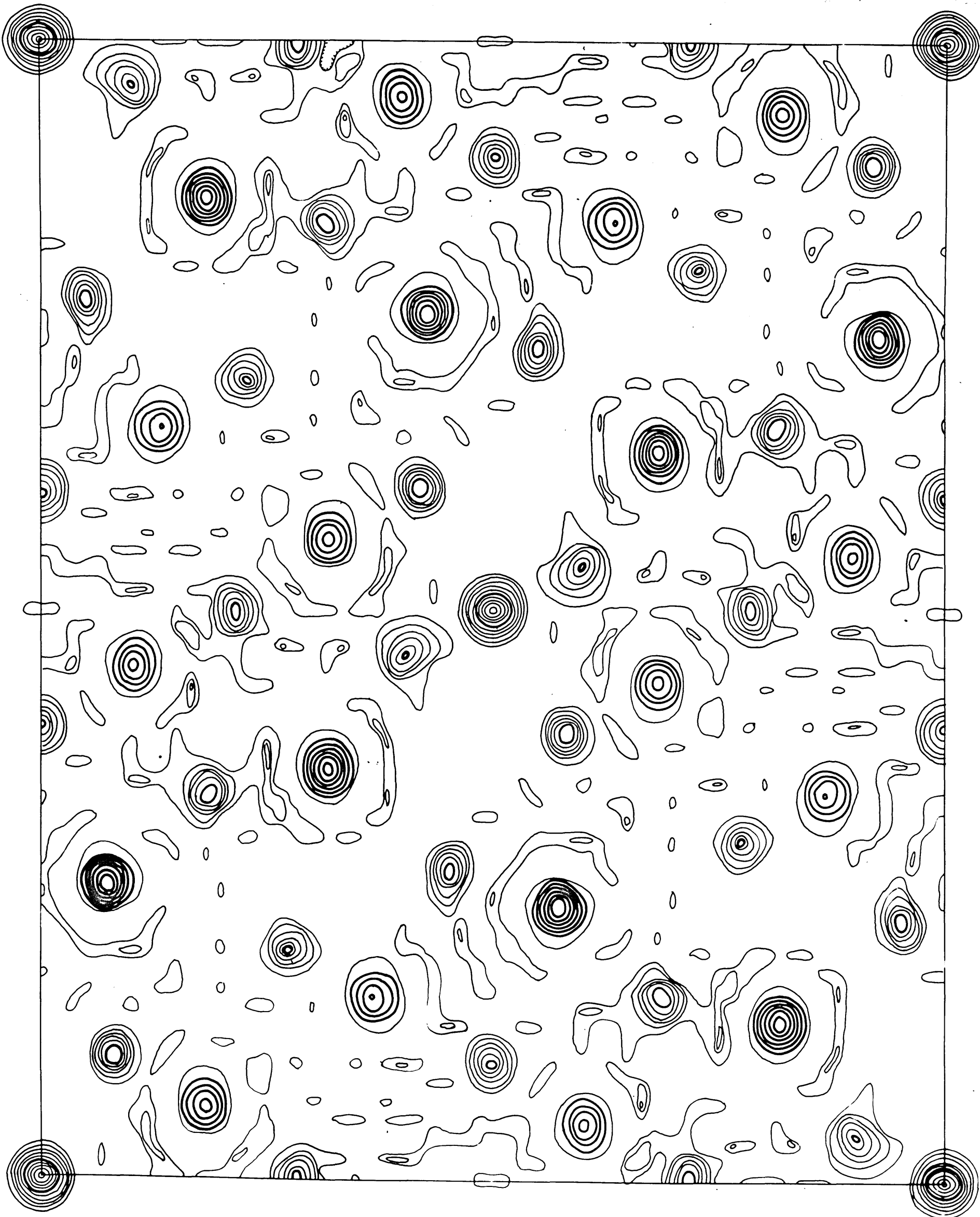


Fig. 28 Final electron-density map  $\rho(\underline{xy})$ .

0

a



b

refinement of the electron-density map, Fig. 26, should naturally indicate the sulfur peaks, it was considered useful to see how the image-seeking method would narrow the allowed region for the S atoms. This process was carried out by further constructing a  $b+c$   $\underline{M}_8$  map based on the rotation peaks  $b$  and  $c$ , both Sb-Sb rotation peaks. This map is shown in Fig. 27 in broken lines superposed with the previously obtained  $I+a$   $\underline{M}_8$  map, which is drawn in full lines. Since these two  $\underline{M}_8$  maps are based on rotation peaks of different weights (different atomic species), the simple superposition to obtain an  $\underline{M}_{16}$  map could not be done without proper weighting for contours. The final sulfur positions found by the Fourier method are indicated in Fig. 27 by black dots. They are all at locations permitted by the minimum-function maps. Including these sulfur atoms in the structure-factor computation, the refinement of structure I was done by successive difference-Fourier maps. The final atomic coordinates determined by this process are presented in Column III of Table 11. The reliability factor of this projection was computed as  $R = .19$ .

The final electron-density map prepared with signs after the three-dimensional refinement is shown in Fig. 28 for the full unit cell.

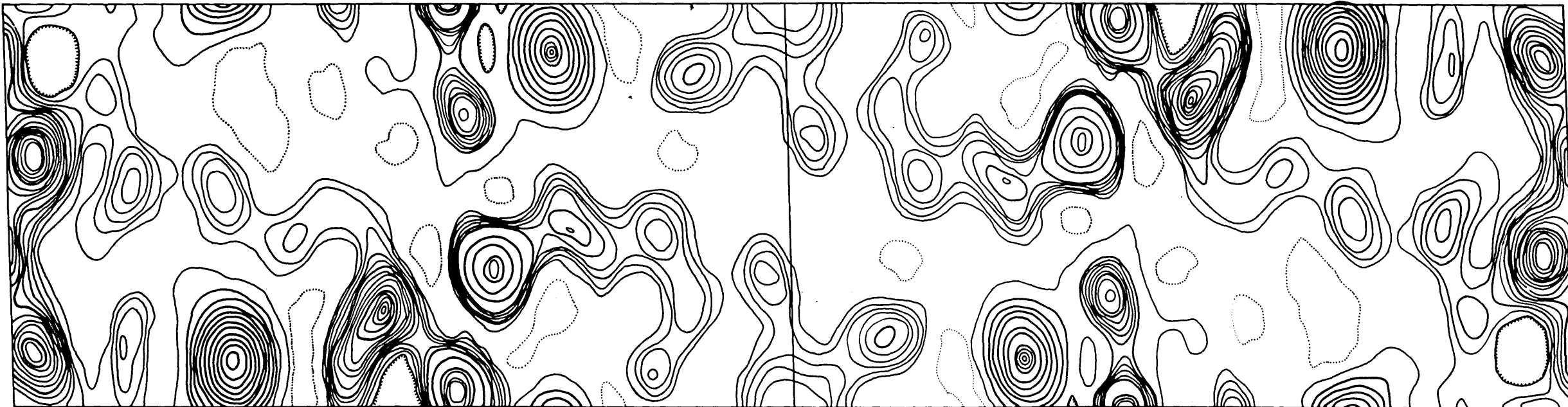
#### Determination of $z$ coordinates of atoms

The  $z$  parameters of the heavy atoms were determined



Fig. 29 Harker section  $\underline{P}(\underline{x}_2^1z)$ . Heavy contours represent the intervals of 5 light contours. The details between the heavy contours are omitted.

c



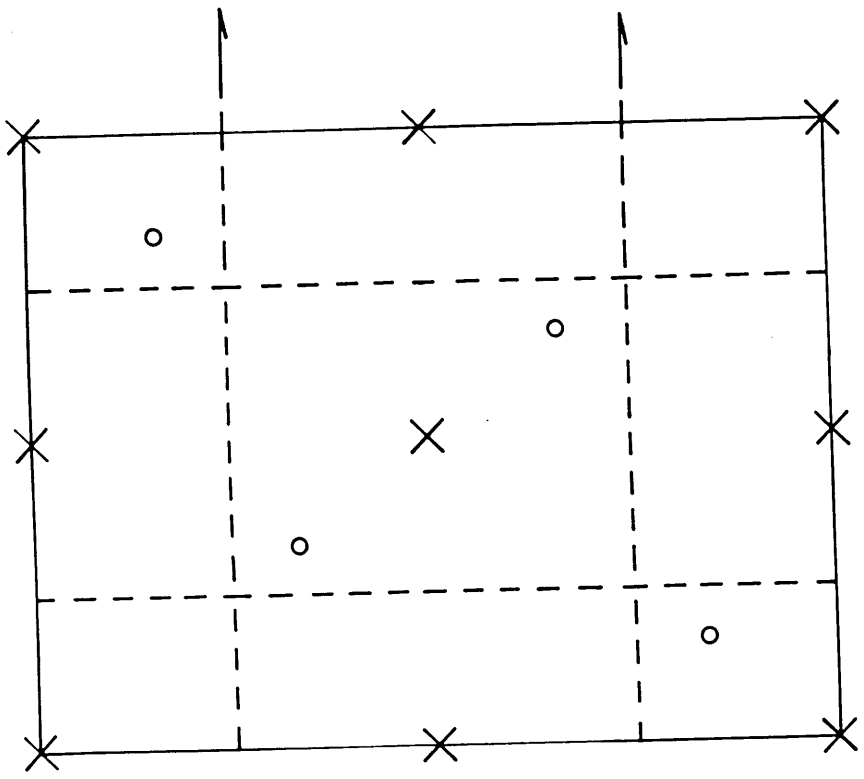
0

$\frac{a}{2}$

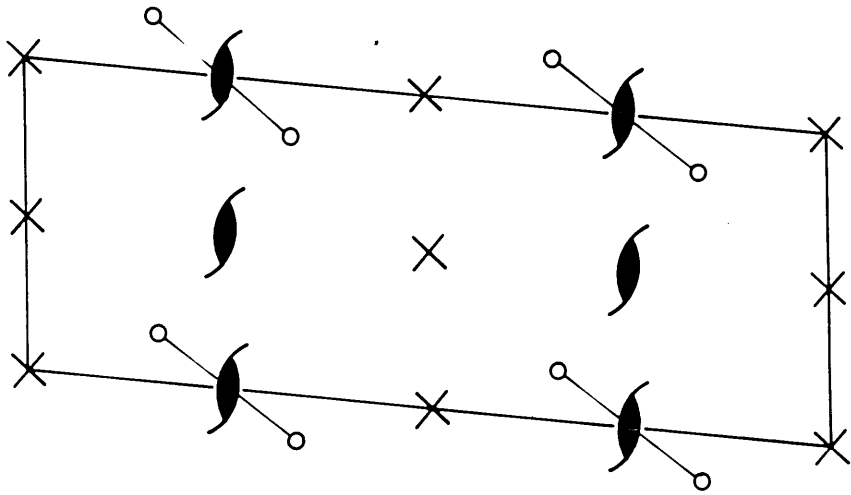
a

Fig. 30 Relations between crystal space, Patterson space, and implication space.

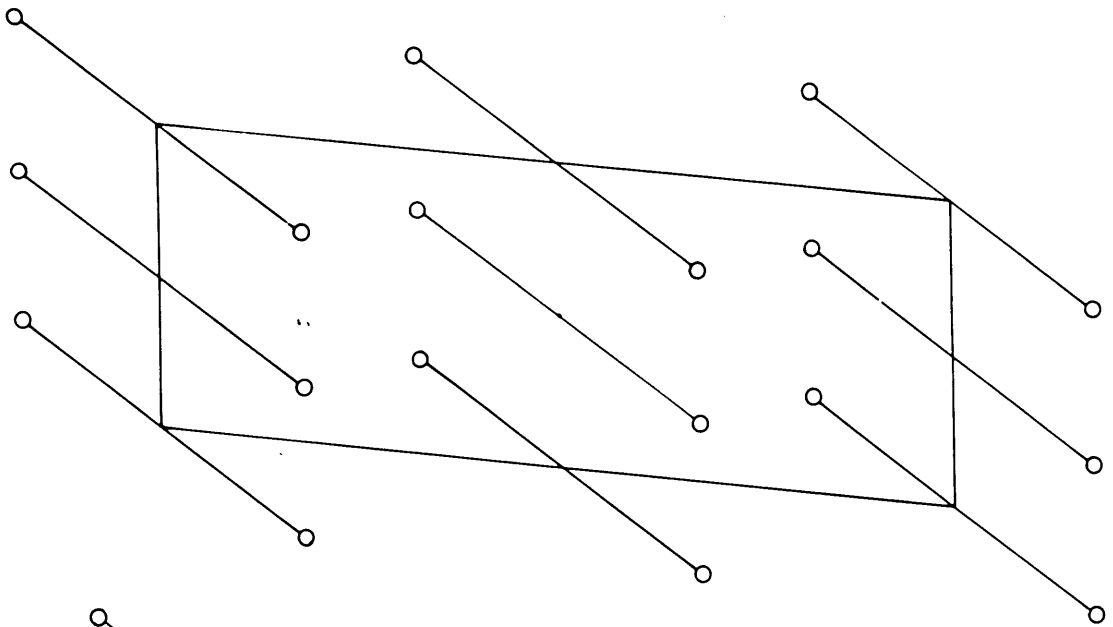
In drawings (a) and (b), space group  $P2_1/a$  is shown in two projections. In crystal space the general equipoints  $4(e)$  are indicated by small circles. Drawing (c) represents the Harker section derived from (b). The origin is shifted from a center of symmetry to a  $2_1$  axis. The sub-multiple translation  $a/2$  is evident. In drawing (d) is shown the corresponding implication space,  $I(x\frac{1}{2}z)$ . The origin is again shifted to a center of symmetry to compare with the crystal space. The 4-fold ambiguity is evident.



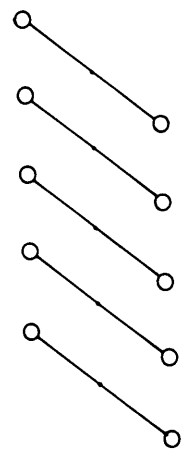
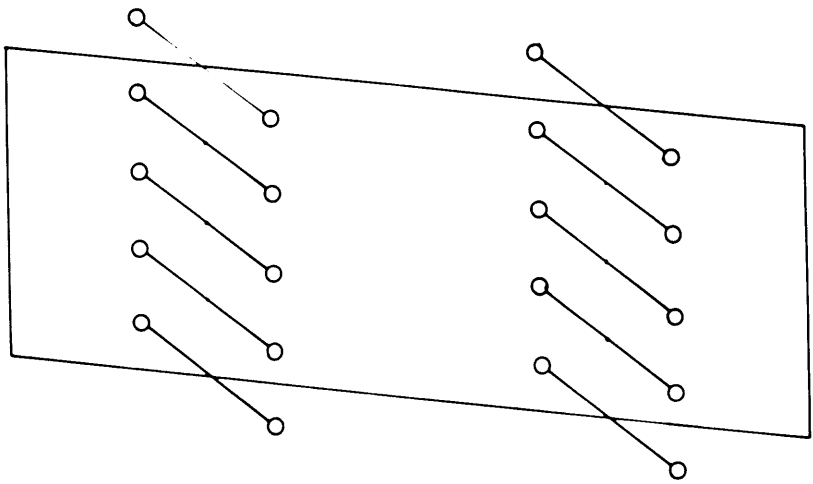
a



b



c



d

Fig. 31 Implication map  $I(\underline{x}\frac{1}{2}\underline{z})$ , and its interpretation. In the upper drawing the implication map is shown. In the lower drawing the  $\underline{x}$  coordinates of the heavy atoms are indicated by circles on the straight line. The atoms related to each other by screw operations are indicated by primes. The  $\underline{z}$  coordinate of each atom can be determined by tracing up the broken line into the implication map. Two-fold ambiguity of the solution is solved if interatomic distances in the projection  $\rho(\underline{xy})$ , Fig. 14, are taken into consideration.

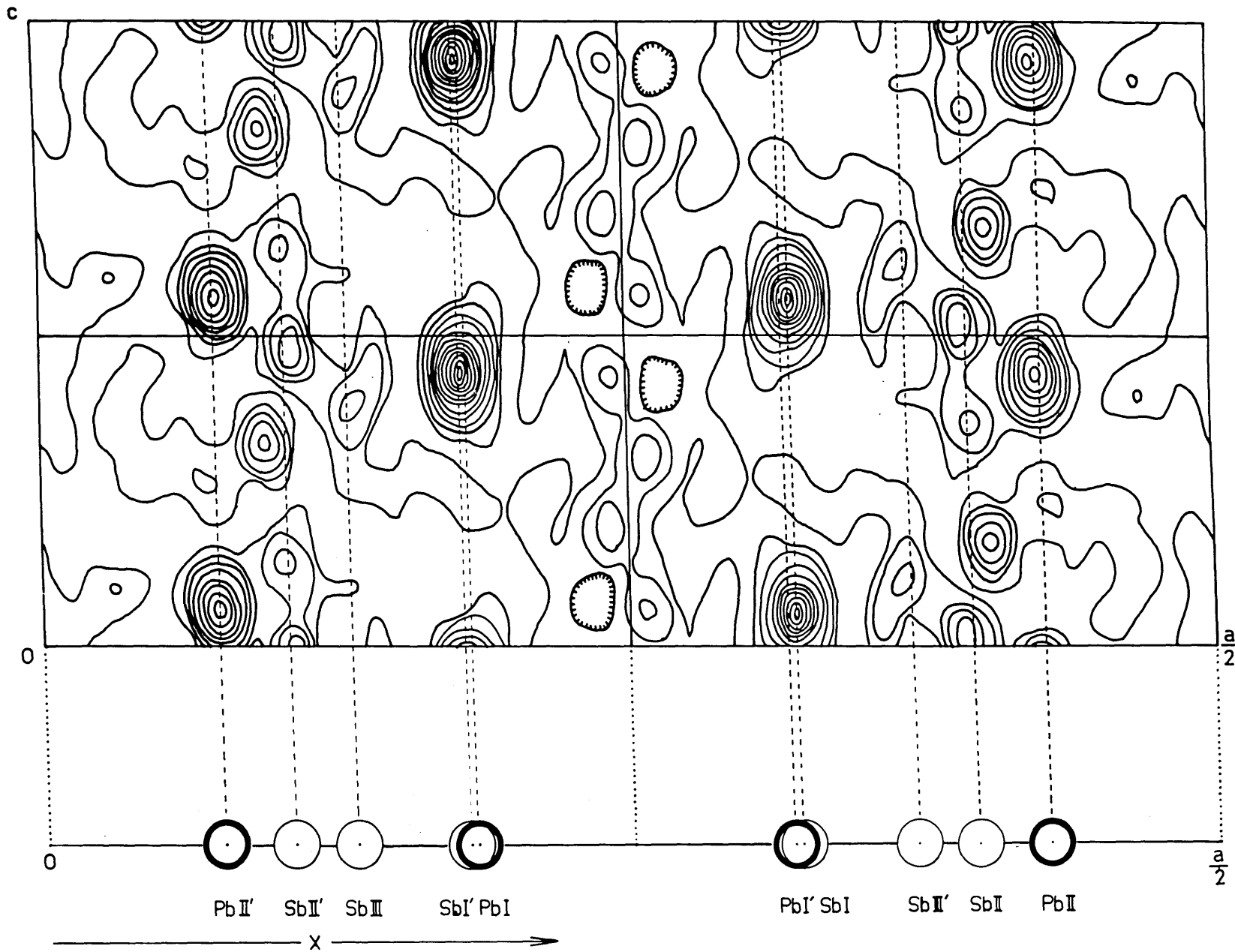


Table 11

Atomic coordinates determined by several methods.

Atom	I		II	III		
	From minimum-function map.		From implication-map	From Fourier maps		
	x	y	z	x	y	z
Pb <sub>I</sub>	.183	.136	.060	.184	.139	.066
Pb <sub>II</sub>	.425	.240	.060	.428	.240	.040
Sb <sub>I</sub>	.320	.436	.480	.320	.436	.488
Sb <sub>II</sub>	.400	.050	.570	.398	.049	.592
Sb <sub>III</sub>	.128	.346	.620	.132	.340	.628
S <sub>I</sub>				.423	.393	.000
S <sub>II</sub>				.102	.043	.460
S <sub>III</sub>				.316	.160	.540
S <sub>IV</sub>				.227	.296	.940
S <sub>V</sub>				.045	.230	.560
S <sub>VI</sub>				.010	.397	.920
S <sub>VII</sub>				.282	.009	.060
Fe				.000	.000	.000
						$R(\underline{hk0}) = .19$
						$R(\underline{h0l}) = .24$
						$R(\underline{hkl}) = .28$

by the implication method<sup>20</sup>. A Harker synthesis  $\underline{P}(\underline{x}\frac{1}{2}\underline{z})$  was performed and the result is shown in Fig. 29. The relations between crystal space, Patterson space, and implication space are illustrated in Fig. 30 for the general equipoints  $2(\underline{e})$  of plane group  $p2$ . There are sub-multiple translation of  $\underline{a}/2$  in these projections. In Fig. 41, therefore, the implication map corresponding to this sub-multiple cell is shown. Underneath the  $\underline{I}(\underline{x}\frac{1}{2}\underline{z})$  map is placed the heavy atoms with the  $\underline{x}$  coordinates determined from  $\rho(\underline{xy})$ . The 4-fold ambiguities were resolved first by assuming as zero the  $\underline{z}$  coordinate of the center of symmetry where the Fe atom is located, then by measuring the projected interatomic distances in  $\rho(\underline{xy})$ . Approximate  $\underline{z}$  coordinates for the Pb atoms were found to be zero, and those for Sb atoms were found to be  $\underline{c}/2$ . The  $\underline{z}$  parameters determined in this way are tabulated in Column II of Table 11. A few extra peaks of medium weights are observed in the implication map, Fig. 31. These are explained as due to interatomic vectors between atoms not related by a screw operation but with  $\underline{y}$  components of nearly  $\frac{1}{2}$ . Such a vector gives part of a Patterson peak in a Harker section.

With an initial set of signs of structure factors determined by the heavy atoms, an electron-density map  $\rho(\underline{xz})$  was obtained, and then refined in the usual way. The final  $\underline{z}$  coordinates determined by the Fourier method are tabulated in Column III of Table 11, along with  $\underline{x}$  and  $\underline{y}$  coordinates. The reliability factor of this projection was computed as



Fig. 18 Final electron-density map  $\rho(\underline{xz})$ .

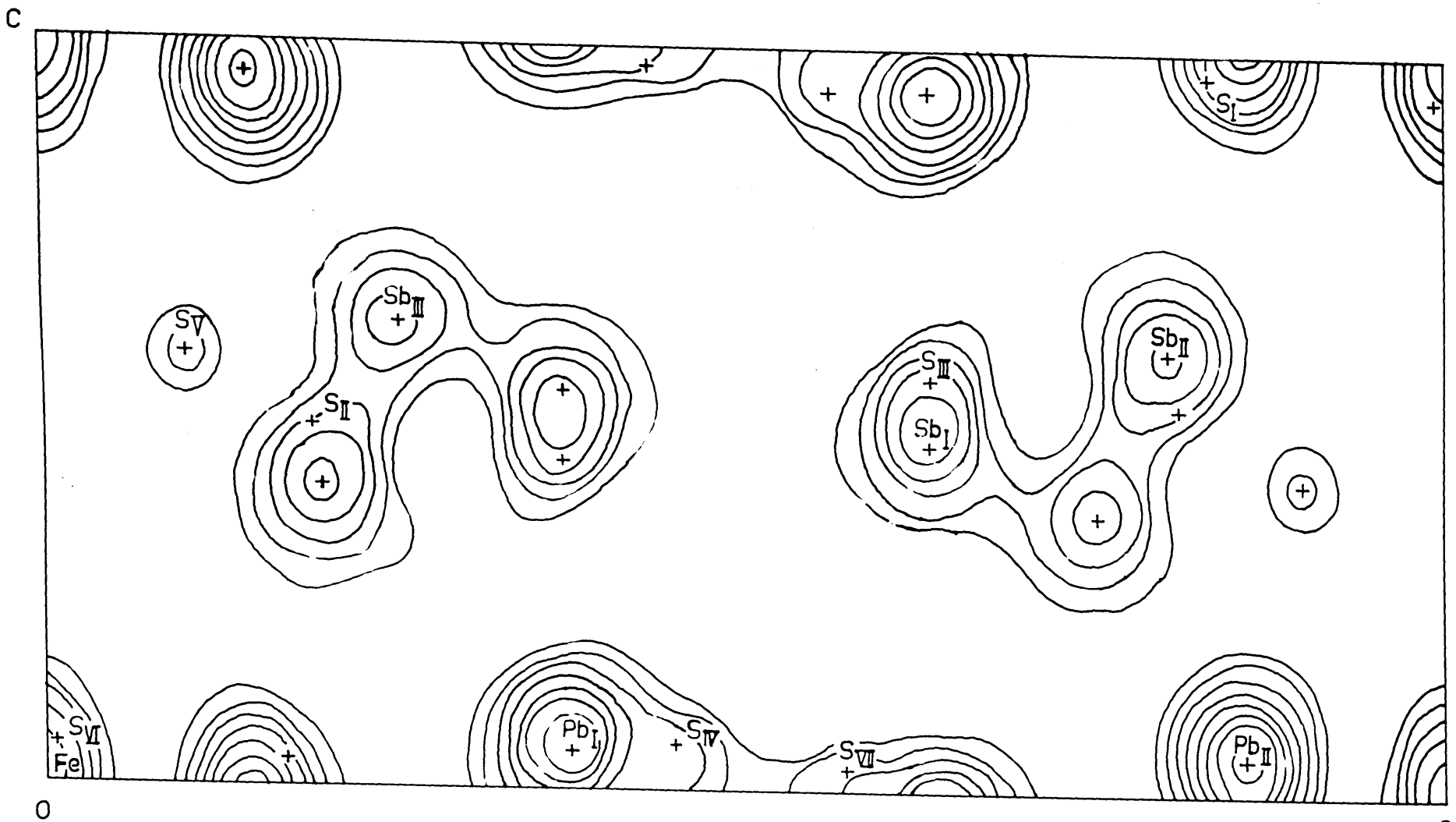
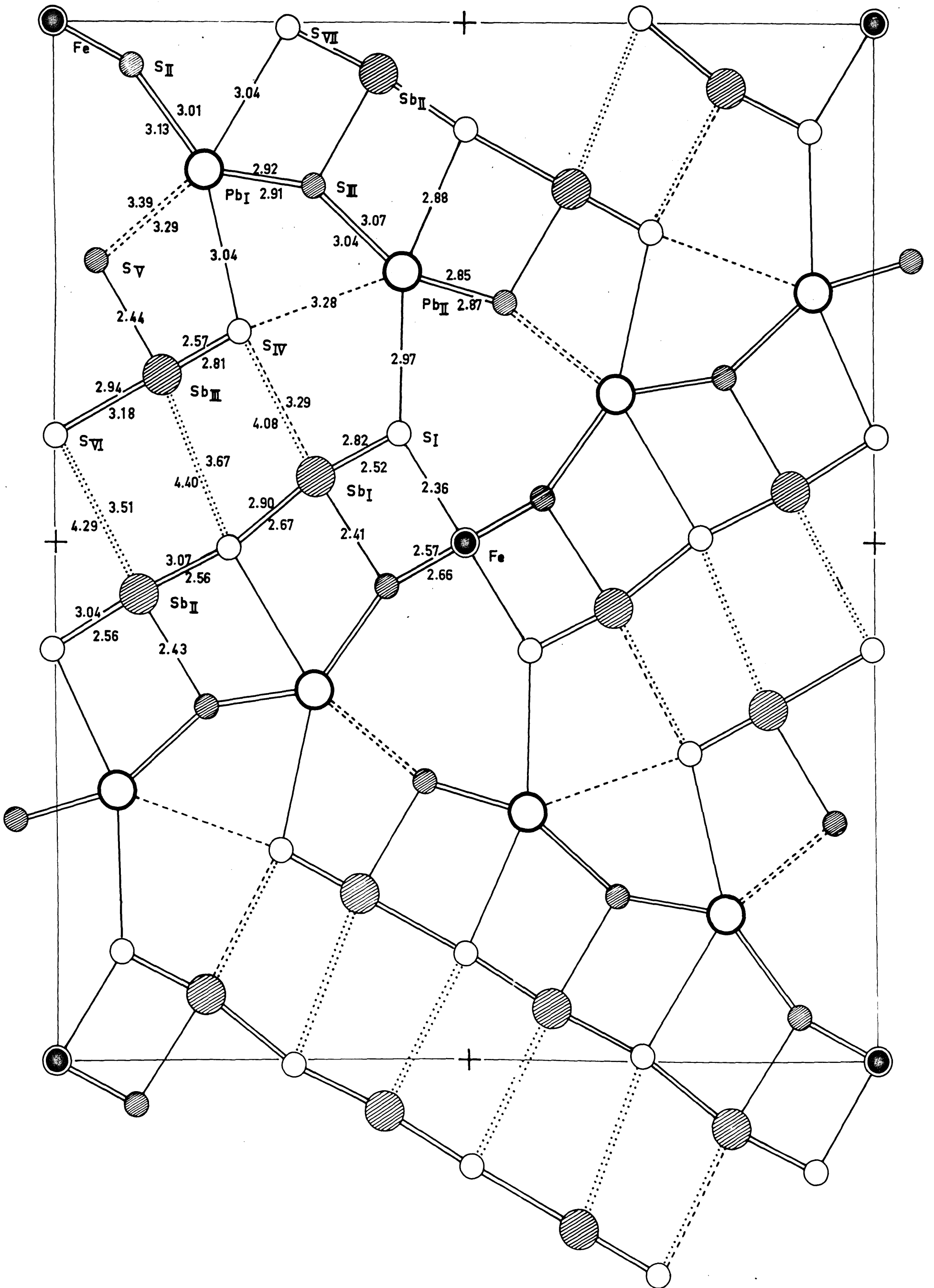


Fig. 33 Schematic representation of the structure. Open circles represent atoms with  $z$  coordinates close to zero, and shaded circles represent atoms with  $z$  coordinates close to  $1/2$ . The chemical bonds between neighboring atoms are indicated by lines. Broken lines are used to show the additional bonds from Pb to S beside the distorted octahedral bonds. Dotted lines indicate the weak bonds between Sb and S. All figures showing interatomic distances are in Å units.



$R = .24$ . This value was considered as low enough to proceed to three-dimensional refinement. The electron-density map  $\rho(\underline{xz})$  of the final structure is shown in Fig. 32.

#### Three-dimensional refinements

The three-dimensional refinement of the structure was performed by the least-squares method developed by Sayre at International Business Machine Corp., New York. The initial reliability factor of 1100  $F(hkl)$ 's was  $R = .28$ . After six cycles of refinement process it went down to  $R = .166$ . Since no allowance was made for the absorption effect, this value was regarded as sufficiently low to assure the accuracy of the structure. The final atomic coordinates are tabulated in Table 12. The comparison between observed and computed structure factors is given in Table 14.

#### Discussion of the structure

The interatomic distances between neighboring atoms are tabulated in Table 13. These distances are also indicated in a diagrammatic representation of the structure, Fig. 33.

If account is taken of the nearest neighbors only, each of the three kinds of Sb atoms has three S atoms at distances of about  $2.5\text{\AA}$ . The Sb and S atoms thus form an  $\text{SbS}_3$  group of trigonal-pyramidal shape. But this  $\text{SbS}_3$  group, described in terms of the three shortest distances, is different in its orientation from the corresponding groups found in the previously determined structures. In other structures of

sulfosalts, one edge of the pyramid is found parallel to the  $4\text{\AA}$  axis. In jamesonite none of the edges is oriented in this way, but one edge is found as approximately parallel to the (001) plane.

Three such groups,  $\text{Sb}_I\text{S}_3$ ,  $\text{Sb}_{II}\text{S}_3$ , and  $\text{Sb}_{III}\text{S}_3$  are arranged in almost straight line parallel to  $120^\circ$ . Each trigonal pyramid shares corners with neighboring pyramids and forms an  $\text{Sb}_3\text{S}_7$  group. The distances between Sb atoms in the group and S atoms in their translation-equivalent group along the  $c$  axis is about  $3.0\text{\AA}$ , and there is no strongly bonded Sb-S layers running parallel to the  $4\text{\AA}$  axis in jamesonite.

This  $\text{Sb}_3\text{S}_7$  group, then, with its centrosymmetrically equivalent group related by inversion centers at  $(\frac{1}{2}00)$  or  $(0\frac{1}{2}0)$ , can be regarded as forming a large  $\text{Sb}_6\text{S}_{14}$  group. The interatomic distance between these two  $\text{Sb}_3\text{S}_7$  groups is not less than  $3.3\text{\AA}$ , so that only a weaker type of chemical bonding occurs between them. If considered in this large group, each Sb atom has altogether 7 S atoms; that is, 3 at about  $2.5\text{\AA}$ , 2 at about  $3.0\text{\AA}$ , and 2 at greater than  $3.3\text{\AA}$  distances. The 2 such  $\text{Sb}_6\text{S}_{14}$  groups in the unit cell located around inversion centers provide interstices of three kinds; these are occupied by Fe and by 2 kinds of Pb atoms.

Six S atoms around inversion centers at (000) and  $(\frac{11}{22}0)$  surround the Fe atom at the center in a distorted octahedral coordination. The Fe-S distances are  $2.36\text{\AA}(2)$ ,  $2.57\text{\AA}(2)$ , and  $2.66\text{\AA}(2)$ , and are similar to those observed in berthierite<sup>4</sup>,

$\text{FeSb}_2\text{S}_4$  (2S at 2.49Å, 1S at 2.45Å, 1S at 2.46Å, and 2S at 2.64Å). As in the latter mineral, Fe-S bonds are regarded as largely ionic in their nature.

In two other kinds of interstices provided by  $\text{Sb}_6\text{S}_{14}$  groups, two kinds of Pb atoms are located. The coordinations of both  $\text{Pb}_I$  and  $\text{Pb}_{II}$  can be regarded, at a first approximation, as distorted octahedra if six S atoms to distance less than 3.1Å are counted. In Fig. 19 these distances are drawn in full lines. As indicated by broken lines in Fig. 19,  $\text{Pb}_I$  has two additional S atoms at about 3.3Å, and  $\text{Pb}_{II}$  has an additional one at 3.3Å. Counting these additional ones, the coordination numbers are 8 for  $\text{Pb}_I$ , and 7 for  $\text{Pb}_{II}$ . Both of these two types of Pb atoms were described in the structures of bournonite,  $\text{CuPbSbS}_3$ , and seligmannite<sup>14</sup>,  $\text{CuPbAsS}_3$ . The  $\text{Pb}_I\text{S}_8$  polyhedron shares one edge with the neighboring  $\text{Pb}_{II}\text{S}_7$  polyhedra. These polyhedra extend parallel to the  $c$  axis, further sharing S atoms with their translation-equivalents. The Pb and S atoms can be considered as forming a  $\text{Pb}_2\text{S}_6$  layer. The  $\text{Pb}_I\text{S}_8$  polyhedron shares an edge with an  $\text{FeS}_6$  octahedron, and a  $\text{Pb}_{II}\text{S}_7$  polyhedron shares a vertex with the  $\text{FeS}_6$  octahedron. If a purely ionic viewpoint is adopted, the formula of jamesonite can be expressed as  $\text{Pb}_4^{++}\text{Fe}^{++}(\text{Sb}_6\text{S}_{14})^{-10}$ .

In the treatment of the crystal chemistry of sulfosalt<sup>8</sup> it is pointed out that the atomic aggregates of metal, submetal, and sulfur atoms found in sulfosalt structures

can be derived from the various kinds of fragments of simpler sulfide structures, such as the galena type. Another way to look at the  $\text{Sb}_6\text{S}_{14}$  group is, therefore, to regard it as one of the basic structural units. This group is, to first approximation, a small fragment of an octahedral layer sharing edges with four neighboring octahedra. Since the regular octahedral arrangement of six sulfur atoms around an Sb atom is not stable, this hypothetical fragment must be rearranged in some way. This is done to satisfy the requirements of the bonding nature of the Sb atoms. In jamesonite each Sb atom has three colsest S atoms and four additional ones to form an  $\text{SbS}_7$  coordination polyhedron. This type of coordination was observed in the Sb atoms in stibnite<sup>22</sup>, and livingstonite<sup>15</sup>, and also in  $\text{Sb}_I$  in berthierite<sup>4</sup>. For the  $\text{Sb}_{II}$  atoms in berthierite the number of additional S atoms is three, and six S atoms surround the Sb atom in distorted octahedral arrangement. These arrangement of additional S atoms seem to be influenced by the existence of the other kinds of metal atoms in the structure.

The cleavage of jamesonite is reported as (1), basal cleavage which is good rather than perfect, and (2), prismatic cleavages ((010)), and ((120)). These cleavages can be explained as the result of the structural nature described above. The cleavage ((120)) occurs as the breaking of the weaker bonds between two  $\text{Sb}_3\text{S}_7$  groups. These bonds are indicated by dotted lines in Fig. 33. For cleavage parallel to (010), breaking of one bond with



length  $2.7\text{\AA}$  is necessary, but this bond density is smaller than in any other direction. As discussed above, the Sb-S distances between groups related by translation  $c$  is about  $3.0\text{\AA}$ , and the two shortest Fe-S distances are parallel to (001). The basal cleavage reported as good is understandable from these facts.

In summary, in the crystal structure of jamesonite, the basic structural principles found among the members of acicular sulfosalts are still observable. But the strongly bonded Sb-S layers or chains running parallel to the acicular axis are not well defined in jamesonite. Although that kind of atomic group can be discernible along the  $c$  axis, the strongest Sb-S bonds are oriented parallel to the (001) plane. The absence of these strongly-bonded layers or chains causes the tendency toward basal cleavage.

Table 12  
 Final coordinates and temperature coefficients  
 of atoms in jamesonite

Atom	x	y	z	B
Pb <sub>I</sub>	.182	.141	.036	1.21
Pb <sub>II</sub>	.425	.240	.062	1.08
Sb <sub>I</sub>	.319	.437	.408	0.75
Sb <sub>II</sub>	.396	.049	.623	0.74
Sb <sub>III</sub>	.130	.340	.620	1.05
S <sub>I</sub>	.419	.395	.968	0.21
S <sub>II</sub>	.095	.042	.524	0.59
S <sub>III</sub>	.316	.158	.555	0.73
S <sub>IV</sub>	.226	.297	.076	0.73
S <sub>V</sub>	.050	.230	.573	0.17
S <sub>VI</sub>	.002	.398	.052	0.71
S <sub>VII</sub>	.285	.004	.027	0.41
Fe	.000	.000	.000	1.08

Note:  $R = .166$  for 1100  $F(hkl)$ 's with this structure.

$B$ -values are determined in the processes of  
 three-dimensional least-squares refinement.

Table 13

Interatomic distances in jamesonite

	S <sub>I</sub>	S <sub>II</sub>	S <sub>III</sub>	S <sub>IV</sub>	S <sub>V</sub>	S <sub>VI</sub>	S <sub>VII</sub>
Pb <sub>I</sub>		3.01Å 3.13	2.91Å 2.92	3.04Å	3.29Å		3.04Å
Pb <sub>II</sub>	2.97Å		3.04 3.08	3.28	2.85 2.87	2.88Å	
Sb <sub>I</sub>	2.52 2.82	2.41				3.29 4.08	2.67 2.90
Sb <sub>II</sub>			2.43			2.56 3.04 3.51 4.29	2.56 3.07
Sb <sub>III</sub>				2.56 2.81	2.44	3.18 2.94	3.67 4.40
Fe	2.36(2)	2.57(2) 2.66(2)					

Table 14  
Observed and Calculated Structure Factors

hkl	F <sub>obs</sub>	F <sub>calc</sub>	hkl	F <sub>obs</sub>	F <sub>calc</sub>	hkl	F <sub>obs</sub>	F <sub>calc</sub>
020	97	- 101	1,14,0	27	- 22	2,18,0	59	+ 69
040	63	+ 20	1,15,0	288	+ 264	2,19,0	78	+ 79
060	151	- 70	1,17,0	113	- 117	310	119	- 143
080	206	+ 182	1,18,0	32	+ 1	320	101	+ 26
0,10,0	585	- 630	1,19,0	18	- 27	330	112	+ 107
0,12,0	158	+ 107	1,20,0	274	+ 293	340	205	- 207
0,14,0	118	+ 116	200	113	- 51	350	310	+ 319
0,16,0	105	+ 71	220	120	- 125	360	411	- 499
0,18,0	127	+ 80	230	31	- 47	370	64	+ 33
0,20,0	292	+ 305	240	347	+ 346	380	190	+ 180
110	52	- 12	250	552	+ 768	3,10,0	183	- 166
120	173	- 126	260	319	- 309	3,11,0	235	+ 226
130	120	+ 83	270	164	- 145	3,12,0	214	+ 194
140	136	+ 78	280	186	+ 144	3,13,0	19	- 7
150	88	- 119	290	96	- 96	3,14,0	64	+ 71
160	149	+ 133	2,10,0	79	+ 69	3,15,0	231	- 214
170	137	+ 122	2,11,0	105	- 88	3,16,0	274	+ 253
180	196	- 162	2,12,0	119	+ 104	3,17,0	32	+ 54
190	88	+ 63	2,13,0	67	+ 69	3,18,0	141	- 132
1,10,0	328	- 325	2,14,0	311	- 317	3,19,0	176	+ 173
1,11,0	112	+ 77	2,15,0	351	- 340	400	273	- 373
1,12,0	169	+ 173	2,16,0	46	- 18	410	279	+ 426
1,13,0	85	- 66	2,17,0	50	+ 12	420	33	+ 34

hkl	Fobs	Fcalc	hkl	Fobs	Fcalc	hkl	Fobs	Fcalc
430	173	- 184	5,14,0	209	- 193	750	217	+ 208
440	117	+ 71	5,15,0	106	+ 91	760	367	+ 454
450	149	- 122	5,16,0	218	+ 210	770	141	- 124
470	259	- 270	5,17,0	151	+ 119	780	131	- 124
480	142	+ 113	5,18,0	181	+ 156	790	228	+ 203
490	369	+ 406	600	47	- 5	7,10,0	146	- 126
4,10,0	414	+ 433	610	54	+ 51	7, 11,0	73	- 56
4,11,0	50	- 62	620	178	+ 210	7,12,0	26	+ 36
4,13,0	53	+ 12	630	54	- 52	7,13,0	104	+ 88
4,14,0	94	+ 86	640	414	- 512	7,14,0	246	- 210
4,15,0	55	- 23	650	47	- 15	7,15,0	65	+ 38
4,16,0	79	+ 60	660	333	+ 345	7,16,0	249	- 238
4,17,0	94	+ 91	670	36	+ 30	7,17,0	163	+ 159
4,18,0	73	- 60	680	86	- 57	800	295	- 351
4,19,0	268	- 280	690	41	- 39	810	213	- 235
510	213	+ 356	6,10,0	41	+ 15	820	205	+ 195
530	114	- 126	6,11,0	223	- 180	830	39	+ 34
540	26	- 1	6,12,0	28	- 11	840	40	- 17
550	31	+ 4	6,13,0	205	+ 204	850	106	- 108
560	215	- 212	6,14,0	361	+ 363	860	258	+ 230
570	33	+ 17	6,15,0	46	+ 28	870	115	+ 106
580	74	+ 71	6,16,0	36	- 28	880	240	- 228
590	265	- 250	6,17,0	59	- 40	890	249	- 220
5,10,0	60	+ 44	710	65	- 63	8,10,0	287	+ 268
5,11,0	400	- 419	720	153	- 167	8,11,0	133	+ 116
5,12,0	178	+ 143	730	181	+ 179	8,12,0	39	- 19
5,13,0	247	+ 231	740	432	+ 498	8,13,0	82	- 50

hkl	Fobs	Fcalc	hkl	Fobs	Fcalc	hkl	Fobs	Fcalc
8,14,0	136	- 136	10,10,0	144	- 123	12,9,0	247	- 211
8,15,0	94	+ 75	10,11,0	265	+ 224	12,10,0	112	- 83
8,16,0	217	- 167	10,12,0	140	- 91	12,11,0	63	- 39
910	314	- 335	10,13,0	229	- 206	12,13,0	108	- 78
920	254	+ 264	10,14,0	36	+ 26	13,10	58	- 34
930	123	+ 107	11,10	270	+ 260	13,20	241	- 209
940	261	- 253	11,30	187	- 167	13,30	129	+ 120
950	92	+ 69	11,40	222	- 186	13,40	136	+ 103
960	77	- 56	11,50	54	- 38	13,60	94	+ 86
970	46	- 11	11,60	51	- 30	13,70	109	+ 75
980	241	+ 219	11,70	245	+ 232	13,80	322	- 273
990	201	+ 168	11,80	115	- 90	13,90	141	- 129
9,10,0	172	+ 162	11,90	170	- 133	13,10,0	51	- 31
9,11,0	183	+ 161	11,10,0	83	+ 55	13,11,0	179	+ 163
9,12,0	255	- 239	11,11,0	56	- 31	13,12,0	101	+ 102
9,13,0	22	- 17	11,12,0	126	- 95	14,00	115	- 93
9,14,0	200	+ 169	11,13,0	123	+ 106	14,10	187	+ 159
9,15,0	155	- 129	11,14,0	228	+ 194	14,20	268	- 210
10,00	313	+ 328	12,00	245	+ 244	14,30	46	- 30
10,10	267	- 262	12,10	81	- 67	14,40	278	+ 238
10,20	247	+ 234	12,20	38	- 37	14,50	74	- 52
10,30	181	+ 182	12,30	168	+ 140	14,60	97	- 89
10,40	36	- 28	12,40	77	+ 64	14,70	73	- 51
10,50	287	- 278	12,50	206	+ 187	14,80	269	+ 222
10,70	96	+ 85	12,60	270	- 233	14,90	153	+ 132
10,80	51	- 33	12,70	288	+ 238	14,10,0	277	+ 234
10,90	65	+ 57	12,80	149	+ 133	15,10	36	- 6

hkl	Fobs	Fcalc	hkl	Fobs	Fcalc	hkl	Fobs	Fcalc
15,20	142	+ 120	0,14, $\bar{1}$	45	+ 53	23 $\bar{1}$	405	- 551
15,30	187	+ 150	0,16, $\bar{1}$	120	+ 104	24 $\bar{1}$	123	+ 113
15,40	140	- 95	0,17, $\bar{1}$	206	+ 205	25 $\bar{1}$	129	+ 122
15,50	22	+ 4	0,18, $\bar{1}$	273	- 298	26 $\bar{1}$	259	- 248
15,60	208	- 179	0,19, $\bar{1}$	38	- 3	27 $\bar{1}$	340	- 316
15,70	68	- 66	11 $\bar{1}$	12	+ 68	28 $\bar{1}$	71	- 60
15,80	105	+ 93	12 $\bar{1}$	150	- 157	29 $\bar{1}$	95	+ 58
16,00	304	+ 244	13 $\bar{1}$	294	- 288	2,10, $\bar{1}$	79	+ 56
16,10	190	+ 162	14 $\bar{1}$	185	+ 154	2,11, $\bar{1}$	28	- 21
16,20	126	- 104	15 $\bar{1}$	38	- 25	2,13, $\bar{1}$	458	+ 506
16,30	278	- 211	16 $\bar{1}$	246	+ 217	2,14, $\bar{1}$	194	- 173
16,40	205	- 170	17 $\bar{1}$	532	+ 535	2,15, $\bar{1}$	63	- 56
			18 $\bar{1}$	92	+ 61	2,16, $\bar{1}$	79	+ 66
00 $\bar{1}$	222	+ 245	19 $\bar{1}$	146	- 125	2,17, $\bar{1}$	92	- 81
01 $\bar{1}$	5	+ 41	1,10, $\bar{1}$	156	- 145	2,18, $\bar{1}$	85	+ 81
02 $\bar{1}$	370	- 374	1,11, $\bar{1}$	82	+ 72	31 $\bar{1}$	135	- 158
03 $\bar{1}$	85	- 94	1,12, $\bar{1}$	250	+ 236	32 $\bar{1}$	121	- 149
04 $\bar{1}$	53	+ 38	1,13, $\bar{1}$	62	+ 36	33 $\bar{1}$	263	+ 288
05 $\bar{1}$	147	+ 97	1,14, $\bar{1}$	186	- 161	34 $\bar{1}$	263	+ 310
06 $\bar{1}$	67	- 50	1,15, $\bar{1}$	54	+ 61	35 $\bar{1}$	124	+ 108
07 $\bar{1}$	242	- 214	1,16, $\bar{1}$	120	- 124	37 $\bar{1}$	308	- 294
08 $\bar{1}$	604	+ 656	1,17, $\bar{1}$	224	- 226	39 $\bar{1}$	117	+ 104
09 $\bar{1}$	47	- 6	1,18, $\bar{1}$	240	- 224	3,10, $\bar{1}$	53	+ 32
0,10, $\bar{1}$	191	+ 132	1,19, $\bar{1}$	153	+ 141	3,11, $\bar{1}$	274	+ 286
0,11, $\bar{1}$	33	+ 1	20 $\bar{1}$	72	- 53	3,12, $\bar{1}$	235	+ 208
0,12, $\bar{1}$	129	+ 96	21 $\bar{1}$	63	- 82	3,13, $\bar{1}$	51	+ 18
0,13, $\bar{1}$	22	- 24	22 $\bar{1}$	127	+ 147	3,14, $\bar{1}$	265	- 241

hkl	Fobs	Fcalc	hkl	Fobs	Fcalc	hkl	Fobs	Fcalc
3,15, $\bar{1}$	117	+ 55	56 $\bar{1}$	162	- 165	71 $\bar{1}$	99	+ 104
3,16, $\bar{1}$	74	+ 71	57 $\bar{1}$	149	+ 136	72 $\bar{1}$	224	- 239
3,17, $\bar{1}$	182	+ 183	58 $\bar{1}$	59	+ 56	73 $\bar{1}$	47	+ 39
3,18, $\bar{1}$	109	- 94	59 $\bar{1}$	208	+ 193	74 $\bar{1}$	335	- 333
40 $\bar{1}$	200	+ 235	5,10, $\bar{1}$	65	- 22	75 $\bar{1}$	272	+ 256
41 $\bar{1}$	402	+ 684	5,11, $\bar{1}$	210	- 209	76 $\bar{1}$	32	+ 1
42 $\bar{1}$	322	+ 455	5,12, $\bar{1}$	165	- 146	78 $\bar{1}$	163	- 145
43 $\bar{1}$	97	+ 98	5,13, $\bar{1}$	160	+ 145	79 $\bar{1}$	81	+ 67
44 $\bar{1}$	56	- 57	5,14, $\bar{1}$	50	- 34	7,10, $\bar{1}$	18	- 32
45 $\bar{1}$	26	+ 25	5,16, $\bar{1}$	187	+ 193	7,11, $\bar{1}$	181	- 169
46 $\bar{1}$	155	+ 154	5,17, $\bar{1}$	26	- 4	7,12, $\bar{1}$	145	+ 127
47 $\bar{1}$	64	- 60	60 $\bar{1}$	79	- 62	7,13, $\bar{1}$	124	+ 111
48 $\bar{1}$	349	- 368	61 $\bar{1}$	149	- 154	7,14, $\bar{1}$	378	+ 370
49 $\bar{1}$	317	+ 339	62 $\bar{1}$	122	+ 133	7,15, $\bar{1}$	83	+ 41
4,10, $\bar{1}$	31	+ 4	63 $\bar{1}$	33	+ 64	7,16, $\bar{1}$	147	- 169
4,11, $\bar{1}$	314	- 310	64 $\bar{1}$	372	- 440	80 $\bar{1}$	314	- 378
4,12, $\bar{1}$	91	- 70	65 $\bar{1}$	335	- 357	81 $\bar{1}$	285	- 310
4,13, $\bar{1}$	130	- 110	66 $\bar{1}$	405	+ 493	82 $\bar{1}$	156	+ 150
4,14, $\bar{1}$	59	+ 42	68 $\bar{1}$	83	+ 68	83 $\bar{1}$	62	- 28
4,15, $\bar{1}$	18	+ 12	69 $\bar{1}$	58	- 54	84 $\bar{1}$	118	+ 112
4,17, $\bar{1}$	18	+ 5	6,10, $\bar{1}$	33	+ 18	85 $\bar{1}$	92	- 74
4,18, $\bar{1}$	258	+ 251	6,11, $\bar{1}$	103	+ 103	86 $\bar{1}$	104	- 86
51 $\bar{1}$	115	- 111	6,12, $\bar{1}$	179	+ 157	87 $\bar{1}$	118	+ 98
52 $\bar{1}$	219	+ 259	6,13, $\bar{1}$	73	- 44	88 $\bar{1}$	154	- 145
53 $\bar{1}$	73	- 85	6,14, $\bar{1}$	190	+ 176	89 $\bar{1}$	247	- 237
54 $\bar{1}$	69	- 55	6,15, $\bar{1}$	178	- 177	8,10, $\bar{1}$	327	+ 331
55 $\bar{1}$	33	+ 42	6,16, $\bar{1}$	232	- 197	8,11, $\bar{1}$	267	+ 245



hkl	F <sub>obs</sub>	F <sub>calc</sub>	hkl	F <sub>obs</sub>	F <sub>calc</sub>	hkl	F <sub>obs</sub>	F <sub>calc</sub>
8,12, $\bar{1}$	69	+ 51	10,9 $\bar{1}$	33	+ 42	12,11, $\bar{1}$	129	+ 119
8,13, $\bar{1}$	30	- 32	10,10, $\bar{1}$	144	+ 97	12,12, $\bar{1}$	147	+ 105
8,14, $\bar{1}$	50	+ 12	10,11, $\bar{1}$	176	- 142	13,1 $\bar{1}$	228	- 200
8,15, $\bar{1}$	31	+ 24	10,12, $\bar{1}$	106	+ 76	13,2 $\bar{1}$	195	- 162
91 $\bar{1}$	144	+ 113	10,13, $\bar{1}$	210	- 177	13,3 $\bar{1}$	178	+ 158
92 $\bar{1}$	42	+ 85	11,1 $\bar{1}$	42	+ 32	13,4 $\bar{1}$	26	- 2
93 $\bar{1}$	185	+ 168	11,2 $\bar{1}$	104	+ 64	13,5 $\bar{1}$	64	- 69
94 $\bar{1}$	28	- 22	11,3 $\bar{1}$	181	- 163	13,6 $\bar{1}$	53	+ 39
95 $\bar{1}$	58	+ 54	11,4 $\bar{1}$	196	+ 155	13,7 $\bar{1}$	26	- 30
96 $\bar{1}$	62	+ 73	11,5 $\bar{1}$	41	+ 27	13,8 $\bar{1}$	41	+ 25
97 $\bar{1}$	264	- 229	11,6 $\bar{1}$	244	+ 204	13,9 $\bar{1}$	154	+ 131
98 $\bar{1}$	62	- 49	11,7 $\bar{1}$	344	+ 305	13,10, $\bar{1}$	73	- 51
99 $\bar{1}$	292	- 270	11,8 $\bar{1}$	32	- 22	13,11, $\bar{1}$	244	+ 214
9,10, $\bar{1}$	203	+ 170	11,9 $\bar{1}$	137	+ 95	14,0 $\bar{1}$	367	+ 313
9,11, $\bar{1}$	73	- 43	11,10, $\bar{1}$	82	+ 82	14,1 $\bar{1}$	67	+ 38
9,12, $\bar{1}$	274	- 258	11,12, $\bar{1}$	213	- 187	14,2 $\bar{1}$	87	+ 60
9,13, $\bar{1}$	79	+ 50	11,13, $\bar{1}$	28	+ 28	14,3 $\bar{1}$	59	- 29
9,14, $\bar{1}$	42	+ 26	12,0 $\bar{1}$	377	+ 406	14,4 $\bar{1}$	305	+ 270
10,0 $\bar{1}$	100	+ 83	12,1 $\bar{1}$	195	- 159	14,5 $\bar{1}$	191	+ 165
10,1 $\bar{1}$	62	+ 50	12,2 $\bar{1}$	268	- 247	14,6 $\bar{1}$	251	- 211
10,2 $\bar{1}$	118	- 99	12,3 $\bar{1}$	161	- 150	14,7 $\bar{1}$	110	- 92
10,3 $\bar{1}$	286	- 278	12,4 $\bar{1}$	26	- 9	14,8 $\bar{1}$	115	- 98
10,4 $\bar{1}$	112	+ 98	12,5 $\bar{1}$	50	- 24	14,9 $\bar{1}$	126	+ 97
10,5 $\bar{1}$	432	- 449	12,6 $\bar{1}$	26	- 28	15,1 $\bar{1}$	60	+ 37
10,6 $\bar{1}$	142	- 119	12,8 $\bar{1}$	308	+ 261	15,2 $\bar{1}$	141	+ 182
10,7 $\bar{1}$	199	+ 163	12,9 $\bar{1}$	181	- 161	15,3 $\bar{1}$	65	+ 25
10,8 $\bar{1}$	206	+ 191	12,10, $\bar{1}$	245	- 235	15,4 $\bar{1}$	65	- 63

hkl	F <sub>obs</sub>	F <sub>calc</sub>	hkl	F <sub>obs</sub>	F <sub>calc</sub>	hkl	F <sub>obs</sub>	F <sub>calc</sub>
15,5 $\bar{1}$	60	+ 37	26 $\bar{1}$	296	- 289	3,14, $\bar{1}$	236	+ 211
15,6 $\bar{1}$	229	- 204	27 $\bar{1}$	173	+ 147	3,15, $\bar{1}$	210	+ 178
15,7 $\bar{1}$	53	- 29	28 $\bar{1}$	42	+ 25	3,17, $\bar{1}$	174	+ 169
11 $\bar{1}$	146	+ 204	29 $\bar{1}$	31	- 18	3,18, $\bar{1}$	153	+ 137
12 $\bar{1}$	361	+ 443	2,10, $\bar{1}$	51	- 33	40 $\bar{1}$	259	+ 298
13 $\bar{1}$	126	+ 86	2,11, $\bar{1}$	36	+ 22	41 $\bar{1}$	328	- 477
15 $\bar{1}$	79	- 79	2,12, $\bar{1}$	388	+ 386	42 $\bar{1}$	46	- 29
16 $\bar{1}$	193	- 157	2,13, $\bar{1}$	274	- 264	43 $\bar{1}$	137	+ 147
17 $\bar{1}$	147	+ 118	2,14, $\bar{1}$	164	- 163	44 $\bar{1}$	51	+ 12
18 $\bar{1}$	360	+ 347	2,15, $\bar{1}$	54	+ 42	45 $\bar{1}$	129	- 97
19 $\bar{1}$	308	- 283	2,16, $\bar{1}$	79	+ 56	46 $\bar{1}$	167	+ 182
1,10, $\bar{1}$	86	- 62	2,17, $\bar{1}$	73	+ 65	47 $\bar{1}$	345	+ 370
1,11, $\bar{1}$	33	+ 24	2,18, $\bar{1}$	140	+ 126	48 $\bar{1}$	76	+ 47
1,12, $\bar{1}$	374	- 372	2,19, $\bar{1}$	46	- 51	49 $\bar{1}$	270	- 289
1,13, $\bar{1}$	209	- 165	31 $\bar{1}$	53	- 61	4,10, $\bar{1}$	51	- 44
1,14, $\bar{1}$	18	- 6	32 $\bar{1}$	267	- 358	4,11, $\bar{1}$	227	+ 214
1,15, $\bar{1}$	223	+ 202	33 $\bar{1}$	424	+ 615	4,12, $\bar{1}$	47	+ 38
1,16, $\bar{1}$	145	+ 149	34 $\bar{1}$	300	- 342	4,13, $\bar{1}$	74	+ 73
1,17, $\bar{1}$	114	- 106	35 $\bar{1}$	38	+ 39	4,16, $\bar{1}$	96	- 79
1,18, $\bar{1}$	47	+ 37	36 $\bar{1}$	18	- 16	4,17, $\bar{1}$	270	- 259
1,19, $\bar{1}$	188	+ 237	37 $\bar{1}$	324	- 341	4,18, $\bar{1}$	64	+ 40
20 $\bar{1}$	150	+ 146	38 $\bar{1}$	260	- 254	51 $\bar{1}$	94	+ 103
21 $\bar{1}$	96	- 123	39 $\bar{1}$	33	- 6	52 $\bar{1}$	231	- 277
22 $\bar{1}$	144	- 184	3,10, $\bar{1}$	79	+ 61	53 $\bar{1}$	288	- 348
23 $\bar{1}$	258	+ 307	3,11, $\bar{1}$	190	+ 176	54 $\bar{1}$	67	+ 9
24 $\bar{1}$	173	+ 199	3,12, $\bar{1}$	138	+ 111	55 $\bar{1}$	109	+ 104
25 $\bar{1}$	172	- 162	3,13, $\bar{1}$	238	- 222	56 $\bar{1}$	68	+ 47

hkl	F <sub>obs</sub>	F <sub>calc</sub>	hkl	F <sub>obs</sub>	F <sub>calc</sub>	hkl	F <sub>obs</sub>	F <sub>calc</sub>
57 $\bar{1}$	358	+ 380	74 $\bar{1}$	113	+ 110	8,15, $\bar{1}$	26	+ 19
58 $\bar{1}$	228	- 223	75 $\bar{1}$	264	+ 257	91 $\bar{1}$	76	- 61
59 $\bar{1}$	146	+ 124	76 $\bar{1}$	71	+ 41	92 $\bar{1}$	63	- 69
5,10, $\bar{1}$	104	+ 87	77 $\bar{1}$	51	- 62	93 $\bar{1}$	170	+ 141
5,11, $\bar{1}$	178	- 180	78 $\bar{1}$	191	+ 158	94 $\bar{1}$	28	+ 37
5,13, $\bar{1}$	212	+ 193	79 $\bar{1}$	50	+ 64	95 $\bar{1}$	83	+ 62
5,14, $\bar{1}$	108	+ 104	7,10, $\bar{1}$	73	+ 74	96 $\bar{1}$	88	+ 73
5,15, $\bar{1}$	72	- 35	7,11, $\bar{1}$	33	- 3	97 $\bar{1}$	246	- 215
5,16, $\bar{1}$	83	- 67	7,12, $\bar{1}$	153	- 243	98 $\bar{1}$	186	+ 135
5,17, $\bar{1}$	168	- 168	7,13, $\bar{1}$	206	+ 332	99 $\bar{1}$	109	+ 75
60 $\bar{1}$	38	- 42	7,14, $\bar{1}$	183	- 154	9,10, $\bar{1}$	142	- 136
61 $\bar{1}$	122	+ 126	7,15, $\bar{1}$	112	- 104	9,11, $\bar{1}$	109	- 77
62 $\bar{1}$	301	+ 353	7,16, $\bar{1}$	53	+ 64	9,12, $\bar{1}$	226	+ 192
63 $\bar{1}$	345	+ 402	80 $\bar{1}$	222	- 227	9,13, $\bar{1}$	87	+ 52
64 $\bar{1}$	117	- 122	81 $\bar{1}$	59	- 49	9,14, $\bar{1}$	42	+ 25
65 $\bar{1}$	265	- 278	82 $\bar{1}$	308	+ 345	10,0 $\bar{1}$	26	+ 29
66 $\bar{1}$	113	+ 123	83 $\bar{1}$	109	- 109	10,2 $\bar{1}$	146	- 123
67 $\bar{1}$	242	+ 226	84 $\bar{1}$	78	+ 74	10,3 $\bar{1}$	370	- 358
68 $\bar{1}$	45	- 30	86 $\bar{1}$	88	- 79	10,4 $\bar{1}$	285	- 242
6,11, $\bar{1}$	113	- 96	87 $\bar{1}$	251	- 225	10,5 $\bar{1}$	327	+ 283
6,12, $\bar{1}$	337	- 301	88 $\bar{1}$	423	- 396	10,6 $\bar{1}$	350	+ 281
6,13, $\bar{1}$	258	- 240	89 $\bar{1}$	50	+ 18	10,7 $\bar{1}$	349	- 294
6,14, $\bar{1}$	100	+ 104	8,10, $\bar{1}$	277	+ 251	10,8 $\bar{1}$	303	+ 263
6,15, $\bar{1}$	100	+ 113	8,11, $\bar{1}$	131	+ 103	10,9 $\bar{1}$	88	- 58
71 $\bar{1}$	53	+ 48	8,12, $\bar{1}$	118	- 96	10,10, $\bar{1}$	167	+ 114
72 $\bar{1}$	322	+ 363	8,13, $\bar{1}$	150	+ 134	10,11, $\bar{1}$	150	+ 101
73 $\bar{1}$	67	- 67	8,14, $\bar{1}$	50	+ 15	10,12, $\bar{1}$	177	+ 136

hkl	F <sub>obs</sub>	F <sub>calc</sub>	hkl	F <sub>obs</sub>	F <sub>calc</sub>	hkl	F <sub>obs</sub>	F <sub>calc</sub>
$\bar{1}0,13,\bar{1}$	288	+ 243	$\bar{1}3,2\bar{1}$	123	- 90	$01\bar{2}$	212	+ 442
$\bar{1}\bar{1},1\bar{1}$	117	+ 121	$\bar{1}3,3\bar{1}$	237	+ 200	$02\bar{2}$	58	- 114
$\bar{1}\bar{1},2\bar{1}$	31	+ 39	$\bar{1}3,4\bar{1}$	53	- 43	$03\bar{2}$	109	- 115
$\bar{1}\bar{1},3\bar{1}$	64	- 57	$\bar{1}3,5\bar{1}$	53	- 44	$04\bar{2}$	13	+ 8
$\bar{1}\bar{1},4\bar{1}$	78	+ 58	$\bar{1}3,6\bar{1}$	170	- 135	$05\bar{2}$	58	- 37
$\bar{1}\bar{1},5\bar{1}$	47	+ 27	$\bar{1}3,7\bar{1}$	117	- 99	$06\bar{2}$	40	- 38
$\bar{1}\bar{1},6\bar{1}$	73	- 52	$\bar{1}3,8\bar{1}$	138	- 89	$07\bar{2}$	26	+ 23
$\bar{1}\bar{1},7\bar{1}$	182	+ 149	$\bar{1}3,9\bar{1}$	205	- 139	$08\bar{2}$	273	+ 263
$\bar{1}\bar{1},8\bar{1}$	46	+ 48	$\bar{1}3,10,\bar{1}$	47	+ 35	$09\bar{2}$	350	+ 339
$\bar{1}\bar{1},9\bar{1}$	131	+ 92	$\bar{1}3,11,\bar{1}$	182	+ 151	$0,10,\bar{2}$	236	- 217
$\bar{1}\bar{1},10,\bar{1}$	79	- 67	$\bar{1}4,0\bar{1}$	188	+ 160	$0,11,\bar{2}$	159	- 172
$\bar{1}\bar{1},11,\bar{1}$	186	- 156	$\bar{1}4,1\bar{1}$	41	+ 9	$0,12,\bar{2}$	46	+ 70
$\bar{1}\bar{1},12,\bar{1}$	65	+ 34	$\bar{1}4,2\bar{1}$	77	+ 52	$0,13,\bar{2}$	92	+ 47
$\bar{1}\bar{1},13,\bar{1}$	69	- 36	$\bar{1}4,3\bar{1}$	112	- 87	$0,14,\bar{2}$	41	+ 97
$\bar{1}2,0\bar{1}$	158	+ 144	$\bar{1}4,4\bar{1}$	376	+ 323	$11\bar{2}$	214	+ 345
$\bar{1}2,1\bar{1}$	437	+ 425	$\bar{1}4,5\bar{1}$	91	+ 77	$12\bar{2}$	355	- 356
$\bar{1}2,2\bar{1}$	213	- 191	$\bar{1}4,6\bar{1}$	354	- 279	$13\bar{2}$	141	+ 117
$\bar{1}2,3\bar{1}$	123	+ 93	$\bar{1}4,7\bar{1}$	63	+ 61	$14\bar{2}$	72	+ 46
$\bar{1}2,4\bar{1}$	58	- 23	$\bar{1}5,1\bar{1}$	54	- 50	$15\bar{2}$	147	- 128
$\bar{1}2,5\bar{1}$	38	+ 25	$\bar{1}5,2\bar{1}$	227	- 186	$18\bar{2}$	223	- 194
$\bar{1}2,6\bar{1}$	95	- 79	$\bar{1}5,3\bar{1}$	135	- 102	$19\bar{2}$	155	- 123
$\bar{1}2,8\bar{1}$	205	+ 161	$\bar{1}5,4\bar{1}$	186	- 140	$1,10,\bar{2}$	123	- 113
$\bar{1}2,9\bar{1}$	348	+ 291	$\bar{1}5,5\bar{1}$	47	+ 31	$1,11,\bar{2}$	244	- 223
$\bar{1}2,10,\bar{1}$	36	+ 5	$\bar{1}5,6\bar{1}$	85	+ 64	$1,12,\bar{2}$	297	+ 272
$\bar{1}2,11,\bar{1}$	390	- 338	$\bar{1}5,7\bar{1}$	227	+ 176	$1,14,\bar{2}$	122	- 120
$\bar{1}2,12,\bar{1}$	158	+ 123				$21\bar{2}$	94	+ 102
$\bar{1}3,1\bar{1}$	68	+ 28	$00\bar{2}$	602	+ 700	$22\bar{2}$	64	- 65

hkl	F <sub>obs</sub>	F <sub>calc</sub>	hkl	F <sub>obs</sub>	F <sub>calc</sub>	hkl	F <sub>obs</sub>	F <sub>calc</sub>
23 $\bar{2}$	141	- 152	46 $\bar{2}$	218	+ 214	6,11, $\bar{2}$	99	+ 85
24 $\bar{2}$	101	- 108	47 $\bar{2}$	327	- 352	71 $\bar{2}$	81	+ 69
25 $\bar{2}$	473	+ 544	49 $\bar{2}$	85	+ 77	72 $\bar{2}$	195	- 229
27 $\bar{2}$	219	- 187	4,10, $\bar{2}$	376	+ 420	73 $\bar{2}$	146	- 163
29 $\bar{2}$	49	- 64	4,11, $\bar{2}$	133	+ 123	74 $\bar{2}$	210	+ 217
2,10, $\bar{2}$	73	+ 77	4,12, $\bar{2}$	31	+ 29	75 $\bar{2}$	133	+ 141
2,11, $\bar{2}$	208	- 174	4,13, $\bar{2}$	22	- 6	76 $\bar{2}$	315	+ 307
2,12, $\bar{2}$	47	+ 143	52 $\bar{2}$	177	+ 226	77 $\bar{2}$	87	+ 86
2,13, $\bar{2}$	190	+ 196	53 $\bar{2}$	172	- 208	78 $\bar{2}$	223	- 237
31 $\bar{2}$	71	- 76	54 $\bar{2}$	113	- 120	79 $\bar{2}$	33	+ 40
32 $\bar{2}$	137	+ 154	55 $\bar{2}$	104	+ 85	7,11, $\bar{2}$	31	- 17
33 $\bar{2}$	249	+ 293	56 $\bar{2}$	182	- 164	80 $\bar{2}$	73	- 74
34 $\bar{2}$	91	+ 97	57 $\bar{2}$	118	+ 110	81 $\bar{2}$	154	- 154
35 $\bar{2}$	236	+ 222	58 $\bar{2}$	249	+ 238	82 $\bar{2}$	176	+ 163
37 $\bar{2}$	296	- 296	59 $\bar{2}$	62	+ 52	83 $\bar{2}$	301	+ 309
38 $\bar{2}$	177	+ 180	5,10, $\bar{2}$	133	+ 108	84 $\bar{2}$	149	+ 149
39 $\bar{2}$	156	+ 163	5,11, $\bar{2}$	199	- 194	85 $\bar{2}$	53	+ 20
3,10, $\bar{2}$	246	- 230	5,12, $\bar{2}$	88	- 90	87 $\bar{2}$	347	+ 353
3,11, $\bar{2}$	33	+ 19	60 $\bar{2}$	108	+ 97	88 $\bar{2}$	162	- 141
3,12, $\bar{2}$	31	- 3	61 $\bar{2}$	137	- 147	89 $\bar{2}$	274	- 265
3,13, $\bar{2}$	96	- 91	62 $\bar{2}$	250	+ 298	8,10, $\bar{2}$	63	+ 52
40 $\bar{2}$	320	- 420	64 $\bar{2}$	236	- 250	91 $\bar{2}$	299	- 340
41 $\bar{2}$	90	+ 107	65 $\bar{2}$	285	- 291	93 $\bar{2}$	200	+ 228
42 $\bar{2}$	74	+ 92	66 $\bar{2}$	97	+ 78	94 $\bar{2}$	92	- 93
43 $\bar{2}$	138	- 147	68 $\bar{2}$	155	- 127	95 $\bar{2}$	50	+ 41
44 $\bar{2}$	38	- 28	69 $\bar{2}$	76	- 57	97 $\bar{2}$	41	- 64
45 $\bar{2}$	95	- 113	6,10, $\bar{2}$	41	- 56	98 $\bar{2}$	41	- 20

hkl	F <sub>obs</sub>	F <sub>calc</sub>	hkl	F <sub>obs</sub>	F <sub>calc</sub>	hkl	F <sub>obs</sub>	F <sub>calc</sub>
99 $\bar{2}$	158	+ 120	$\bar{1},12,\bar{2}$	47	- 44	$\bar{4}1\bar{2}$	320	- 420
10,0 $\bar{2}$	217	+ 217	$\bar{1},13,\bar{2}$	101	- 81	$\bar{4}2\bar{2}$	50	+ 40
10,1 $\bar{2}$	73	- 71	$\bar{2}0\bar{2}$	88	- 116	$\bar{4}4\bar{2}$	71	+ 78
10,2 $\bar{2}$	185	- 178	$\bar{2}2\bar{2}$	60	- 64	$\bar{4}5\bar{2}$	100	+ 100
10,3 $\bar{2}$	236	+ 238	$\bar{2}3\bar{2}$	118	+ 125	$\bar{4}6\bar{2}$	97	- 87
10,4 $\bar{2}$	69	+ 52	$\bar{2}4\bar{2}$	415	+ 505	$\bar{4}7\bar{2}$	68	+ 59
10,5 $\bar{2}$	213	- 195	$\bar{2}5\bar{2}$	88	+ 39	$\bar{4}9\bar{2}$	374	- 389
10,6 $\bar{2}$	96	+ 83	$\bar{2}6\bar{2}$	387	- 402	$\bar{4},10,\bar{2}$	137	- 125
10,7 $\bar{2}$	181	+ 156	$\bar{2}7\bar{2}$	63	+ 59	$\bar{4},11,\bar{2}$	238	+ 227
10,8 $\bar{2}$	205	+ 157	$\bar{2}8\bar{2}$	144	+ 113	$\bar{5}1\bar{2}$	59	+ 106
11,1 $\bar{2}$	241	+ 228	$\bar{2}9\bar{2}$	83	+ 70	$\bar{5}4\bar{2}$	33	- 23
11,3 $\bar{2}$	101	+ 79	$\bar{2},10,\bar{2}$	85	+ 53	$\bar{5}5\bar{2}$	99	- 94
11,4 $\bar{2}$	295	- 267	$\bar{2},11,\bar{2}$	41	- 31	$\bar{5}6\bar{2}$	163	+ 148
11,5 $\bar{2}$	65	- 52	$\bar{2},12,\bar{2}$	31	+ 28	$\bar{5}7\bar{2}$	42	+ 45
11,6 $\bar{2}$	168	- 141	$\bar{2},13,\bar{2}$	142	- 140	$\bar{5}8\bar{2}$	41	+ 35
12,0 $\bar{2}$	279	+ 235	$\bar{3}1\bar{2}$	150	- 182	$\bar{5}9\bar{2}$	81	- 82
12,1 $\bar{2}$	118	- 97	$\bar{3}2\bar{2}$	73	+ 74	$\bar{5},10,\bar{2}$	133	+ 122
12,2 $\bar{2}$	106	- 99	$\bar{3}3\bar{2}$	49	+ 44	$\bar{5},11,\bar{2}$	197	- 199
12,3 $\bar{2}$	108	- 96	$\bar{3}4\bar{2}$	67	+ 69	$\bar{5},12,\bar{2}$	185	- 166
$\bar{1}1\bar{2}$	91	- 119	$\bar{3}5\bar{2}$	86	+ 106	$\bar{6}1\bar{2}$	79	- 75
$\bar{1}3\bar{2}$	119	- 86	$\bar{3}6\bar{2}$	349	+ 386	$\bar{6}3\bar{2}$	83	+ 78
$\bar{1}4\bar{2}$	218	- 207	$\bar{3}7\bar{2}$	173	+ 174	$\bar{6}4\bar{2}$	314	- 325
$\bar{1}6\bar{2}$	311	- 290	$\bar{3},10,\bar{2}$	105	- 91	$\bar{6}5\bar{2}$	483	- 544
$\bar{1}7\bar{2}$	258	+ 212	$\bar{3},11,\bar{2}$	347	+ 359	$\bar{6}6\bar{2}$	364	+ 361
$\bar{1}8\bar{2}$	104	+ 102	$\bar{3},12,\bar{2}$	228	- 193	$\bar{6}8\bar{2}$	95	+ 69
$\bar{1},10,\bar{2}$	214	+ 195	$\bar{3},13,\bar{2}$	59	+ 54	$\bar{6},11,\bar{2}$	183	+ 164
$\bar{1},11,\bar{2}$	206	+ 190	$\bar{4}0\bar{2}$	273	+ 345	$\bar{7}1\bar{2}$	88	- 83

hkl	F <sub>obs</sub>	F <sub>calc</sub>	hkl	F <sub>obs</sub>	F <sub>calc</sub>	hkl	F <sub>obs</sub>	F <sub>calc</sub>
$\bar{7}2\bar{2}$	90	+ 105	$\bar{10},1\bar{2}$	105	+ 100	$11\bar{3}$	87	- 78
$\bar{7}3\bar{2}$	240	+ 256	$\bar{10},2\bar{2}$	341	+ 328	$12\bar{3}$	64	+ 41
$\bar{7}4\bar{2}$	131	- 111	$\bar{10},3\bar{2}$	41	- 38	$13\bar{3}$	224	- 210
$\bar{7}5\bar{2}$	196	+ 183	$\bar{10},4\bar{2}$	169	- 153	$14\bar{3}$	22	+ 38
$\bar{7}6\bar{2}$	88	- 81	$\bar{10},5\bar{2}$	316	+ 283	$15\bar{3}$	99	- 41
$\bar{7}7\bar{2}$	126	- 117	$\bar{10},6\bar{2}$	28	+ 28	$16\bar{3}$	36	- 16
$\bar{7}8\bar{2}$	38	- 32	$\bar{10},7\bar{2}$	59	- 30	$17\bar{3}$	332	+ 352
$\bar{7}9\bar{2}$	156	+ 136	$\bar{10},8\bar{2}$	79	- 44	$18\bar{3}$	201	+ 192
$\bar{7},10,\bar{2}$	200	+ 177	$\bar{11},1\bar{2}$	140	+ 132	$19\bar{3}$	153	+ 190
$\bar{8}0\bar{2}$	465	- 557	$\bar{11},2\bar{2}$	46	+ 21	$1,10,\bar{3}$	245	- 249
$\bar{8}2\bar{2}$	91	+ 128	$\bar{11},3\bar{2}$	191	- 156	$20\bar{3}$	119	- 143
$\bar{8}3\bar{2}$	187	+ 174	$\bar{11},4\bar{2}$	201	- 173	$21\bar{3}$	46	- 59
$\bar{8}6\bar{2}$	146	+ 128	$\bar{11},6\bar{2}$	249	- 219	$22\bar{3}$	117	+ 140
$\bar{8}7\bar{2}$	113	+ 75	$\bar{12},0\bar{2}$	212	+ 175	$23\bar{3}$	186	- 173
$\bar{8}8\bar{2}$	195	- 144	$\bar{12},2\bar{2}$	22	- 12	$24\bar{3}$	236	- 93
$\bar{8}9\bar{2}$	67	- 52	$\bar{12},3\bar{2}$	96	- 88	$26\bar{3}$	73	+ 38
$\bar{8},10,\bar{2}$	460	+ 452				$27\bar{3}$	162	- 143
$\bar{9}1\bar{2}$	132	+ 130	$00\bar{3}$	181	+ 432	$28\bar{3}$	42	- 39
$\bar{9}2\bar{2}$	250	- 244	$01\bar{3}$	100	+ 177	$2,10,\bar{3}$	132	+ 114
$\bar{9}3\bar{2}$	26	- 29	$03\bar{3}$	76	- 79	$31\bar{3}$	64	- 38
$\bar{9}4\bar{2}$	176	+ 152	$04\bar{3}$	85	- 56	$32\bar{3}$	190	- 247
$\bar{9}5\bar{2}$	103	+ 68	$05\bar{3}$	142	+ 127	$33\bar{3}$	36	+ 9
$\bar{9}6\bar{2}$	53	+ 36	$06\bar{3}$	38	+ 50	$34\bar{3}$	110	- 76
$\bar{9}7\bar{2}$	67	- 52	$07\bar{3}$	245	- 220	$35\bar{3}$	82	+ 142
$\bar{9}8\bar{2}$	213	- 195	$08\bar{3}$	169	+ 136	$36\bar{3}$	115	- 103
$\bar{10},0\bar{2}$	101	+ 119	$09\bar{3}$	96	+ 82	$37\bar{3}$	106	- 110

hkl	F <sub>obs</sub>	F <sub>calc</sub>	hkl	F <sub>obs</sub>	F <sub>calc</sub>	hkl	F <sub>obs</sub>	F <sub>calc</sub>
38 $\bar{3}$	73	- 73	75 $\bar{3}$	108	+ 95	24 $\bar{3}$	222	+ 266
39 $\bar{3}$	53	+ 56	76 $\bar{3}$	227	+ 234	25 $\bar{3}$	261	- 297
40 $\bar{3}$	213	- 273	77 $\bar{3}$	256	+ 60	26 $\bar{3}$	228	- 236
41 $\bar{3}$	205	+ 280	80 $\bar{3}$	87	- 63	27 $\bar{3}$	44	- 80
42 $\bar{3}$	290	+ 379	81 $\bar{3}$	288	- 325	28 $\bar{3}$	36	+ 17
43 $\bar{3}$	138	+ 156	82 $\bar{3}$	46	- 32	29 $\bar{3}$	76	+ 63
44 $\bar{3}$	62	+ 5	83 $\bar{3}$	115	- 116	2,10, $\bar{3}$	28	- 39
47 $\bar{3}$	88	+ 95	84 $\bar{3}$	92	+ 89	32 $\bar{3}$	247	- 347
48 $\bar{3}$	245	- 241	85 $\bar{3}$	164	- 128	33 $\bar{3}$	164	+ 265
49 $\bar{3}$	165	+ 164	86 $\bar{3}$	50	+ 51	35 $\bar{3}$	45	+ 61
51 $\bar{3}$	162	+ 176	87 $\bar{3}$	26	- 46	36 $\bar{3}$	136	+ 157
52 $\bar{3}$	109	+ 122	91 $\bar{3}$	63	- 102	38 $\bar{3}$	169	- 178
53 $\bar{3}$	154	+ 160	93 $\bar{3}$	126	+ 121	39 $\bar{3}$	79	- 88
56 $\bar{3}$	96	- 99	94 $\bar{3}$	122	- 96	40 $\bar{3}$	67	+ 56
57 $\bar{3}$	79	- 72	12 $\bar{3}$	145	+ 171	41 $\bar{3}$	144	- 172
59 $\bar{3}$	123	- 117	13 $\bar{3}$	141	+ 148	42 $\bar{3}$	210	- 277
60 $\bar{3}$	46	+ 6	14 $\bar{3}$	64	+ 75	43 $\bar{3}$	74	+ 83
61 $\bar{3}$	41	- 37	15 $\bar{3}$	79	- 62	44 $\bar{3}$	145	+ 111
63 $\bar{3}$	227	+ 257	16 $\bar{3}$	88	- 71	47 $\bar{3}$	181	+ 174
64 $\bar{3}$	224	- 341	17 $\bar{3}$	146	- 136	48 $\bar{3}$	296	+ 333
65 $\bar{3}$	58	- 65	18 $\bar{3}$	262	+ 289	49 $\bar{3}$	212	- 206
66 $\bar{3}$	310	+ 347	19 $\bar{3}$	64	- 46	51 $\bar{3}$	146	+ 166
67 $\bar{3}$	117	+ 93	1,10, $\bar{3}$	38	- 34	52 $\bar{3}$	41	+ 58
68 $\bar{3}$	60	+ 80	20 $\bar{3}$	96	+ 96	53 $\bar{3}$	199	- 207
72 $\bar{3}$	69	- 50	21 $\bar{3}$	13	+ 14	54 $\bar{3}$	59	- 46
73 $\bar{3}$	99	+ 110	22 $\bar{3}$	122	- 151	55 $\bar{3}$	59	+ 53
74 $\bar{3}$	36	+ 1	23 $\bar{3}$	112	- 140	57 $\bar{3}$	214	+ 210



hkl	F <sub>obs</sub>	F <sub>calc</sub>	hkl	F <sub>obs</sub>	F <sub>calc</sub>	hkl	F <sub>obs</sub>	F <sub>calc</sub>
$\bar{5}9\bar{3}$	168	- 170	$07\bar{4}$	109	- 118	$\bar{2}2\bar{4}$	54	- 96
$\bar{6}0\bar{3}$	50	+ 25	$11\bar{4}$	135	+ 290	$\bar{2}3\bar{4}$	38	+ 58
$\bar{6}1\bar{3}$	47	- 28	$12\bar{4}$	138	- 161	$\bar{2}4\bar{4}$	146	+ 211
$\bar{6}2\bar{3}$	120	+ 126	$13\bar{4}$	91	- 90	$\bar{2}5\bar{4}$	196	+ 358
$\bar{6}3\bar{3}$	345	+ 417	$14\bar{4}$	54	+ 55	$\bar{2}6\bar{4}$	99	- 132
$\bar{6}4\bar{3}$	50	+ 56	$22\bar{4}$	104	+ 140	$\bar{3}2\bar{4}$	53	- 92
$\bar{6}5\bar{3}$	42	- 37	$23\bar{4}$	165	- 200	$\bar{3}3\bar{4}$	96	+ 174
$\bar{6}6\bar{3}$	74	- 65	$24\bar{4}$	112	- 152	$\bar{3}4\bar{4}$	28	- 60
$\bar{6}7\bar{3}$	163	+ 149	$25\bar{4}$	69	+ 64	$\bar{3}5\bar{4}$	33	- 42
$\bar{7}2\bar{3}$	155	+ 156	$26\bar{4}$	22	+ 24	$\bar{4}0\bar{4}$	227	+ 385
$\bar{7}3\bar{3}$	132	+ 125	$31\bar{4}$	41	- 57	$\bar{4}1\bar{4}$	68	- 94
$\bar{7}4\bar{3}$	233	- 226	$33\bar{4}$	101	+ 127	$\bar{4}2\bar{4}$	45	- 47
$\bar{7}5\bar{3}$	118	+ 105	$34\bar{4}$	106	+ 171	$\bar{5}1\bar{4}$	46	- 87
$\bar{7}6\bar{3}$	85	- 90	$35\bar{4}$	47	+ 70	$\bar{5}2\bar{4}$	63	- 82
$\bar{7}7\bar{3}$	169	- 155	$40\bar{4}$	46	- 67	$\bar{5}3\bar{4}$	87	- 112
$\bar{8}0\bar{3}$	73	- 37	$41\bar{4}$	31	+ 50			
$\bar{8}1\bar{3}$	118	- 111	$42\bar{4}$	124	+ 169			
$\bar{8}2\bar{3}$	158	+ 171	$43\bar{4}$	177	+ 180			
$\bar{8}6\bar{3}$	96	+ 65	$51\bar{4}$	131	- 189			
$\bar{9}1\bar{3}$	217	+ 210	$52\bar{4}$	106	+ 158			
$\bar{9}2\bar{3}$	192	- 171	$53\bar{4}$	47	- 48			
			$\bar{1}2\bar{4}$	71	+ 97			
$01\bar{4}$	179	+ 285	$\bar{1}3\bar{4}$	28	+ 39			
$02\bar{4}$	26	- 38	$\bar{1}4\bar{4}$	64	- 96			
$03\bar{4}$	128	- 163	$\bar{1}5\bar{4}$	41	+ 55			
$04\bar{4}$	45	- 24	$\bar{1}6\bar{4}$	88	- 125			
$06\bar{4}$	42	+ 48	$\bar{2}1\bar{4}$	31	+ 30			

## PART III

## Crystal chemistry of the sulfosalt minerals

Introduction

The purpose of this paper is to discuss certain basic structural principles concerning the crystal chemistry of mineral sulfosalts by examining the crystal structures already determined, and to propose a new scheme of classification based on these principles. Three earlier investigators, Hofmann<sup>23</sup>, Berry<sup>24</sup>, and Hellner<sup>25</sup>, have made contributions to the problem, but a full treatment of the subject has not yet been presented.

---

Footnote

The term sulfosalt in the present paper is used for the chemical compounds with formula  $A_m B_n X_p$  where

A = Cu, Ag, Pb, Hg, Fe

B = As, Sb, Bi

X = S

The terminology used here is therefore narrower than the one used in Dana's System of Mineralogy<sup>11</sup>, by excluding the elements Tl, Mn, V, Sn, and Ge. The reason for their omission is lack of structural data. The condition  $n:p \neq 1:1$  for sulfosalt, used in Dana, will be followed here. Thus such minerals as arsenopyrite, FeAsS, and related compounds are not treated in this paper.

To understand the crystal chemistry of a group of minerals it is necessary to know (1) the relations between the chemical formula and corresponding structural motifs, and (2) the nature of the chemical bonds characteristic of the minerals under consideration.

In the case of the silicate minerals, these two points have been well recognized. The silica to oxygen ratios in the chemical formula are directly related to the kinds of polymerization of the structural motif, the Si-O tetrahedron. Also the purely ionic approach to the nature of the chemical bonds in silicates has been successfully used to explain the various problems involved in the crystal chemistry of the silicates<sup>26</sup>.

The situation is different for the sulfosalt minerals. As to the nature of the chemical bonds in sulfosalts, it is more difficult to understand than the one in the silicates. Because of the tendency of sulfur atom to be deformed more easily, compared with oxygen, by the adjacent cations, the bonds between the sulfur atom and the metallic atoms have been considered as more covalent in their nature. The ionic approach to explain the structures of sulfides or sulfosalts as the packing of charged spheres has failed. But the purely covalent approach to the problem is also not adequate because of the existence of partial metallic character of the bonds. The evidences of this metallic character are the lusters, colors, and intrinsic semi-conductivities of many minerals of this group. Although

the discussion in more detail will be given in a later section, the complete understanding of the nature of chemical bonds in sulfides and sulfosalts is yet to come.

It is true that a well defined structural motif, such as the Si-O tetrahedron in silicates, can be recognized in the sulfosalt structures. It is an  $\text{Sb}(\text{As}, \text{Bi})\text{S}_3$  group. These Sb and S atoms are located at the vertices of a trigonal pyramid. But the difficulty in describing the sulfosalt structures in terms of this structural motif is twofold. The first factor for the complication is that this coordination polyhedron is open. The term open is used since the metal atom is not located at the center of polyhedral arrangement of non-metal atoms. Instead, This  $\text{Sb}(\text{As}, \text{Bi})$  atom locates itself at one of the vertices of polyhedron with sulfur atoms at the other three vertices.

The three  $\text{Sb}(\text{As}, \text{Bi})\text{-S}$  bonds to form this group can be understood as covalent bonds involving three p electrons of the  $\text{Sb}(\text{As}, \text{Bi})$  atom. Except for a few example such as the structure of proustite,  $\text{Ag}_3\text{AsS}_3$ , the pure covalent bond between the  $\text{Sb}(\text{As}, \text{Bi})$  atom and the S atom is not present in the sulfosalt crystals. In other structures, the second and the third closest neighboring S atoms will approach the  $\text{Sb}(\text{As}, \text{Bi})$  atom from the open side of the coordination polyhedron. If the interatomic distances between the  $\text{Sb}(\text{As}, \text{Bi})$  atom and these additional S atoms are considered, we must conclude that a weak but a distinct chemical bond, other than Van der Waals type, exists between them. As the result of

these additional coordinations of sulfur atoms, the above-discussed  $\text{Sb(As,Bi)-S}_3$  group is obscured in the structure.

In comparison with the silicate minerals the situation can be summarized as follows: In silicate crystals, the structural framework can be described by the geometrical shape and polymerization of the first coordination polyhedron, the Si-O tetrahedron. To describe the structures of sulfosalts, not only these factors but the relative arrangement of the groups built by a first coordination polyhedron,  $\text{Sb(As,Bi)-S}_3$  unit, plays an important role. Each submetal atom in the group obtains additional S atoms, in its second coordination. These S atoms are at the larger distances from the submetal atom, and actually belong to the first coordination of the central atom in the neighboring group. The number and the arrangement of these additional S atoms are not arbitrary.

If the additional S atoms close to the  $\text{Sb(As,Bi)}$  atom are included, a larger coordination polyhedron can be defined. The  $\text{Sb(As,Bi)}$  atom is located at the center of this polyhedron. The shape and dimensions of this second coordination polyhedron are found to be almost identical in every structure. This fact suggests describing the sulfosalt structures as the stacking of the second coordination polyhedra, and classifying the minerals according to the modes of stacking. The subject will be discussed in the next two sections.

The second factor to obscure the  $\text{Sb(As,Bi)-S}_3$  unit in the structure is the relative strengths of bonds between the  $\text{Sb(As,Bi)}$  and S atoms compared with the bonds between

the other metal atom and S atom. In the silicates the Si-O bonds are stronger than any other bonds between a metal ion and oxygen. The difference can be measured from the extremely high value of ionization potential value of  $\text{Si}^{4+}$  compared with another cation in the structure. If the same measure is applied to the sulfosalts, the value of ionization potential of submetal ion is larger than those of the metal ions, but the difference is not so distinct as in the silicates. Thus the affinities of S atoms to the submetal and metal atoms are sometimes in a similar, and sometimes in a different order. In the former case, the Sb(As,Bi) atom plays almost the same role as the coexisting metal atoms such as Pb or Ag. The structure of this type of sulfosalts is closely related to the structures of simple sulfides. The detailed discussion will be found in Section 4.

When the bonds between the Sb(As,Bi) atom and the S atoms are the stronger ones in the structure, the close relation to the structure of the sulfides of Sb or Bi, namely stibnite type,  $\text{Sb}_2\text{S}_3$ , is observed. Among the sulfosalt minerals the members of the so-called acicular group provide the most abundant structural data. In these structures the atomic group of Sb(As,Bi) and S can be considered to form the structural framework to a certain extent. The systematic treatment of the combination of Sb(As,Bi)- $\text{S}_3$  units into the larger groups will be given in Section 3.

In the following sections the discussion will be approached from the more geometrical viewpoint than the physico-

chemical one. The state of knowledge concerning the nature of chemical bonds in this group of minerals is not yet well established. Nevertheless, certain principles can be obtained from the results of the geometrical treatments. In Sections 3, 4, and 6, the related subjects will be discussed.

Up to date the following crystal structures of the sulfosalts listed in Table 15 are known. In the accompanying illustrations these structures are represented either in clinographic projections or by projections along the shortest axis. The important interatomic distances are also found in the illustrations.

Table 15. The sulfosalt structures previously determined.

Name	Formula	Figures	Isomorphs
Tetrahedrite	$(\text{Cu,Fe})_{12}\text{Sb}_4\text{S}_{13}$	Fig. 62	Tennantite, $(\text{Cu,Fe})_{12}\text{Sb}_4\text{S}_{13}$
Enargite	$\text{Cu}_3\text{AsS}_4$	Fig. 63	
Proustite	$\text{Ag}_3\text{AsS}_3$	Fig. 65	Pyrargyrite, $\text{Ag}_3\text{SbS}_3$
Chalcostibite	$\text{CuSbS}_2$	Fig. 55	Emplectite, $\text{CuAsS}_2$
Aikinite	$\text{CuPbBiS}_3$	Fig. 40	
Berthierite	$\text{FeSb}_2\text{S}_4$	Fig. 53	
Galenobismutite	$\text{PbSb}_2\text{S}_4$	Fig. 58	
Seligmannite	$\text{CuPbAsS}_3$	Fig. 41	Bournonite, $\text{CuPbSbS}_3$
Livingstonite	$\text{HgSb}_4\text{S}_8$	Fig. 13	
Jamesonite	$\text{FePb}_4\text{Sb}_6\text{S}_{14}$	Fig. 33	

## 1. Geomeyrical basis of crystal chemistry of sulfosalts

Coordination polyhedra. In the crystal structures of sulfosalts the sulfur atoms surround the metallic or submetallic atoms in numbers and configurations characteristic of the central atoms. These sulfur atoms can be regarded as occupying the vertices of certain polyhedra around the central metallic or submetallic atoms. The description of these coordination polyhedra can be done in two stages.

First coordination polyhedra. The observed interatomic distances between the central atom and the sulfur atoms can be grouped into two or more kinds. If account is taken of the sulfur atoms closest to the central atom, the simpler polyhedron can be traced. This is defined as the first coordination polyhedron. The chemical bonds between the central atom and the sulfur atoms in the first coordination represent the strongest bonds characteristic of the central atom. They are almost identical in every structure. The description of the coordination for each kind of central atom is given below.

Ag: Ag tends to have two strong linear bonds of presumably sp character. Examples are found in pyrargyrite<sup>27</sup>, and in s sulfide, stromeyerite<sup>28</sup>. Detailed crystal-structure analysis of sulfosalts containing Ag is lacking, but probably this type of the first coordination prevails rather than the tetrahedral one. In this connection the interatomic distances between Ag and S atoms in the galena-type structures of sulfosalts need to be described in more



detail.

Hg: Hg has also, as its first coordination, two linearly arranged S atoms as found in cinnabar<sup>13</sup>, and in livingstonite<sup>15</sup>.

Cu: Cu always forms tetrahedral bonds of presumably  $sp^3$  character except one case of trigonal coordination found in tennantite<sup>29</sup>. In tennantite, however, this trigonally coordinated Cu is found together with the usual tetrahedrally coordinated one. Other examples of the tetrahedral coordination are found in enargite<sup>30</sup>, chalcostibite<sup>31</sup>, aikinite<sup>6</sup>, seligmannite<sup>21</sup>, and bournonite<sup>21</sup>.

Fe: In two out of three minerals containing Fe among sulfosalt minerals, i.e. in berthierite<sup>4</sup>, and in jamesonite<sup>7</sup>, the Fe has an octahedral coordination of six S atoms. This octahedron is slightly distorted in both cases. In the tetrahedrite group the tetrahedral coordination is assumed for the Fe atoms substituting Cu atoms. In sulfides the tetrahedral coordination is the common one.

As, Sb, Bi: These three submetallic atoms have three orthogonally directed bonds of presumably p character to form a trigonal pyramidal arrangement with the nearest three S atoms. One exception is the As atoms in enargite. In enargite, a tetrahedral coordination around the As atom is found.

Pb: As its first coordination, Pb atom has either a regular octahedral arrangement of six S atoms at equal distances, or a significantly distorted octahedral arrangement of six closest S atoms. The former case is known in the structure of galena. In every determined

structure of sulfosalts, the Pb atom is in the center of the latter type coordination polyhedron.

Second coordination polyhedra. Second coordination is defined as the arrangement of S atoms generally associated with the central atoms at larger distances than the S atoms in the first coordination. The second coordination polyhedron is defined as the polyhedral arrangement of S atoms including these additional S atoms around the central atoms. The number and configuration of these S atoms in the second coordination are not so uniquely defined as in case of the first coordination. For the submetal and Pb atoms the geometrical shape of the second coordination polyhedra have several possibilities, depending on the number of additional S atoms at larger distances. The nature of the chemical bonds between the central atom and the S atoms at these larger distances is not clearly understood. The descriptions for each central atom are as follows:

Ag, Hg: Ag, and Hg atoms have four more S atoms at the larger distances. With the two S atoms in the first coordination they form a distorted octahedron.

As, Sb, Bi: These atoms have three possibilities in their second coordinations. (1) three more S atoms, (2) four more S atoms, and (3) five more S atoms. With three S atoms in the first coordination the resulting second coordination polyhedra in respective cases are (1) distorted octahedron, (2) 7-vertex-8-hedron, and (3) 8-vertex-11-hedron. The geometry of these complex polyhedra will be discussed below.

Pb: Beside the six S atoms in a distorted octahedral arrangement in the first coordination, a Pb atom tends to have at larger distances (1) one more S atom, or (2) two more S atoms. The resulting second coordination polyhedra are similar in their geometry to the above-described ones for submetallic atoms.

Geometry of polyhedra. In Figs. 34, 35, and 36 the geometry of the tetrahedron, octahedron, and complex polyhedra are illustrated. In these figures the several orientations of polyhedra are shown by the clinographic projection. For each orientation of the polyhedra, the projection along the vertical axis, and bond configuration are also illustrated. In Table 16 the probable dimensions of these polyhedra are listed assuming the probable interatomic distances, or center to vertex distances. A brief description is necessary for the geometry of complex polyhedra which are characteristics of As, Sb, Bi, and Pb atoms.

(1) 7-vertex-8-hedron, Figs. 36a and 36b. This polyhedron has 7 vertices and 8 faces. In the regular octahedron all the eight faces are triangles. In this polyhedron there are six triangular faces and two rectangular faces. This 8-hedron can be derived from the usual octahedron in the following way. In Fig. 35b the regular octahedron is shown so that the edges of square cross section of it are horizontal and vertical. The length of an octahedral edge is assumed as  $4\text{\AA}$ . If a vertex (designated by letter O in Fig. 35) is replaced by two points parallel to the edges of the cross section, and if

a new polyhedron is traced including these two points as its vertices, an 8-hedron with 7 vertices is obtained.

Obviously there are two regular ways to perform this. One is to replace by two points horizontally apart ( by points 2 and 2' in Fig. 35), and the other by two points vertically apart ( by points 1 and 1' in Fig. 35). The resulting two are respectively shown in Figs. 36b and 36a. These two polyhedra are exactly identical except in their orientations. If projected along the  $4\overset{\circ}{\text{A}}$  axis, i.e. the vertical edge of the octahedron, however, two kinds of projections are obtained. One is a 4-gon (Fig. 36a), and the other is a 5-gon (Fig. 36b).

The second coordination polyhedra found in the structure of stibnite,  $\text{Sb}_2\text{S}_3$ , are of only one kind in geometrical shape, the 7-vertex-8-hedron. But there are two kinds in their orientations with respect to the  $4\overset{\circ}{\text{A}}$  axis of the structure. The orientations represented by Figs. 36a, and 36b are respectively associated with  $\text{Sb}_{\text{II}}$ , and  $\text{Sb}_{\text{I}}$  of stibnite. If projected along the  $4\overset{\circ}{\text{A}}$  axis there are 4-gons and 5-gons as shown in Figs. 37 and 46.

If the two new points placed to obtain this polyhedron are separated by not exactly the same length as the octahedral edge, or not parallel to it, a distortion of the polyhedron is produced.

The structure of galena,  $\text{PbS}$ , can be regarded as the open stacking of regular octahedra. The square cross-sections of the octahedra are oriented parallel to the (110) plane. Part of the structure is represented by the

projection on (110) in Fig. 38. If all the atoms in one part of the structure (part B in Fig. 38) separated by a plane parallel to  $(\bar{1}10)$ , glide by amount of  $2\text{\AA}$ , i.e. a half the distance of an octahedral edge, the projection illustrated in Fig. 39 will result. There is a double layer of 7-vertex-8-hedra in the galena-type structure (between two dash-and-dots lines in Fig. 39). In this idealized case, however, the interatomic distances between the same kinds of atoms, indicated by dotted lines, are too small, and a further distortion will result. A small fragment of this type of layer was described in the structure of jamesonite as an  $\text{Sb}_6\text{S}_{14}$  group<sup>7</sup>, Fig. 33. The relation discussed here is important in understanding the sulfosalt structures as related to the simple sulfide structures, and will be resumed in Section 4.

(2) 8-vertex-11-hedron, Fig. 36c. This polyhedron has 8 vertices and 11 faces. Among 11 faces, 10 are triangular, and one is rectangular. Although the other kinds of polyhedra with 8 vertices are conceivable, the one found in the sulfosalt structures is this type with 11 faces. The relation of this polyhedron to a regular octahedron and a 7-vertex-8-hedron can be understood from Fig. 35 and Fig. 36. As the central atom of this coordination polyhedron, Bi and Pb in galenobismutite<sup>5</sup>, and Pb in seligmannite and jamesonite, are known.

Interstomic distances in second coordination polyhedra.

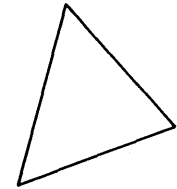
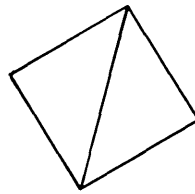
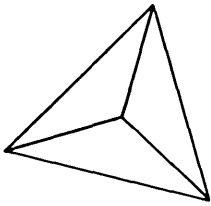
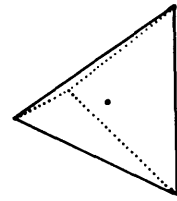
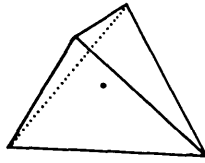
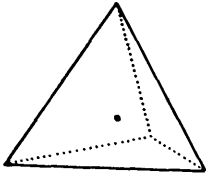
If the strength of chemical bonds is considered in terms of interatomic distances, the bonds between the central

atom and S atoms in the second coordination are the weaker ones. When an S atom belongs to, at the same time, a first coordination of one atom and to a second coordination of the other, this S atom is subject to the two competing forces. As the result, in some cases, the observed interatomic distances between the central atom and S atoms in the second coordination will change within certain limits. In case of jamesonite, some of the Sb-S distances of this type can be understood only as the van der Waals bonds. Nevertheless, the geometrical shapes of the coordination polyhedra in even such cases are similar to the ones, for example, found in the stibnite structure. This fact suggests the primary stability of the second coordination polyhedra in the sulfosalt structures. The deviations in the observed Sb-S distances are considered to be the result of the secondary influences, such as relative arrangement of neighboring polyhedra, or kinds of other metallic atoms in the structure.

The nature of the first and the second coordination polyhedra of each kind of the central atom are tabulated in Table 17.

Sulfosalt structures as open stacking of second coordination polyhedra. In the following discussions the viewpoint is taken that the crystal structure is to be regarded as a three-dimensional open stacking of the above-discussed second coordination polyhedra. In the open stacking of the polyhedra, the sharing of all the polyhedral faces is not considered. In other words,

Fig. 34 Geometry of tetrahedron. In drawings a, tetrahedron is orientated so that a three-fold axis is vertical. In drawings b, a two-fold axis is set as vertical. In drawings c, an edge of tetrahedron is set as vertical. In the top row, tetrahedra thus oriented are shown in clinographic projection. The second row shows the projection of these tetrahedra projected along the vertical axes. The third and the fourth rows show the bonds between the central atom and S atoms located at the vertices. In the fourth row, this central atom is represented by large circle. The figures accompanying are respectively, a distance between a vertex and opposite face, a distance between opposite two edges, and a length of an edge, which is assumed as  $4.0\text{\AA}$ .



**a**

**b**

**c**

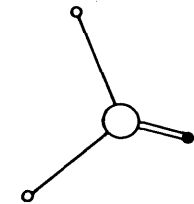
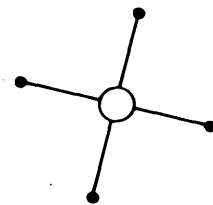
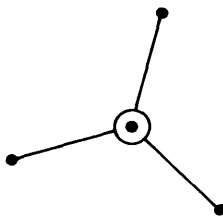
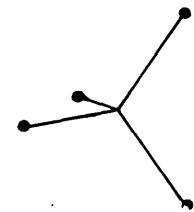
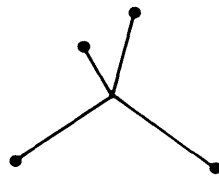
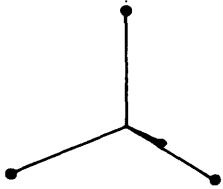
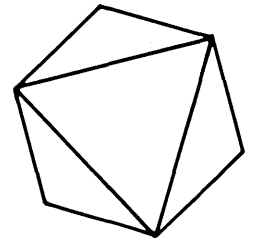
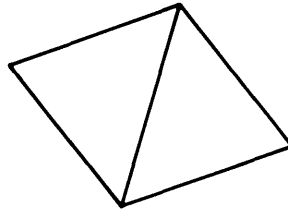
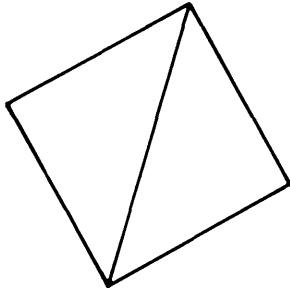
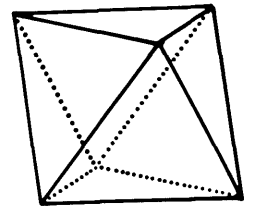
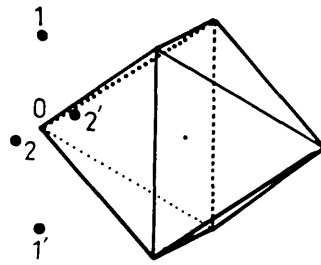
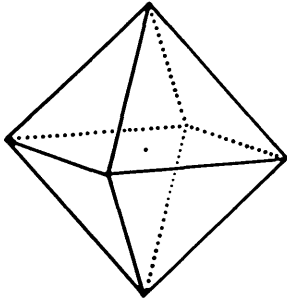




Fig. 35 Geometry of octahedron. A 4-fold axis, a 2-fold axis, and a 3-fold axis of an octahedron are respectively taken as vertical axis in drawings a, b, and c. The length of an octahedral edge is assumed as  $4.0\text{\AA}$ , and distances between opposite vertices, and between opposite faces are indicated in drawings a, and c. The top row is the clinographic projection, the second row is the projection along the vertical axis. The third and fourth row show bonds between the central atom and S atoms at the vertices in the two kinds of projection. The large circles in the fourth row indicate the central atoms.



a

b

c

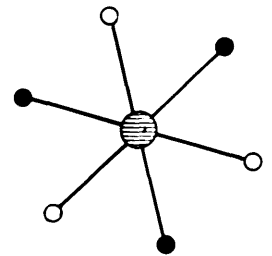
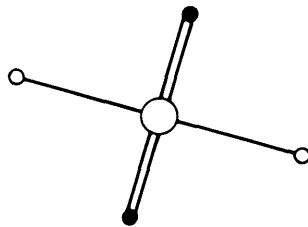
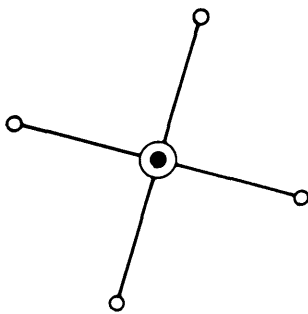
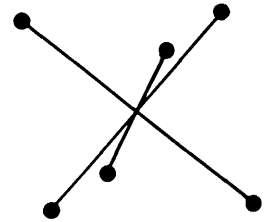
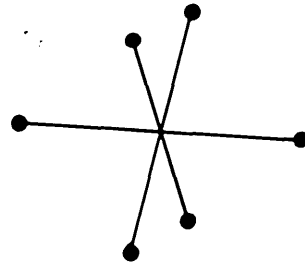
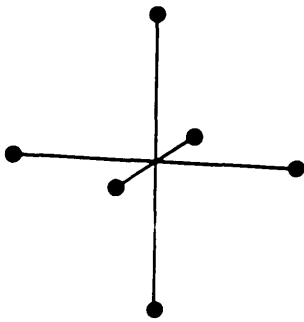
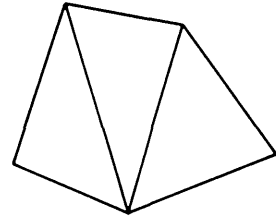
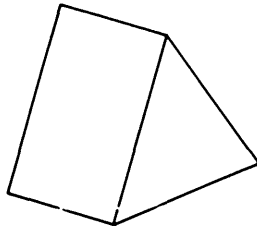
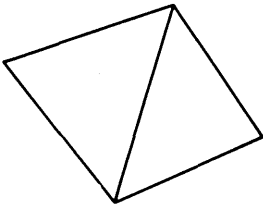
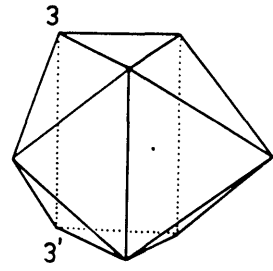
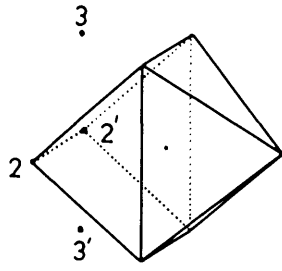
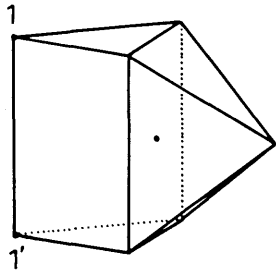


Fig. 36 Geometry of complex polyhedra. In drawings a, and b are illustrated 7-vertex-8-hedron. The numbers 1, 1', 2, 2' correspond the same numbers given in Fig. 35b. The derivation of this polyhedron from a regular octahedron is explained in text. In drawings c, an 8-vertex-11-hedron is shown. If a vertex 2' in Fig. 36b is replaced by points 3, and 3' and a new polyhedron is constructed with these points as two of its vertices, the 11-hedron is obtained. Top row shows clinographic projection, and second row shows projection along the vertical axis, i.e. along the edge of original octahedron. Since this edge is kept intact to derive the complex polyhedra, the heights of these polyhedra in the orientations illustrated are  $4.0\text{\AA}$ . The third and fourth rows show the bonds between the central atom and S atoms located at the vertices of polyhedra.



a

b

c

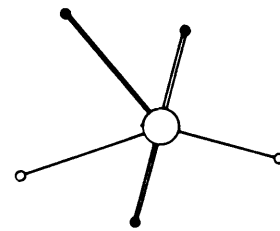
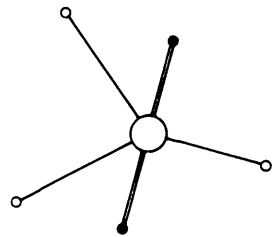
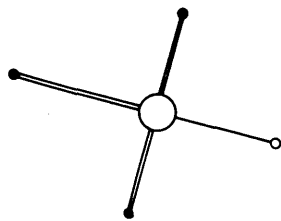
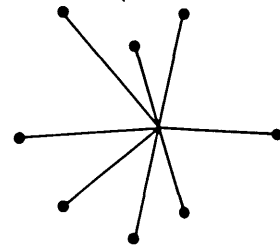
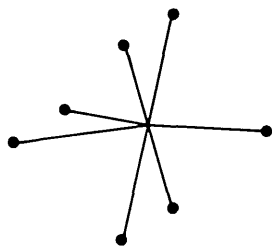
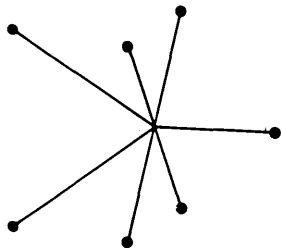


Table 16. Dimensions in tetrahedron and octahedron

(1) tetrahedron.

$\underline{d}$  = center to vertex distance,  $\underline{a}$  = edge length,  
 $\underline{b}$  = height of vertex, and  $\underline{c}$  = distance between opposite edges.

	$\underline{d}$	$\underline{a}$	$\underline{b}$	$\underline{c}$
Regular	2.45Å	4.00Å	3.26Å	2.82Å
Cu-S, the shortest.	2.20	3.59	2.93	2.54
Cu-S, the largest.	2.76	4.51	3.67	3.18

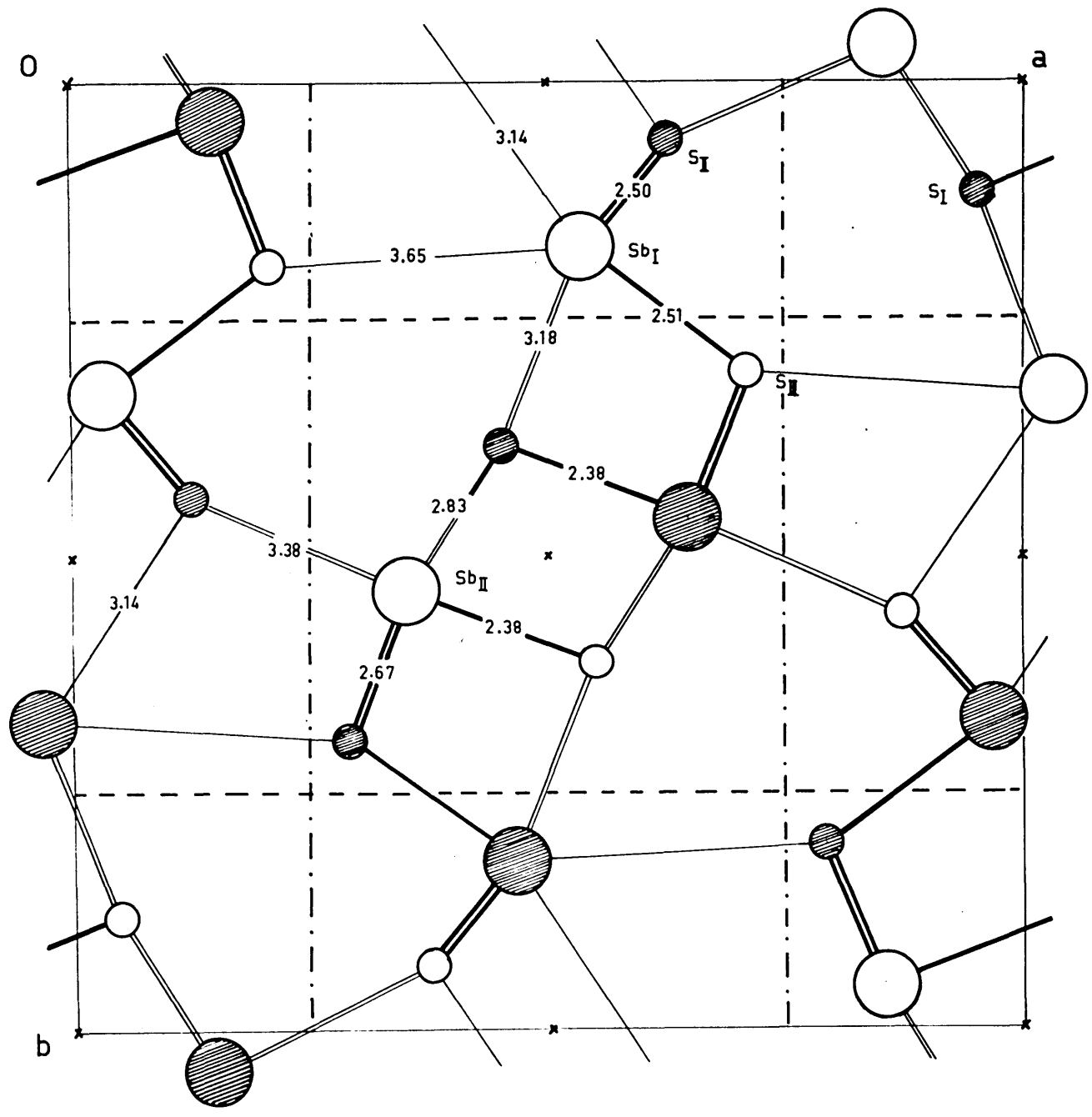
In regular tetrahedron, length of a tetrahedral edge is assumed as 4.00Å. One of the shortest and the largest Cu-S distances observed are given, and other dimensions are computed assuming a regular tetrahedron.

(2) octahedron.

$\underline{d}$  = center to vertex distance,  $\underline{a}$  = distance between opposite two vertices,  $\underline{b}$  = length of an edge, and  $\underline{c}$  = distance between opposite two faces.

	$\underline{d}$	$\underline{a}$	$\underline{b}$	$\underline{c}$
Regular	2.84Å	5.68Å	4.00Å	3.27Å
Pb-S	2.97	5.93	4.19	3.42 in galena
Sb-S	2.74	5.48	3.88	3.17 in stibnite (averaged)
Fe-S	2.64 2.45	5.38 4.90	3.37 3.46	3.05 2.84 in berthierite "

Fig. 37 Schematic representation of the structure of stibnite,  $\text{Sb}_2\text{S}_3$ . Open circles represent the atoms with  $\underline{z}$  coordinates zero. Shaded circles represent the atoms with  $\underline{z}$  coordinates  $1/2$ . Interatomic distances are in Å unit.



1Å

Fig. 38 Schematic drawing of the structure of galena. Small circles represent S atoms, and large circles Pb atoms. The projection on (110) is shown. Projections of octahedra shown in Fig. 35b are evident. Dotted line indicates a trace of a plane parallel to (110). If height of atoms represented by open circles is assumed as zero, then height of atoms represented by shaded circles is  $2.1\text{\AA}$ .

Fig. 39 Schematic drawing to illustrate a double layer of 7-vertex-8-hedra in galena structure. Part A of the galena structure in Fig. 38 is glided parallel to (110) relative to part B. The amount of gliding is  $2.1\text{\AA}$ . The projections of 7-vertex-8-hedra illustrated in Fig. 36a are evident.





Table 17

The first and the second coordination polyhedra  
characteristics of the central atoms in sulfosial<sup>ca</sup> structures

Atom	First coordination		Second coordination	
	C.N.*	Polyhedron	C.N.	Polyhedron
Cu	4	tetrahedron		
Ag	2	linear	6	distorted octahedron
Hg	2	linear	6	distorted octahedron
Fe	6	distorted octahedron		
Pb	6	regular octahedron	7	7-vertices-8-hedron
	6	distorted octahedron	8	8-vertices-11-hedron
As	3	trigonal pyramid	6	distorted octahedron
Sb	3	trigonal pyramid	7	7-vertices-8-hedron
Bi	3	trigonal pyramid	8	8-vertices-11-hedron

\* C.N. stands for coordination number.

Note: The following exceptions are known.

- Cu, in one case, 3 triangle
- As, in one case, 4 tetrahedron
- Fe, in one case, 4 tetrahedron

In space-filling by polyhedra, there must be open space in the shape of tetrahedra, etc., which does not belong to any one of the polyhedra. To understand the sulfosalt structures, the building principle is the stacking of the second coordination polyhedra sharing edges or vertices (in few cases polyhedral face). As discussed above, for the most important atoms in sulfosalts, namely submetallic atoms and Pb atom, there are several possibilities concerning the kinds of the polyhedra they can assume. The reason why the certain kind of coordination is realized in one structure but not in the other is not clearly understood. The first factor to determine the actual coordination is the kind of central atom and the ratio of the number of S atoms to the number of metallic atoms in the structure. But it must also depend on the number and kinds of coexisting different metallic atoms, i.e. on the nature of coexisting polyhedra.

From the above statement it can be deduced that the group of atoms including one or more of these versatile atoms, other metallic atom, and S atoms will crystallize in many kinds of structures with the proper ratio between the numbers of these atoms in the formula. In other words, there will be many minerals representing, for example, a Pb-Sb-S system. And actually the situation is observed. Excluding the doubtful species, 9 such minerals are known<sup>11</sup>. This fact is in distinct contrast to sulfide minerals representing Pb-S, and Sb-S systems. Galena, and stibnite are respectively the only minerals known of these systems.

There is not always a simple relation between the

dimensions characteristic of the polyhedra, and the dimensions defined as a unit cell in the resulting structure. The unit cell dimensions are certainly the result of periodicity in the way these polyhedra are stacked, but the relative orientation of one polyhedron to the other can not be guessed from the given unit cells. In some cases, however, there is one shortest unit cell dimension which is directly related to one of the characteristic dimensions of the coordination polyhedra. In these cases the following assumptions are reasonably made: (1) this dimension is found common to all coexisting polyhedra in the structure, and (2) these polyhedra are orientated so that this common dimension is parallel to the direction of the unit cell length. The most recurring shortest dimensions of the sulfosalt unit cells are approximately 4Å, 6Å, and 8Å. These dimensions should be in close relation to the polyhedral dimensions in the structures. From Fig. 34, 35 and 36, and Table 16, these dimensions are understood in terms of polyhedron or a small group of polyhedra as follows:

4Å unit. This unit is found as (1) an edge of Cu-S tetrahedron, and (2) an edge of Pb-S, Sb(As,Bi)-S octahedron, and (3) an edge of the distorted Fe-S octahedron, and finally (4) an edge of complex polyhedra around the atoms Pb, Sb(As,Bi).

6Å unit. This unit is found as (1) a body diagonal of octahedron with edge length of 4Å, and (2)  $2c$  in two tetrahedra sharing an edge between them ( $c$  is given in Table 16), and  $2c$  in two octahedra sharing a face between them ( $c$  is in

Table 16).

8Å unit. This unit is found as twice the above-mentioned 4Å dimension. The stacking of any two of the polyhedra with 4Å edge will result in this unit.

Classification of sulfosalt minerals. The present structural knowledge of sulfosalt minerals is not enough to classify all the structural types based on the principle of the open stacking of coordination polyhedra. Nevertheless, there is one group of sulfosalts, concerning which this principle can be considered as well established. This is the acicular group of sulfosalts. The members of this group are characterized by one unit cell dimension of about 4Å, and the acicular to thin tabular forms in crystal habits. The building principles found in all the previously determined crystal structures of this group can be stated as follows: For the members of the acicular group of sulfosalts, the structure building principle is the open stacking of the second coordination polyhedra. They are stacked so that the 4Å dimensions in all the polyhedra are orientated parallel to each other.

From the crystallographic and morphological viewpoints, these minerals should be grouped together not only for the convenience of description, but as the definite group based on the structure building principle. In the usual classification based on the chemical formula of minerals, Table 18 \*, the above mentioned grouping can not be achieved. Therefore, the new scheme of classification of sulfosalt minerals to be proposed here is primarily based on the shortest unit cell dimensions of the crystals.

## Footnote for Table 18's.

In Table 18's the chemical classifications of the sulfosalt minerals are given. All the known minerals are classified according to the kind or kinds of metallic elements in the chemical formula. The scheme of classification is listed below.

Sulfosalt minerals containing Cu. . . . .	Table 18a
" Ag (Fe,Hg). . .	Table 18b
" Pb. . . . .	Table 18c
" Cu and Ag . . .	Table 18d
" Cu and Pb . . .	Table 18e
" Ag (Fe) and Pb.	Table 18f
" Ag, Cu and Pb .	Table 18g

In each group of minerals the species with known crystallographic data and those without them are listed separately.

For the well established species the minerals are listed in the increasing order of the chemical parameter defined as

$$f = (\text{Cu} + \text{Ag} + \text{Pb} + \text{As} + \text{Sb} + \text{Bi}) / \text{S}.$$

For each mineral, The following data are given; the name, chemical formula,  $f$ , crystal system, space group, unit cell dimensions, crystal habit,  $Z$  ( number of formula in the cell), cleavage, and investigator.

Table 18a. Sulfosalt minerals containing Cu.

Mineral	Chemical Formula	f	Crystal System	Space Group	Unit Cell Dimensions	Z	Crystal Habit	Cleavage	Note	Investigator
(synthetic)	$\text{Cu}_6\text{Bi}_{10}\text{S}_{18}$	0.89	mono.	C2/m	$a = 13.08, b = 4.00, c = 14.07$ $\beta = 99^\circ 24.5'$	1				Nuffield <sup>60</sup> (1947)
Chalcostibite	$\text{CuSbS}_2$	1.0	orht.	Pnam	$a = 6.01, b = 14.46, c = 3.78$	4	Bladed crystals flattened {010}, often elongated to [001].	{010} perfect, {001}, {100} less so.	Structure known.	Hofmann <sup>31</sup> (1933)
Emplectite	$\text{CuBiS}_2$	1.0	orht.	Pnam	$a = 6.13, b = 14.51, c = 3.89$	4	Prismatic [001], flattened {010}.	{010} perfect, {001} less so.	Structure known.	Hofmann <sup>31</sup> (1933)
Cuprobismuthite	$\text{CuBiS}_2$	1.0	mono.	C2/m	$a = 17.65, b = 3.93, c = 15.24$ $\beta = 100^\circ 30'$	12				Nuffield <sup>62</sup> (1952)
Enargite	$\text{Cu}_3\text{AsS}_4$	1.0	orht.	Pnm	$a = 6.46, b = 7.43, c = 6.18$	2	Tabular {001}, prismatic [001].	{110} perfect, {100}, {010} distinct {001} indistinct	Structure known.	Pauling and Weinbaum <sup>30</sup> (1934)
Famatinite	$\text{Cu}_3\text{SbS}_4$	1.0	orht.						Isomorph of enargite?	
Tennantite	$(\text{Cu,Fe})_{12}\text{As}_4\text{S}_{13}$	1.23	isom.	I43m	$a = 10.09$	2	Tetrahedral.	None.	Structure known.	Pauling and Neumann <sup>29</sup> (1934)
Tetrahedrite	$(\text{Cu,Fe})_{12}\text{Sb}_4\text{S}_{13}$	1.23	isom.	I43m	$a = 10.40$	2	Tetrahedral.	None.	Structure known.	Machatschki <sup>43</sup> (1928)
Wittichenite	$\text{Cu}_3\text{BiS}_3$	1.33	orth.	$P2_12_12_1$	$a = 7.66, b = 10.31, c = 6.69$	2	Tabular {001}, also acicular to columnar.			Nuffield <sup>60</sup> (1947)
Klaprothite	$\text{Cu}_6\text{Bi}_4\text{S}_9$	1.11	orth.?							
Epigenite	$(\text{Cu,Fe})_5\text{AsS}_6$	1.0	orht.?							
Stylopyrite	$(\text{Cu,Ag,Fe})_3\text{SbS}_3$	1.33	mono.?							

Table 18b. Sulfosalt minerals containing Ag (Hg,Fe).

Mineral	Chemical Formula	f	Crystal System	Space Group	Unit Cell Dimensions	Z	Crystal Habit	Cleavage	Note	Investigator
Pavonite	$\text{AgBi}_3\text{S}_5$	0.8	mono.	C2/m	$a = 13.35, b = 4.03, c = 16.34$ $\beta = 94^\circ 30'$	4	Bladed crystals elongated to [010].			Nuffield <sup>47</sup> (1954)
Smithite	$\text{AgAsS}_2$	1.0	mono.	A2/a or Aa	$a = 17.20, b = 7.76, c = 15.16$ $\beta = 101^\circ 12'$	24	Thin tabular {100}, also equant.	{100} perfect		Peacock <sup>65</sup> (1946)
Miargyrite	$\text{AgSbS}_2$	1.0	mono.	C2/c	$a = 13.17, b = 4.39, c = 12.83$ $\beta = 98^\circ 30'$	8	Thick tabular {001} or {110}.	{010} imperfect, {100}, {101} trace.	Pseudo-isom. sub-multiple cell.	Hofmann <sup>53</sup> (1938) Graham <sup>42</sup> (1951)
Aramayoite	$\text{Ag}(\text{Sb}, \text{Bi})\text{S}_2$	1.0	tri.	$\bar{1}$	$a = 7.72, b = 8.82, c = 8.30$ $\alpha = 100^\circ 23', \beta = 90^\circ 00', \gamma = 103^\circ 54'$	6	Thin plate {010}.	{010} perfect, {100} fair, {001} trace.	Pseudo-isom. sub-multiple cell	Graham <sup>42</sup> (1951)
Matildite	$\text{AgBiS}_2$	1.0	orth.	I?	$a = 3.918, b = 4.406, c = 5.662$	1	Rarely as indistinct prism.	None.	Pseudo-isom. sub unit cell	Graham <sup>42</sup> (1951)
Proustite	$\text{Ag}_3\text{AsS}_3$	1.33	hex.	R3c	$a = 10.77, c = 6.86$ $a_{rh} = 6.86, \alpha = 103^\circ 30.5'$	6	Prismatic [001].	{101} distinct, {012} very perfect.	Structure known.	Harker <sup>27</sup> (1936)
Xanthoconite	$\text{Ag}_3\text{AsS}_3$	1.33	mono.	C2/c	$a = 11.97, b = 6.20, c = 16.95$ $\beta = 110^\circ 10'$	8	Tabular {001}, or elongated [010].	{001} distinct.	Dimorph of proustite.	Peacock <sup>67</sup> (1951)
Pyrargyrite	$\text{Ag}_3\text{SbS}_3$	1.33	hex.	R3c	$a = 11.04, c = 6.20$ $a_{rh} = 7.00, \alpha = 103^\circ 59'$	6	Prismatic [001].	{101} distinct.	Structure known.	Harker <sup>27</sup> (1936)
Pyrostilpnite	$\text{Ag}_3\text{SbS}_3$	1.33	mono.	P2 <sub>1</sub> /c	$a = 6.84, b = 15.84, c = 16.59$ $\beta = 117^\circ 09'$	4	Small lath [001], or plate flattened to {010}.	{010} perfect.	Dimorph of pyrargyrite.	Peacock <sup>67</sup> (1951)
Stephanite	$\text{Ag}_5\text{SbS}_4$	1.67	orth.	Cmc2	$a = 7.70, b = 12.32, c = 8.48$	4	Short prismatic to tabular {001}, or elongated [100].	{010}, {021} imperfect.		Taylor <sup>69</sup> (1940)
Polyargyrite	$\text{Ag}_{24}\text{Sb}_2\text{S}_{15}?$	1.73?	isom.				Cubo-octahedron			
Berthierite	$\text{FeSb}_2\text{S}_4$	0.75	orth.	Pnam	$a = 11.44, b = 14.12, c = 3.76$	4	Prismatic [001] to fibrous.	Prismatic rather indistinct.		Buerger and Hahn <sup>4</sup> (1955)
Livingstonite	$\text{HgSb}_4\text{S}_8$	0.625	mono.	A2/a	$a = 30.25, b = 4.00, c = 21.49$	8	Minute needles elongated [010].	{001} perfect, {010}, {100} poor.		Niizeki and Buerger <sup>15</sup> (1957)



Table 18c. Sulfosalt minerals containing Pb.

Mineral	Chemical Formula	f	Crystal System	Space Group	Unit Cell Dimensions	Z	Crystal Habit	Cleavage	Note	Investigator
Sartorite	$PbAs_2S_4$	0.75	mono.	?	$a = 77.9, b = 83.0, c = 78.6$	320	Prismatic.	{100} fair.	Pseudo cell with orth. symmetry is taken with $a' = 19.48, b' = 4.15, c' = 7.86$	Peacock and Berry <sup>64</sup> (1940)
Zinkenite	$PbSb_2S_4$	0.75	hex.	$C6_3$	$a = 44.06, c = 8.60$	80 or 81	Thin prismatic to fibrous.	{110} indistinct.		Nuffield <sup>58</sup> (1945)
Galenobismutite	$PbBi_2S_4$	0.75	orth.	Pnam	$a = 11.73, b = 14.47, c = 4.076$	4	Needles [001], flattened {100}.	{110} good	Structure known	Wickman <sup>5</sup> (1951)
Robinsonite	$Pb_7Sb_{12}S_{25}$	0.76	tri.	$P\bar{1}$	$a = 16.51, b = 17.62, c = 3.97$ $\alpha = 96^\circ 04', \beta = 96^\circ 22', \gamma = 91^\circ 12'$	1	Slender prismatic [001].	None.		Berry et al <sup>50</sup> (1952)
Baumhauerite	$Pb_4As_6S_{13}?$	0.77?	mono.	$P2_1/m$	$a = 22.68, b = 8.32, c = 7.92$ $\beta = 97^\circ 17'$	3 or 4	Short prismatic [010], tabular {100}.	{100} perfect		Peacock <sup>64</sup> (1940)
Rathite	$Pb_7As_9S_{10}?$	0.80?	mono.	$P2_1/m$	$a = 25.00, b = 7.91, c = 8.42$ $\beta = 99^\circ 00'$	2	Prismatic [001].	{100} perfect		Berry <sup>64</sup> (1940)
Cosalite	$Pb_2Bi_2S_5$	0.80	orth.	Pbnm	$a = 19.04, b = 23.81, c = 4.05$	8	Prismatic to needle [001].			Berry <sup>46</sup> (1939)
Bourangerite	$Pb_5Sb_4S_{11}$	0.82	mono.	$P2_1/a$	$a = 21.52, b = 23.46, c = 8.07$ $\beta = 100^\circ 48'$	8	Long prismatic to acicular.	{100} good	Strong sub-cell with $c' = 4.035$	Berry <sup>48</sup> (1940)
Falkmannite	$Pb_3Sb_2S_6$	0.83	mono.	$P2_1/a?$	$a = 15.67, b = 19.06, c = 4.02$ $\beta = 91^\circ 50'$	4	needles [001].	{001}		Hiller <sup>17</sup> (1955)
Gratonite	$Pb_9As_4S_{15}$	0.86	hex.	$R3m$	$a = 17.69, c = 7.83$ $a_{rh} = 10.54, \alpha = 114^\circ 05'$	3	Prismatic [001].	None.		Palache and Fisher <sup>63</sup> (1940)
Jordanite	$Pb_4As_7S_9?$	0.86?	mono.	$P2_1/m$	$a = 8.89, b = 31.65, c = 8.40$ $\beta = 118^\circ 21'$	?	Tabular {010}.	{010} very perfect	Sub-cell with $c' = 4.20$	Peacock and Berry <sup>64</sup> (1940)
Geocronite	$Pb_5(As,Sb)_2S_8$	0.88	mono.	$P2_1/m$	$a = 8.97, b = 31.90, c = 8.49$	3	Tabular {001}.	{011} distinct		Douglass <sup>51</sup> (1954)

Table 18c. (Continued)

Mineral	Chemical Formula	f	Crystal System	Space Group	Unit Cell Dimensions	Z	Crystal Habit	Cleavage	Note	Investigator
Fuloppite	$Pb_3Sb_8S_{15}$	0.73	mono.	C2/c or Cc	$a = 13.36, b = 11.67, c = 16.88$ $\beta = 94^\circ 41'$	4	Pyramidal, short prismatic [201].	{112} very good		Nuffield <sup>58</sup> (1945)
Plagionite	$Pb_5Sb_8S_{17}$	0.76	mono.	C2/c or Cc	$a = 13.45, b = 11.81, c = 19.94$ $\beta = 107^\circ 11'$	4	Thick tabular {001}, short prismatic [201].	{112} very good		Nuffield and Peacock <sup>55</sup> (1944)
Heteromorphite	$Pb_7Sb_8S_{19}$	0.79					Pyramidal.	{112} good		
Semseyite	$Pb_9Sb_8S_{21}$	0.82	mono.	C2/c or Cc	$a = 13.61, b = 11.99, c = 23.59$ $\beta = 105^\circ 49'$	4	Tabular {001}, prismatic [010].	{112} perfect		Nuffield and Peacock <sup>55</sup> (1944)
Chiviatite	$Pb_3Bi_8S_{15}$	0.73					Columnar aggregates			
Dufrenysite	$Pb_2As_2S_5$	0.80	mono.				Tabular {010},	{010} perfect		
Gütermannite	$Pb_{10}As_6S_{19}$	0.84					Massive, compact			
Gongarrite	$Pb_4Bi_2S_7$	0.87					Irregular to platy mass.			
Beegerite	$Pb_6Bi_2S_9$	0.90					Crystal indistinct.			

Table 18d. Sulfosalt minerals containing Cu and Ag.

Mineral	Chemical Formula	f	Crystal System	Space Group	Unit Cell Dimensions	Z	Crystal Habit	Cleavage	Note	Investigator
Polybasite	$(\text{Ag}, \text{Cu})_{16}(\text{Sb}, \text{As})_2\text{S}_{11}$	1.64	mono.	C2/m	$a = 26.12, b = 15.08, c = 23.89$ $\beta = 90^\circ 00'$	16	Short tabular {001}.	{001} imperfect	Pseudo hex. cell with $a' = 15.08, c' = 23.84$	Peacock and Berry <sup>66</sup> (1947)
Pearceite	$(\text{Ag}, \text{Cu})_{16}\text{As}_2\text{S}_{11}$	1.64	mono.	C2/m	$a = 12.61, b = 7.28, c = 11.88$	2	Short tabular {001}.	None	Pseudo hex. cell with $a' = 7.28, c' = 11.88$	Peacock and Berry <sup>66</sup> (1947)

Table 18e. Sulfosalt minerals containing Cu and Pb.

Mineral	Chemical Formula	f	Crystal System	Space Group	Unit Cell Dimensions	Z	Crystal Habit	Cleavage	Note	Investigator
Meneghinite	$\text{Pb}_{13}\text{CuSb}_7\text{S}_{24}$	0.83	orth.	Fbnm for sub-cell	$a = 11.36, b = 24.04, c = 8.26$	2	Slender prismatic [001], also fibrous.	{010} perfect, {001} difficult.	Strong sub-cell with $c' = 4.13$	Berry and Moddle <sup>49</sup> (1941)
Seligmannite	$\text{PbCuAsS}_3$	1.0	orth.	Fm2m	$a = 8.081, b = 8.747, c = 7.636$	4	Equant to short prismatic [001], also tabular {001}.	Very poor on {001}, {100}, {010}.	Structure known	Hellner <sup>21</sup> (1956)
Bournonite	$\text{PbCuSbS}_3$	1.0	orth.	Fm2m	$a = 8.162, b = 8.711, c = 7.811$	4	Short prismatic to tabular {001}.	{010} imperfect, {100}, {010} less good	Structure known	Hellner <sup>21</sup> (1956)
Aikinite	$\text{PbCuBiS}_3$	1.0	orth.	Fm3m	$a = 11.65, b = 4.00, c = 11.30$	4	Prismatic to acicular 001.	Very indistinct	Structure known	Wickman <sup>6</sup> (1953)
Gladite	$\text{PbCuBi}_5\text{S}_9$	0.78	orth?				Prismatic.			
Razabanyite	$\text{Pb}_3\text{Cu}_2\text{Bi}_{10}\text{S}_{19}$	0.79					Massive.			
Hammarite	$\text{Pb}_2\text{Cu}_2\text{Bi}_4\text{S}_9$	0.89					Short prismatic to acicular.			
Berthonite	$\text{Pb}_2\text{Cu}_7\text{Sb}_5\text{S}_{13}$	1.08					Massive.			





The further possibility of this kind of classification was illuminated by the recently analysed structures of seligmannite and bournonite<sup>21</sup>. The schematic representation of their structures is reproduced in Fig. 41. As contrasted with sulfosalts in the above-discussed group, especially to aikinite, their Bi-analogue, these two minerals have the following characteristics. Their crystal habits are equant to short prismatic, and their shortest unit cell dimensions are respectively  $7.64\text{\AA}$ , and  $7.81\text{\AA}$ . In their structures, however, there are mirror planes perpendicular to these shortest axes. Consequently the structures are divided into two units related by the mirror operations. In these building units with one dimension of  $3.82\text{\AA}$ , and  $3.91\text{\AA}$ , it was shown that the structure building principle by the stacking of polyhedra is essentially same as stated above. The structural scheme of aikinite is reproduced for comparison in Fig. 40.

Also in numbers of sulfosalts minerals the existence of a  $4\text{\AA}$  sub-multiple unit cell is reported. Most well studied examples are andorite IV, and andorite VI of Donnay and Donnay<sup>32</sup>. In both structures the strong pseudo-unit cell with  $a = 13.03\text{\AA}$ ,  $b = 19.15\text{\AA}$ , and  $c' = 4.29\text{\AA}$  is found. In the former mineral four such cells give the true unit cell with  $c = 17.16\text{\AA}$ , and in the latter mineral six of them give the true unit cell with  $c = 25.74\text{\AA}$ .

The above-mentioned two groups of sulfosalts can be defined as (1) sulfosalts with shortest unit cell dimension of  $8\text{\AA}$ , but with asymmetric unit with  $4\text{\AA}$ , and (2) sulfosalts

with sub-multiple unit cell with  $4\overset{\circ}{\text{A}}$  dimension.

The structure building principle for these groups is assumed here, if the building unit with  $4\overset{\circ}{\text{A}}$  length is considered, as identical for the acicular group. Although the structure determination of the minerals in these groups are lacking, these groups are treated as closely related ones to the acicular group in the present classification.

Chemical parameter f. The next shortest dimension to be considered is  $6\overset{\circ}{\text{A}}$ . The structures associated with this dimension have been identified as closely related to the galena type structure. In his discussion on this group of sulfosalts, Hellner<sup>25</sup> introduced two chemical parameters,  $f_1$  and  $f_2$ . These are defined by the following formula:

$$f_1 = \frac{\text{Ag} + \text{Pb} + \text{Sb}(\text{As}, \text{Bi})}{\text{S}}$$

and

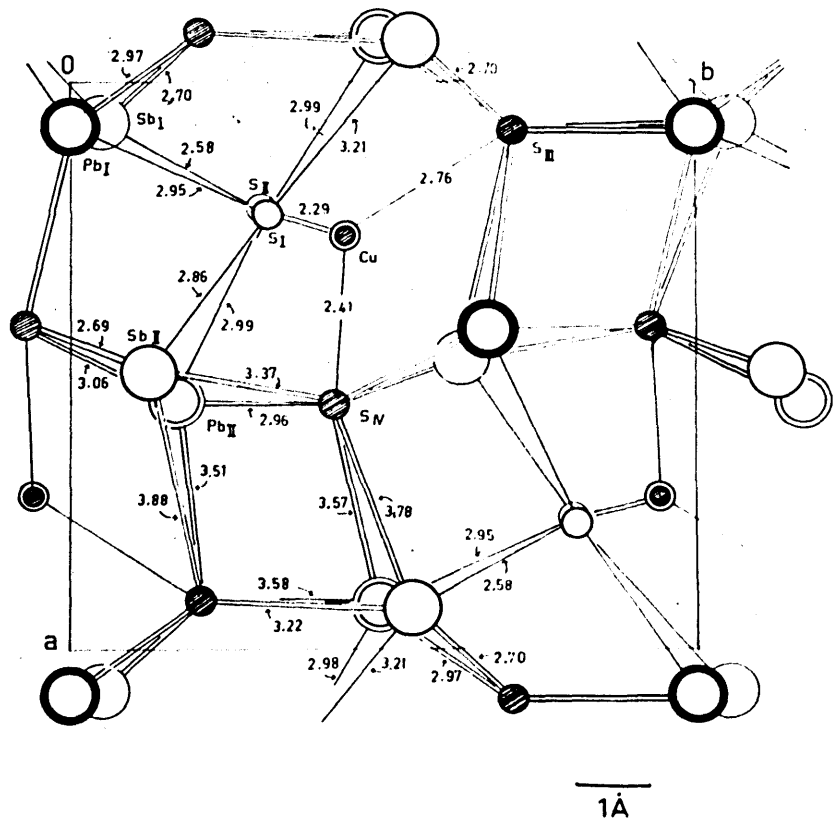
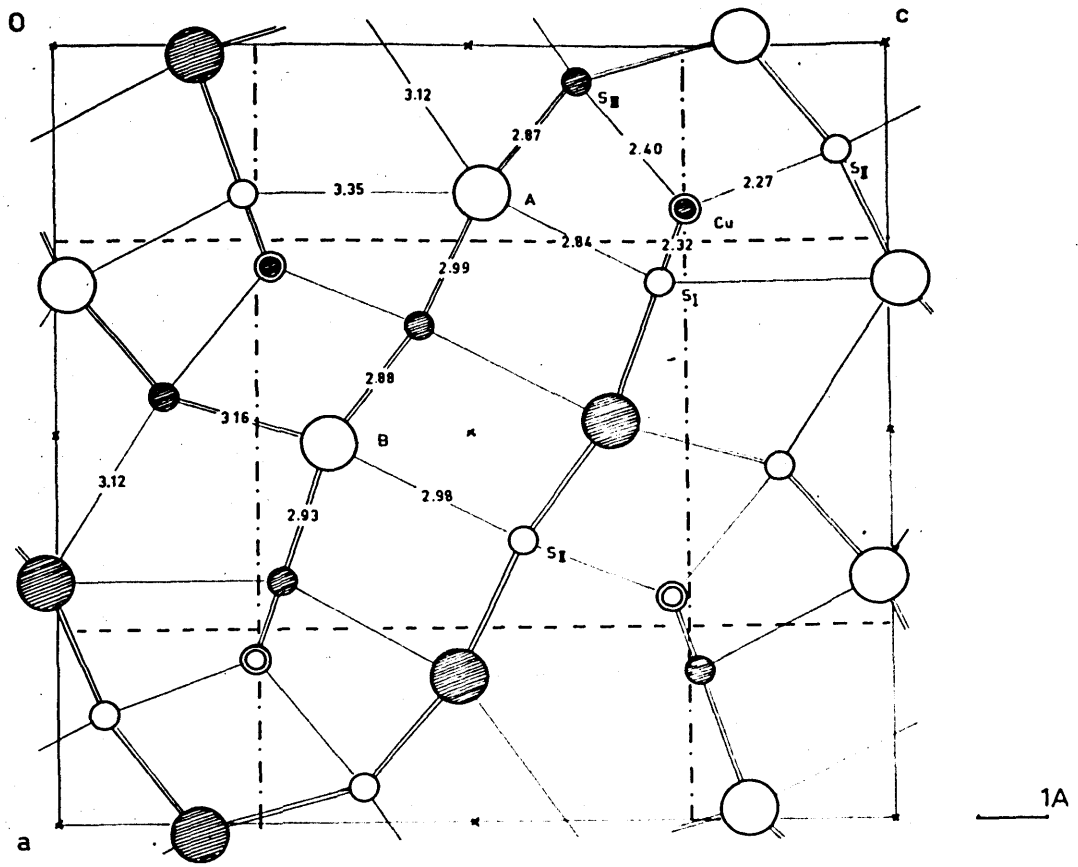
$$f_2 = \frac{\text{Ag} + \text{Pb}}{\text{Sb}(\text{As}, \text{Bi})}$$

In the above formula each symbol represents the number of each atomic specie in the chemical formula. Thus in galena,  $\text{PbS}$ ,  $f_1 = 1.0$  and  $f_2 = \text{an infinite}$ . The similarity of the sulfosalts structures to the galena-type is therefore defined by two factors, i.e. identity of unit cell dimension with about  $6\overset{\circ}{\text{A}}$ , and the value of  $f_1$  equal to 1.0 or very close to it. The minerals satisfying these two conditions are grouped together. The structure of galena as the stacking of regular octahedra was already treated in an earlier section. If the existence of atomic species other than Pb does not

Fig. 40 Structural scheme of aikinite,  $\text{CuPbBiS}_3$ . (After Wickman<sup>5</sup>). Open circles represent atoms with  $y$  coordinate equal to zero, and shaded circles represent  $y$  coordinates equal to  $1/2$ . Accompanying figures indicate the interatomic distances in Å unit.

Fig. 41 Structural scheme of bournonité,  $\text{CuPbSbS}_3$ . (After Hellner<sup>21</sup>.) The projection of the whole unit cell on (001) is given. Heavy open circles represent the atoms with  $z$  coordinates equal to zero. Light open circles represent the atoms with  $z$  coordinates equal to  $1/2$ . These atoms are on the mirror planes. Shaded circles represent atoms with  $z$  coordinates very close to  $1/4$ .





disturb this octahedral arrangement, the structure scheme of galena will be kept essentially intact. Ag, and Sb(As,Bi) atoms, as discussed already, may have distorted octahedra as their second coordination polyhedra.

Similar chemical parameter can be defined for the sulfosalts containing Cu as only the metallic element.

The parameter  $f_3$  is defined as follows:

$$f_3 = \frac{\text{Cu} + \text{Sb(As,Bi)}}{\text{S}}$$

In the fourth group of the present classification, the minerals with  $f_3$  values equal to 1.0 are grouped together.

In the most general treatment, parameter  $f$  can be defined as

$$f = \frac{\text{Cu} + \text{Ag} + \text{Pb} + \text{Sb(As,Bi)}}{\text{S}} .$$

In the fifth group the sulfosalts with values of  $f$  greater than 1.0 are classified. The reason for this classification will be developed in a later section.

Finally, the minerals with unknown structural principles are grouped together. They are plagioclase series, and two hexagonal minerals, gratonite, and zinkenite.

The principles of classification are tabulated in Table 19. All the minerals are classified according to these principles and listed in Table 19's.

The detailed treatment of each group will be found in the following sections.

Table 19

Classification of sulfosalts minerals based on the probable stacking type of the second coordination polyhedra.

Group A (acicular group). Minerals characterized by one unit cell dimension of  $4A$ , and acicular to thin tabular forms in crystal habit. For the minerals of this group  $f = 1.0$ .

Group A'. This group is sub-divided into two groups.

Group A'-1 (Bournonite group). Minerals characterized by one unit cell dimension of about  $8A$ , but with asymmetric unit of  $4A$ .  $f$ -values are less than  $1.0$

Group A'-2 (Andorite group). Minerals with one pseudo (sub-multiple) unit cell dimension of  $4A$ , and  $f$  values less than  $1.0$ .

Group B (Galena-type group). Minerals characterized by ~~a~~ the shortest unit cell dimension of about  $6A$ , and  $f_1 = 1.0$ .

Group C (Tetrahedrite group). Minerals characterized by an isometric symmetry, and chemical parameter  $f_3 = 1.0$ .

Group D (Pyrargyrite group). Minerals with chemical parameter  $f$ -values greater than  $1.0$

Group E In this group are included plagionite series, and two hexagonal minerals zinkenite, and glatonite.

2. Polygonal network of the projected structures of minerals in group A and A'.

Introduction. The three dimensional treatment of the open stacking of polyhedra is not easy. For the minerals in group A and A' of Table 19, to which most numerous sulfosalts belong, the existence of a  $4\text{\AA}$  dimension allows an easier treatment. If projected along this  $4\text{\AA}$  axis, all the atoms in the structure will be clearly resolved. The orientations of polyhedra of various kinds with respect to this axis were treated in the previous section. A polygon obtained as the projection of each polyhedron, therefore, can be understood with definite shapes and probable dimensions. Thus the three dimensional structures will reflect their nature in their projections although with certain ambiguities.

The coordination polygons in the projections are obtained by connecting all the S atoms to the neighboring S atoms surrounding the same central atom. The two dimensional space is now divided into sets of polygons sharing their sides. In this paper this network is termed as a polygonal network representing each structure. The polygonal network must possess the translational and plane group symmetry elements of the original projection. These polygonal networks are illustrated for all the known structures of acicular sulfosalts in Fig. 42 to Fig. 48.

Corresponding to the table of coordination polyhedra,

Fig. 42 Polygonal network of the structure of chalcostibite,  $\text{CuSbS}_2$  projected on (001). The structure is represented diagrammatically in Fig. 55.

The large circles represent Sb atoms, and the small circles Cu atoms. The S atoms are located at the points of network.

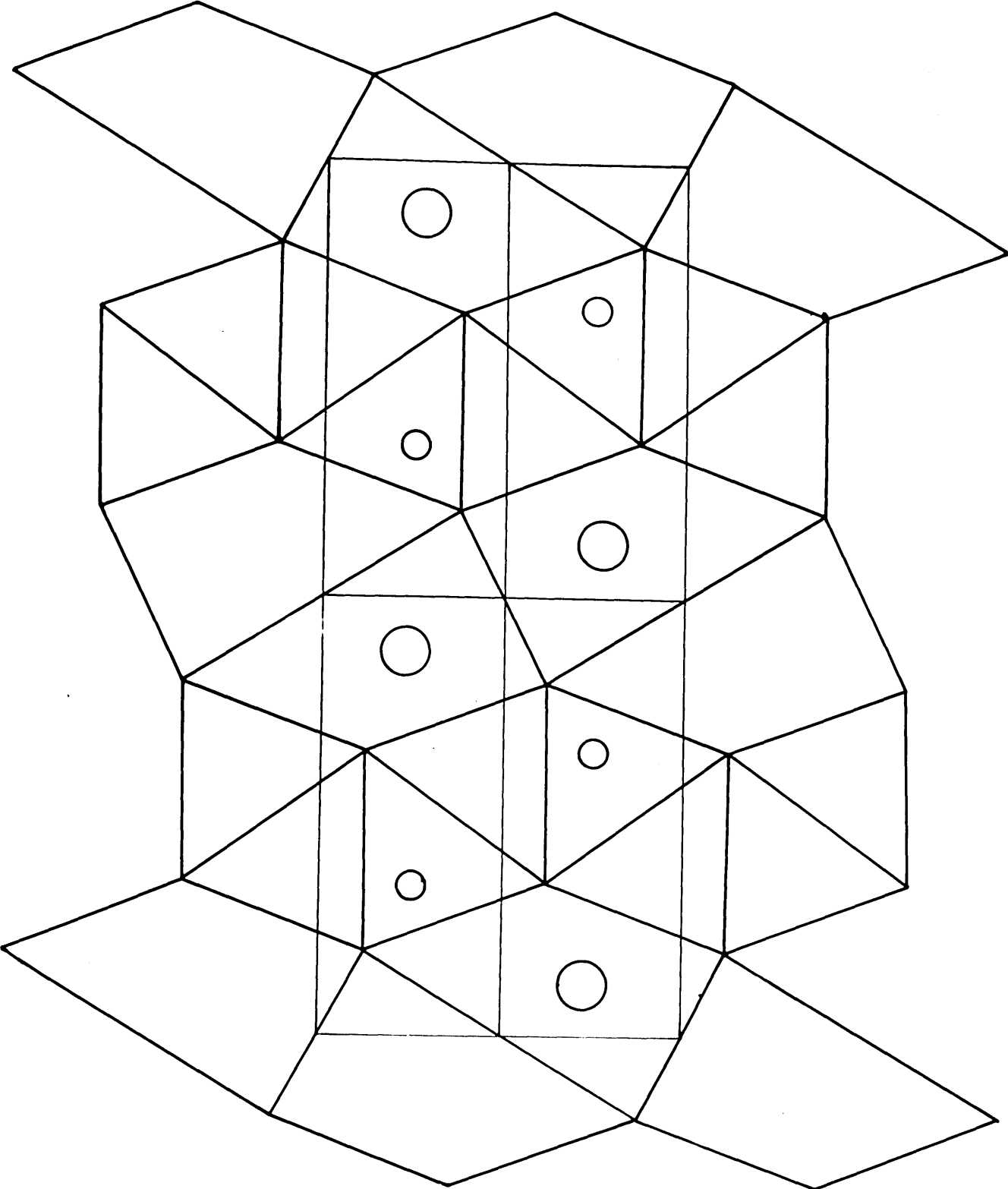


Fig. 43 Polygonal network of the structure of aikinite,  $\text{CuPbBiS}_3$  projected on (010). The schematic representation of the structure is given in Fig. 40. The large circles represent Pb or Bi atoms, and the small circles Cu atoms.

This is essentially also the polygonal network of the structure of stibnite. The large circles represent Sb atoms, and the triangle in which Cu atoms are located will be vacant.

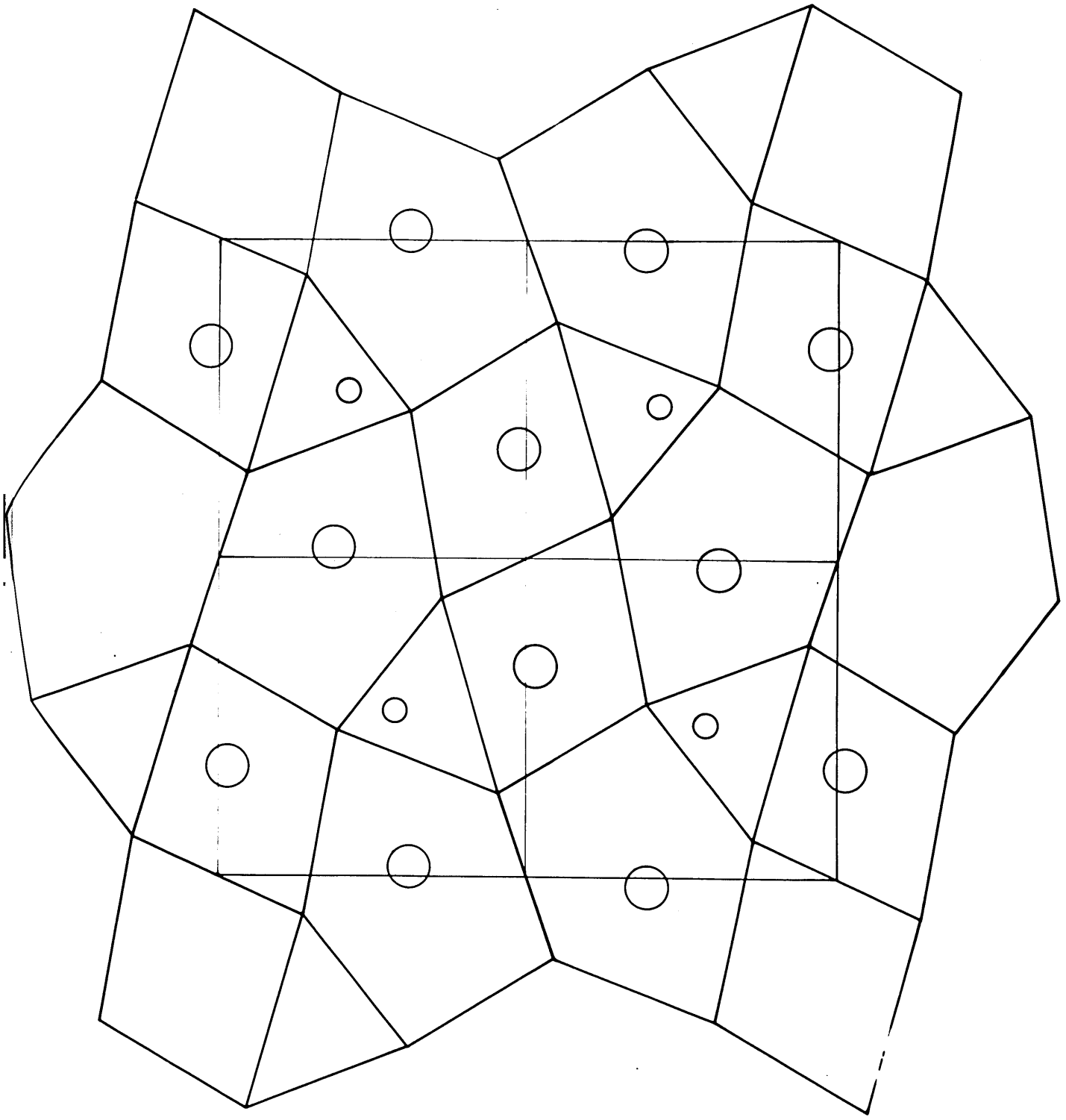




Fig. 44 Polygonal network of the structure of bournonite,  $\text{CuPbSbS}_3$  projected on (001), Fig. 41.

The large circles represent Sb atoms, the large circles in heavy lines represent Pb atoms, and the small circles Cu atoms.

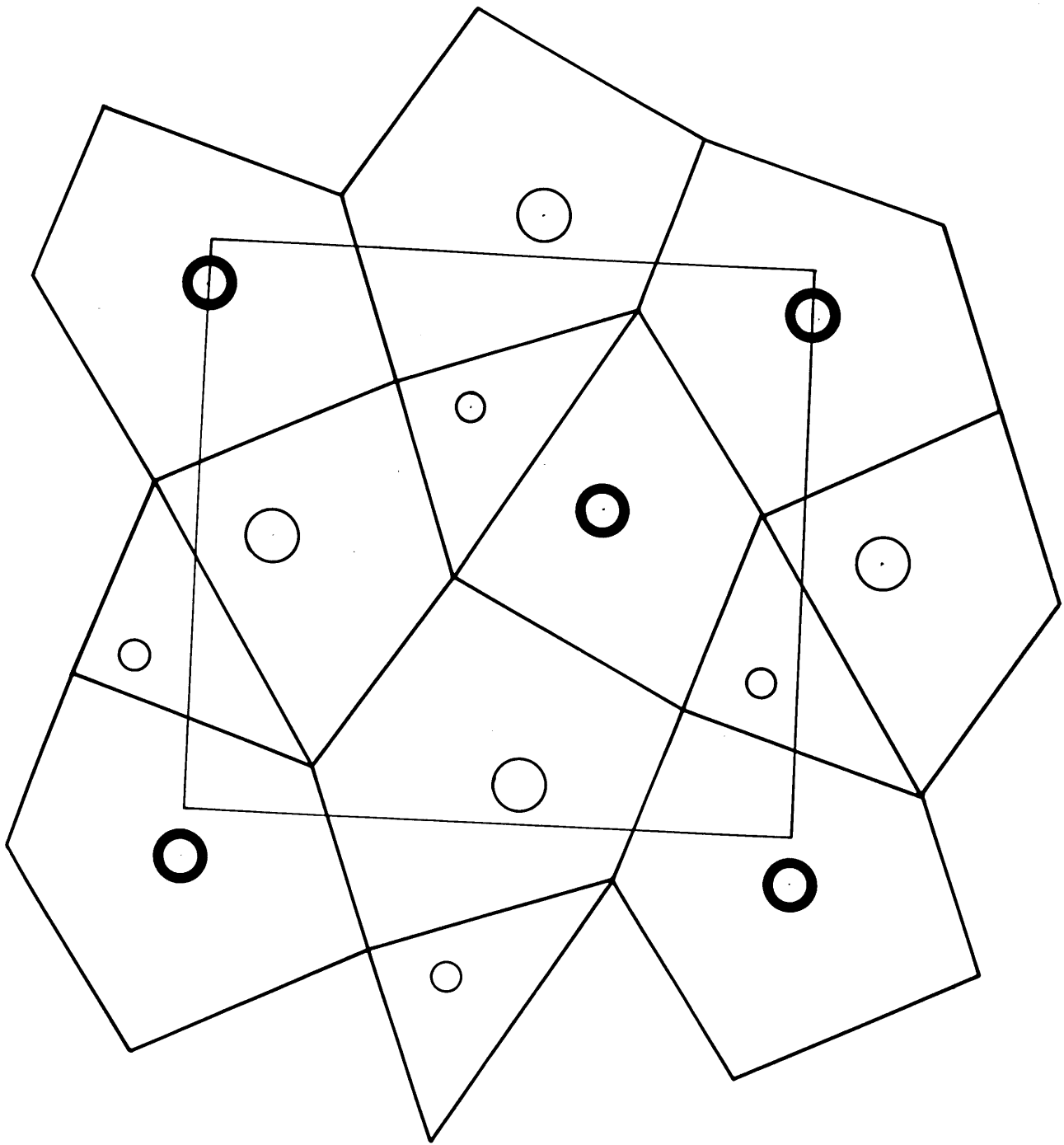


Fig. 45 Polygonal network of the structure of berthierite,  $\text{FeSb}_2\text{S}_4$  projected on (001), Fig. 53.

The large circles represent Sb atoms, and the small circles Fe atoms.

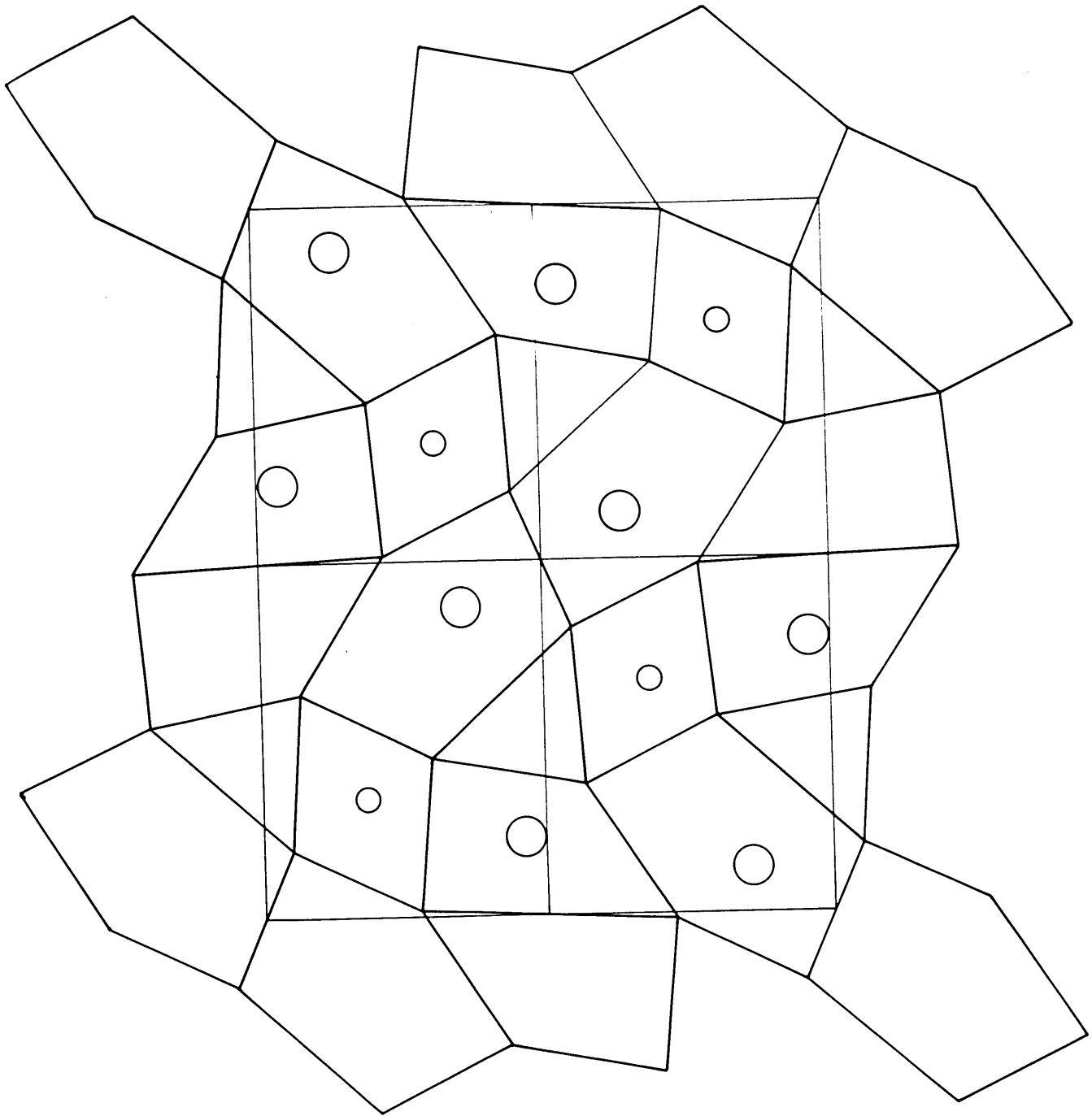


Fig. 46 Polygonal network of the structure of galenobismutite,  $\text{PbBi}_2\text{S}_4$ , projected on (010), Fig. 58. The heavy circles represent Pb atoms, and the light circles Bi atoms.

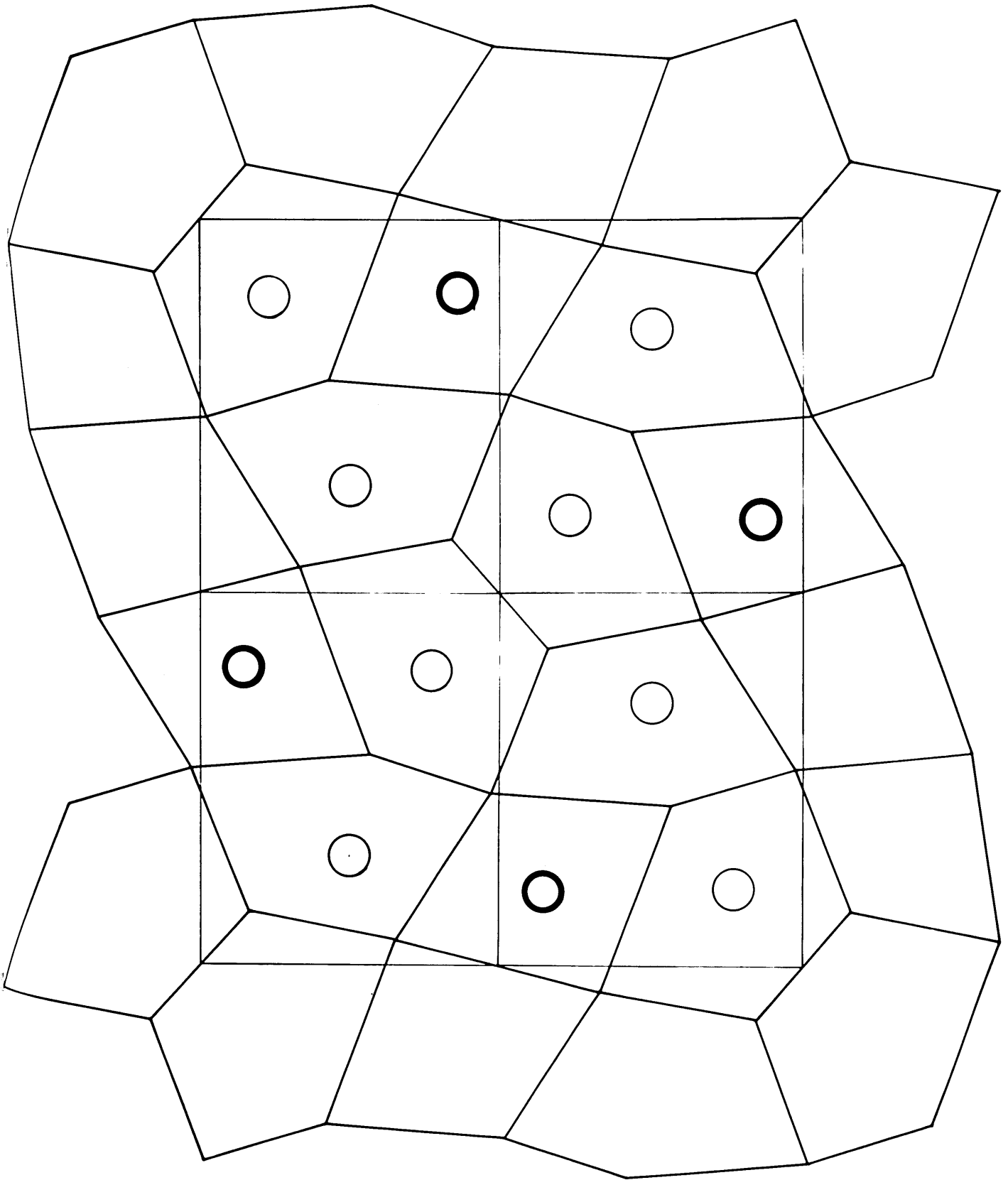


Fig. 47 Polygonal network of the structure of jamesonite,  $\text{FePb}_4\text{Sb}_6\text{S}_{14}$  projected on (001), Fig. 33. The large heavy circles represent Pb atoms, the large circles Sb atoms, and the small black circles Fe atoms.

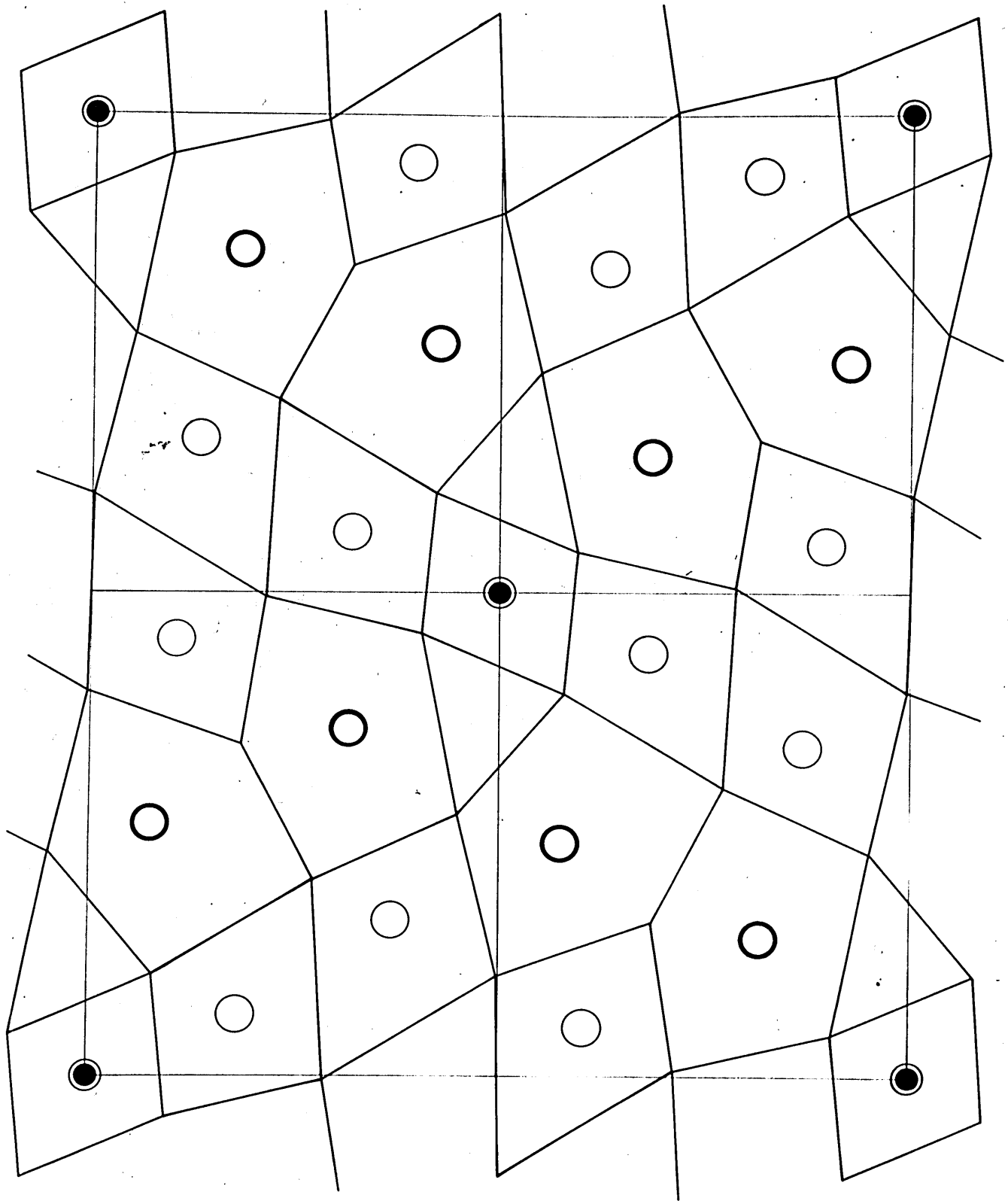




Fig. 48 Polygonal network of the structure of livingstonite,  $\text{HgSb}_4\text{S}_8$  projected on (010), Fig. 13 and Fig. 14.

Large circles represent Hg atoms, and small circles Sb atoms.

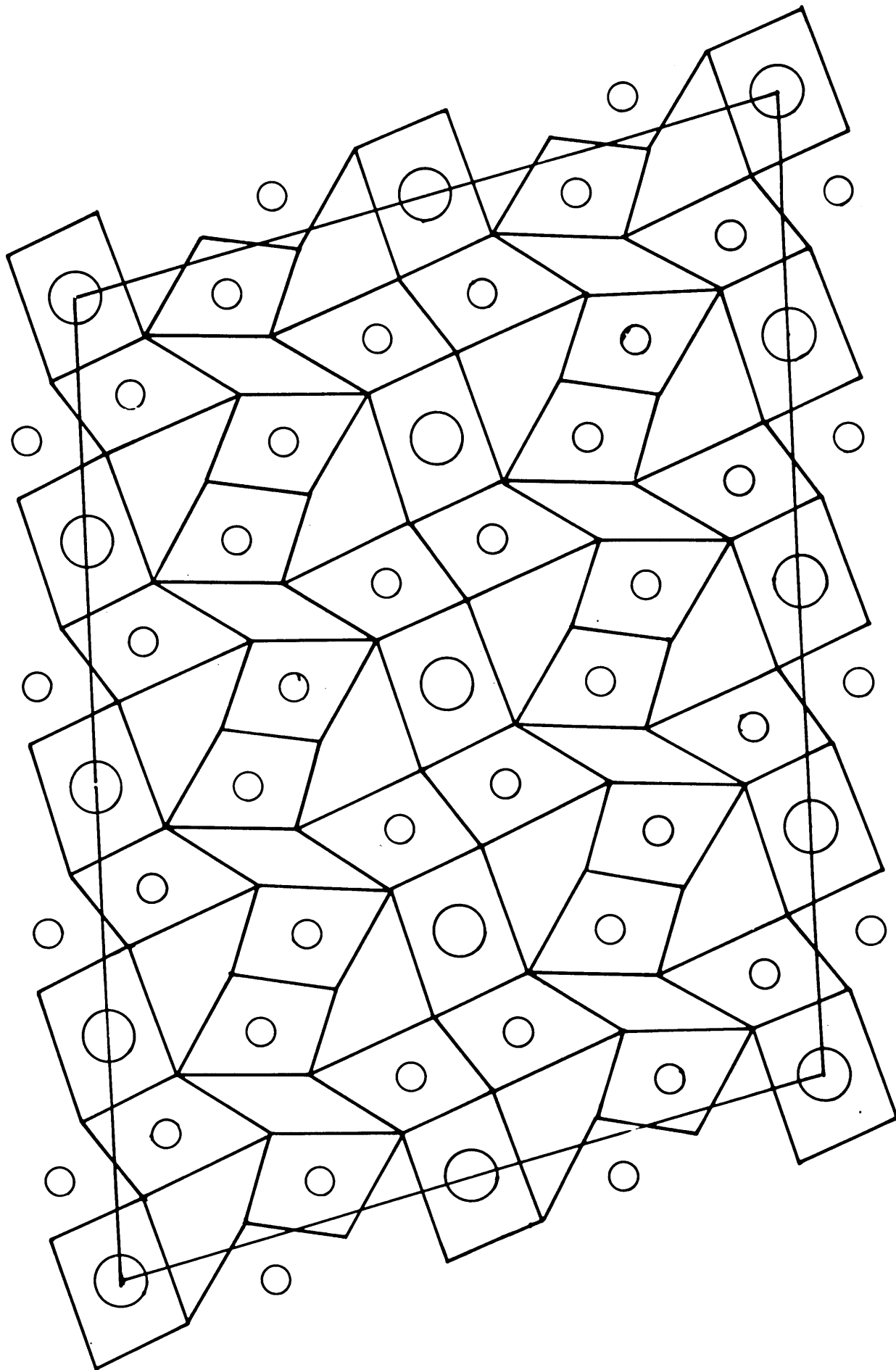


Table 20.

The second coordination polyhedra and the corresponding coordination polygons in the projection along 4A axis of the sulfosalt structures.

Atom	Second Coordination Polyhedra	Coordination Polygons
Cu	tetrahedron	3-gon (triangle)
Ag	distorted octahedron	4-gon
Fe	"	"
Hg	"	"
Pb	regular octahedron	"
Pb	(1) distorted octahedron	4-gon
As	(2) 7-vertices-8-hedron	4-gon or 5-gon
Sb		
Bi	(3) 8-vertices-11-hedron	5-gon

a table for the coordination polygons in the projected structures can be prepared. They are tabulated in Table 20.

Nature of polygonal network. Another point of view for discussing this polygonal network is the plane network described in some detail by Wells<sup>33,34,35</sup>. The nature of the network can be specified by the number of points in the translational or asymmetric unit, and their nature of connectedness. The connectedness is defined as the number of polygonal sides which terminate at a point. This number is equal to the number of polygons which share the point in common if the exceptional situation of loop<sup>33,34</sup> is not considered.

The nature of a polygonal network also can be described by the kinds and number of polygons in the unit. These characteristics of networks of each sulfosalt structure are tabulated in Table 21.

From examining the polygonal networks of sulfosalts structures, the following empirical rules can be obtained.

- (1) Except in the case of chalcostibite, Fig. 42, and of livingstonite, Fig. 48, the connectedness found in the networks is three and four.
- (2) In chalcostibite, all the connectedness is five, and in livingstonite, these five-connected points are found with four-connected points.
- (3) The polygons with more than six sides are not found.
- (4) There are, as in stibnite, Fig. 43, berthierite,

Table 21

Polygonal networks of the projections of acicular sulfosalts.

Minerals and Figures	Points in network					Polygons in network			
	P	p <sub>3</sub>	p <sub>4</sub>	p <sub>5</sub>	$\frac{2X}{(X-2)}$	h <sub>3</sub>	h <sub>4</sub>	h <sub>5</sub>	Jh <sub>j</sub>
Chalcostibite Fig. 42	2	0	0	2	$\frac{10}{13}$	$\frac{2}{3}$	$\frac{1}{3}$	0	$\frac{10}{3}$
Stibnite Aikinite Fig. 43	3	0	4	0	4	$\frac{1}{3}$	$\frac{1}{3}$	$\frac{1}{3}$	4
Seligmannite Fig. 44	6	0	6	0	4	$\frac{1}{3}$	$\frac{1}{3}$	$\frac{1}{3}$	4
Berthierite Fig. 45	4	0	4	0	4	$\frac{1}{4}$	$\frac{2}{4}$	$\frac{1}{4}$	4
Galenobismutite Fig. 46	4	2	2	0	$\frac{14}{3}$	0	$\frac{1}{3}$	$\frac{2}{3}$	$\frac{14}{3}$
Jamesonite Fig. 47	7	1	6	0	$\frac{54}{13}$	$\frac{1.5}{6.5}$ $= \frac{2}{13}$	$\frac{3.5}{6.5}$ $= \frac{7}{13}$	$\frac{2}{6.5}$ $= \frac{4}{13}$	$\frac{54}{13}$
Livingstonite Fig. 48	8	2	4	2	4	1	0	0	4

In all the above example the relation  $3h_3 + 4h_4 + 5h_5 = \frac{2X}{(X-2)}$  is seen to hold. X is computed as,

$$X = \frac{3p_3 + 4p_4 + 5p_5}{P}$$

Fig 44 and jamesonite, Fig. 48, unoccupied triangles. These triangles are the projections of the open space in the three dimensional stacking of polyhedra.

(5) There are unoccupied 4-gons in livingstonite. One of them is caused by the existence of  $S_2$  group in the structure, and the other is the result of projecting the open space in the polyhedral stackings.

Solution of polygonal network. The two kinds of specifications to be applied to the polygonal network were described in the above paragraph. One is the number and nature of the points in the networks, and the other is the number and nature of the polygons in the networks. By the solution of polygonal network, the relations between these two viewpoints are implied. The polygonal network will be given in terms of the number and connectedness of the points. The solution can be obtained in the number and kinds of polygons to be constructed with these points.

Polygonal network and chemical formula. To understand the relation between the polygonal network and chemical formula of the mineral, the following table of correspondency is useful.

Network theory	Chemical formula
Total number of points in the unit, P	Total number of S atoms
Total number of polygons, N	Total number of coordination polygons including unoccupied ones.

Network theory	Chemical formula
Total number of occupied polygons, $N_0$	Total number of metallic and submetallic atoms.
3-gon	Cu-triangle, or vacant triangle
4-gon	4-gons with central atoms Ag, Fe, Hg, Sb(As,Bi), and Pb.
5 gon	5-gons with central atoms Sb(As,Bi) and Pb.

Theorem of network theory. Wells has shown that

$$h_3 + h_4 + h_5 + h_p = 1 \dots\dots\dots(1)$$

and  $3h_3 + 4h_4 + 5h_5 + ph_p = 6 \dots\dots\dots(2)$

if all points are three-connected, and instead of (2),

$$3h_3 + 4h_4 + 5h_5 + ph_p = 4 \dots\dots\dots(3)$$

if all points are four-connected. In these formula  $h_p$  represents the fraction of p-gon in the unit of network.

Now in general the following two theorems can be proved.

Theorem 1. In two dimensional network, if all points are q-connected, the following two relations hold:

$$h_3 + h_4 + h_5 + h_p = 1$$

$$3h_3 + 4h_4 + 5h_5 + ph_p = \frac{2q}{(2-2)} \dots\dots\dots(4)$$

where  $h_p$  is the fraction of p-gon in the unit of network.

The proof Theorem 1 will be found in Appendix IV.

Theorem 2. If there are q-connected points and r-connected points in the ratio of Q : R in the two dimensional network, instead of (4), the following relation holds:

$$3h_3 + 4h_4 + 5h_5 + \dots + ph_p = \frac{2X}{(X-2)} \quad (5)$$

where

$$X = \frac{qQ + rR}{Q + R}$$

The proof of Theorem 2 is given in Appendix V. The significance of this theorem is that in a mixed network an averaged connectedness per point plays the same role of the single value of connectedness in a uniform network.

Ambiguities in the solution of polygonal network.

By means of the above-stated two theorems the solution in terms of number and kinds of polygon can be obtained if the nature of connectedness is given in the problem. But in applying these theorems to the problem of the projections of sulfosalt structures three kinds of ambiguities should be mentioned.

(1) Ambiguity in the nature of connectedness. The connectedness in all-hexagon networks is 3, and the connectedness in all-triangle network is 6. These two values of connectedness can be treated as extreme cases. As observed before, the connectedness found in major parts of the projection of sulfosalt structures is three and four, and in a few cases five. There is no way to pre-determine the value of connectedness from the given chemical formula. But there is one theorem which limits the value of connectedness in relation to the chemical formula.

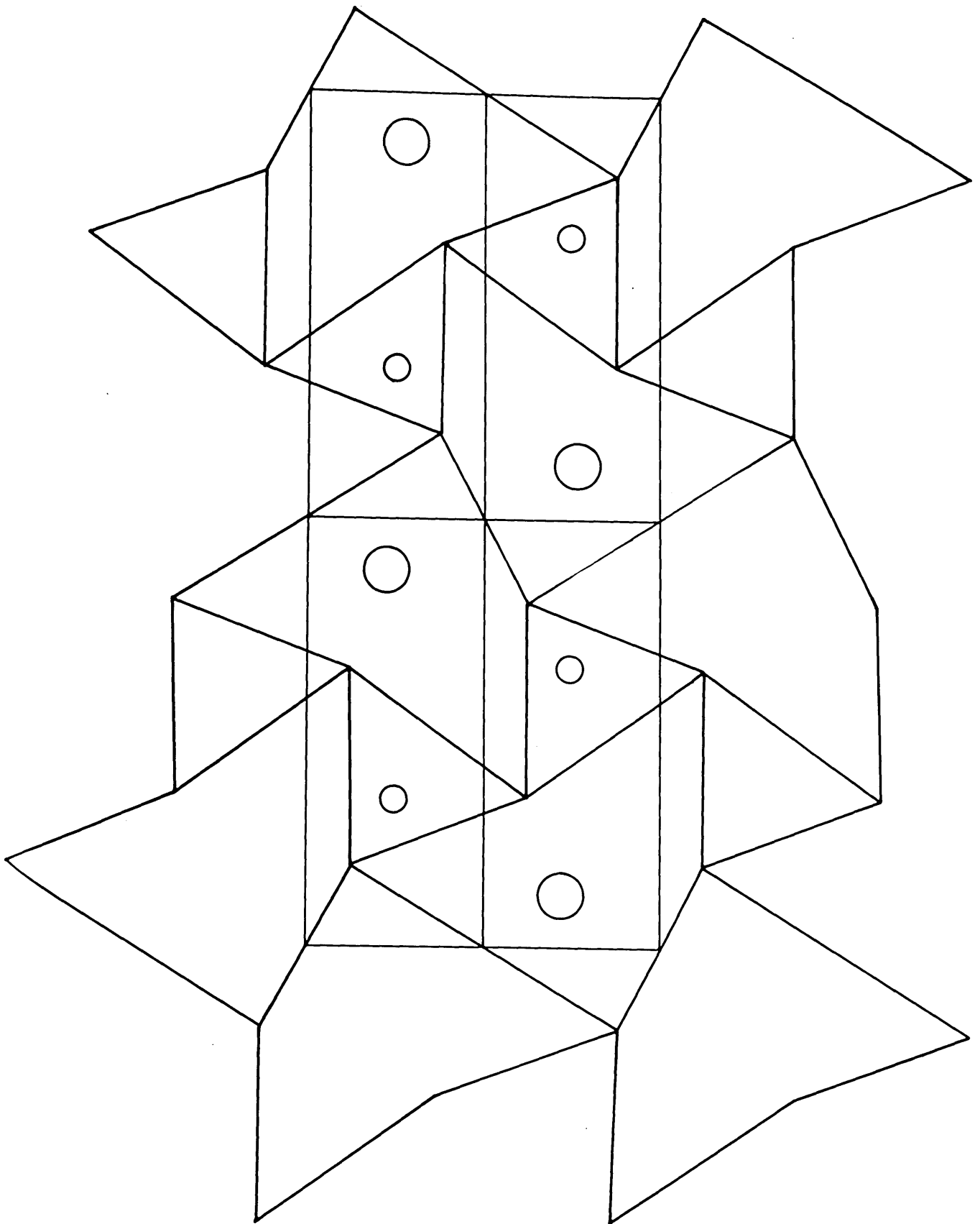


Theorem 3. If the chemical parameter  $f$  has a value greater than 1.0, the existence of the connectedness larger than 4 must be assumed in the network.

The proof of this theorem is given in Appendix VI. In the network of chalcostibite, Fig. 42, it is found that all the points are 5-connected. But the value of  $f_3$  of the mineral,  $\text{CuSbS}_2$  is equal to 1.0. Actually the idealized network of this structure can be constructed with points of 4-connectedness only as the above theorem implies. This idealized network is shown in Fig. 49. In the actual network the distortion of 5-gons associated with Sb atoms are such that one angle becomes greater than  $\pi$ . To avoid such polygons the division of each 5-gon into one 3-gon and one 4-gon was made, and the connectedness of the points is increased to 5. This 4-gon is associated with Sb, and consequently the 3-gon is vacant. The same kind of discussion applies to the other case of exception to the above theorem, the network of livingstonite, Fig. 48. Here a 6-gon with one angle greater than  $\pi$  is divided into two 4-gons by an additional line. One of the 4-gons is vacant, and some of the points become 5-connected.

(2) Ambiguity in the nature of the polygons. The possible polygons to be associated with each central atom are listed in Table 20. For the atoms Pb, and Sb(As,Bi), there are always two possibilities, i.e. 4-gon or 5-gon. There is no way to resolve this point.

Fig. 49 Alternative representation of the polygonal network of chalcostibite projection. In this network, there are 3-connected and 4-connected points. In the network illustrated in Fig. 42, there were only 5-connected points.



(3) Ambiguity due to the probable existence of the vacant triangles. There is no criterion for finding the existence and number of the vacant triangles. As will be shown in the later examples, this ambiguity increases the number of possible solutions two-fold or more.

Systematic solution of the polygonal network. There are two kinds of approach to solve the given networks depending on the nature of the problem. The first kind of problem is to find the solution from a given chemical formula without any assumption concerning the nature of connectedness. The second problem is to find the solution from a given chemical formula assuming that the connectedness of points is a mixture of 3 and 4, a most general case in the projections of acicular sulfosalts. The second kind approach will be treated systematically below.

The problem here is to exhaust the possible network types given the number of points in the unit of the network. In terms of crystal chemistry, it amounts to stating that, given the number of S atoms in the formula in the asymmetric unit, exhausting the possible types of projections in terms of the coordination polygons.

The solutions can be obtained by applying the above-stated Theorem 1 and 2. The systematic steps are given in Theorem 4. The derivation of this theorem by means of earlier theorems is treated in Appendix VII.

Theorem 4. The possible types of the polygonal networks for the given chemical formula can be derived by the following steps: Only 3-connected and 4-connected points are assumed in the networks.

Step 1. Determine the exact chemical formula in the asymmetric unit.

Step 2. Assign the possible kinds of polygons to metallic or submetallic atoms.

Step 3. If the total number of polygons in the unit is found as an integer, the possible combinations of  $p_3$  (number of 3-connected points) and  $p_4$  (number of 4-connected points) in the unit is given by

$$\begin{aligned} p_3 &= 2n && \text{where } n = 0, 1, 2, \dots, P/2 \text{ if } P \text{ is} \\ p_4 &= P-2n && \text{even, and} \\ &&& n = 0, 1, 2, 3, \dots, (P-1)/2 \\ &&& \text{if } P \text{ is odd.} \end{aligned}$$

where  $P$  is the total number of points in the unit.

Step 4. If  $P$  and  $n$  are fixed, the total number of polygons,  $N$ , is given by

$$N = P - n$$

Step 5. If  $P$  and  $n$  are fixed,  $n_3$ ,  $n_4$ , and  $n_5$  can be determined by

$$\begin{aligned} 0 &\leq n_3 \leq \frac{P-3n}{2} \\ n_5 &= n_3 + 2n \\ n_4 &= N - n_3 - n_5. \end{aligned}$$

Step 6. Among the solutions there are those with  $N_0$  equal to the number of metallic and submetallic atoms in the formula. These are the possible solutions representing the projection.

When the given formula does not include Cu atoms, that is, when there is no ambiguity due to the vacant triangle, the number of the possible solutions is given by the following theorem:

Theorem 5. The number of possible solutions representing the given chemical formula is

$$P - N_0 + 1$$

where P is the number of S atoms in the formula,  $N_0$  is the number of central atoms (metals and submetals) in the formula. The proof of this theorem is given in Appendix VIII.

For minerals berthierite,  $\text{FeSb}_2\text{S}_4$  and galenobismutite,  $\text{PbBi}_2\text{S}_4$ ,  $P = 4$  and  $N_0 = 3$ . By Theorem 5, the number of possible solutions in this case is two. In one of the following examples it is shown that these two minerals represent one or the other of these two solutions.

Examples of the systematic treatment. In Table 19a, the sulfosalt minerals of the group A are tabulated. The minerals are listed in the increasing order of P, i.e. the number of S atoms in the formula. The systematic solutions are illustrated below for the smaller values of P.

Example 1,  $P = 2$ . The solutions are worked out most easily by a tabular form. It is shown below for the case of  $P = 2$ .

P	$p_3$	$p_4$	n	N	$(P-3n)/2$	$n_3$	$n_4$	$n_5$	Examples
2	0	2	0	2	1	0	2	0	matildite
						1	0	1	chalcostibite
2	0	1	1	-					

By step 3 of Theorem 6, the possible values of  $n$  can be determined. In the present case they are 0 and 1. Also by step 3, the possible combinations of  $p_3$  and  $p_4$  are computed as in the second and third columns of table shown above.

By step 4, for each combination of  $p_3$  and  $p_4$ , or for each value of  $n$ , the possible number of polygons,  $N$ , is determined.

By step 5, the upper limit of  $n_3$  is evaluated by  $(P - 3n)/2$ . The possible values of  $n_3$  can be tabulated at once starting from zero to this upper limit. If this upper limit is not an integer,  $n_3$  will be listed to the closest integer. In the present case they are found to be 0 and 1. From each value of  $n_3$ , the values of  $n_5$ , and then  $n_4$  are easily computed by formula of step 5.

There are two solutions in case of  $P = 2$ . One of them represents a network of all 4-gons, and can be considered to represent a projection of the galena-type given in Fig. 38.

The second solution is a network in which 3-gons and 5-gons are found in the ratio of 1 : 1. This represents the ideal case of the projection of chalcostibite, Fig. 49.

The actual network of chalcostibite was shown in Fig. 48. In Fig. 50 the second kind of arrangement of 3-gons and 5-gons in the ratio of 1 : 1 is illustrated. In Fig. 49 the two successive sides of 5-gons are shared with neighboring 3-gons. In Fig. 50 the alternative two sides of 5-gons are shared with 3-gons. These two drawings illustrate that the diagrammatic representation of the solution obtained is not uniquely fixed.

Example 2,  $P = 3$ . The possible values of  $n$  are 0 and 1. The solutions are worked out in a tabular form below.

P	$p_3$	$p_4$	n	N	$(P - 3n)/2$	$n_3$	$n_4$	$n_5$	Example
3	0	3	0	3	1.5	0	3	0	trivial
						1	1	1	stibnite aikinite
	2	1	1	2	0.5	0	0	2	no example

The network representing the projection of stibnite is illustrated in Fig. 43. The difference between stibnite and aikinite is the existence of a vacant triangle in the former structure and the filling of it by a Cu atom in the latter case. The network representing the projection of asymmetric unit of seligmannite is



Table 19a. Group A.

The sulfosalt minerals of this group are characterized by one unit cell dimension of approximately  $4\text{\AA}$ , and by their crystal habits as acicular to elongated thin tabular forms.

Mineral	Space Group	Unit Cell Dimensions	Plane Group of Projection	Formula in Asymmetric Unit of Projection	No. of S in Formula	Structure
Matildite	orth.	$a = 3.92, b = 4.05, c = 5.66$		$\text{AgBiS}_2$	2	Known, need refinement.
Chalcostibite	Pnam	$c = 3.78, a = 6.01, b = 14.46$	pgg	$\text{CuSbS}_2$	2	Known
Emplectite	Pnam	$c = 3.89, a = 6.13, b = 14.51$	pgg	$\text{CuBiS}_2$	2	"
Stibnite	Pnma	$b = 3.83, c = 11.20, a = 11.28$	pgg	$\text{Sb}_2\text{S}_3$	3	"
Aikinite	Pnma	$b = 4.00, c = 11.30, a = 11.65$	pgg	$\text{CuPbBiS}_3$	3	"
Berthierite	Pnam	$c = 3.76, a = 11.44, b = 14.12$	pgg	$\text{FeSb}_2\text{S}_4$	4	"
Galenobismutite	Pnam	$c = 4.08, a = 11.74, b = 14.47$	pgg	$\text{PbBi}_2\text{S}_4$	4	"
Pavonite	C2/m	$b = 4.03, a = 13.35, c = 16.34$ $\beta = 94^\circ 30'$	p2	$\text{AgBi}_3\text{S}_5$	5	Unknown
(synthetic)	C2/m	$b = 4.00, a = 13.08, c = 14.70$ $\beta = 99^\circ 24'$	p2	$\text{Cu}_{1.5}\text{Bi}_{2.5}\text{S}_{4.5}$	4.5	Unknown
Cuprobismuthite	C2/m	$b = 3.93, a = 6.01, b = 14.46$ $\beta = 100^\circ 21'$	p2	$\text{Cu}_3\text{Bi}_3\text{S}_6$	6	Unknown
Falkmannite	P2 <sub>1</sub> /a	$c = 4.02, a = 15.67, b = 19.06$ $\beta = 91^\circ 50'$	pgg	$\text{Pb}_3\text{Sb}_2\text{S}_6$	6	Unknown
Jamesonite	P2 <sub>1</sub> /a	$c = 4.03, a = 15.57, b = 18.89$ $\beta = 91^\circ 48'$	pgg	$\text{Fe}_{0.5}\text{Pb}_2\text{Sb}_3\text{S}_7$	7	Known
Livingstonite	A2/a	$b = 4.00, c = 21.49, a = 30.25$ $\beta = 104^\circ 12'$	p2	$\text{HgSb}_4\text{S}_8$	8	"
Cosalite	Pbnm	$c = 4.05, a = 19.04, b = 23.81$	pgg	$\text{Pb}_4\text{Sb}_4\text{S}_{10}$	10	Unknown
Robinsonite	P $\bar{1}$	$c = 3.97, a = 16.51, b = 17.63$ $\alpha = 96^\circ 04', \beta = 96^\circ 22', \gamma = 91^\circ 12'$	p2	$\text{Pb}_{3.5}\text{Sb}_3\text{S}_{12.5}$	12.5	"
Kobellite	Pnmm	$c = 4.01, a = 22.57, b = 34.01$	pmg	$\text{FePb}_6\text{Bi}_4\text{Sb}_2\text{S}_{16}$	16	"
Cannizzarite A	P2/m	$b = 4.10, a = 4.13, c = 15.5$ $\beta = 99^\circ 00'$	p2	$\text{Pb, Bi, S}$	?	"
Cannizzarite B	C2/m	$b = 4.10, a = 7.07, c = 15.5$ $\beta = 99^\circ 00'$	p2	"	?	"
(synthetic)	P2/m	$b = 4.08, a = 4.11, c = 18.58$ $\beta = 93^\circ 35'$	p2	"	?	"
(synthetic)	F2/m	$b = 4.08, a = 7.03, c = 37.16$ $\beta = 93^\circ 35'$		"	?	"

Fig. 50 Idealized network of the chalcostibite projection. This represent one type of arrangement of 3-gons and 5-gons in the ratio of 1 : 1, and with two 4-connected points in the asymmetric unit. The second type of arrangement is shown in Fig. 51.

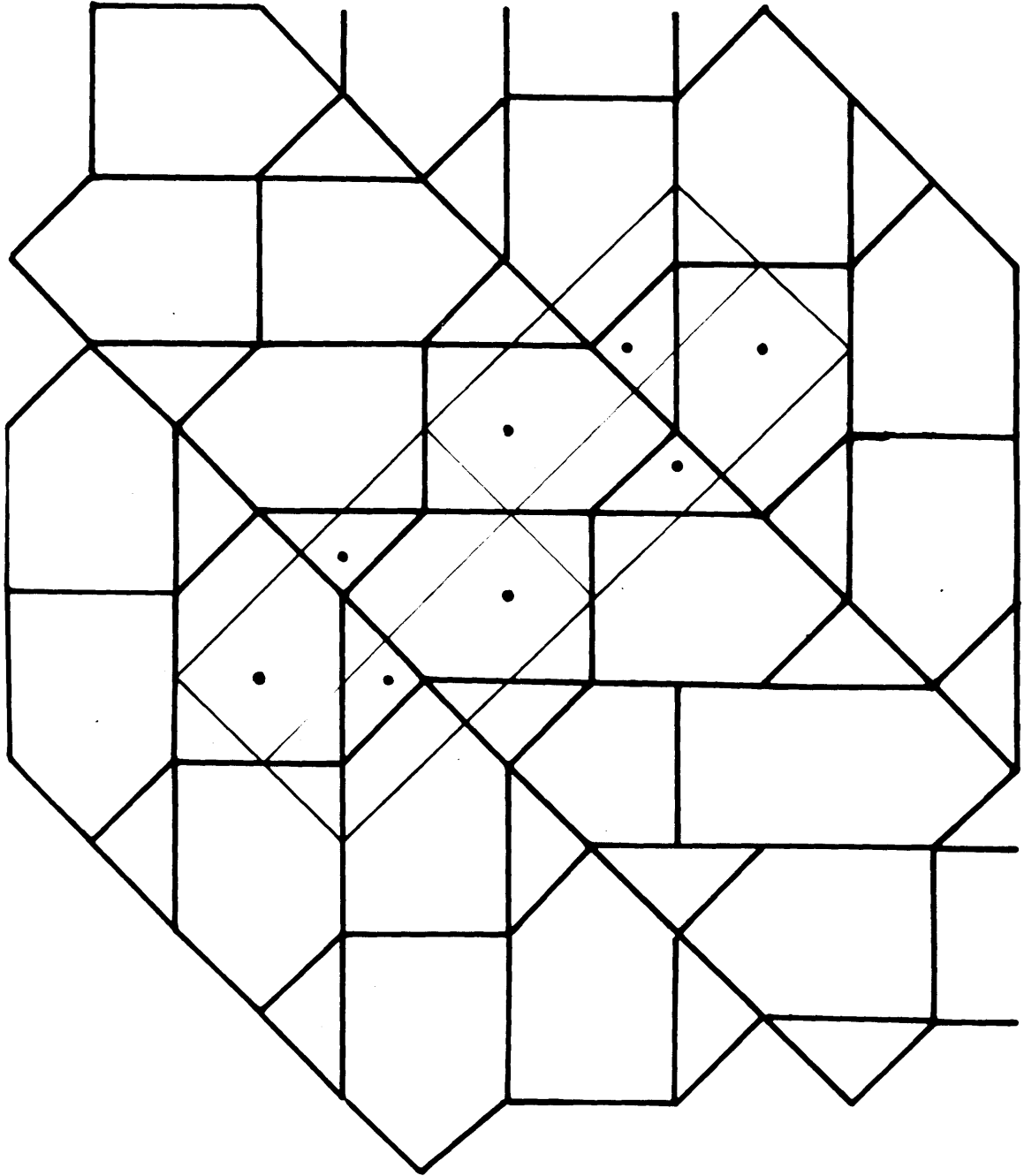
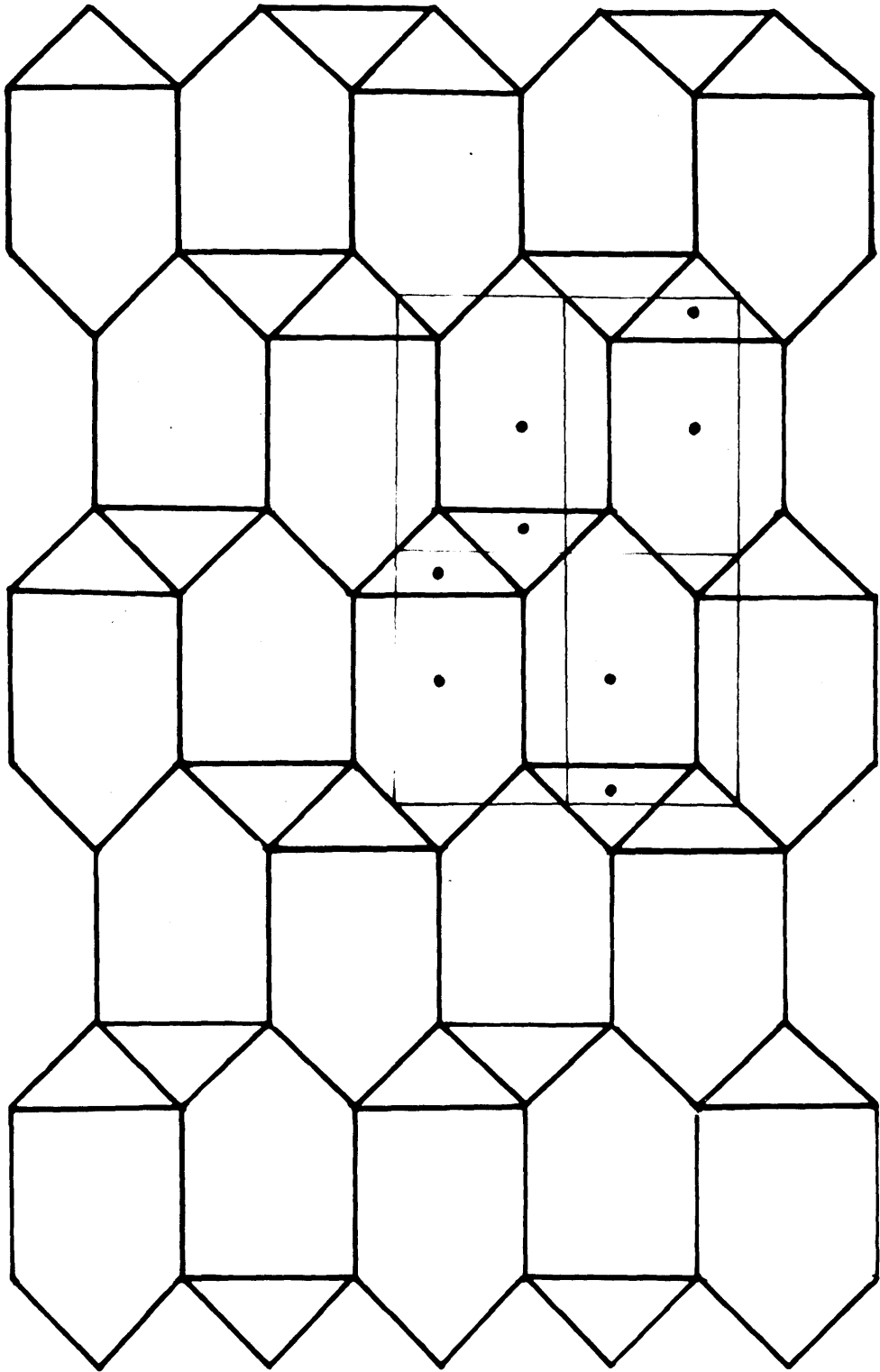


Fig. 51 The second type of arrangement of 3-gons and 5-gons. In the asymmetric unit of projection there is one of each. The two points in the unit are both 4-connected.



illustrated in Fig. 44. In this network there are also 3-gons, 4-gons, and 5-gons in the ratio of 1:1:1, and  $P = 6$ . The difference in the relative arrangement of polygons between aikinite and seligmannite can be seen from Fig. 43 and Fig. 44.

The first solution can be considered as three units of the galena-type network, and therefore is a trivial one.

The third solution with all 5-gons is not yet found among the projections of known sulfosalts.

Example 3,  $P = 4$ .

Solutions are worked out in a tabular form below.

P	$p_3$	$p_4$	n	N	$(P-3n)/2$	$n_3$	$n_4$	$n_5$	Example
4	0	4	0	4	2	0	4	0	trivial
						1	2	1	berthierite
						2	0	2	unknown
	2	2	1	3	0.5	0	1	2	galeno-bismutite

In the case of berthierite, Fig. 45, Fe and  $Sb_I$  are associated with 4-gons, and  $Sb_{II}$  with a 5-gon, and there is a vacant 3-gon. In the case of galenobismutite, Fig. 46, Pb is associated with a 4-gon, all Bi with 5-gons, and no vacant 3-gon is found in the network.

For the third solution, there are two possibilities. If the Cu atom is associated with two 3-gons the possible chemical formula is, for example,  $Cu_2Sb_2S_4$ . If there are

one Cu-3-gon and one vacant 3-gon, the possible formula is  $\text{CuSb}_2\text{S}_4$ . The first compound can be regarded as two unit cells of chalcostibite, and the second compound is unknown.

Example 4,  $P = 5$ .

The solutions are given in a table form below.

P	$p_3$	$p_4$	n	N	$(P-3n)/2$	$n_3$	$n_4$	$n_5$
5	0	5	0	5	2.5	0	5	0
						1	3	1
						2	1	2
	2	3	1	4	1	0	2	2
						1	0	3

In Table 19a the only example with  $P = 5$  is the mineral pavoniye,  $\text{AgBi}_3\text{S}_5$ . For pavonite,  $N_0 = 4$ , and the 3-gon is to be considered as vacant. So the possible solutions for this mineral are the following two:

	$p_3$	$p_4$	$n_3$	$n_4$	$n_5$
(1)	0	5	1	3	1
(2)	2	3	0	2	2

Example 5, Jamesonite,  $\text{FePb}_4\text{Sb}_6\text{S}_{14}$ .

In the asymmetric unit of projection there is  $\text{Fe}_{0.5}\text{Pb}_2\text{Sb}_3\text{S}_7$ . Thus  $P = 7$ , and  $N_0 = 5.5$ . This is a case where  $N$  in the unit is half an integer. The steps corresponding to those given

in Theorem 6 are found in Appendix IX. The possible solutions with  $P = 7$  are as follows.

	$p_3$	$p_4$	$n_3$	$n_4$	$n_5$
(i)	0	7	1.5	4	1.5
(ii)	1	6	1	3.5	2
(iii)	2	5	0.5	3	2.5
(iv)	3	4	0	2.5	3

Since Fe is definitely to be associated with 4-gons, the value of  $n_4$  is expected as a half integer. Two solutions among the above-listed four can be selected as probable ones. The actual network, Fig. 47, is represented by (ii) with one vacant triangle in the asymmetric unit of projection. In jamesonite Fe and Sb are associated with 4-gons, and Pb with 5-gons.

#### Summary of the polygonal network theory.

The method developed by Wells in his treatment of the geometrical basis of crystal chemistry was generalized and applied to the crystal chemistry of sulfosalts. The solutions were systematically obtained for given  $P$ , the number of points in the unit of networks. These solutions represent the projections of structures with given  $S$  atoms in the asymmetric unit of projection. All the projections of the known acicular sulfosalts find their representative networks among the solutions obtained. This fact is considered as the theoretical confirmation of the basic assumption, the principle of open stackings of coordination polyhedra. Because of the openness in the structure, the ambiguity due to the vacant 3-gons



in the networks could not be resolved. This ambiguity prevented the unique solutions for the minerals with unknown structures. But if the basic assumptions are correct, the actual structures of these minerals should find their representative networks among the possible solutions.

### 3. The Sb(As,Bi)-S chains and layers

Introduction. In the previous section the structures of the sulfosalts of the acicular group were treated from the viewpoint of open stacking of the second coordination polyhedra. The shortcoming of this treatment is twofold. First, the satisfactory application of the principle was possible only in the form of the polygonal network theory. Thus the projections of the structures, not the three-dimensional structures themselves, have been considered. Second, the important structural motifs found among the members of acicular sulfosalts were obscured. These motifs are the various kinds of the atomic groups composed of Sb(As,Bi) atoms and S atoms, in the shapes of chains and layers running parallel to the acicular axes of the minerals. The building unit of these groups is an  $\text{Sb(As,Bi)S}_3$  trigonal pyramid. Since this is the first coordination polyhedron, the discussion of the features has been necessarily neglected in the previous section. In this section the building up of the larger Sb(As,Bi)-S groups from this unit will be considered in detail. The discussion is similar to the familiar polymerization of the Si-O tetrahedra in silicate crystal chemistry. In the following descriptions, the submetallic atoms, As, Sb, and Bi will be represented simply by Sb.

Electronic configurations of Sb, and S atoms, and structures of the elements Sb and S. Each one of the three

submetallic atoms, As, Sb, and Bi has four outer orbitals. They are respectively  $4s4p^3$ ,  $5s5p^3$ , and  $6s6p^3$ . There are five electrons to fill these orbitals. In the normal case two electrons are paired and fill the s orbital, and the remaining three electrons are unpaired and occupy three p orbitals. These three electrons in the p states are capable of forming three covalent bonds.

The structures of the metallic forms of As, Sb, and Bi are well known, but the nature of the chemical bonds in these submetals has not been quite clearly presented. These metals provide a type example of the Brillouin zone theory of the metallic bonds<sup>36</sup>. Regarding their rhombohedral crystal structure as a distorted NaCl type, the deviation has been explained as due to accommodating the five outer electrons in the first Brillouin zone. Recently Krebs<sup>37</sup> presented another picture from the concept of covalent bonds resonating among six positions. The structure of these submetals is a double layered structure. In the double layer each atom forms three strongest bonds of p character to the three closest neighbors in the layer. There are, however, three additional atoms at larger distances in the adjacent layer. The six neighbors form a distorted octahedron around the central atom. Krebs' interpretation is that three p bonds resonate among six positions, which can be accounted for if positive and negative region of the p wave function are considered. The difference between the two kinds of interatomic distances is explained as the result

of the difference in the probability of resonance toward first three, and second three neighbors. According to Krebs, this resonance is responsible for the metallic nature of these elements.

Pauling<sup>38</sup> recently treated the valence states of these elements in alloy with true metallic atoms. He predicted that these atoms would have metallic valences between 1 and 1.5 in a metallic state. With the single bond radii of these atoms as

$$\begin{aligned} R_1 &= 1.210\text{\AA} \text{ for As} \\ &= 1.391\text{\AA} \text{ for Sb} \\ &= 1.510\text{\AA} \text{ for Bi} \end{aligned}$$

and his formula to compute the bond number,

$$R_n = R_1 - 0.300 \log_{10} n$$

he found that As in Cu and Ag; Sb in Pb, Tl, Cu, and Ag; Bi in Pb and Au; all have this metallic valence. The values he found were between 1.00 and 2.10.

It is interesting to note that if computed with these  $R_1$  values, then the valences of As, Sb, and Bi in the elements are computed as (see Appendix X) 2.31, 2.45, and 2.74 respectively. These values are considered as intermediate between the metallic valences and covalent valences with three p electrons of each atom.

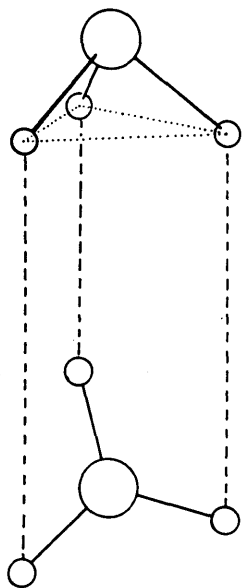
Whatever the true nature of the chemical bonds in these elements, it is to be noted that these atoms have a tendency to obtain additional neighbors beside the three bonded by covalent bonds of p character.

Sulfur has also four outer orbitals,  $3s3p^3$  and six electrons to fill them. Two electrons are paired and are in the s orbital. Two further are paired and in one of p orbitals, and the remaining two are unpaired and occupy two p orbitals. In orthorhombic sulfur, the unit of structure is the  $S_8$  molecule, which has the form of a puckered 8-membered ring. The S-S distance in this molecule is 2.12A, and interbond angle is  $105^\circ$ . The chemical bonds holding the ring are considered as two covalent bonds of p character due to the two unpaired electrons. Exact nature of the behavior of S atom in various environments is not well understood. The simpler varieties are the tetrahedral one in ZnS, and the octahedral one in PbS. From the covalent approach they are explained as, respectively,  $sp^3$  hybrid bonds<sup>39</sup>, and resonating 3p bonds<sup>37</sup>.

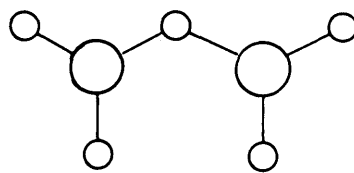
Independent  $SbS_3$  pyramid. If the covalency of 3 and 2 are associated with Sb and S atoms, the first unit to be considered is an  $SbS_3$  group of atoms. In this unit three covalent bonds of the Sb atom are satisfied within the unit, but one of the two bonds of each S atom is not satisfied. The formula corresponding to the notations for Si-O groups can be written as  $(SbS)_3$ . The number 3 indicates the unsatisfied three covalent bonds associated with this group. An example of this unit is found in the structures of proustite,  $Ag_3AsS_3$  and pyrargyrite,  $Ag_3SbS_3$ . The detailed discussion of these structures will be found in section 5.

Fig. 52. Schematic representations of Sb-S groups. The large circles represent Sb atoms, and small circles S atoms.

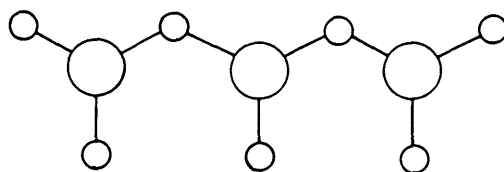
- (a)  $\text{SbS}_3$  trigonal pyramid.
- (b)  $\text{Sb}_2\text{S}_5$  group.
- (c)  $\text{Sb}_3\text{S}_7$  group.
- (d)  $\text{Sb}_4\text{S}_8$  ring.
- (e)  $\text{SbS}_2$  chain with a projection along the chain axis.



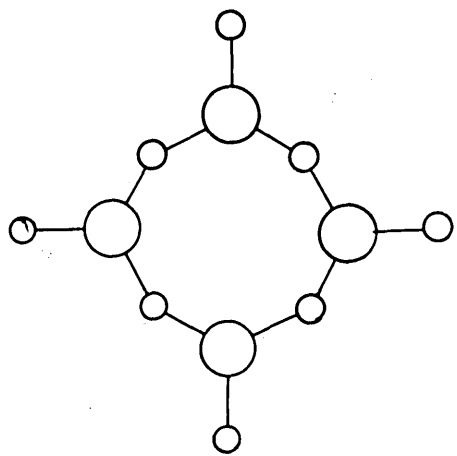
a



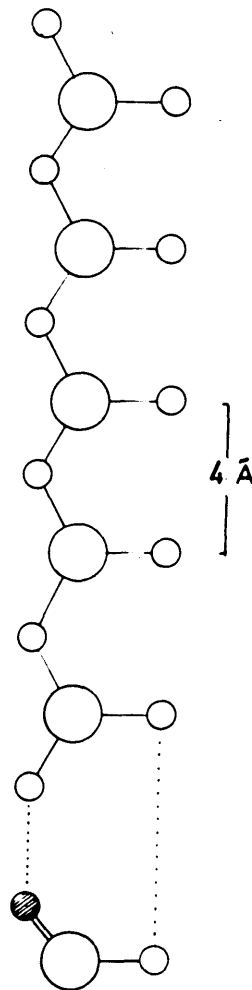
b



c



d



e

The geometry of this unit is illustrated in Fig. 52a.

Although the theoretical interbond angles between three p bonds are  $90^\circ$ , the observed angles in the structures are about  $100^\circ$ .

Finite group of Sb and S atoms. If two adjacent  $\text{SbS}_3$  groups share one S atom between them, groups such as  $\text{Sb}_2\text{S}_5$  and  $\text{Sb}_3\text{S}_7$  will be obtained. These are illustrated in Fig. 52b and 52c. The formulas of these groups can be given as  $(\text{Sb}_2\text{S}_5)^4$ , and  $(\text{Sb}_3\text{S}_7)^5$ . Larger groups are also conceivable. The  $\text{Sb}_3\text{S}_7$  group is found in jamesonite,  $\text{FePb}_4\text{Sb}_6\text{S}_{14}$ . In the structure of jamesonite, Fig. 33, two  $\text{Sb}_3\text{S}_7$  groups related by a center of symmetry form the larger double group of  $\text{Sb}_6\text{S}_{14}$ , although the Sb-S distances between two groups are of the order of Van der Waals distances. No example of the  $\text{Sb}_2\text{S}_5$  group is known. Although an example has not been found yet, closed groups such as  $(\text{Sb}_4\text{S}_8)^4$ , Fig. 52d, are theoretically possible.

$\text{SbS}_2$  chain. If an infinite number of  $\text{SbS}_3$  groups share one S atom between neighboring groups, a single chain of the composition  $\text{SbS}_2$  is obtained. This chain is schematically represented in Fig. 52e. This chain is found in the structure of berthierite,  $\text{FeSb}_2\text{S}_4$ , Fig. 53. The projection of this chain on the plane normal to the chain axis is also shown in Fig. 52e, and comparison of this with Fig. 53 indicates this chain in the structure. In every other example the chain is associated with its centrosymmetric



Fig. 53a Schematic representation of the structure of berthierite,  $\text{FeSb}_2\text{S}_4$  projected on (001) after Buerger and Hahn<sup>4</sup>. Open circles represent the atoms with z coordinates equal to zero, and shaded circles those with z coordinates equal to 1/2. Figures indicate the interatomic distances in Å unit.

Fig. 53b. Schematic representation of the projection of berthierite given for the four unit cells. The shaded circles in Fig. 53a are filled in.

$\text{SbS}_2$  chains are emphasized. An octahedral coordination around Fe atom, and  $\text{Sb}_4\text{Fe}_2\text{S}_8$  building unit is shown.

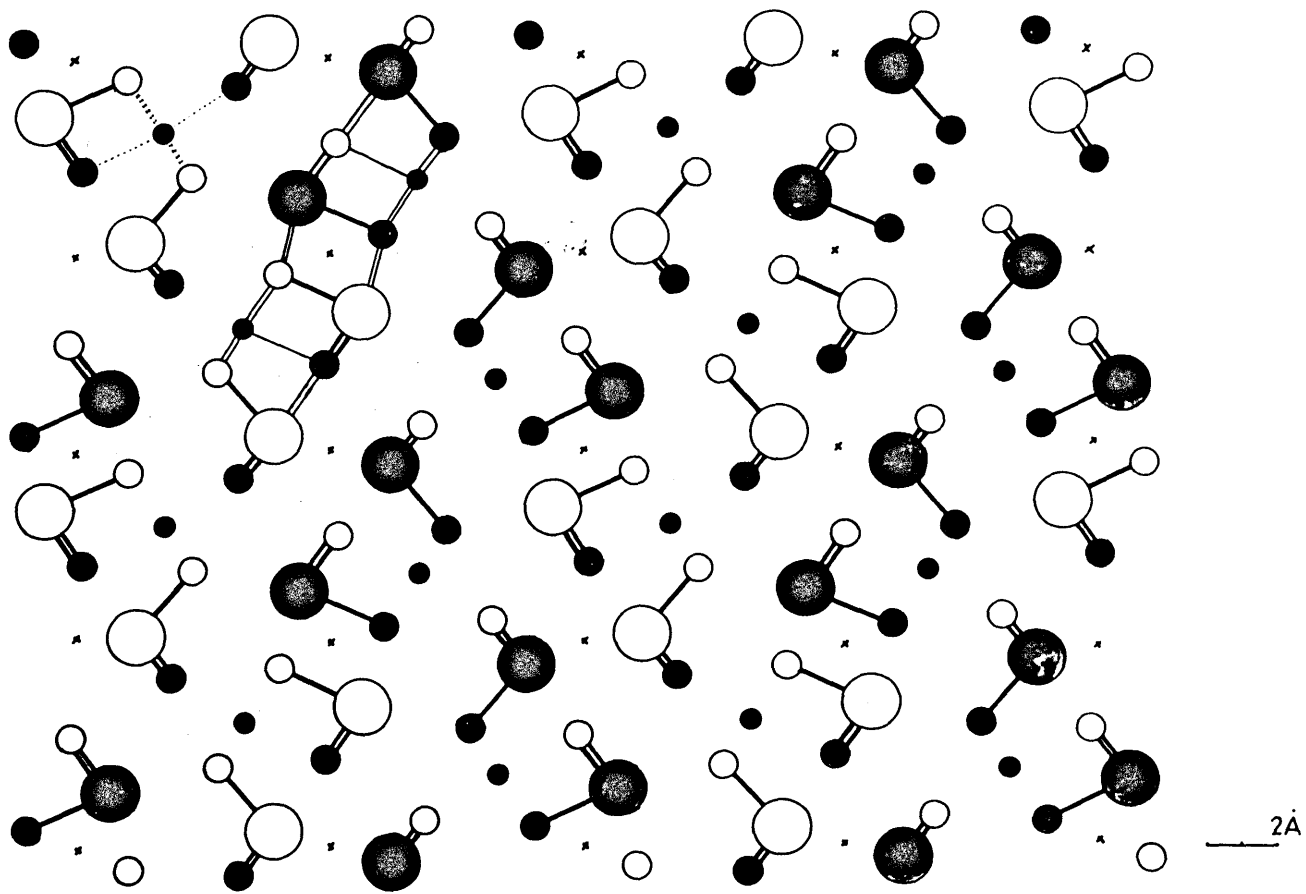
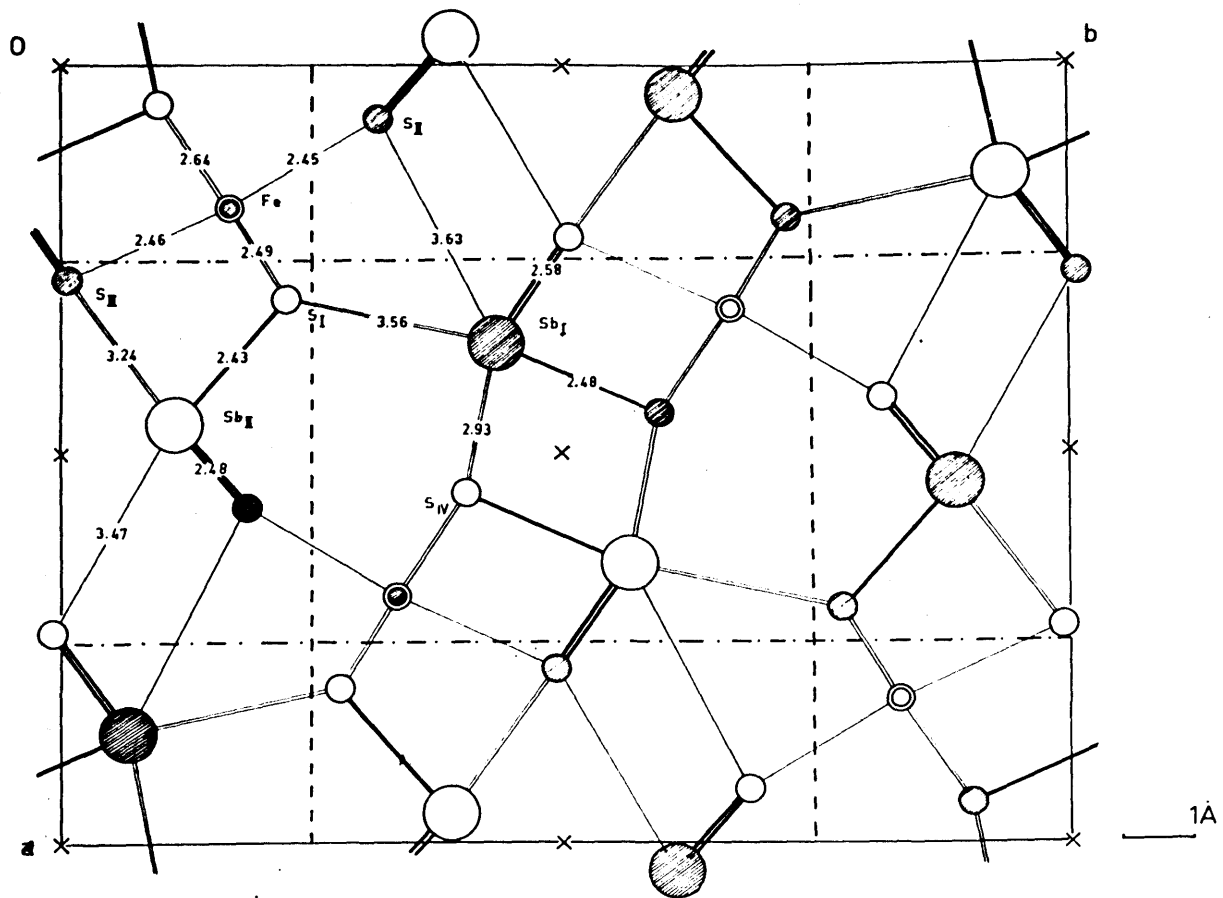


Fig. 54 Schematic representations of Sb-S groups.

(cont.)

- (a)  $\text{Sb}_2\text{S}_4$  double chain, with a projection.
- (b)  $\text{Sb}_2\text{S}_3$  band.
- (c)  $\text{Sb}_4\text{S}_6$  double band.
- (d)  $\text{Sb}_2\text{S}_3$  sheet, only a part is shown.

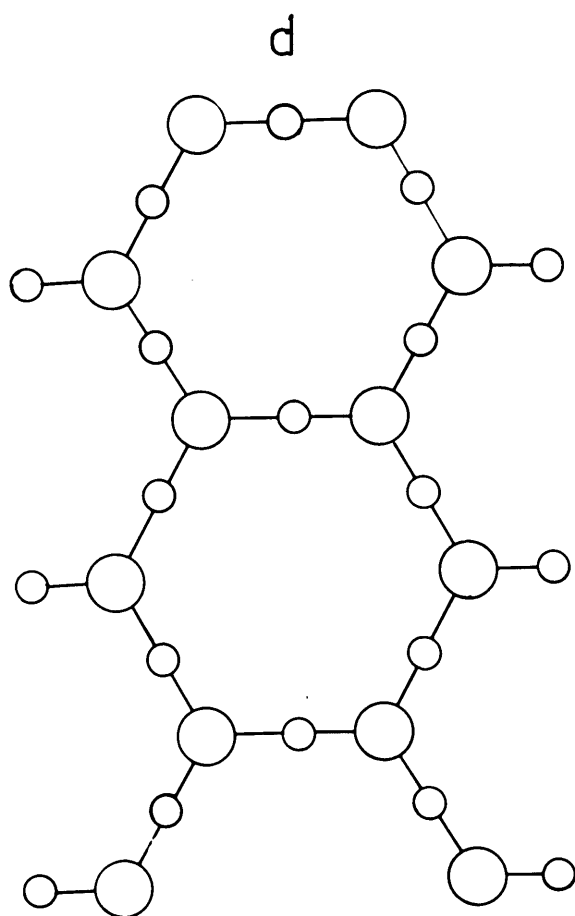
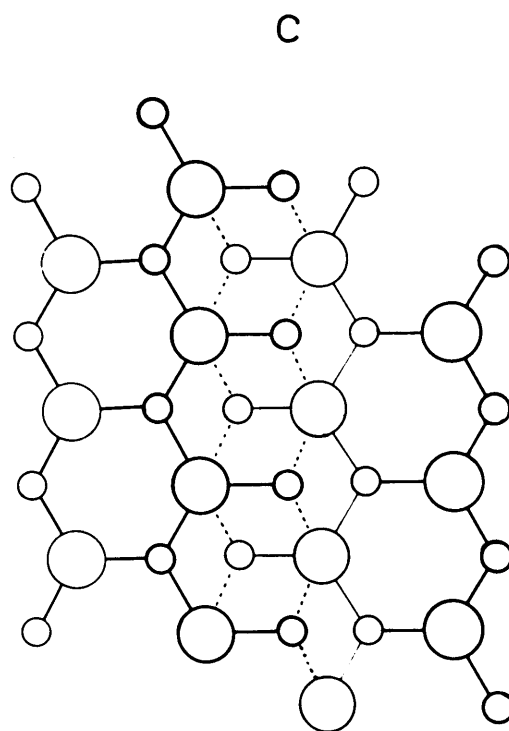
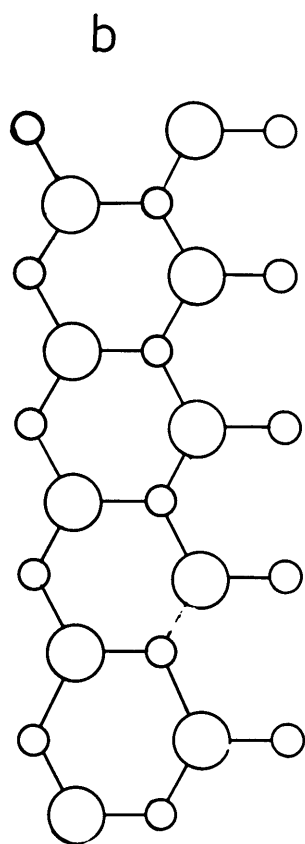
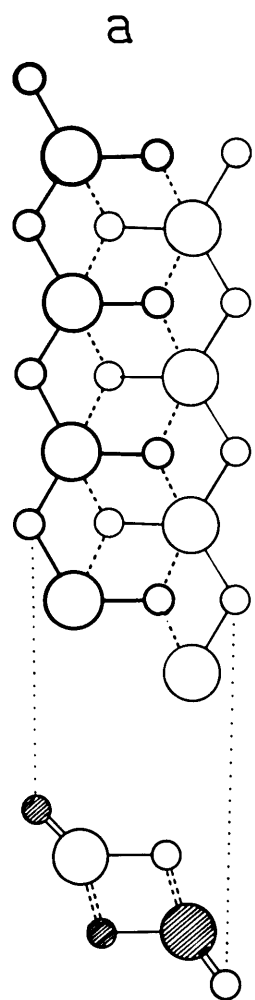
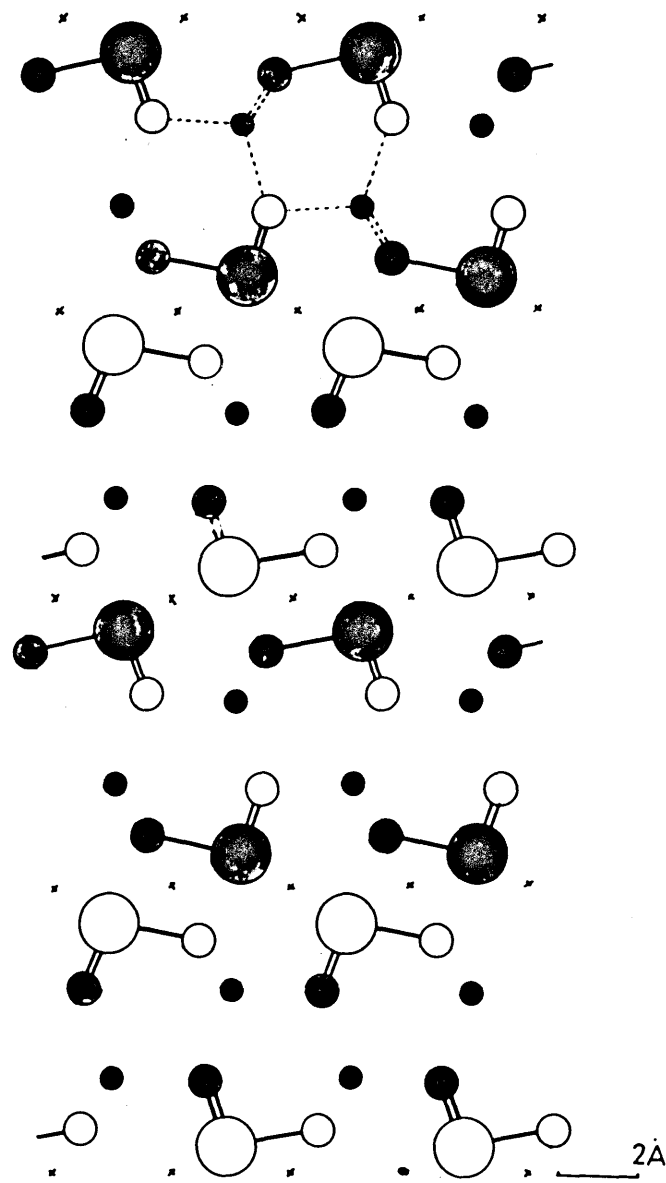
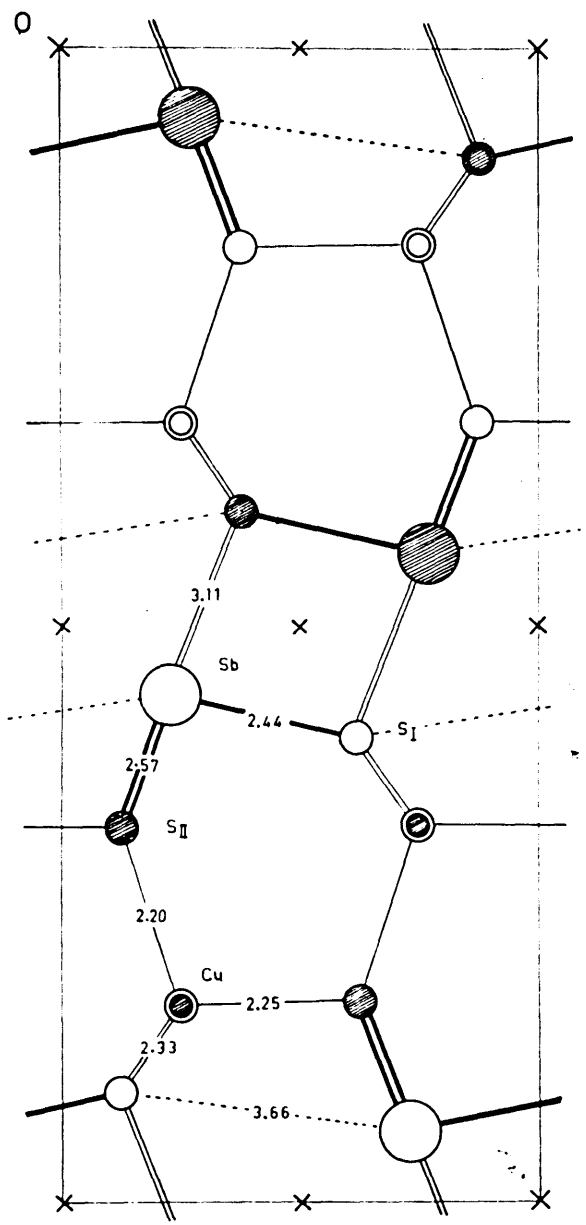


Fig. 55a Schematic representation of the structure of chalcostibite,  $\text{CuSbS}_2$  projected on (001), after Hofmann<sup>31</sup>.

Open circles represent the atoms with z coordinates equal to zero, and the shaded circles represent the atoms with z coordinates equal to 1/2. Figures represent the interatomic distances in A unit.

Fig. 55b. Schematic representation of the four unit cells of chalcostibite. The shaded circles in Fig. 55a are filled in. The  $\text{SbS}_2$  chains are indicated.



or two-fold screw equivalent in the structure and forms a double chain of composition  $\text{Sb}_2\text{S}_4$ . One of the  $\text{SbS}_2$  chains in berthierite is this type.

Double chain  $\text{Sb}_2\text{S}_4$ . The double chain  $\text{Sb}_2\text{S}_4$  is schematically illustrated in Fig. 53a with its projection along the chain axis. In this chain each Sb atom has 5 neighboring S atoms, i.e., three closest ones and two additional ones at slightly larger distances. These S atoms can be considered as located at the vertices of an octahedron with one vertex unoccupied. One kind of S atoms in this double chain has three neighboring Sb atoms. Thus at this stage of building up of Sb-S groups, the purely covalent viewpoint cannot be followed, since the actual interatomic distances found in the chain indicate the bond type as non-Van der Waals type. Examples are found in the structures of berthierite, of chalcostibite, Fig. 54 and of livingstonite, Fig. 13. The interatomic distances between the Sb and S atoms of two  $\text{SbS}_2$  chains are sometimes, as in livingstonite, comparable to the closest Sb-S distances in the chain, and in the other example, as in chalcostibite, quite large ones (over 3.0A).

$\text{Sb}_2\text{S}_3$  band. Another kind of group can be formed from the two  $\text{SbS}_2$  chains. In forming  $\text{Sb}_2\text{S}_4$  double chains no further sharing of S atoms occurs. If two  $\text{SbS}_2$  chains share one kind of S atoms between them, then the  $\text{Sb}_2\text{S}_3$  type band, Fig. 53b, is obtained. This band itself has not

been found in the sulfosalt structures. In the  $Sb_2S_3$  band schematically shown in Fig. 54b all the Sb atoms have three neighboring S atoms, and the formula can be expressed as  $(Sb_2S_3)^1$  indicating one remaining covalence of the S atom. The one  $SbS_2$  chain can be oriented with respect to the other to satisfy this remaining one covalent bond of the S atom within the  $Sb_2S_3$  band. This additional bond is indicated by the dotted lines in Fig. 54b. The formula of this type of  $Sb_2S_3$  band is expressed, therefore, as  $(Sb_2S_3)^0$  indicating that all the theoretical covalent bonds are used up in the group. Two of these  $(Sb_2S_3)$  group, usually related by a center of symmetry, form the  $Sb_4S_6$  double band. An example is the structure of stibnite,  $Sb_2S_3$  illustrated in Fig. 37. In this double band every Sb atom has five neighboring S atoms.

Although not illustrated, Sb-S bands of larger size can be conceived. The formula of such bands can be expressed as  $Sb_3S_4$ ,  $Sb_4S_5$ , and generally as  $Sb_nS_{n+1}$ .

$Sb_2S_3$  sheet. The  $SbS_2$  chain considered in the previous groups was, as shown in Fig. 52a, the kind in which all the bonds from the Sb to S atom with one unsatisfied valence are orientated in same direction. Another kind of  $SbS_2$  chain can be imagined if the above-mentioned Sb-S bonds are orientated alternately to the opposite directions. Two of this type of  $SbS_2$  chain are shown in Fig. 54d sharing one kind of S atoms between them. If this group is extended



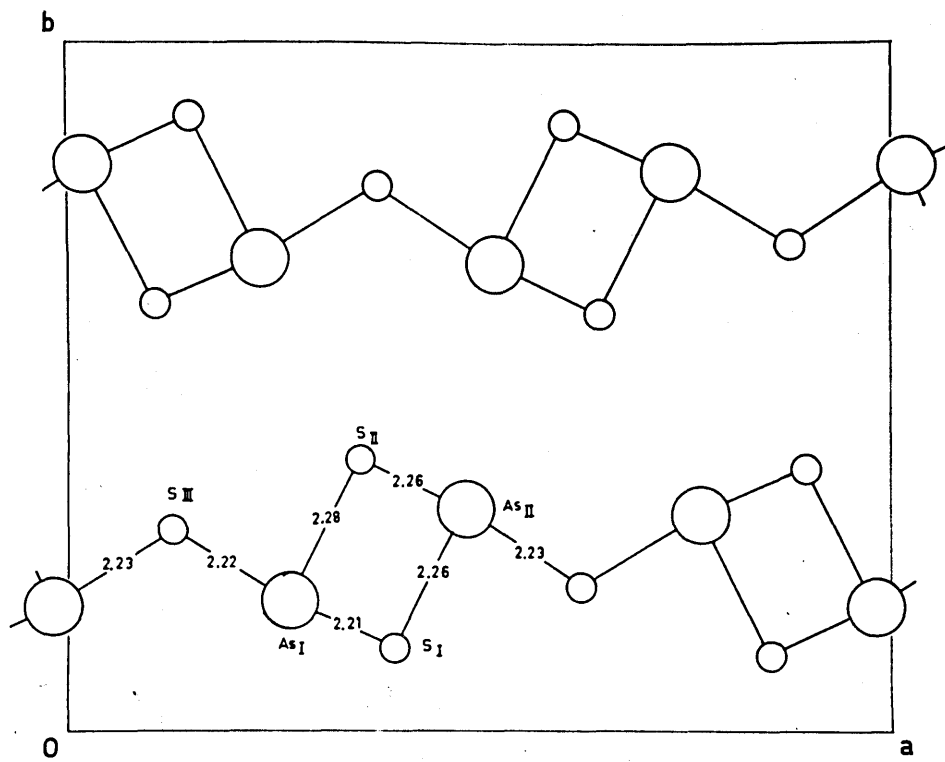
to infinite size, the two-dimensional Sb-S sheet is obtained. The composition of this sheet is  $\text{Sb}_2\text{S}_3$ . In this sheet each Sb atom has three S atoms, and each S atom has two Sb atoms as the neighbors. All the covalent bonds of Sb and S are used up within this sheet. An example of this group is known in the structure of orpiment<sup>40</sup>,  $\text{As}_2\text{S}_3$ . In the orpiment structure, Fig. 56, the chemical bonds between the successive sheets are considered as Van der Waals type.

$\text{Sb}_4\text{S}_8$  group. In the structure of livingstonite, Fig. 13, two double chains of composition  $\text{Sb}_2\text{S}_4$  are arranged close to each other, and an  $\text{S}_2$  group (one S from each double chain) is formed between them. The S-S distance of this group is 2.07Å, and bond between these two S atoms is considered as covalent as in the case of the same group found in pyrite, marcasite, and covellite.

Structure of stibnite. The structural unit of stibnite is, as described above, an  $\text{Sb}_4\text{S}_6$  double group, or an  $(\text{Sb}_2\text{S}_3)_2^0$  double group. When this group is arranged in the unit cell of the structure, the result is that each Sb atom has two more additional S atoms as its neighbors. The schematic representation of four unit cells of stibnite is shown in Fig. 57. These two additional S atoms belong to the adjacent  $\text{Sb}_4\text{S}_6$  groups, and are located at further distances than the five atoms already described. Altogether the coordination number provided by Cl atoms,

Fig. 56 Schematic representation of the structure of orpiment,  $\text{As}_2\text{S}_3$  after Morimoto<sup>40</sup>.

Figures represent the interatomic distances in Å units. An  $\text{As}_2\text{S}_3$  sheet is indicated by heavy lines in the projection on (010).



1Å

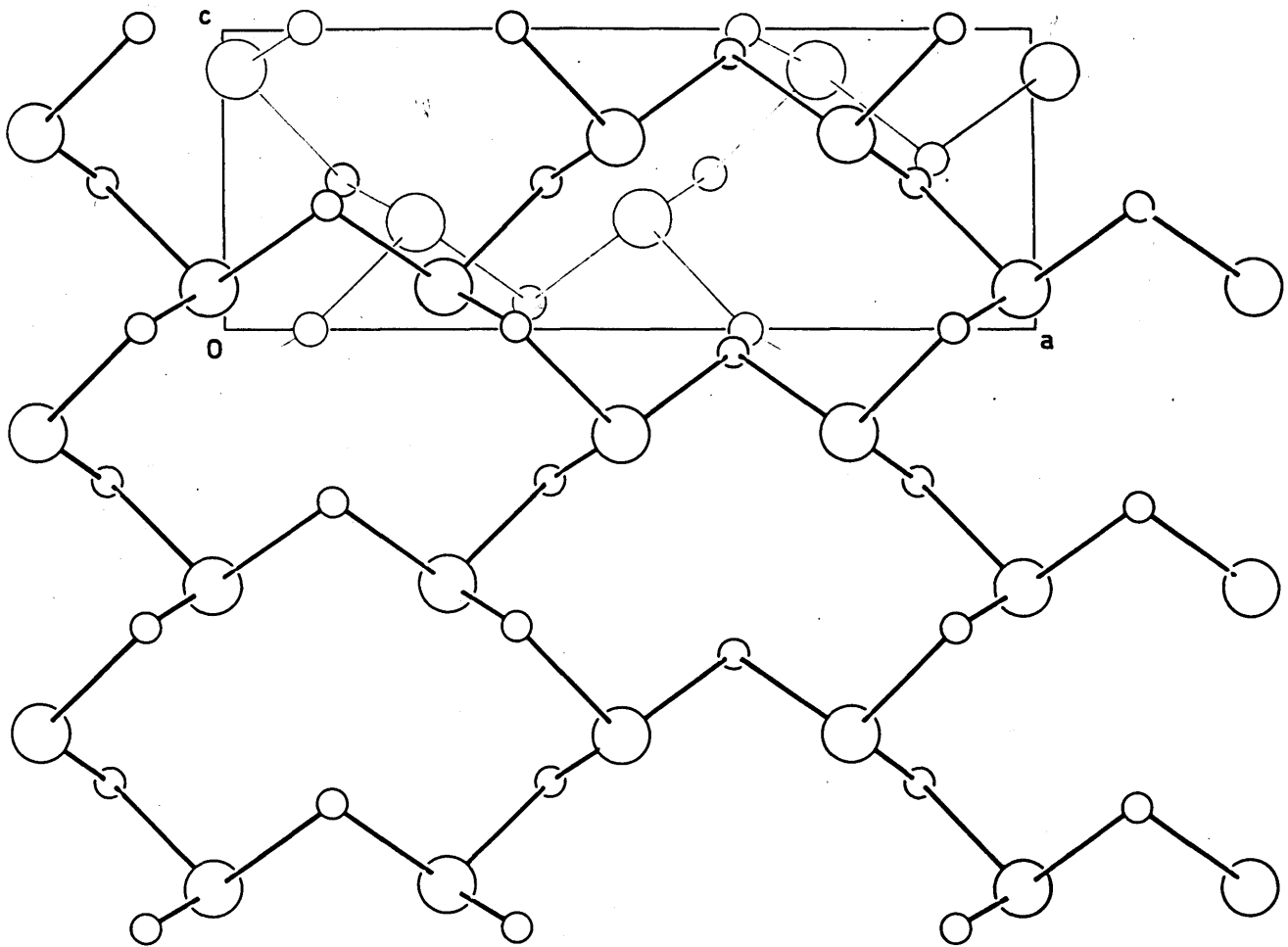
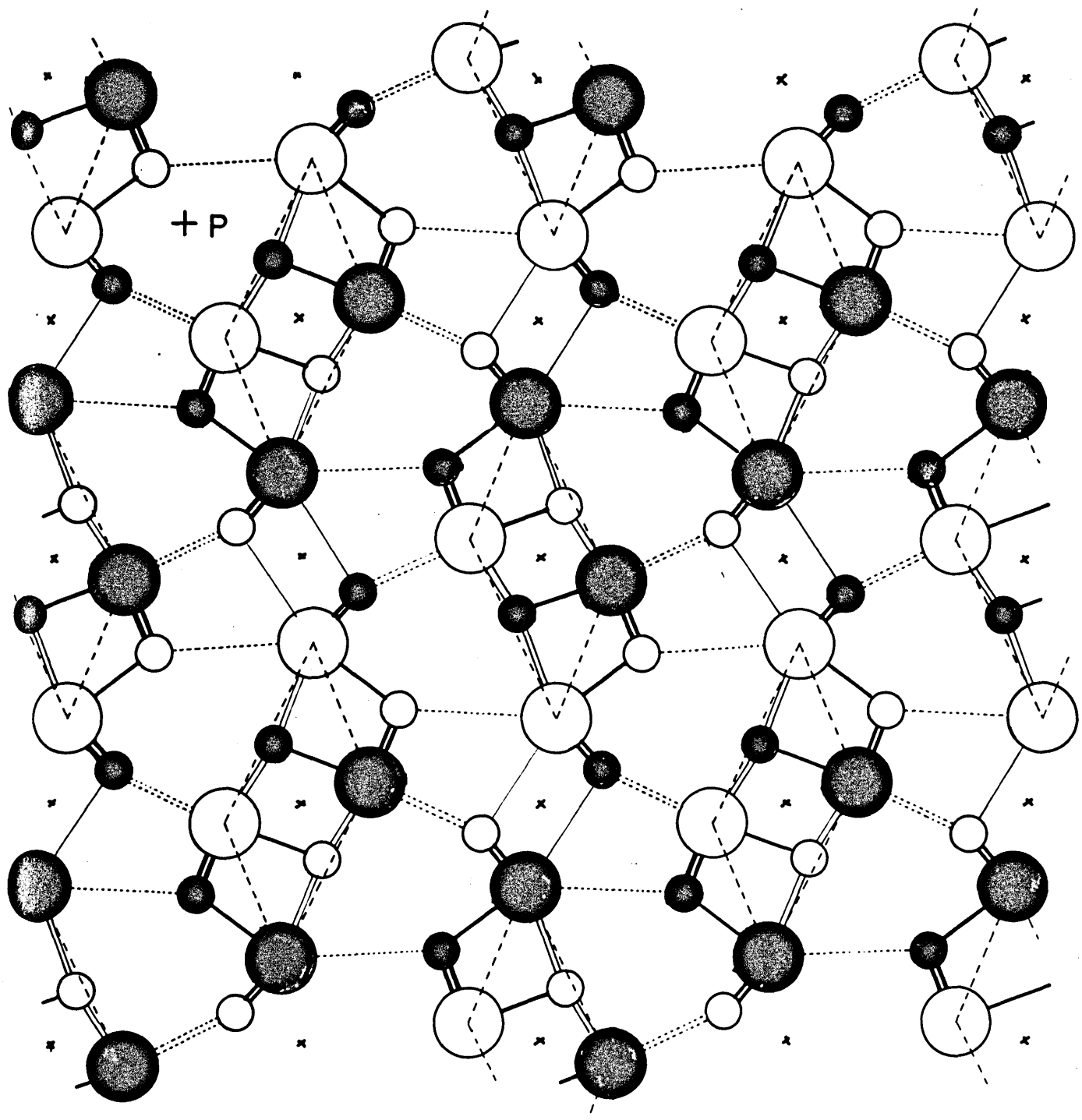


Fig. 57 Schematic representation of the structure of stibnite,  $\text{Sb}_2\text{S}_3$ . The projection of four unit cells are shown.

Large circles represent Sb atoms, and small circles S atoms. Open circles indicate the height zero, and shaded circles one half.

$\text{Sb}_4\text{S}_6$  double bands are indicated by outlined 4-gons.



+ P

2Å

of each Sb atom increases to seven, and the second coordination polyhedron of Sb atom is completed at this stage.

Chains and double chains of Metal-Sulfur in sulfosalt structures. When the chains or bands of Sb-S group described above are discernible in the sulfosalt structures, the metal atoms can be regarded as playing the cementing role for these Sb-S groups. But if considered in terms of their own coordination, the chains or double chains of metal-sulfur coordination polyhedra can be recognized. The kinds of chains found in the structures are as follows.

Cu-S tetrahedral chain. The successive tetrahedra share one corner between them in this chain. The axis of the chain is parallel to the 4A unit of the tetrahedron, Fig. 34, and Table 16. Examples are found in every structure of the acicular sulfosalts containing Cu. The chain itself has the chemical composition of  $\text{CuS}_3$ , and corresponds to the  $\text{SiO}_3$  chain in the pyroxenes. The difference between these two chains is the orientations of the alternating tetrahedra with respect to the chain axis.

The same kind of chain as  $\text{CuS}_3$  was found in the crystal structures of  $\text{K}_2\text{CuCl}_3$ , and its isomorphs,  $\text{Cs}_2\text{AgCl}_3$ , and  $\text{Cs}_2\text{AgI}_3$ . In these structures<sup>41</sup> the chains of tetrahedra of  $\text{CuCl}_3$ , or  $\text{AgCl}_3$ ,  $\text{AgI}_3$  run parallel to the 4A axis of the structure, and in the interstices

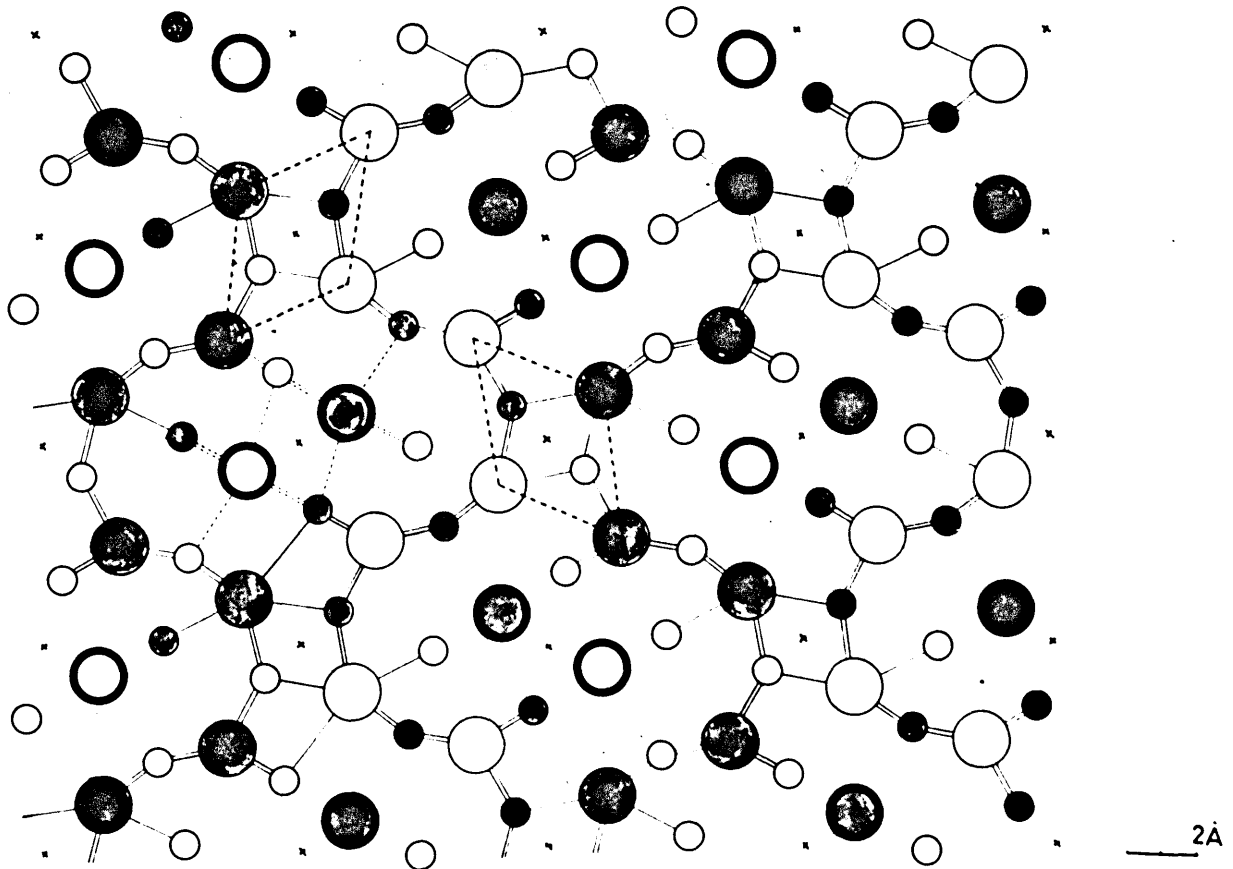
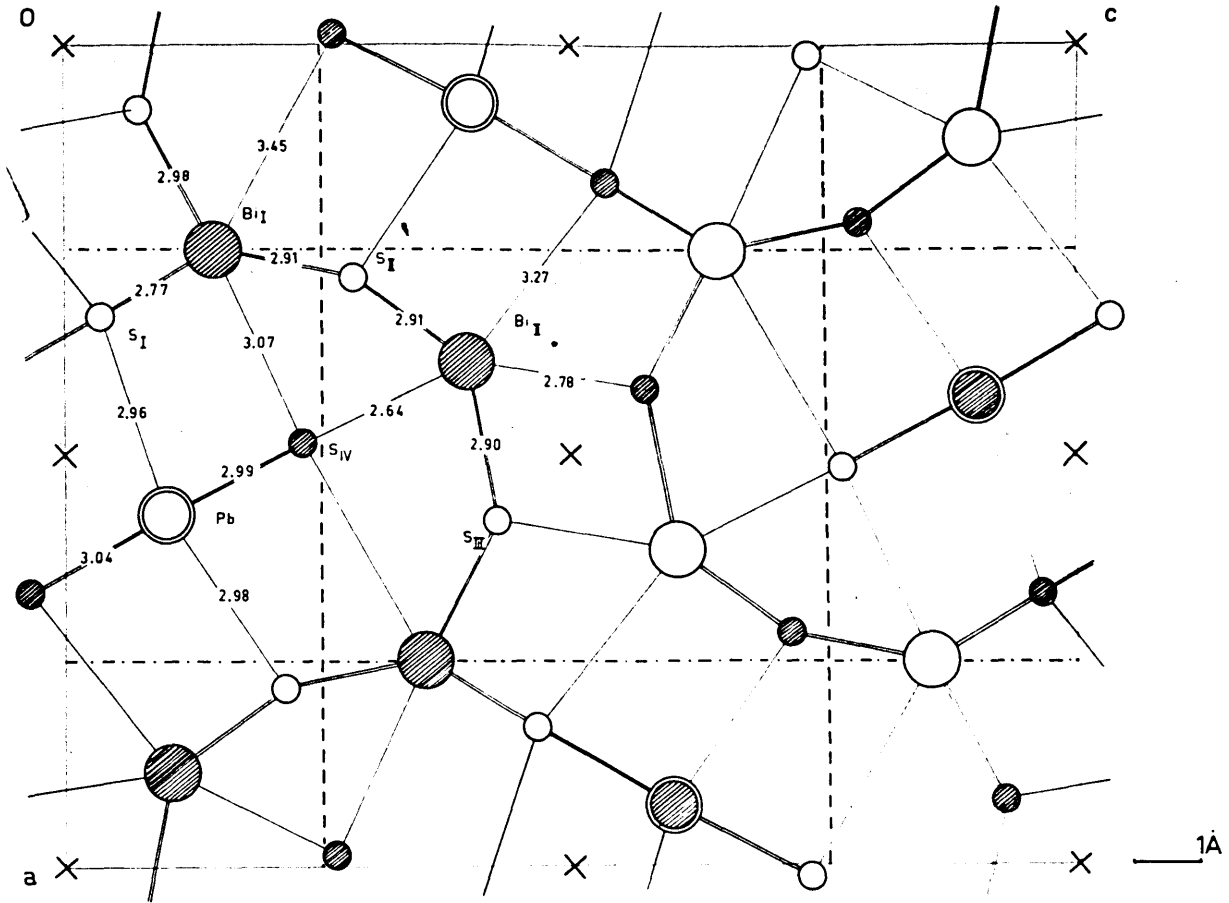
large cations locate themselves. Since Brink showed that the Pauling's electrostatic rules are satisfied in the structures, these structures can be treated as ionic. They are interesting since they are isostructural with one of the acicular sulfosalts, aikinite  $\text{CuPbBiS}_3$ . In the latter structure, if the same viewpoint is taken, the atoms Pb and Bi can be considered as occupying the interstices provided by the  $\text{CuS}_3$  chains. The difference between them is that in the more ionic  $\text{K}_2\text{CuCl}_3$  structure, the cation K is surrounded by seven Cl atoms at nearly equal distances, but in the more covalent structure of aikinite Bi(Pb) has, among the seven closest S atom neighbors, the three most strongly bonded ones.

Metal-sulfur octahedral chains. The second example of metal-sulfur chains is an octahedral chain formed by successive octahedra sharing two opposite edges with adjacent octahedra. Fe-S chains are found in the structures of berthierite and jamesonite. An Hg-S chain is found in livingstonite. The composition of the chain itself can be expressed as  $\text{MS}_4$ . If two such chains of octahedra further share between them edges of octahedra, a double chain of composition  $\text{MS}_3$  can be obtained. An example is found in the Pb-S double chain in the structure of galenobismutite,  $\text{PbBi}_2\text{S}_4^5$ . The structure of the mineral is schematically represented in Fig. 58.

Fig. 58a Schematic representation of the structure of galenobismutite,  $\text{PbBi}_2\text{S}_4$  projected on (010), after Wickman<sup>5</sup>. Open circles represent atoms with y coordinates equal to zero, and shaded circles represent atoms with y coordinates equal to 1/2.

Fig. 58b Schematic representation of four unit cells of galenobismutite. The shaded circles in Fig. 58a are filled in.





Polyhedral interstices provided by two or more chains: The metallic atoms may be considered as occupying interstices of proper shape and dimensions formed by S atoms of several Sb-S chains or bands. As illustrated in Fig. 59 the tetrahedral and octahedral interstices are easily provided by two or more parallel chains.

The tetrahedral interstices are provided by two chains. One chain provides three S atoms, and the second chain one S atom, Fig. 59a. An example is the Cu-S tetrahedron in aikinite. Tetrahedral interstices also can be provided by three chains as in chalcostibite.

The octahedral interstices are provided by either two chains, Fig. 59b or by three chains, Fig. 59c. The former case is observed in berthierite, and the latter case in jamesonite, both for the Fe-S octahedron.

Interstices surrounded by seven or more S atoms from three chains are also known. These interstices are to be accommodated by Pb atoms. Examples can be seen in jamesonite and seligmannite.

It is observed that the sulfur atoms with more than two submetallic neighbors in the chain further participate in forming interstices, and form chemical bonds with the metallic atoms that occupy these interstices. From the interatomic distances between metallic and S atoms observed in sulfosalts, listed in Table 22, the metal-S bonds are considerably ionic in minerals. Thus for some compounds

Fig. 59 Schematic representation of tetrahedral and octahedral coordination of the metal atoms in the acicular sulfosalts. Large circles represent Sb atoms, small circles S atoms, and small black circles metal atoms.

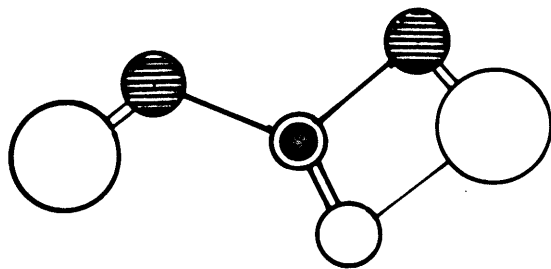
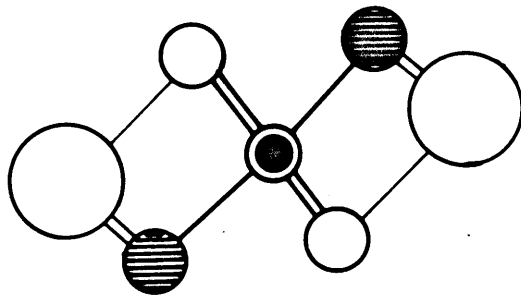
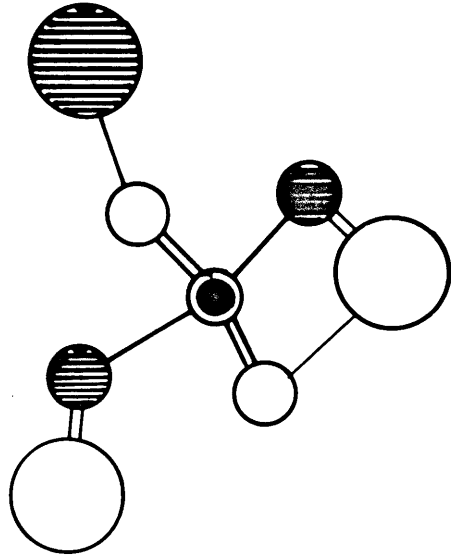


Table 22  
Metal-S distances in sulfosalts (in Å units)

<u>Pb-S</u> c.f. in galena 2.97(6)	
Pb in galenobismutite	2.96, 2.98, 2.99(2), 3.04
Pb <sub>I</sub> in aikinite	2.88(2), 2.93(2), 2.98, 3.16(2)
Pb <sub>II</sub> in aikinite	2.84, 2.87(2), 2.99(2), 3.12, 3.35
Pb <sub>I</sub> in bournonite	2.96(2), 2.99, 3.06(2), 3.51(2)
Pb <sub>II</sub> in bournonite	2.95, 2.97(2), 2.98, 3.22(2), 3.57(2)
Pb <sub>I</sub> in jamesonite	2.91, 2.92, 3.01, 3.04, 3.04, 3.13, 3.29, 3.39
Pb <sub>II</sub> in jamesonite	2.87, 2.87, 2.88, 2.97, 3.04, 3.07, 3.28
<u>Fe-S</u> c.f. in pyrite 2.26(6)	
Fe in berthierite	2.45, 2.46, 2.49(2), 2.64(2)
Fe in jamesonite	2.36(2), 2.57(2), 2.66(2)
<u>Cu-S</u>	
Cu in chalcostibite	2.20, 2.25, 2.33(2)
Cu in enargite	2.31 (2), 2.33(2)
Cu <sub>I</sub> in tennantite	2.28(4)
Cu <sub>II</sub> "	2.29, 2.39(2)
Cu in aikinite	2.32(2), 2.27, 2.40
Cu in bournonite	2.29(2), 2.41, 2.76
<u>Ag-S</u>	
Ag in proustite	2.40(2)
<u>Hg-S</u>	
Hg in livingstonite	2.37(2), 2.34(2), 3.38(2)

an ionic representation of the chemical formula is possible. For example, berthierite can be expressed as  $\text{Fe}^{2+}(\text{SbS}_2)_2^{--}$ , and jamesonite as  $\text{Fe}^{2+}\text{Pb}_4^{2+}(\text{Sb}_6\text{S}_{14})^{10-}$ .

The relation between the first and second coordination polyhedra of Sb(As,Bi) atom. In section 2, the structures of the acicular sulfosalts were considered in terms of the second coordination polyhedra of metallic and submetallic atoms. In this section the same structures were described in terms of Sb-S groups. These groups were composed of Sb-S<sub>3</sub> trigonal pyramids, i.e., the first coordination polyhedra of the Sb(As,Bi) atom. By definition, the second coordinations include the first coordinations. The relation between these two kinds of coordination of submetallic atoms is illustrated in Fig. 60.

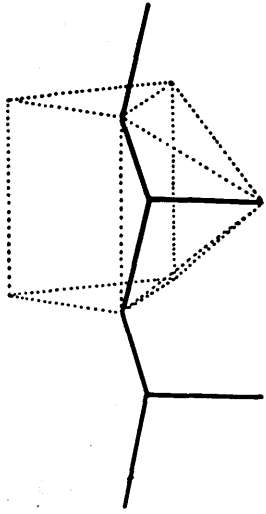
In Fig. 60e, the Sb<sub>2</sub>S<sub>3</sub> band of the stibnite structure is shown with its centrosymmetrical equivalent (in dotted lines). In this figure the second coordination polyhedra are also outlined. It was already pointed out that the only kind of polyhedron found in two kinds of orientation, is the 7-vertex-8-hedron. In one kind of chain this polyhedron is extended into a chain by sharing its two opposite triangular faces with adjacent polyhedra. In the other the sharing of two opposite edges is observed. The three shortest Sb-S bonds are indicated, and the small circles at the corners of polyhedra indicate the additional

Fig. 60 Relations between the first coordination and the second coordination of Sb atoms in the acicular sulfosalts.

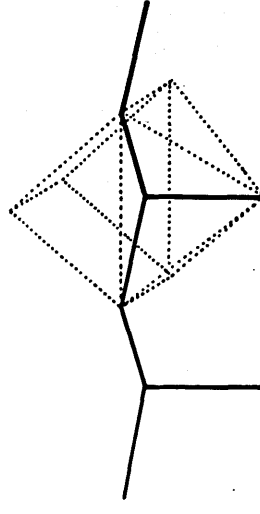
The first coordination is represented by heavy lines, and the second coordination by dotted lines.

- (a)  $\text{SbS}_2$  chain in relation to 7-vertex-8-hedron.
- (b) " " "
- (c)  $\text{SbS}_2$  chain in relation to 8-vertex-11-hedron.
- (d)  $\text{SbS}_3$  group in relation to 7-vertex-8-hedron.
- (e)  $\text{Sb}_4\text{S}_6$  double bands of stibnite is shown in relation to the stacking of polyhedra.

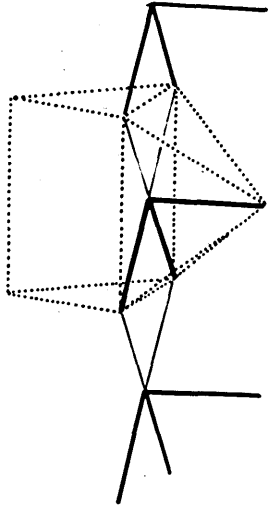
a



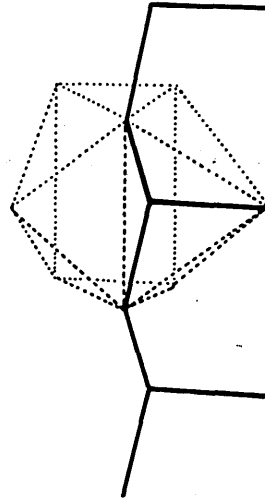
b



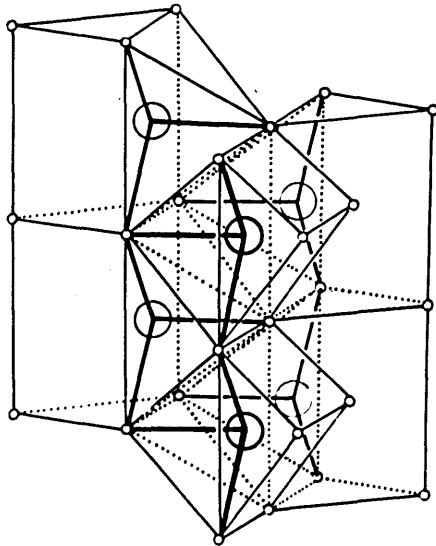
d



c



e





S atoms. The orientations of the three closest S neighbors in the various kinds of Sb(As,Bi) second coordination polyhedra are illustrated in Fig. 60a, 60b, and 60d.

These three strong bonds share two of the S atoms with adjacent configurations, and are built into strongly bonded chains of Sb and S.

It will be noticed, however, that this orientation is not the only one for the three nearly orthogonally directed bonds with respect to the polyhedron. Since two of the three bonds are in the square close-section of the geometrically related octahedron, the orientation illustrated in Fig. 60c is also possible. In this case, although some weaker bonds are directed in the proper direction of chaining (as indicated by light lines), the strong ones are not connected to each other. It will be noticed from the drawing that there are possibilities of extending these three strong bonds horizontally, and this situation is actually observed in jamesonite.

Cleavage of acicular sulfosalts. If the cleavage of the mineral is understood as the distribution of the weaker chemical bonds in a way parallel to the macroscopic crystallographic planes, the cleavage of the acicular sulfosalts will be prismatic. It is so since the above-mentioned planes are parallel to the axis of strongly bonded Sb-S groups, and are thus parallel to the

acicular axis of the crystal. It must be understood, however, that not only the acicular habit, or the existence of  $4\overset{\circ}{\text{Å}}$  dimension in the unit cell, but the orientation of three strong Sb-S bonds with respect to the second coordination polyhedra is responsible to this kind of cleavage.

In case the orientation of these bonds occurs as illustrated in Fig. 60c, then there can be a cleavage normal to the acicular axis. This is observed in the above mentioned structure of jamesonite. Other acicular sulfosalts with this basal cleavage are owyeeite and falkmannite.

Submultiple unit cell dimension of  $4\overset{\circ}{\text{Å}}$  in sulfosalt structures. In the diagrams of Fig. 60's, the chains are drawn so that each successive polyhedron is identical with the adjacent ones. In other words, they are translation equivalents of each other. The value of this translation is  $4\overset{\circ}{\text{Å}}$ . It is conceivable that in some case the successive polyhedra are not identical with each other. Then the dimension  $4\overset{\circ}{\text{Å}}$  is not the true period of repetition, but will be a sub-multiple dimension of a larger unit cell with  $n$  times the  $4\overset{\circ}{\text{Å}}$  dimension. No structural data are available for this kind of sulfosalt, but the feature may occur in the structure of seligmannite.

There are two kinds of atom having the second coordinations constituting chains. They are Pb and submetallic

atoms. If the center atoms of successive polyhedra are not the same kind, but alternate between these two kinds, the configurations of the coordinating S atoms will not be identical, but similar to each other. In this case the doubling of the  $4\text{\AA}$  unit results as a true unit cell dimension, but a strong sub-multiple unit cell with a  $4\text{\AA}$  dimension will be observed too. It is interesting to note that such sub-multiple unit cells are observed in sulfosalt structures including Pb atoms.

Table 19b. Group A'.

The sulfosalts of this group are characterized either by an asymmetric unit with  $4\text{\AA}$  dimension, or by a sub-multiple unit with  $4\text{\AA}$  dimension. The value of the chemical parameter  $f$  of the minerals of this group is equal to or less than 1.0.

In the following table, name, formula, space group, and asymmetric or sub-multiple dimension of  $4\text{\AA}$  length are given. A sub-multiple dimension is indicated by a prime, and an asymmetric dimension is indicated by a double prime.

Smithite $\text{AgAsS}_2$	A2/a	$b = 7.76, b'' = 3.88$
Stephanite $\text{Ag}_5\text{SbS}_4$	Cmc2	$a = 7.70, a'' = 3.85$
Boulangerite $\text{Pb}_5\text{Sb}_4\text{S}_{11}$	$P2_1/a$	sub-cell with $c' = 4.035$
Sartorite $\text{PbAs}_2\text{S}_4$	Pseudo orth. cell	with $b' = 4.15$
Geocronite $\text{Pb}_5\text{Sb}_2\text{S}_8?$	Pseudo orth. cell	with $c' = 4.24$
Jordanite $\text{Pb}_{28}\text{As}_{14}\text{S}_{49}?$	$P2_1/m$	sub-cell with $c' = 4.20$
Baumhauerite $\text{Pb}_4\text{As}_6\text{S}_{13}?$	$P2_1/m$	$b = 8.32, b'' = 4.16$
Benjaminite $\text{Pb}(\text{Cu}, \text{Ag})_2\text{Bi}_4\text{S}_9$	Pseudo mono. cell	with $b' = 4.06$
Hutchinsonite $\text{Pb}_4(\text{Ag}, \text{Cu})_2\text{As}_{10}\text{S}_{20}$	Fbca	$c = 8.14, c'' = 4.07$
Meneghinite $\text{Pb}_{13}\text{CuSb}_7\text{S}_{24}$	Fbnm	$c = 8.26, c'' = 4.13$
Seligmannite $\text{CuPbAsS}_3$	Pn2m	$c = 7.636, c'' = 3.818$
Bournonite $\text{CuPbSbS}_3$	Pn2m	$c = 7.811, c'' = 3.906$
Owyheeite $\text{Pb}_5\text{Ag}_2\text{Sb}_6\text{S}_{15}$	Pseudo orth. cell	with $c' = 4.095$

Table 19b (cont.)

Andorite IV	Pmma?	sub cell with $c' = 4.29$
Andorite VI	Pnma?	sub cell with $c' = 4.29$
Rathite	$P2_1/n$	$b = 7.91, b'' = 3.96$

---

Note

Among the above-listed minerals , only seligmannite and bournonite have determined structures. Therefore the classification based on the existence of a 4A unit in one way or other must be considered as a tentative one until much more structural data become available.

4. Relation between sulfosalts structures and simple sulfide structures.

Sulfosalts of group B. The sulfosalts of this group are characterized by a shortest unit cell dimension of about 6A, including with sub unit cell with the same dimension, and with the chemical parameter  $f_1$  equal to 1.0. The minerals are listed in Table 19c. These structures are related to the structure of galena, PbS, although the detailed structure analysis has not yet been presented. The possible relations between these sulfosalts and the galena-type structure were discussed in section 2. The nature of chemical bonds in galena was treated by Krebs<sup>37</sup> as resonating covalent bonds.

In the last part of the previous section, the second coordinations of Pb atoms similar to those of submetallic atoms were discussed. It is also possible for the submetallic atoms to have a second coordination more characteristics of Pb atoms, such as a distorted octahedral one. The same situation applies to the Ag atoms. To satisfy their first coordination, Ag needs two linearly arranged S neighbors, and the submetallic atoms three S neighbors. These first coordination will be realized within the distorted octahedral arrangement of six S atoms. Graham<sup>42</sup> pointed out that each of galena-type powder lines of the high-temperature forms of Pb-Ag-Sb or Pb-Ag-Bi systems split, when cooled down, into a set of fine structure lines. These systems are considered to crystallize

Table 19c.

## Group B.

The sulfosalts minerals in this group is characterized by one shortest unit cell dimension of about  $6\text{\AA}$ , and by a value of chemical parameter  $f_1 = 1.0$  or very close to it.

Matildite $\text{AgBiS}_2$	orth. $c = 5.66, a = 3.92, b = 4.05$	$f_1 = 1.0$
Miargyrite $\text{AgSbS}_2$	mono. $b = 4.39, c = 12.83, a = 13.17$	$f_1 = 1.0$
Aramayoite $\text{Ag}(\text{Bi}, \text{Sb})\text{S}_2$	tri. $a = 7.72, b = 8.82, c = 8.30$ $= 100^\circ 23', = 90^\circ 00', = 103^\circ 54'$	$f_1 = 1.0$
Diaphorite $\text{Pb}_4\text{Ag}_6\text{Sb}_6\text{S}_{16}$	mono. $c = 5.89, a = 15.83, b = 32.23$	$f_1 = 1.0$
Freislebenite	mono. $c = 5.88, a = 7.53, b = 12.79$ $= 92^\circ 14'$	$f_1 = 1.0$
Lengenbachite $\text{Pb}_6(\text{Ag}, \text{Cu})_2\text{As}_4\text{S}_{13}?$	mono. $a' = 5.80, b' = 5.75, c' = 18.36$	$f = 0.92?$

Probably smithite belongs to this group.

Smithite  
 $\text{AgAsS}_2$

mono.  $a = 17.20, b = 7.76, c = 15.16$   
 $= 101^\circ 12'$

with  $a' = a/3 = 5.73, b' = 2b = 15.52$ , and

$$c' = 2c = 30.32$$

a relation with diaphorite is observed.

in a disordered galena-type structure at the higher temperature, and, when the temperature is lowered, to recrystallize into structures in which the S atoms near the different kinds of metallic or submetallic atoms rearrange themselves to satisfy different requirements of chemical bonds.

There is another kind of possible distortion when submetallic atoms are introduced into the PbS type structure. It is the changing of the coordination number of some of the atoms from six to seven or more.

Relation between atomic ratio in the formula and C.N. ratio in the structure. If structures can be considered as the open stacking of the second coordination polyhedra, and all the atoms belong to at least one of polyhedra, then the following relation must hold.

The atomic ratio between the metallic and S atoms in the chemical formula is the inverse ratio between the C.N. (coordination number) of metallic atom and C.N. of S atom achieved in the structure. When there are more than two kinds of coordinations in the structure, the relation holds for the averaged C.N.'s.

The proof can be given as follows.

The averaged number of coordination times the number of metallic atoms equals the number of S atoms counted as many times as each S atoms belong to the several polyhedra. This can be expressed as

$$\overline{\text{C.N.}}_{\text{Metal}} \text{ times No.}_{\text{Metal}} = \text{No.}_{\text{S}} \text{ times } \underline{K}$$

Now as the average, each S atom belongs to the metallic



atoms whose number is given by averaged C.N. of S. This value is  $\bar{K}$ . Therefore,

$$\overline{\text{C.N.}}_{\text{Metal}} \text{ times } \text{No.}_{\text{Metal}} = \text{No.}_{\text{S}} \text{ times } \overline{\text{C.N.}}_{\text{S}}$$

or

$$\frac{\text{No.}_{\text{Metal}}}{\text{No.}_{\text{S}}} = \frac{\overline{\text{C.N.}}_{\text{S}}}{\overline{\text{C.N.}}_{\text{Metal}}}$$

The left hand side of the equation is equal to the chemical parameter defined as,

$$f = \text{No.}_{\text{Pb,Ag,Cu,Sb(As,Bi)}} / \text{No.}_{\text{S}}$$

Relation between C.N. and chemical parameter  $f = 1.0$ .

From the formula obtained above, if the value of  $f$  is equal to 1.0, then an averaged C.N. of metallic atoms is equal to that of one of the S atoms. When there is only one kind of coordination in the structure, the number of S atoms surrounding the metallic atom is equal to the number of metallic atoms surrounding S atom. The simplest example is when C.N. = 4, or 6. The case when C.N. = 4 will be discussed immediately later. The case when C.N. = 6 is applied to the present discussion of the structures related to galena. These structures will be termed as the structures with 4 to 4, or 6 to 6 coordinations. The example of 7 to 7 coordinations in the sulfosalts are unknown.

The possible type of deviation in C.N., keeping the value of  $f$  equal to 1.0, in sulfosalt structures, therefore, will occur when the averaged coordinations of metal and S atoms achieve the same value between 6 and 7. No example

is

is known to represent such structure.

Relation between C.N. and deviation of f-value from 1.0. The f-values of the acicular sulfosalts are all less than 1.0 except these including Cu atoms. By examining the structures determined it is found that the C.N. of the S atoms in the structures of the acicular sulfosalts is not greater than 6. It takes the value of either 5 or 6. And it was already pointed out that C.N.<sub>Metal</sub> for these structures, if Cu is excluded, is greater than 6. Thus these structures can be regarded as the rearrangement of the galena-type with a defect of S atoms.

The deviation of the f value from 1.0 as an indication of this type of deviation from the galena-type structure fails to hold if the formula contains Cu. For example in aikinite,  $\text{CuPbBiS}_3$ , a structure closely related to the stibnite type, the value of f is equal to 1.0. This is so since the averaged C.N. is related with the given chemical formula. In aikinite, the C.N. of each metallic atom is, Cu = 4, Pb = 7, and Bi = 7. The average C.N. is 6. And C.N.<sub>S</sub> of aikinite is 6.

Fragments of 6 to 6 coordination type in the sulfosalt structures. In examining the structures of sulfosalts it is noticed that the arrangements of the metallic or sub-metallic atoms with 6 or more coordination are not completely arbitrary. The situation can be expressed by saying that fragmental layers or double layers are stable in the structure.

These are fragments of the simpler structures with (1) 4 to 4 coordination, (2) 6 to 6 coordination, and (3) 7 to 7 coordination. In sulfide structures the 4 to 4 coordination is found in ZnS, but not in FeS, pyrrhotite, or in CuS as covellite. The 6 to 6 coordination is only found in PbS, and not in any of FeS or AgS. The 7 to 7 coordination is hypothetical.

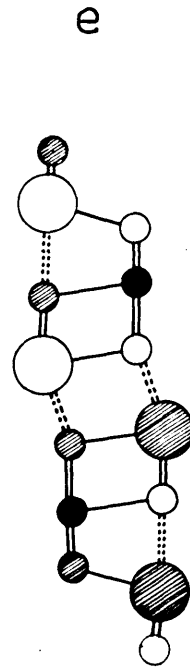
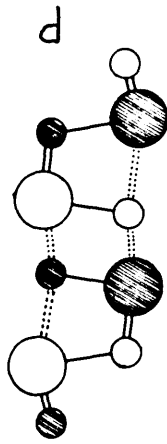
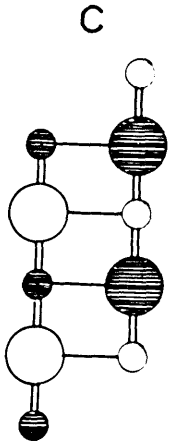
These fragmental layers are illustrated in Fig. 61. Fig. 61a is a representation of part of the galena type coordination, Fig. 38. Fig. 61b is the same kind of layer found in the projection of chalcostibite.

In Fig. 61c is illustrated a smaller fragment from the 6 to 6 coordination-type structure. Fig. 61d is a corresponding group found in the projection of stibnite, and actually this represents the projection of the  $\text{Sb}_4\text{S}_6$  double band discussed in the previous section. Fig. 61e is a similar part found in the projection of berthierite. It is noticed that the Fe atoms play the same role as the Sb atoms from the present viewpoint. Fig. 61f is a group of atoms found in the projection of livingstonite. The  $\text{Sb}_2\text{S}_4$  double chains are cemented together by Hg atoms and are built into the layer of composition  $\text{Hg}_2(\text{Sb}_2\text{S}_4)_2$ .

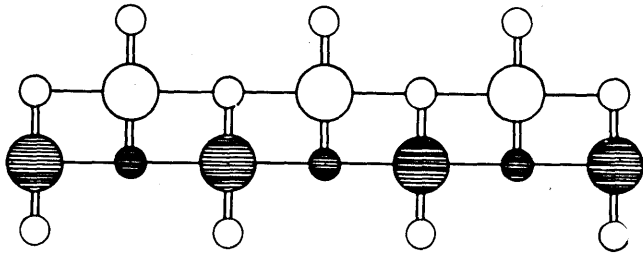
The structure of galenobismutite, Fig. 58 is an interesting example from the present viewpoint. If Bi atoms at the same height  $y = 0$  or  $1/2$  are followed in Fig. 58b, by following the doubled lines, two kinds of S-shaped groups are recognized. Each group corresponds to

Fig. 61 Fragments from the galena-type structure in the structures of the acicular sulfosalts. They are illustrated as shown in projection along the 4A axis.

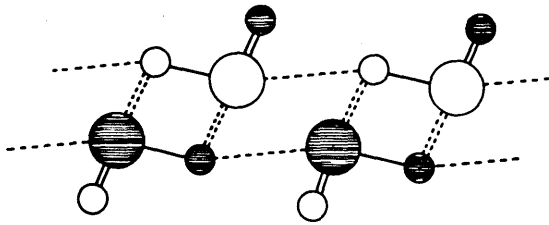
- (a) A fragment of galena-type structure, Fig. 38.
- (b) Fragment illustrated in (a) distorted and found in the projection of chalcostibite.
- (c) Another fragment of the galena type.
- (d) An  $\text{Sb}_4\text{S}_6$  double band in the projection of stibnite.
- (e) An  $\text{Fe}_2\text{Sb}_4\text{S}_8$  band in the projection of berthierite.
- (f) An  $\text{HgSb}_2\text{S}_4$  layer in the projection of livingstonite.



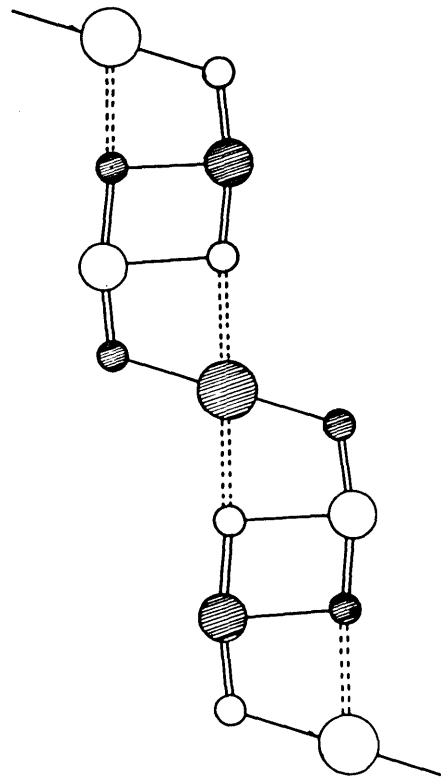
a



b



f



one of the layer illustrated in Fig. 61a. And it will be found that the Pb atoms are located within the large interstices provided by these S-shaped groups. Pb atoms here form double chains of octahedra.

The  $\text{Sb}_6\text{S}_{14}$  group in jamesonite has been studied from the several viewpoints. This group is also regarded as a fragment of a simpler structure. Comparison between the projection of the structure, Fig. 33 and the schematic representation of a 7 to 7 layer given in Fig. 39 shows that this  $\text{Sb}_6\text{S}_{14}$  group can be considered as a small part of the hypothetical structure with 7 to 7 coordination.

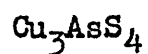
Minerals of group C. The minerals of this group are characterized by isometric or orthorhombic crystal classes and the value of the chemical parameter  $f_3$  is equal to 1.0, thus indicating Cu atoms in the formula. These minerals have the crystal structures closely related to the structures of sphalerite or wurtzite, both  $\text{ZnS}$ , and have a 4 to 4 coordination in the ideal case.

In tetrahedrite<sup>43</sup> and tennantite<sup>29</sup>, with formulas respectively  $\text{Cu}_{12}\text{Sb}_4\text{S}_{13}$ , and  $\text{Cu}_{12}\text{As}_4\text{S}_{13}$ , the value of  $f_3$  is computed as  $16/13 = 1.23$ . Thus from the result of the principle developed earlier in this section, the averaged C.N.<sub>S</sub> is greater than the averaged C.N.<sub>Metal</sub>. What is found as a deviation from the structure of sphalerite with 4 to 4 coordination is as follows: The coordination of the As or Sb atom is not a tetrahedral one but a flat pyramidal

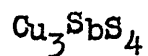
Table 19d. Group C.

The sulfosalts in this group are characterized by the value of the chemical parameter  $f_3$  equal to 1.0, but the minerals with  $4\text{\AA}$  dimension as the shortest unit cell dimension are excluded.

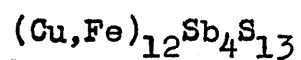
Enargite orth.  $a = 6.46$ ,  $c = 6.18$ ,  $b = 7.43$



Famatinite no crystallographic data



Tetrahedrite isom.  $a = 10.40$



Tennantite isom.  $a = 10.09$

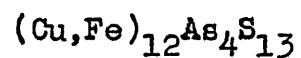
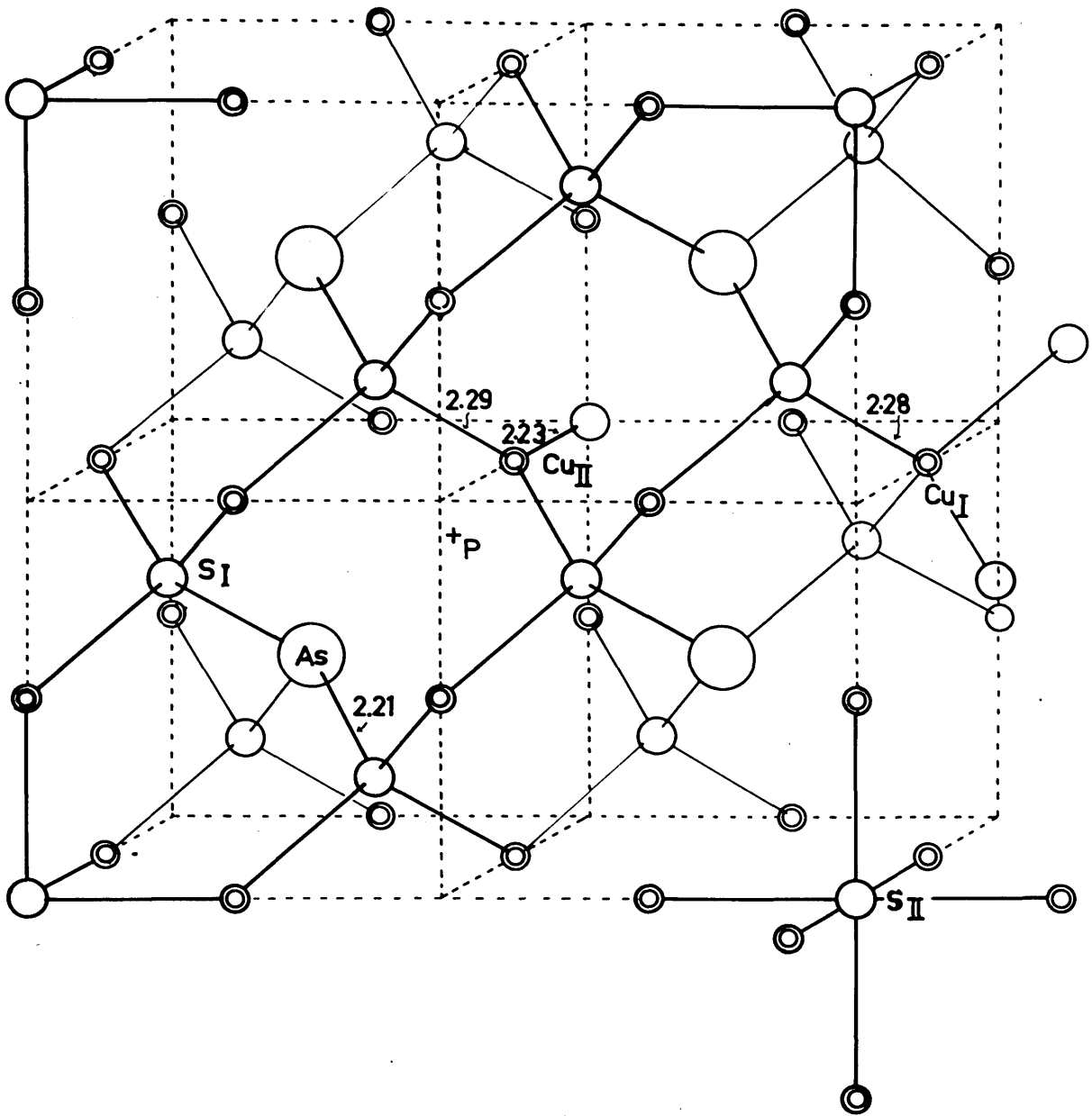


Fig. 62 Structure of tennantite,  $(\text{Cu,Fe})_{12}\text{As}_4\text{S}_{13}$  after Pauling and Neumann<sup>29</sup>.

A cross indicated by letter P is where the fourth S atom to complete a tetrahedral arrangement around an As atom is missing.





one as if the fourth vertice of the tetrahedron is not occupied. And half the Cu atoms have triangular coordination instead of a tetrahedral one. As to the S atoms, 12 out of 13 S atoms are surrounded by 4 metallic atoms, but the remaining one S atom is surrounded by six metallic atoms. The coordination numbers observed are as follows:

$$6\text{Cu} = 3, 6\text{Cu} = 4, 4\text{As} = 3, \text{ and } \overline{\text{C.N.}}_{\text{Metal}} = 27/8 = 3.38$$

$$12\text{S} = 4, 1\text{S} = 6, \text{ and } \overline{\text{C.N.}}_{\text{S}} = 54/13 = 4.15.$$

The perspective drawing of the structure is illustrated in Fig. 62.

Enargite,  $\text{Cu}_3\text{AsS}_4$ , is only the example of a structure with 4 to 4 coordination among sulfosalts. The relation of this structure to the structure of wurtzite is illustrated in Fig. 63. In Fig. 63a and Fig. 63b the perspective drawings of the structures of wurtzite and enargite respectively are given. The structure of enargite can be regarded also as a double layer of Cu-S tetrahedra of wurtzite type sandwiched between single layers of As-S tetrahedra of wurtzite type. This can be seen from the projections of both structures illustrated in Fig. 63c and 63d.

Although from mathematical considerations, alternately occurring layers of Cu-S and Sb-S tetrahedra are possible with any thickness of layer, the double layer of Cu-S seems to be the most stable one of fragments of tetrahedral

framework structure. Another example is found in the structure of chalcostibite, which will be discussed immediately below. As already mentioned, the CuS structure is not a 4 to 4 coordinated one. And AsS or As<sub>2</sub>S<sub>3</sub> compounds are examples of perfect three to two coordinated structure.

The tetrahedral bonds in sulfide structures are not yet completely understood. This type of bond can be explained, from the covalent viewpoint, as an sp<sup>3</sup> hybrid bond. It can also be explained from the ionic viewpoint as the coordination determined by the size-ratio between cation and anion. But the reason why Fe, and Cu, both of which do not crystallize in a structure with 4 to 4 coordination with S, can achieve this coordination in the structure of chalcopyrite, FeCuS<sub>2</sub> is not yet clearly understood. One approach was made by Ahrens<sup>26</sup>. In discussing the structure of chalcopyrite, he termed the structure as a compromised one with respect to ionization potential values. An averaged value of the ionization potentials of Fe<sup>2+</sup>, and Cu<sup>2+</sup> is computed as the same order as that of Zn<sup>2+</sup>, 18 e.v. Although the physical reality of the averaged ionization is not at all clear, the same kind of treatment can be applied to enargite, Cu<sub>3</sub>As<sup>5+</sup>S<sub>4</sub><sup>2-</sup>. The respective ionization potential values are, I<sub>Cu</sub><sup>+</sup> = 7.7, I<sub>As</sub><sup>5+</sup> = 52.6 and the averaged one is  $\bar{I} = 18.9$  e.v.

The structure of emphacite, CuAsS<sub>2</sub>. The structures of

emplectite,  $\text{CuAsS}_2$ , and its isomorph chalcostibite,  $\text{CuSbS}_2$ , are worth while investigating closely from two points of interest. First, the value of  $f_3$ , which is equal to 1.0, and a similarity of the formula to that of enargite, suggest 4 to 4 coordination. Actually this is not found in the structure. In the structure, however, a close relation with the wurtzite structure is observed. The fact was first pointed out by Wells<sup>44</sup>, but his account was incomplete. The second point of interest is their acicular habit and unit cells with a  $4\text{\AA}$  dimension, suggesting similarity to the structures of the acicular sulfosalts. There are  $\text{SbS}_2$  chains in the structure.

In Fig. 63c, the projection of the wurtzite structure is illustrated. Suppose part of the Zn atoms (these are indicated by letter P) are replaced by Cu atoms and another part by Sb atoms. The strong tendency of Sb atoms to have three closest neighbors rather than tetrahedrally arranged ones will cut the fourth bond of the original Zn-S tetrahedral coordination. This fourth bond is the one passing across the dotted lines in Fig. 63c. The resulting projection will be like Fig. 63e. The projection of the structure of chalcostibite, Fig. 55, indicates the existence of this layer in the structure.

In Fig. 64 another viewpoint for regarding the structure of chalcostibite is illustrated. The layers of Sb-S

Fig. 63

(A) The structure of wurtzite in an orthohexagonal unit cell.

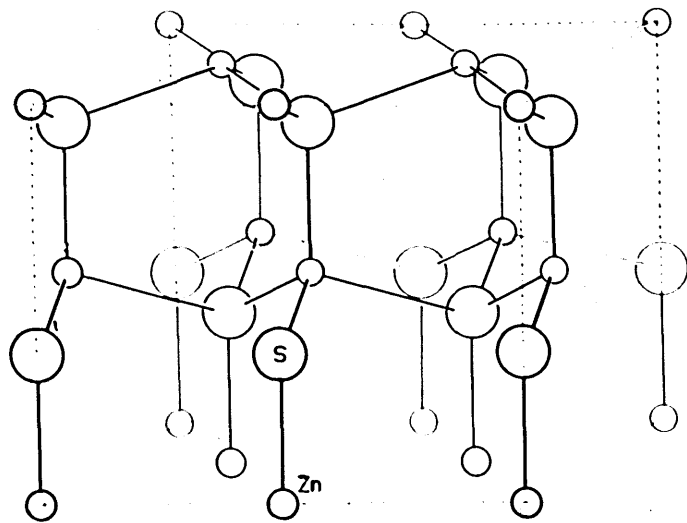
(B) The structure of enargite after Pauling and Weinbaum<sup>30</sup>.

(C) A projection of the structure of wurtzite.

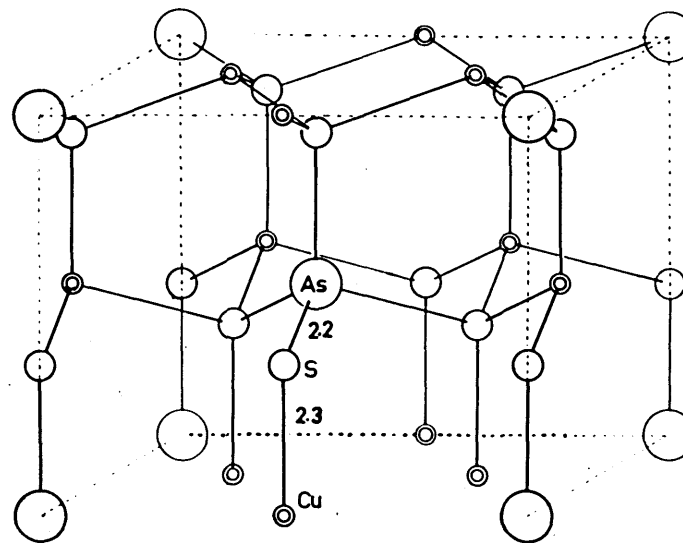
(D) A projection of the structure of enargite.

In (C) and (D), projections are on the plane normal to (120) and traces of (001) are set horizontally.

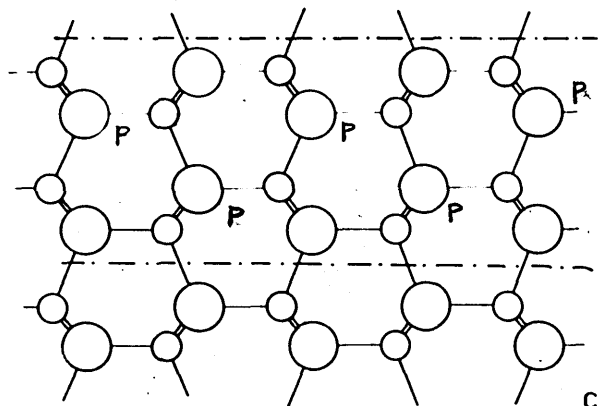
(E) Idealized band in emplectite composed of Cu, As, and S atoms.



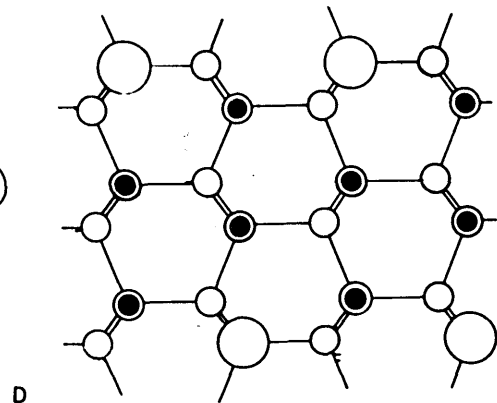
A



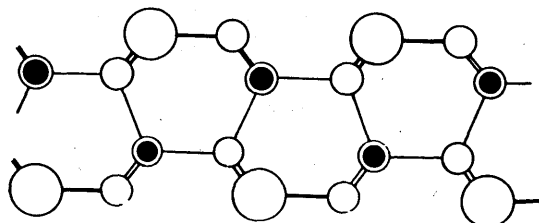
B



C



D



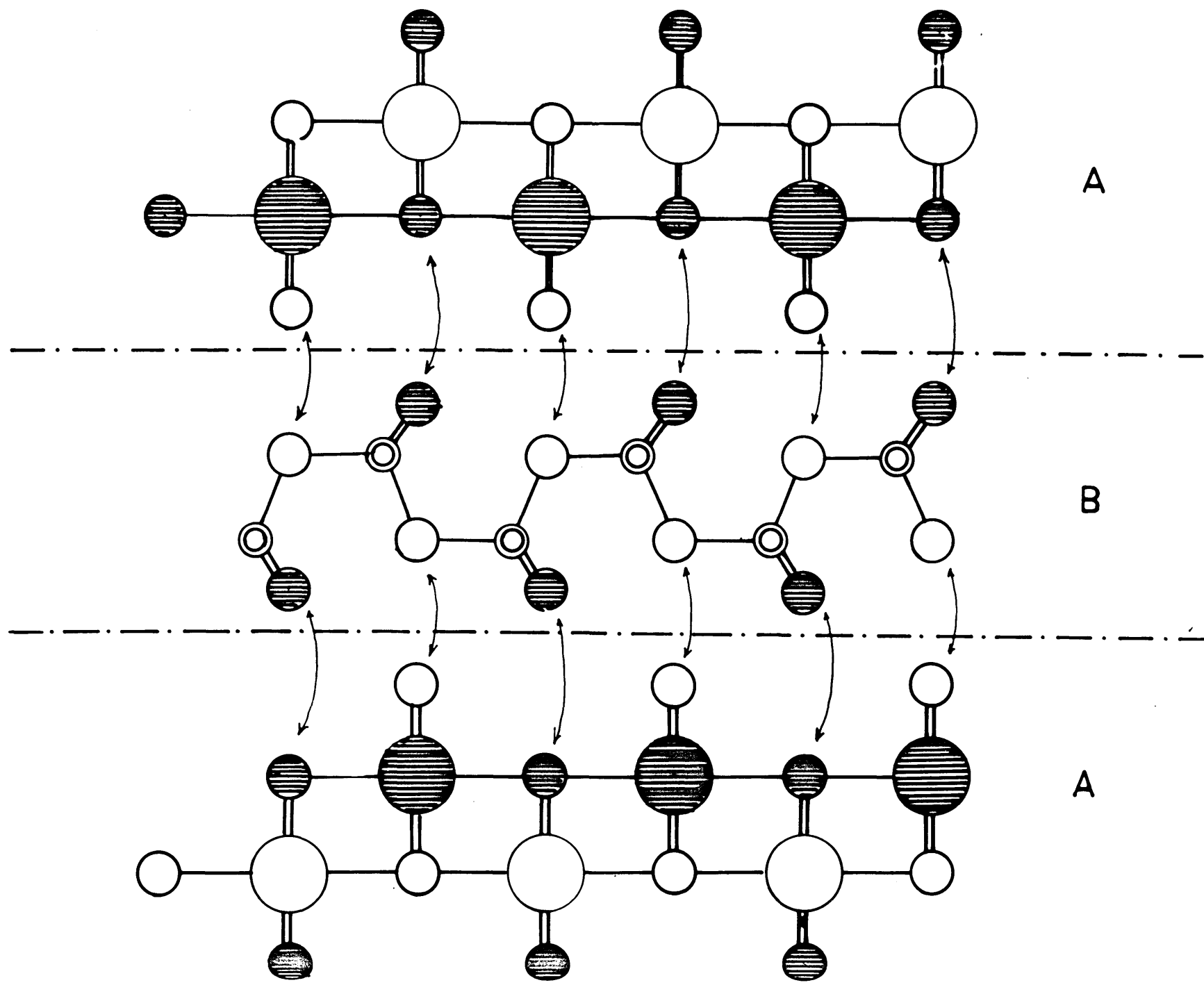
E

Fig. 64 Interpretation of the structure of chalcostibite, Fig. 55.

Drawing A illustrates a double layer of octahedra of Sb and S. This is also shown in Fig. 61b.

Drawing B illustrates a double layer of Cu-S tetrahedra.

The S atoms indicated by arrows are the ones to be shared between layers A and B.





octahedra, and Cu-S tetrahedra are shown to occur alternately. These layers share the S atoms indicated by arrows between them. After the distortions in the regularity of layers illustrated in Fig. 64, the structure given in Fig. 55 results.

The structures of enargite and emplectite can be expressed in the following way from the above considerations.

Enargite,  $\text{Cu}_3\text{AsS}_4 = (\text{Cu-S double layer of tetrahedra})$   
plus (As-S layer of tetrahedra).

Emplectite,  $\text{CuAsS}_2 = (\text{Cu-S double layer of tetrahedra})$   
plus (As-S layer of distorted octahedra).

5. Minerals with chemical parameter  $f$  greater than 1.0.

The minerals in this group are listed in Table 19e. Only the sulfosalts containing Cu or Ag, or both, belong to this group. If the value of  $f$  is greater than 1.0 then an averaged C.N.<sub>S</sub> is greater than an averaged C.N.<sub>Metal</sub>.

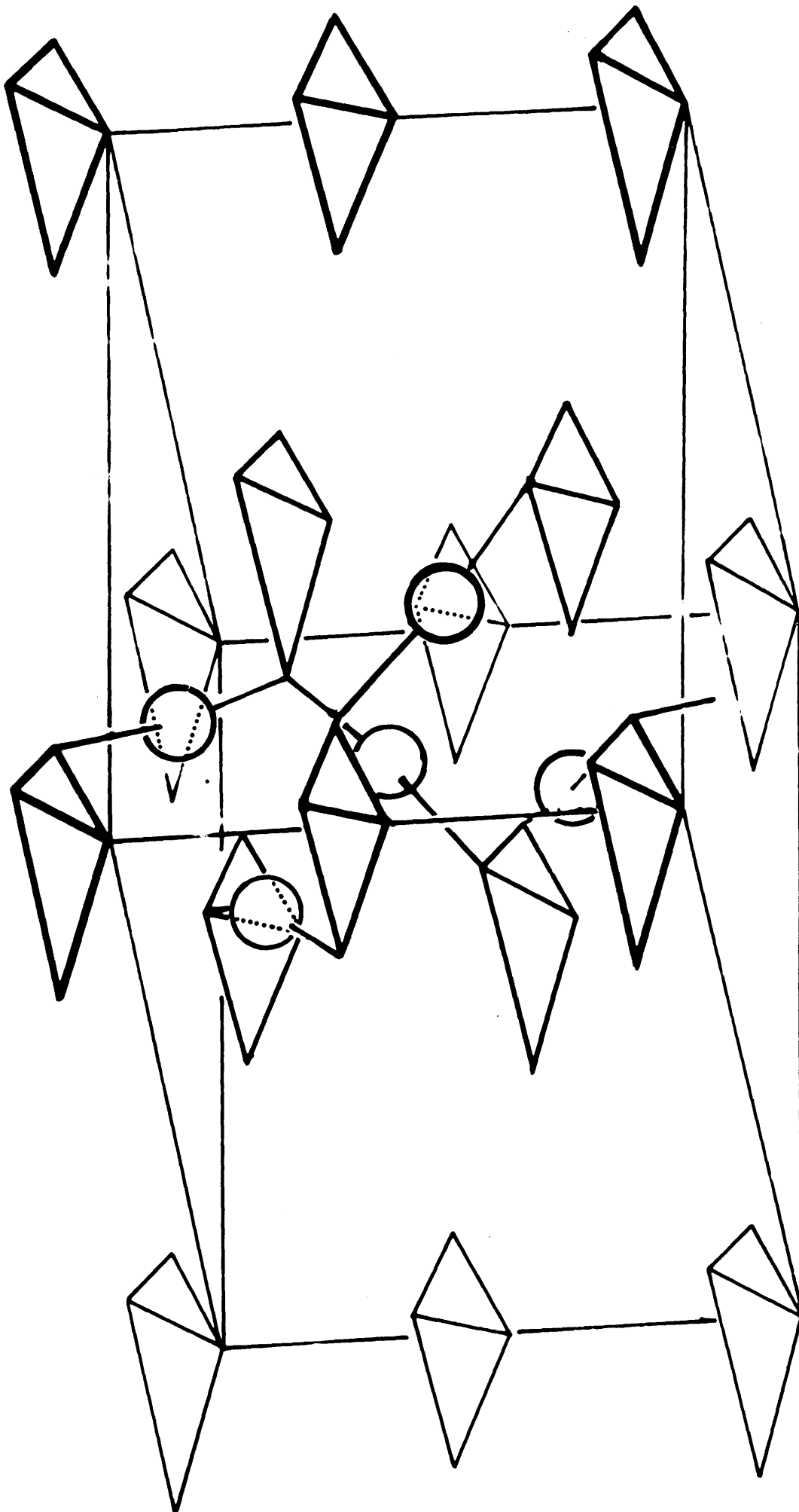
Minerals containing Ag. The second coordination polyhedron of the Ag atom is a distorted octahedron. Thus the C.N. of Ag is 6. The C.N. of the submetallic atoms is greater than 6. The above-mentioned relation between C.N.'s of S and metal atoms is achieved when the value of averaged C.N.<sub>S</sub> becomes greater than 6. In the crystal structures of proustite,  $\text{Ag}_3\text{AsS}_3$  and pyrargyrite,  $\text{Ag}_3\text{SbS}_3$  this situation is observed. S atoms in these structures are surrounded by eight metallic and submetallic atoms. In these structures, however, this situation is closely related to the occurrence of independent  $\text{SbS}_3$  groups of trigonal pyramidal shape. The interatomic distances between the Sb and S atoms in the different groups are larger than 4.0Å. Within the large space provided by these groups Ag atoms are located. Each Ag atom is surrounded by 6 S atoms and each S atom is surrounded by 6 Ag atoms. Each S atom has further two additional neighbors, one Sb of an  $\text{SbS}_3$  group and the other Sb in the adjacent group. The structures can be understood in terms of covalent bonds between Ag and S, and Sb and S, with covalency of 2 and 3 for each metallic atom. The minerals are more covalent in

Table 19e. Group D.

The sulfosalts in this group are characterized by the values of the chemical parameter  $f$  greater than 1.0.

Froustite	hex.	$a = 10.77, c = 6.86$	
$\text{Ag}_3\text{AsS}_3$			$f = 1.33$
Xanthoconite	mono.	$a = 11.97, b = 6.20, c = 16.95$	
$\text{Ag}_3\text{AsS}_3$		$= 110^\circ 10'$	$f = 1.33$
Pyrargyrite	hex.	$a = 11.04, c = 8.72$	
$\text{Ag}_3\text{SbS}_3$			$f = 1.33$
Pyrostipnite	mono.	$a = 6.84, b = 15.84, c = 6.24$	
$\text{Ag}_3\text{SbS}_3$		$= 117^\circ 09'$	$f = 1.33$
Polybasite	mono.	$a = 26.12, b = 15.08, c = 23.89$	
$(\text{Ag}, \text{Cu})_{16}(\text{Sb}, \text{As})_2\text{S}_{11}$		$90^\circ 00'$	$f = 1.64$
Pearceite	mono.	$a = 12.16, b = 7.28, c = 11.88$	
$(\text{Ag}, \text{Cu})_{16}\text{As}_2\text{S}_{11}$		$= 90^\circ 00'$	$f = 1.64$
Wittichenite	orth.	$a = 7.66, b = 10.31, c = 6.69$	
$\text{Cu}_3\text{BiS}_3$			$f = 1.33$
Stephanite	orth.	$a = 7.70, b = 12.32, c = 8.48$	
$\text{Ag}_5\text{SbS}_4$			$f = 1.66$

Fig. 65 Schematic representation of the structure of proustite,  $\text{Ag}_3\text{AsS}_3$ , after Harker<sup>27</sup>. Trigonal pyramids represent  $\text{AsS}_3$  groups. At the apex of the pyramids are located As atoms. S atoms are located at the three corners of basal triangles. Ag atoms are represented by circles. Only part of the total Ag atoms are illustrated. There are two interpenetrating spiral chains of  $\text{Ag}_3\text{AsS}_3$  composition. The parts of these chains are indicated by straight lines bonding Ag and S atoms.



their physical nature than most of the sulfosalt minerals. The lusters of these minerals are adamantine, and the colors are reddish rather than blackish. A part of the structure is illustrated in Fig. 65.

It is not to be definitely stated that this occurrence of independent  $\text{SbS}_3$  groups is always associated with  $f$ -value greater than 1.0. Nevertheless, there are two further examples to suggest the relation in the sulfosalt minerals. The minerals xanthoconite<sup>67</sup> and pyrostitpnite<sup>67</sup> are dimorphs of proustite and pyrargyrite respectively. The structures of these minerals have not yet been investigated. These minerals have also the adamantine lusters and reddish colors. They exhibit sometimes crystal habits similar to the acicular sulfosalts. Since an Sb-S bonds in  $\text{SbS}_3$  group can be regarded as more covalent than an Sb-S bonds in the larger coordination, these physical properties suggest the existence of these groups in these minerals too.

The physical properties of mineral stephanite,  $\text{Ag}_5\text{SbS}_4$  is similar to the one observed in the more metallic sulfosalts. A different scheme of arrangement of atoms which causes  $\overline{\text{C.N.}}_{\text{S}}$  to be larger than six may be found in the structure.

Minerals containing Cu. The examples are tetrahedrite and tennantite, which are described in an earlier section, and wittichenite  $\text{Cu}_3\text{BiS}_3$ . In physical properties wittichenite is the more metallic one, but no structural study has been done on the mineral.

Minerals containing Cu and Ag. There are two minerals with the highest f-values among the sulfosalts. They are polybasite, and pearceite.

Minerals in group E. There are six minerals which could not be classified into any of the previously discussed groups. They are four minerals of the plagiionite series, and the two hexagonal minerals zinkenite and gratonite.

These sulfosalts contain Pb as the only metallic atom in the formula, and all have f-values less than 1.0. These minerals represent problems to be investigated for a further understanding of the crystal chemistry of sulfosalts.

Table 19e. Group E.

In this group are included the following minerals.

Plagionite series.

Fuloppite  $Pb_3Sb_8S_{15}$

Plagionite  $Pb_5Sb_8S_{17}$

Heteromorphite  $Pb_7Sb_8S_{19}$

Semseyite  $Pb_9Sb_8S_{21}$

Two hexagonal minerals

Zinkenite  $PbSb_2S_4$

Gratonite  $Pb_9As_4S_{15}$



## 6. Summary

In the previous sections a certain number of relations between the chemical formula and the structures of sulfosalt minerals have been discussed. They can be summarized as follows. To interpret the sulfosalt structures the principle of the stacking of the second coordination polyhedra has been proposed. The kinds of these polyhedra were discussed for the central metallic atoms. This principle was confirmed in the form of the polygonal network theory. This theory was successfully applied to the members of acicular group of sulfosalts and closely related minerals. The possible modes of polyhedral stackings for the rest of the sulfosalt minerals were considered, and the minerals were classified according to this principle.

It was shown that if the chemical parameter  $f$  of the mineral is equal to 1.0, the coordination number of metallic and submetallic atoms must be equal to the coordination number of the S atoms. There are two such cases. When there is only one kind of coordination number in the structure, namely 6 or 4, the structure is closely related to the galena type or ZnS type. The second case is when two or more kinds of coordination numbers are found in the structure. In this case it was shown that the above-mentioned equality holds for the averaged coordination numbers. And this kind of equality can be achieved by two ways. The first, simpler structure is composed of alternating

layer

layers from the galena type and ZnS type structures. This is realized in the structure of chalcostibite,  $\text{CuSbS}_2$ .

Some distortions in these layers when coexisting were indicated. The second structural type can be illustrated by the structure of aikinite,  $\text{CuPbBiS}_3$ . In this structure, by introducing a  $\text{CuS}_3$  chain sharing S atoms with  $\text{Sb}_2\text{S}_3$  bands of the stibnite structure, the equality of the averaged coordination numbers was achieved.

If the value of  $f$  is smaller than 1.0, the coordination numbers of the submetallic or Pb atoms are shown to be necessarily greater than 6. The resulting structures increase the similarity toward the structure of stibnite,  $\text{Sb}_2\text{S}_3$ . These structures can be regarded as intermediate between the simple sulfide type and stibnite type in certain ways. It was pointed out that, in these structures, the structures with 6 to 6, or 4 to 4 coordinations are only stable as small fragments. In other words these coordinations are realized in only part of the structures. Also in these structures, some kinds of  $\text{Sb}(\text{As}, \text{Bi})\text{-S}$  groups, usually in chains or double chains, are discernible. The geometry of these groups was treated in detail. If these chains or double chains are strongly bonded, the structure will be acicular type. The axis of the chain is parallel to the acicular axis of the crystal. When this  $\text{Sb-S}$  group is a finite one, or when the chains are recognized as only loosely bonded, several modifications of the structure

compared with the acicular ones may be observed. As the first possibility, the crystal habit will still be acicular. The structure has one shortest unit cell dimension of  $4\overset{\circ}{\text{A}}$ , and two other larger dimensions. But the tendency of cleavage perpendicular to the acicular axis will develop. This was observed in jamesonite. As the second possibility, this  $4\overset{\circ}{\text{A}}$  dimension will not exist as a true translation, but as the submultiple translation of the unit cell. This can be looked upon as follows. The dimension  $4\overset{\circ}{\text{A}}$  is characteristic of  $\text{Sb-S}_3$  pyramidal group, from which these chains are built. In the chains the successive  $\text{Sb-S}_3$  groups are translation equivalents of each other. If the chain slightly collapses the regularity of  $4\overset{\circ}{\text{A}}$  repetition along the chain will be lost, and instead the larger translation unit will result. The crystal habit will be thick tabular to prismatic or equant. As the third possibility the structure of seligmannite can be taken as an example. In this structure, the central atoms for the ideally translation-equivalent groups are of different kind, and slightly different kind of coordination is required for each atom. The unit cell translation is doubled, and the  $4\overset{\circ}{\text{A}}$  dimension exists as a unit associated with the asymmetric unit of the structure.

If the value of  $f$  is greater than 1.0 it was shown that the one possible case is when the coordination number

of the submetallic atoms and Cu atoms become three. When there are independent  $\text{Sb-S}_3$  pyramidal group in the structure, the resulting crystals are, above all, more covalent in the nature of their chemical bonds. This fact was observed in proustite, and xanthoconite. There are minerals with  $f$  value greater than 1.0 and with metallic luster, such as stephanite,  $\text{Ag}_5\text{SbS}_4$ . The structural scheme of this mineral is not yet known.

The structures of sulfosalts in one way resembles the sulfide structures. Structural features observed in the sulfides are also found in sulfosalts. This is true especially concerning the nature of the first coordination of each metallic or submetallic atom. But on the other hand, the existence of one or more kinds of metallic atoms with submetallic ones seems to give more ionic character in the chemical bonds compared with sulfide crystals. This does not imply that the resulting crystal is more ionic. The resulting structure is metallic to a certain extent. According to Pauling's theory of the metallic bond, pure covalent bonds can not give metallic character because of the lack of non-synchronized resonances. Thus the deviation from pure covalent bonds to the type observed in sulfosalts, weak but distinct residual bonds, must be related to the observed partial metallic nature of the minerals. The coordination numbers will increase from the characteristically small one for the pure covalent bonds to the larger

ones, but not the quite large ones as observed in metals or alloys.

Further understanding of the crystal chemistry of sulfosalts must be carried out from a more thorough investigation of the chemical bonds in the structures. It seems to be most important to have a clear picture concerning the behavior of the submetallic atoms in the structures of sulfosalts.

## PART IV

## Appendix L

Historical Introduction to the  
Crystal-structure analysis of sulfosalts

The first crystal structure of a sulfosalt determined by the x-ray diffraction method was the structure of tetrahedrite,  $(\text{Cu,Fe})_{12}\text{Sb}_4\text{S}_{13}$  by Machtschki (1928)<sup>43</sup>. This was followed by the structure analyses of tennantite,  $(\text{Cu,Fe})_{12}\text{As}_4\text{S}_{13}$  and of enargite,  $\text{Cu}_3\text{AsS}_4$  by Pauling et al (1934)<sup>29,30</sup>. These three structures were shown to be related to the structures of sphalerite, and wurtzite,  $\text{ZnS}$ . Meanwhile Hofmann determined the crystal structure of emplectite,  $\text{CuBiS}_2$ , and its isomorph chalcostibite,  $\text{CuSbS}_2$  and pointed out the similarity of these structures to that of stibnite<sup>22,31</sup>,  $\text{Sb}_2\text{S}_3$ . These three structures have flat unit cells with one edge of length  $4\text{\AA}$ , and as discussed by Bragg<sup>45</sup>, exhibit the crystal habit which is the reverse of the unit cell, that is, they grow in needles, elongated thin tabular or prism forms. Although there were numbers of sulfosalts minerals with this type of crystal habit, it was ten years later when a new contribution was made by Buerger (1951)<sup>18</sup> on the crystal structure of berthierite,  $\text{FeSb}_2\text{S}_4$ . Before Bragg published his Atomic Structure of Minerals, there were two other sulfosalt structures determined. They were

proustite,  $\text{Ag}_3\text{AsS}_3$ , and its isomorph pyrargyrite,  $\text{Ag}_3\text{SbS}_3$  determined by Harker<sup>27</sup> as the first example of his method of Harker section.

Although Hofmann<sup>53</sup> indicated the similarity between the idealized structure of myargyrite,  $\text{AgSbS}_2$  and the NaCl type structure, and placed aramayoite,  $\text{Ag}(\text{Sb},\text{Bi})\text{S}_2$  as isostructure with myargyrite, satisfactory studies of both minerals have not yet been presented. Later Graham<sup>42</sup> established that the high-temperature form of the systems Ag-Sb-S and Ag-Bi-S crystallizes in the disordered galena type structures. He also showed that myargyrite, aramayoite, and matildite,  $\text{AgBiS}_2$ , have pseudo isometric unit cells with comparable dimensions to the unit cell of galena. The exact atomic coordinates of these structures, however, are still to be determined.

Although their studies did not cover the field of the crystal-structure determinations, the group of Canadian mineralogists at the Toronto University (Peacock, Berry, Nuffield, Graham, Robinson, et al) made a continuous and extensive contributions in the crystallographic and chemical studies of sulfosalts. Since 1939 when Berry presented the first paper on cosalite<sup>46</sup>, to the latest one by Nuffield on pavonite<sup>47</sup> in 1954, altogether 18 papers were published under the series title of "Studies of mineral sulpho-salts". Not only do they establish the crystallographic data for many species, and make apparent the intricate nature of the chemistry and crystallography of sulfosalts, but their results have served as guides to

the structure investigators of this field.

Buerger, in his paper on the minimum function method of crystal-structure analysis<sup>18</sup>, noticed that the unit cells of sulfosalts with acicular habits were the most favorable to be approached by his method, and solved the structure of berthierite accordingly. This structure was later refined by Buerger and Hahn. This method was later applied in the crystal structure determinations of jamesonite<sup>7</sup>,  $\text{FePb}_4\text{Sb}_6\text{S}_{14}$ , and of livingstonite,  $\text{HgSb}_4\text{S}_8^3$ , by Niizeki and Buerger. Further two structures of the acicular sulfosalts were solved by Wickman by means of direct interpretations of Patterson diagrams. His analyses were carried out on aikinite<sup>5</sup>,  $\text{CuPbBiS}_3$ , and on galenobismutite<sup>6</sup>,  $\text{PbBi}_2\text{S}_4$ . Recently Hellner and Leineweber<sup>21</sup> presented their paper on the crystal structures of bournonite,  $\text{CuPbSbS}_3$ , and its isomorph seligmannite,  $\text{CuPbAsS}_3$ . The crystal habits of the last two minerals are columnar, and the shortest unit cell dimension is not 4A, but 8A. The relation between these structures and that of previously determined aikinite, their Bi analogue, was pointed out by authors. Finally in recent discussion, Hellner<sup>25</sup> stated that the crystal structures of diaphorite,  $\text{Pb}_4\text{Ag}_6\text{Sb}_6\text{S}_{16}$ , and of freislebenite,  $\text{Pb}_4\text{Ag}_4\text{Sb}_4\text{S}_{12}$  are galena-type. All the known types of the sulfosalt structures are represented in illustrations as listed in Table 15 of the main text.



PAGES (S) MISSING FROM ORIGINAL

PAGES (S) MISSING FROM ORIGINAL

PAGES (S) MISSING FROM ORIGINAL

PAGES (S) MISSING FROM ORIGINAL

PAGES (S) MISSING FROM ORIGINAL

Appendix IV

Proof of Theorem 1.

In his original paper in Acta Cryst.<sup>33</sup>, Wells presented the special cases of the theorem 1 for the 3-connected, and 4-connected networks without any proof. But in his recent publication, The Third Dimension in Chemistry<sup>35</sup>, a proof for the above-mentioned cases is found. The proof presented here is different from Wells'.

First, two Lemmas are given.

Lemma 1. Given  $t$  points in the unit of a plane network,  $2t$  triangles can be constructed by connecting these points with straight lines in such a way that no point is left inside any resulting triangle.

Proof. Suppose, in the resulting network, there are  $t$  points and  $xt$  triangles, and no point is left inside any triangle. Put an additional point inside each triangle. Connect the point to the three corner points of the triangle. The three new triangles are constructed and one original triangle is destroyed per each additional point. In the resulting network, there are  $t + xt$  points and  $3xt$  triangles, and no point is left inside any triangle. Thus by the assumption, the following relations must hold.

$$x ( t + xt ) = 3xt$$

Solving this equation we obtain  $x = 2$ . Q.E.D.

Lemma 2. Given  $t$  points in the unit of a plane network, the number of  $q$ -gons constructed by connecting

these points in such a way that no point is left inside any resulting q-gon is  $2/(q-2)$ .

Proof. Suppose there are  $t$  points and  $xt$  q-gons in the unit of network, and no point is left inside any q-gon. Put one additional point in each q-gon, and connect this point to the  $q$  corners of each q-gon.  $Q$  new triangles are constructed, and one original q-gon is destroyed per each additional point. In the resulting network, there are  $t + xt$  points and  $qxt$  triangles, and no point is left inside any triangle. By Lemma 1, the following relation must hold.

$$qxt = 2 ( t + xt )$$

Solving this equation we obtain

$$x = \frac{2}{q - 2} \quad \text{Q.E.D.}$$

Definition: Reciprocal network.

Given is a network in which all points are q-connected and there are  $n_3$  3-gons,  $n_4$  4-gons, etc.  $n_p$  p-gons. If a representative point is put inside each polygon, and these points are connected by straight lines, a new network can be constructed. The resulting network is defined as the reciprocal network of the original network. In the given example, the reciprocal network is the network of q-gons constructed with  $N$  points, where  $N$  is the total number of polygons in the original network. Among the  $N$  points in the reciprocal network, there are  $n_3$  3-connected points,  $n_4$  4-connected points etc.,  $n_p$  p-connected points. Generally, the number of points

in the original network is equal to the number of polygons in its reciprocal network, and vice versa. And also the number of connectedness of points, and the number of sides of the polygons are in a reciprocal relation to each other in the two kinds of networks.

Theorem 1. For the network of all  $q$ -connected points,

$$h_3 + h_4 + h_5 + \dots + h_p = 1,$$

$$3h_3 + 4h_4 + 5h_5 + \dots + ph_p = 2q/(q - 2),$$

where  $h_p$  represents the fraction of  $p$ -gon.

Proof. The first equation is an alternative way of saying the total number of polygons in the unit of network.

Let the total number of polygons be  $N$ , and number of 3-gon, 4-gon, etc.,  $p$ -gon be  $n_3, n_4, \dots, n_p$ .

Then

$$n_3 + n_4 + n_5 + \dots + n_p = N.$$

Dividing both sides of equation by  $N$ ,

$$n_3/N + n_4/N + \dots + n_p/N = 1.$$

Putting  $n_p/N = h_p$  we obtain the result.

The following formula,

$$3n_3 + 4n_4 + 5n_5 + \dots + pn_p,$$

represents the number of points counted as many times as the corner points of each polygon. Since each  $q$ -connected point is shared by  $q$  polygons, and counted as many as  $q$  times, the total number of points counted only once is given as

$$P = \frac{1}{q} (3n_3 + 4n_4 + \dots + pn_p) \quad (1)$$



Now consider the network reciprocal to the given one. By the definition above, we have, in this reciprocal network,  $N$  points and  $P$   $q$ -gons. By Lemma 2 the following relation holds between  $N$ ,  $P$ , and  $q$ .

$$P = 2N/(q - 2). \quad (2)$$

From (1) and (2) we obtain

$$3n_3 + 4n_4 + 5n_5 + \dots + pn_p = 2qN/(q - 2).$$

By dividing both sides of equation by  $N$ ,

$$3h_3 + 4h_4 + 5h_5 + \dots + ph_p = 2q/(q - 2).$$

Q.E.D.

The values at the right hand side of the equation can be evaluated for each value of  $q$ , as shown below:

$q$	$2q/(q - 2)$
3	6
4	4
5	$10/3 = 3.33$
6	3
7	$14/5 = 2.8$

## Appendix V

## Proof of Theorem 2

Lemma 3. If a network in which there are  $q$ -gons and  $r$ -gons in the ratio of  $Q : R$ , is constructed from  $t$  points, the following relation holds between  $t$ ,  $N$  (total number of polygon),  $q$ ,  $r$ ,  $Q$ , and  $R$ ;

$$N = 2t/(x - 2), \text{ where } X = (qQ + rR)/(Q + R)$$

Proof. Let the total number of  $q$ -gons and  $r$ -gons in the network be related to the number of points by

$$N = xt,$$

By assumption, the number of  $q$ -gons is given by

$$n_q = \frac{Q}{Q + R} N,$$

and that of  $r$ -gons is given by

$$n_r = \frac{R}{Q + R} N.$$

Put an additional point in each polygon, and connect the point with every corner points of the polygon. In the resulting new network, there are only triangles. The number of triangles constructed from one  $q$ -gon is  $q$ , and that from one  $r$ -gon is  $r$ . Thus the total number of triangles obtained is

$$\begin{aligned} n_3 &= \frac{qQN}{Q + R} + \frac{rRN}{Q + R} \\ &= \frac{(qQ + rR)N}{Q + R} \\ &= \frac{(qQ + rR)xt}{Q + R}. \end{aligned}$$

The number of points in the resulting network is, on the other hand,

$$P = t + xt.$$

Relating these two equations by Lemma 1,

$$\frac{(qQ + rR)xt}{Q + R} = 2(t + xt).$$

Let

$$\frac{(qQ + rR)}{Q + R} = X,$$

then

$$xXt = 2(t + xt).$$

Solving this equation for x, we obtain

$$x = 2/(X - 2).$$

Thus finally,

$$\begin{aligned} N &= xt \\ &= \frac{2t}{X - 2}. \end{aligned} \quad \text{Q.E.D.}$$

Theorem 2. For the plane network in which q-connected points and r-connected points are found in the ratio of  $Q : R$ , and with  $n_3$  3-gons,  $n_4$  4-gons, etc., and  $n_p$  p-gons, the following relation holds.

$$3h_3 + 4h_4 + 5h_5 + \dots + ph_p = \frac{2X}{X - 2},$$

where

$$X = \frac{qQ + rR}{Q + R}.$$

Proof. The following formula,

$$3n_3 + 4n_4 + \dots + pn_p,$$

represents the number of points counted as many times as the corner points of each polygon. The q-connected point is shared by q polygons, and the r-connected point is shared by r polygons. Thus each q-connected point is counted q times, and each r-connected point r times. Since there are these two kinds of points in the ratio of  $Q : R$ , as an

average, each point is  $(qQ + rR)/(Q + R)$  connected, and is counted as many times as this value. Let this averaged value be expressed by  $X$ , then the total number of points counted only once,  $P$ , is given by

$$P = \frac{1}{X} (3n_3 + 4n_4 + \dots + pn_p).$$

Consider next the network reciprocal to the given network. There are  $N$  points and  $P$  polygons, and there are, among the  $N$  polygons,  $q$ -gons and  $r$ -gons in the ratio of  $Q : R$ .

By Lemma 3,

$$P = \frac{2N}{X - 2}. \quad (2)$$

From equations (1) and (2) we obtain

$$3n_3 + 4n_4 + 5n_5 + \dots + pn_p = \frac{2XN}{X - 2}.$$

By dividing both sides of equation by  $N$ , we have the final result;

$$3h_3 + 4h_4 + 5h_5 + \dots + ph_p = \frac{2X}{X - 2}.$$

Q.E.D.

## Appendix VI

## Proof of Theorem 3.

Theorem 3. If the chemical parameter  $\underline{f}$  has a value greater than 1.0, the existence of a connectedness larger than 4 must be assumed in the network.

Proof. Let the number of points and the number of polygons in the unit of the network be respectively P, and N. From Lemma 3, and the reciprocal relation given in the definition (Appendix I), the following relation is obtained:

$$\frac{N}{P} = \frac{X - 2}{2},$$

where

$$X = \frac{qQ + rR}{Q + R},$$

for the mixed network with q-connected and r-connected points.

Now as seen from the correspondance table, page 157, P is the number of S atoms in the unit. If  $N_0$  is the number of metal atoms, and N is the number of polygons,

$$N_0 \leq N.$$

The chemical parameter  $\underline{f}$  is defined as

$$f = (Cu + Ag + Pb + As + Sb + Bi)/S,$$

therefore,

$$f = \frac{N_0}{P} \geq \frac{X - 2}{2}.$$

The case of a mixed network of 3-connected, 4-connected, and 5-connected points is considered.

The evaluations of X, and  $(X - 2)/2$  for the network where all points are of one kind, are tabulated below:

q	x	$(x - 2)/2$
3	6	0.5
4	4	1.0
5	10/3	$2\frac{2}{3}$

Thus for all 4-connected network,  $\underline{f} = 1.0$ .

Equality occurs only when  $N = N_0$ .

For a network in which 4-connected points mix with 3-connected points,  $\underline{f} \leq 1.0$ .

For a network in which 4-connected points mix with 5-connected points,  $\underline{f} \geq 1.0$ .

Therefore, when  $f \geq 1.0$ , the network should include points with connectedness of 5.

## Appendix VII

## Proof of Theorem 4.

The proof is given in four steps. First, a preliminary theorem is proved in Lemma 4. Then steps 3, 4, and 5 will be proved.

Lemma 4. In the network of 3-connected points, and 4-connected points the number of each kind of point is given as  $p_3$  and  $p_4$ . If the total number of points,  $P$ , in the unit is even, then  $p_4$  is even. And if  $P$  is odd, then  $p_4$  is odd.

Proof. For the mixed network of 3-connected and 4-connected points,

$$X = (3p_3 + 4p_4)/P, \quad (1)$$

since  $q = 3$ ,  $r = 4$ ,  $Q = p_3$ ,  $R = p_4$ , and  $p_3 + p_4 = P$ .

Thus,

$$\frac{2}{X - 2} = \frac{2P}{(p_3 + 2p_4)}. \quad (2)$$

As seen in the proof of Theorem 3,

$$P = 2N/(X - 2). \quad (3)$$

From (2) and (3),

$$P = 2PN/(p_3 + 2p_4), \quad (4)$$

and

$$N = (p_3 + 2p_4)/2. \quad (5)$$

From (5), if  $N$  is an integer,  $p_3 + 2p_4$  must be an even integer. Since

$$p_3 + 2p_4 = P + p_4,$$

if  $P$  is even,  $p_4$  must be even to make  $P + p_4$  even.

Also if  $P$  is odd,  $p_4$  must be odd.

Proof of Step 3.

The maximum value of  $p_4$  is  $P$ , and the minimum value is zero. By Lemma 4,  $p_4$  can assume the following values:

$$p_4 = P - 2n,$$

where  $n = 0, 1, 2, \dots, P/2$ ,

if  $P$  is even, and

$$p_4 = P - 2n,$$

where  $n = 0, 1, 2, \dots, (P - 1)/2$ ,

if  $P$  is odd.

Since  $p_3 = P - p_4$ ,

$$p_3 = 2n.$$

Proof of Step 4.

From Lemma 4,

$$N = (p_3 + 2p_4)/2.$$

If  $P$  and  $n$  are fixed, then since

$$p_4 = P - 2n, \text{ and } p_3 = P - p_4,$$

we have  $N = (P + p_4)/2$ ,

$$= (P + P - 2n)/2,$$

$$= P - n.$$

Proof of Step 5.

In the network only 3-gons, 4-gons, and 5-gons are assumed. Let the total number of polygons be  $N$ , then

$$N = n_3 + n_4 + n_5.$$

By Theorem 2,

$$3n_3 + 4n_4 + 5n_5 = 2XN/(X - 2). \quad (1)$$



By Lemma 4, for the network with a mixed connectedness of 3 and 4,

$$X = (3p_3 + 4p_4)/P,$$

and 
$$N = (p_3 + 2p_4)/2.$$

Substituting these expressions into (1),

$$3n_3 + 4n_4 + 5n_5 = 3p_3 + 4p_4. \quad (2)$$

If  $P$  and  $n$  are fixed,

$$p_4 = P - 2n, \text{ and } p_3 = 2n.$$

Substituting these values into (2),

$$3n_3 + 4n_4 + 5n_5 = 4P - 2n. \quad (3)$$

Also, 
$$n_4 = N - n_3 - n_5. \quad (4)$$

From (3) and (4),

$$n_5 - n_3 = 2n, \text{ or } n_5 = n_3 + 2n. \quad (5)$$

If  $n_3$  can be fixed, then  $n_5$  can be computed from (5), and  $n_4$  from (4) for the fixed  $n$ .

The minimum value  $n_3$  can assume is zero.

Since  $n_3 + n_5 \leq N$ , the maximum value  $n_3$  can assume is obtained as following:

With (5),

$$n_3 + n_3 + 2n \leq N.$$

Thus

$$n_3 \leq \frac{N}{2} - n.$$

With relation,

$$N = P - n \text{ (Step 4),}$$

we obtain

$$n_3 \leq \frac{P - 3n}{2}$$

## Appendix VIII

## Proof of Theorem 5.

If Cu is not included in the chemical formula, the possible polygons to be associated with metal atoms are 4-gons and 5-gons, and

$$n_4 + n_5 = N_0, \quad (1)$$

where  $N_0$  is the number of the occupied polygons.

And

$$N_0 \leq N,$$

where  $N$  is the number of all the polygons.

For each value of  $N$  obtained with the fixed values of  $P$  and  $n$ , there is a solution which satisfies condition(1).

If the number of polygons,  $N$ , becomes less than  $N_0$ , such a solution is, though mathematically possible, without meaning to represent the chemical formula.

Thus the minimum value of which  $N$  has a meaning is  $N_0$ .

The maximum value of  $N$  is  $P$  since  $N$  can be expressed as

$$N = P - n,$$

and the minimum  $n$  is zero.

Thus the values of  $N$  as

$$N_0, N_0 + 1, N_0 + 2, \dots P$$

give  $P - N_0 + 1$  solutions which satisfy the condition (1).

## Appendix IX

## Solutions of jamesonite.

From Lemma 4,

$$N = (p_3 + 2p_4)/2.$$

Therefore if  $N$  is a half an integer,  $p_3 + 2p_4$  must be an integer. Thus  $p_4$  can be an integer or a half an integer, but  $p_3$  must be an integer. In case  $P$  is an integer, however,  $p_4$  can not be a half integer.

Thus corresponding to Step 3 of Theorem 4, we have

$$p_4 = P - n,$$

where  $n = 0, 1, 2, \dots, P$ .

With this relation, at Step 4 we obtain

$$N = P - \frac{n}{2}.$$

And as Step 5,

$$3n_3 + 4n_4 + 5n_5 = 4P - n.$$

And finally

$$n_5 = n_3 + n.$$

Also,

$$n_3 = (2P - 3n)/4.$$

In case of jamesonite,  $P = 7$ .

The solutions are worked out in a table form below.

P	$p_3$	$p_4$	n	N	$(2P-3n)/4$	$n_3$	$n_4$	$n_5$	
7	0	7	0	7	3.5	0	7	0	(1)
						0.5	6	0.5	
						1	5	1	
						1.5	4	1.5	
						2	3	2	
						2.5	2	2.5	
						3	1	3	
3.5	0	3.5							
1	6	1	6,5	2.75	0	5.5	1	(2)	
					0.5	4.5	1.5		
					1	3.5	2		
					1.5	2.5	2.5		
					2	1.5	3		
					2.5	0.5	3.5		
2	5	2	6	2	0	4	2	(3)	
					0.5	3	2.5		
					1	2	3		
					1.5	1	3.5		
					2	0	4		
3	4	3	5.5	1.25	0	2.5	3	(4)	
					0.5	1.5	3.5		
					1	0.5	4		

In jamesonite formula no Cu atom is contained. Therefore 3-gons must be vacant, and the total number of 4-gons and 5-gons must be equal to the number of metal and submetal atoms in the formula.

$$n_4 + n_5 = 5.5,$$

since in the asymmetric unit of projection there are  $\frac{1}{2}$ Fe, 2Pb, and 3Sb. Among the above-obtained solutions only four solutions indicated by (1), (2), (3), and (4) satisfy the condition.

PAGES (S) MISSING FROM ORIGINAL

## Bibliography

- 1) W. E. Richmond, Crystallography of livingstonite: Amer. Min., 21 (1936), 719.
- 2) D. H. Gorman, An x-ray study of the mineral livingstonite: Amer. Min., 36 (1951), 480-483.
- 3) M. J. Buerger and N. Niizeki, The crystal structure of livingstonite,  $\text{HgSb}_4\text{S}_8$ : Amer. Min., 39 (1954), 319-320.
- 4) M. J. Buerger and T. Hahn, The crystal structure of berthierite,  $\text{FeSb}_2\text{S}_4$ : Amer. Min., 40 (1955), 226-238.
- 5) F. E. Wickman, The crystal structure of galenobismutite,  $\text{PbBi}_2\text{S}_4$ : Arkiv. Min. Geol., 1 (1951), 219-225.
- 6) F. E. Wickman, The crystal structure of aikinite,  $\text{CuPbBiS}_3$ : Arkiv Min. Geol., 1 (1953), 501-507.
- 7) N. Niizeki and M. J. Buerger, The crystal structure of jamesonite,  $\text{FePb}_4\text{Sb}_6\text{S}_{14}$ : Ph.D. Thesis, Part II., Department of Geology and Geophysics, M. I. T., Z. Kristallogr., 108 (1957)
- 8) N. Niizeki, The crystal chemistry of the mineral sulfosalts: Ph.D. Thesis, Part III., Department of Geology and Geophysics, M. I. T.
- 9) Ralph H. V. M. Dawton, The integration of large numbers of x-ray reflections: Proc. Phy. Soc., 50 (1938), 919-925.
- 10) E. R. Howells, D. C. Phyllips, and D. Rogers, Experimental investigation and x-ray detection of center of symmetry: Acta Cryst., 3 (1950), 210-214.

11) C. Palache, H. Berman, and C. Frondel, The System of Mineralogy (1952), John Wiley and Sons, New York: 485-486.

12) A. J. C. Wilson, Determination of absolute from relative x-ray intensity data: *Nature*, 150 (1942), 151-152.

13) K. L. Aurivillius, On the crystal structure of cinnabar: *Acta Chem. Scand.*, 4 (1950), 1413-1436.

14) L. G. Berry, Studies of mineral sulpho-salts: II. Jamesonite from Cornwall and Bolivia: *Min. Mag.*, 25 (1940), 597-608.

15) N. Niizeki and M. J. Buerger, The crystal structure of livingstonite,  $\text{HgSb}_4\text{S}_8$ : Ph.D. Thesis, Part I., Department of Geology and Geophysics, M. I. T., *Z. Kristallogr.*, 108 (1957).

16) S. C. Robinson, Owheelite: *Amer. Min.*, 34 (1949), 398-402.

17) J. E. Hiller, Uber den Falkmanit und seine Unterscheidung von Bourangerit: *Jb. Min.*, 1 (1955).

18) M. J. Buerger, A new approach to crystal-structure analysis: *Acta Cryst.*, 4 (1951), 531-544.

19) P. R. Pinnock, C. A. Taylor and H. Lipson, A re-determination of the structure of triphenylene: *Acta Cryst.*, 9 (1956), 173-179.

- 20) M. J. Buerger, The interpretation of Harker section: J. Appl. Phys., 17 (1946), 579-595.
- 21) E. Hellner and G. Leineweber, Über komplex zusammengesetzte sulfidische Erze: I. Zur Struktur des Bournonits,  $\text{PbCuSbS}_3$  und Seligmannits,  $\text{PbCuAsS}_3$ : Z. Kristallogr., 107 (1956), 150-154.
- 22) W. Hofmann, Die Struktur der Mineral der Antimonitgruppe: Z. Kristallogr., 86 (1933), 225-245.
- 23) W. Hofmann, Ergebnisse der Strukturbestimmung komplexer Sulfide. II. Beitrag zur Kristallchemie der Sulfosalze des Arsens, Antimons, und Wismuts: Z. Kristallogr., 92 (1935), 161-185.
- 24) L. G. Berry, Studies of mineral sulpho-salts: VII. A systematic arrangement on the basis of cell dimensions: Univ. Toronto Stud., Geol. Ser., 48 (1943), 1-30.
- 25) E. Hellner, Diskussionsbemerkung: Fortshr. Min., 34 (1956), 50-51.
- 26) L. H. Ahrens, The use of ionization potentials. Part II. Anion affinity and geochemistry: Geochim. Cosmochim. Acta 3 (1953), 1-29.
- 27) D. Harker, The application of the three-dimensional Patterson method and the crystal structures of proustite,  $\text{Ag}_3\text{AsS}_3$  and pyrargyrite,  $\text{Ag}_3\text{SbS}_3$ : J. Chem. Phys. 4 (1936), 381-390.
- 28) A. J. Freuh, The crystal structure of stromyerite,  $\text{AgCuS}$ : a possible defect structure: Z. Kristallogr., 106 (1956), 299-307.



- 29) L. Pauling and E. W. Neumann, The crystal structure of binnite,  $(\text{Cu,Fe})_{12}\text{As}_4\text{S}_{13}$ , and the chemical composition and structures of minerals of the tetrahedrite group: *Z. Kristallogr.*, 88 (1934), 54-62.
- 30) L. Pauling and S. Weinbaum, The crystal structure of enargite,  $\text{Cu}_3\text{AsS}_4$ : *Z. Kristallogr.*, 88 (1934), 48-53.
- 31) W. Hofmann, Strukturelle und morphologische Zusammenhänge bei Erzen vom Formetyp  $\text{ABC}_2$ . I. Die Struktur von Wolfsbergit  $\text{CuSbS}_2$  und Emplektit  $\text{CuBiS}_2$  und deren Beziehungen zu der Struktur von Antimonit  $\text{Sb}_2\text{S}_3$ : *Z. Kristallogr.*, 84 (1933), 177-203.
- 32) J. D. Donnay and G. Donnay, Syntaxial intergrowth in the andorite series: *Amer. Min.*, 39 (1954), 161-171.
- 33) A. F. Wells, The geometrical base of crystal chemistry, Part I and Part II: *Acta Cryst.*, 7 (1954), 535-544.
- 34) A. F. Wells, The geometrical base of crystal chemistry, Part III and Part IV: *Acta Cryst.*, 7 (1954), 545-554.
- 35) A. F. Wells, *The Third Dimension in Chemistry* (1956), Oxford, at the Clarendon Press.
- 36) N. F. Mott and F. W. Jones, *Properties of Metals and Alloys* (1936), Oxford. Also see R. E. Peierls, Chapt. V, *Quantum Theory of Solids* (1955), Oxford.
- 37) C. A. Coulson, *Valence* (1952), Oxford.
- 38) L. Pauling and P. Pauling, On the valence and atomic size of silicon, germanium, arsenic, antimony, and bismuth in alloy: *Acta Cryst.*, 9 (1956), 121-130.

- 39) H. Krebs, Der Einfluss homoopolarer Bindungsanteile auf die Struktur anorganischer Salz. II. Halbleiter und legierungsartige Phasen: Acta Cryst., 9 (1956), 95-108.
- 40) N. Morimoto, The crystal structure of orpiment,  $As_2S_3$  refined: Min. Jour., 1 (1954), 160-169.
- 41) C. Brink and C. H. MacGillavry, The crystal structure of  $K_2CuCl_3$  and isomorphous substances: Acta Cryst., 2 (1949), 158-163.
- 42) A. R. Graham, Matildite, aramayoite, myargyrite: Amer. Min., 36 (1951), 436-449.
- 43) F. Machatschki, Präzisionsmessungen der Gitterkonstanten verschiedener Fehlerze. Formel und Struktur derselben: Z. Kristallogr., 68 (1928), 204-222.
- 44) A. F. Wells, Structural Inorganic Chemistry, 2nd. Ed. (1950), Oxford.
- 45) W. L. Bragg, Atomic Structure of Minerals: (1937), Cornell Univ. Press, Ithaca.
- 46) L. G. Berry, Studies of mineral sulpho-salts: I - Cosalite from Canada and Sweden: Univ. Toronto Stud., Geol. Ser., 42, (1939), 23-30.
- 47) E. W. Nuffield, Studies of mineral sulpho-salts: XVIII - Pavonite, new mineral: Amer. Min., 39 (1954), 447-452.
- 48) L. G. Berry, Studies of mineral sulpho-salts: III - Boulangerite and "epiboulangerite": Univ. Toronto Stud., Geol. Ser., 44 (1940), 5-19

49) L. G. Berry and D. A. Moddle, Studies of mineral sulpho-salts: V - Meneghinite from Ontario and Tuscany: Univ. Toronto Stud., Geol. Ser., 46 (1941), 5-17.

50) L. G. Berry, J. J. Fahey, and E. H. Bailey, Robinsonite, a new lead antimony sulphide: Amer. Min., 37 (1952), 438-446.

51) R. M. Douglass, M. J. Murphy, and A. Pabst, Geocronite: Amer. Min., 39 (1954), 908-928.

52) A. R. Graham, R. M. Thompson, and L. G. Berry, Studies of mineral sulpho-salts: XVII - Cannizzarite: Amer. Min., 38 (1953), 536-544.

53) W. Hofmann, Die Struktur von Miargyrit,  $\text{AgSbS}_2$ : Sitzungsber. Preuss. Akad. Wiss. Phys.-Math. Kl., (1938), 111-119.

54) T. Ito, N. Morimoto, and R. Sadanaga, The crystal structure of realger,  $\text{AsS}$ : Acta Cryst., 5 (1952), 775-782.

55) E. W. Nuffield, and M. A. Peacock, Studies of mineral sulpho-salts: VIII - Plagionite and semseyite: Univ. Toronto Stud., Geol. Ser., 49 (1944), 17-40.

56) E. W. Nuffield, Studies of mineral sulpho-salts: IX - Lengenbachite: Trans. Roy. Soc. Canada, 38 (1944), 59-64.

57) E. W. Nuffield, Studies of mineral sulpho-salts: X - Andorite, ramdohrite, fizelyite: Trans. Roy. Soc. Canada, 39 (1945), 41-49.

58) E. W. Nuffield, Studies of mineral sulpho-salts: XII - Fuloppite and zinkenite: Univ. Toronto Stud., Geol. Ser., 50 (1945), 41-49.

59) E. W. Nuffield, X-ray measurements on hutchinsonite: Univ. Toronto Stud., Geol. Ser., 51, 79-81.

- 60) E. W. Nuffield, Studies of mineral sulpho-salts: XI - Wittichenite (klaprothite): Econ. Geol., 42 (1947), 147-160.
- 61) E. W. Nuffield, Observations on kobellite: Univ. Toronto Stud., Geol. Ser., 52 (1948), 86-89.
- 62) E. W. Nuffield, Studies of mineral sulpho-salts: XVII - Cuprobismuthite: Amer. Min., 37 (1952), 447-452.
- 63) C. Palache, and D. J. Fisher, Gratonite - a new mineral from Cerro De Pasco, Peru: Amer. Min., 25 (1940), 255-265.
- 64) M. A. Peacock and L. G. Berry, Rontogenographic observations on ore minerals: Univ. Toronto Stud., Geol. Ser., 44 (1940), 47-69.
- 65) M. A. Peacock, Crystallography of artificial and natural smithite: Univ. Toronto Stud., Geol. Ser., 50, 81-84.
- 66) M. A. Peacock and L. G. Berry, Studies of mineral sulpho-salts: XIII - Polybasite and pearceite: Min. Mag., 28 (1947), 1-13.
- 67) M. A. Peacock, Studies of mineral sulpho-salts: XV - Xanthoconite and pyrostitpnite: Min. Mag., 29 (1951), 346-358.
- 68) S. C. Robinson, Studies of mineral sulpho-salts: XIV - Artificial sulphantimonites of lead: Univ. Toronto Stud., Geol. Ser., 52 (1948), 54-70.
- 69) E. D. Taylor, Stephanite morphology: Amer. Min., 25 (1940), 327-337.
- 70) G. Tunell and L. Pauling, The atomic arrangement and bonds of the gold-silver ditellurides: Acta. Cryst., 5 (1952), 375-381.

## ACKNOWLEDGMENT

The author would like to express his sincere thanks to Professor Martin J. Buerger for his helpful guidance during the course of this work. Only with his continuous encouragement could this thesis be realized, and only with his patience in correcting the numerous mistakes in the English usage by the author could this work be finished as the scientific presentation.

Thanks are also due to Dr. Theodor Hahn for his discussions on many occasions during his stay in our laboratory.

The author wishes to acknowledge the encouragements given by the staff members and his colleagues in the Department of Geology and Geophysics. While he was engaged in the tedious task of collecting the three-dimensional intensity data, he was assisted by Dr. Hahn and Mr. Gordon Seele. The computations of Fourier syntheses involved were performed by the " Whirlwind I " digital computer. Dr. Stephen M. Simpson of the Department did the programming and gave his help in starting the operations.

Finally the author's deep thanks are due to his parents in Japan who morally and financially supported his extended stay in this country, and to Professor Teiichi Ito of the Tokyo University who introduced him to the experience of scientific apprentice at the Massachusetts Institute of Technology.

## Biographical Note

Nobukazu Niizeki was born on November 17, 1925 in Tokyo, Japan. He was the son of Yasutaro Niizeki and Hisako Niizeki. His elementary and secondary educations were obtained mainly in Tokyo. His undergraduate education was completed at the Mineralogical Institute, Science Department, of the Tokyo University, Tokyo. He majored in mineralogy, and graduated in March, 1952, with a degree of Rigakushi, an approximate equivalent to B.S.

In September of 1952, he was admitted to the Graduate School of the Massachusetts Institute of Technology where he worked towards a Ph.D. in geology. He held an appointment as a third-time teaching assistant in the Department of Geology and Geophysics in 1952 and 1953. From September, 1954 to February, 1957 he was appointed as a half-time research assistant in crystallography. In 1956 he was elected to ZX. He is also a member of the American Crystallographic Association.